Mercury Adsorption from South African Coal Fired Power Plants using Modified and Unmodified Fly Ash

Varnika Govender

[MSc.(Eng.) and BSc.(Eng.), UKZN]

A thesis submitted in the School of Chemical Engineering
University of KwaZulu-Natal
Durban

In fulfilment of the requirements for the degree
Doctor of Philosophy in Engineering, Chemical Engineering

February 2024

Supervisors: Professor David Lokhat and Professor Milan Carsky

Declaration

The work presented in this thesis was carried out in the Reactor Technology Research Group in the School of Chemical Engineering at the University of KwaZulu-Natal, Durban from January 2019 to December 2023 under the supervision of Professor D. Lokhat and Professor M Carsky.

This thesis is submitted as the full requirement for the degree PhD. (Eng).:

I, Varnika Govender, therefore, declare that:

(i) The research reported in this dissertation, except where otherwise indicated, is my original work.

(ii) This thesis has not been submitted for any degree or examination at any other university.

(iii) This dissertation does not contain other persons' data, pictures graphs or other information, unless specifically acknowledged as being sourced from another person's.

(iv) This thesis does not contain other persons' writing, unless specifically acknowledged as being sourced from other researchers. Where other written sources have been quoted, then:

(a) Their words have been re-written, but the general information attributed to them has been referenced.

(b) Where their words have been used, their writing has been placed inside quotation marks, and referenced.

(v) This thesis does not contain text, graphics or tables copied and pasted from the internet, unless specifically acknowledged, and the source being detailed in the dissertation and in the References sections.

....

Varnika Govender

As the candidate's Supervisor I agree to the submission of this thesis:

Professor David Lokhat

As the candidate's Co-Supervisor I agree to the submission of this thesis:

……..

Professor Milan Carsky

Acknowledgments

I would like to thank:

- My supervisors, Professor David Lokhat and Professor Milan Carsky for their expertise, support, patience, and guidance during this project.

- The NRF for funding of this project.

- The University of Kwazulu-Natal Research Department for the special funding allocated to purchase the Lumex RA915 Mercury Analyser.

- Eskom staff at Camden and Majuba power stations for their assistance in procuring the fly ash required for testing.

- Miss N Hadebe for her expertise and continuous assistance in the laboratory.

- The staff in workshop department of the School of Chemical Engineering for their assistance in setting up and maintenance of the experimental unit.

- Ms N Murugan and Dr V Bharuth from the Microscopy and Microanalysis Unit (MMU) at UKZN – Westville Campus for the assistance with the SEM/EDX analysis.

- My aunt Selvaranie for the motivation, encouragement, and prayers.

- My sister Krivasha and brother-in-law Trevin for all their support and love.

- My parents, Kumeras and Shobana, for all their love and support and for doing everything possible to make this endeavour successful.

- My dearest Lord Muruga for your endless guidance and blessings always. Muruga Saranam.

Abstract

Mercury can be classified as a global pollutant due to its ability to travel vast distances atmospherically, be deposited on land, and enter water sources. It poses significant environmental, human, and animal risks, especially when converted to methylmercury (any toxic compound containing the complex CH3Hg) (Merriam-Webster, 2024). One of the primary anthropogenic sources is from coal-fired power stations. Therefore, effective control measures need to be employed. Fly ash provides a practical, cheap solution by acting as an adsorbent The fly ash can be enhanced by modification with metallic salts such as $CuCl_2$, $FeCl_3$, $ZnCl_2$, and $CuSO_4$. Two South African fly ash samples obtained from Camden and Majuba power stations show excellent adsorption capacity for mercury when modified by $CuCl_2$ and $FeCl_3$. Fly ash characterisation revealed that the two fly ash samples have very similar chemical compositions. However, the pH differs, with the Camden (dark) ash having a lower pH of 8.62 and Majuba (light) ash having a pH of 10.35. The fly ash samples successfully adsorb Hg^0 whilst in the presence of CO_2, which competes for the active sites available for adsorption. The emission control technology is costly, so power stations should meet a specific eligibility criterion. The fly ash adsorption process can be operated as a single pollutant system or a part of sequential pollution systems with co-benefits. The environmental impact should be an essential consideration when operating the pollution control system as the waste generated is classified as hazardous according to NEM: WA (2008).

Table of Contents

List of Figures

List of Tables

List of Photographs

List of Abbreviations

Hg – Mercury

Hg^0 – Elemental Mercury

Hg^{2+} - Mercury Ion

Hg(p) – Particulate Mercury

CO_2- Carbon dioxide

SO_2 – Sulphur dioxide

NOx – Nitrogen oxides

Å – Angstrom

ESPs – Electrostatic Precipitators

FFPs – Fabric Filter Plants

FGD – Flue Gas Delsuphurisation

Chapter 1
Introduction

Mercury is a harmful, highly toxic substance which needs effective control to prevent contamination to humans and the environment. Mercury is primarily emitted from anthropogenic sources such as coal-fired power stations. In South Africa, approximately 90% of electricity is produced in coal-fired power stations. Since these are some of the largest emitters of mercury, effective techniques to remove mercury on an industrial scale from coal gas in an economically viable manner must be explored.

Due to the absence of mercury control measures in coal-fired power stations excess amounts of Hg are emitted (greater than permissible limits). This requires innovative techniques such as removal of mercury using fly ash or modified fly ash to be explored. Fly ash is a relatively cheaper alternative to activated carbon and is an underutilised by-product of power production using coal. This project aims to test the fly ash from multiple power stations in South Africa, which could alleviate the problem of purchasing costly adsorbents, if the fly ash proves to be a successful adsorbent. Previous studies have not conducted extensive experiments on multiples fly ash samples i.e..: only complete experimentation (modification) was done using the best performing fly ash from the initial results. Testing multiple samples allows power plants to utilise ash from the specific plant without the added costs of purchasing a new adsorbent from elsewhere.

Whilst millions of tonnes of fly ash are produced annually, only approximately 10% is utilised in various applications because it is classified as hazardous according to the National Environmental Management Waste Act of 2008 (Department of Environmental Affairs, 2012). This hazardous classification hinders fly ash in many applications since special licenses are required to handle the material. Fly ash has numerous uses, such as cement manufacturing, brick making, road construction, soil conditioner, or to control acid mine drainage (South African Coal Ash Association, 2023). Eskom's power stations are some of the largest producers of fly ash in South Africa and, therefore, already have the necessary procedures in place for waste

management. This project aims to utilise fly ash, a waste product of the coal combustion process, to adsorb mercury. The project will use unmodified and modified fly ash to remove mercury. The fly ash can be modified by metallic salts such as $CuBr_2$, $CuCl_2$, and $FeCl_3$ (Xu et al., 2013). Fly ash removes mercury by adsorption and acts as a catalyst to promote oxidation.

The two variations of mercury removal will be assessed on their ability to reduce the overall mercury concentration. The reduction in mercury concentrations will be measured to determine the efficiency of the process. Relationships between the operating conditions (temperature, pH, unmodified/modified fly ash) and reduction in mercury concentration will be assessed to develop models for use in industrial processes.

This project used a simulated flue gas stream to assess the performance of the fly ash since the adsorption is not selective, and fly ash has an affinity to adsorb multiple impurities such as SO_2 and CO_2. While other control technologies are available to adsorb other pollutants (CO_2, SO_2 and NOx), no specific mercury emission control technology exists. This study aimed to develop a process that could remove mercury from a coal flue gas stream preferentially using adsorption by unmodified fly ash or modified fly ash.

This project scope is multi-faceted in its overall approach because apart from testing a potential sorbent/s for use in industrial applications, an assessment of the infrastructure available at Eskom's power stations, the ability to incorporate the proposed design into existing processes, evaluating utilisation of single control/sequential-control emission technology and an environmental impact evaluation were also done to provide a whole project evaluation.

The research work is expected to provide novel information into mercury capture in South Africa, as Eskom currently has no emission control technology installed to meet this pollution limit requirement.

Chapter 2

Theoretical Background and Literature Review

2.1. South African Electricity Production

Coal accounts for 85% of electricity production in South Africa and is estimated to be the primary source for at least the next decade (International Trade Administration, 2023). It remains one of the most cost-effective methods to produce electricity. Eskom, South Africa's largest electricity producer, relies on coal-fired power stations to produce approximately 90% of its electricity (Eskom, 2016). Eskom also produces and sells electricity to other African countries such as Zimbabwe, Botswana, Namibia, Lesotho, Swaziland, and Mozambique. South Africa has many coalfields concentrated mainly in the Mpumalanga, KwaZulu-Natal and Free State provinces, as seen in Figure 2.1. The abundance of coal in the country makes it an easy and convenient choice as the major source of electricity production. During coal gasification, impurities such as Hg, SO_2, H_2S and NOx are produced. As most of South Africa's electricity is derived from coal combustion, increased amounts of impurities are being released into the environment.

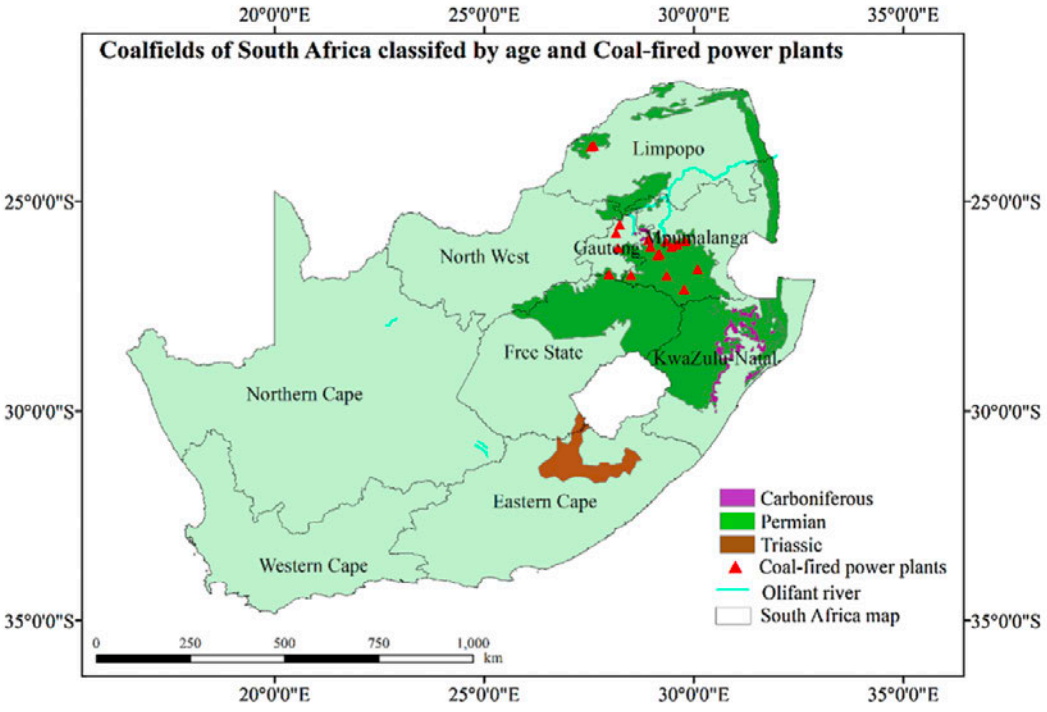

Figure 2.1: Location of South African coalfields and coal fired power plants (Zerizghi et.al, 2022)

2.2. Global Mercury Emissions

Mercury is released into the environment in two ways: naturally and anthropogenically. Natural sources include volcanoes and oceans, whilst anthropogenic sources include fuels, raw products, and industrial processes (United States Environmental Protection Agency, 2023). Figure 2.2 shows global mercury emissions by sector; one of the highest emissions is from the Mining and Coal Combustion Industries.

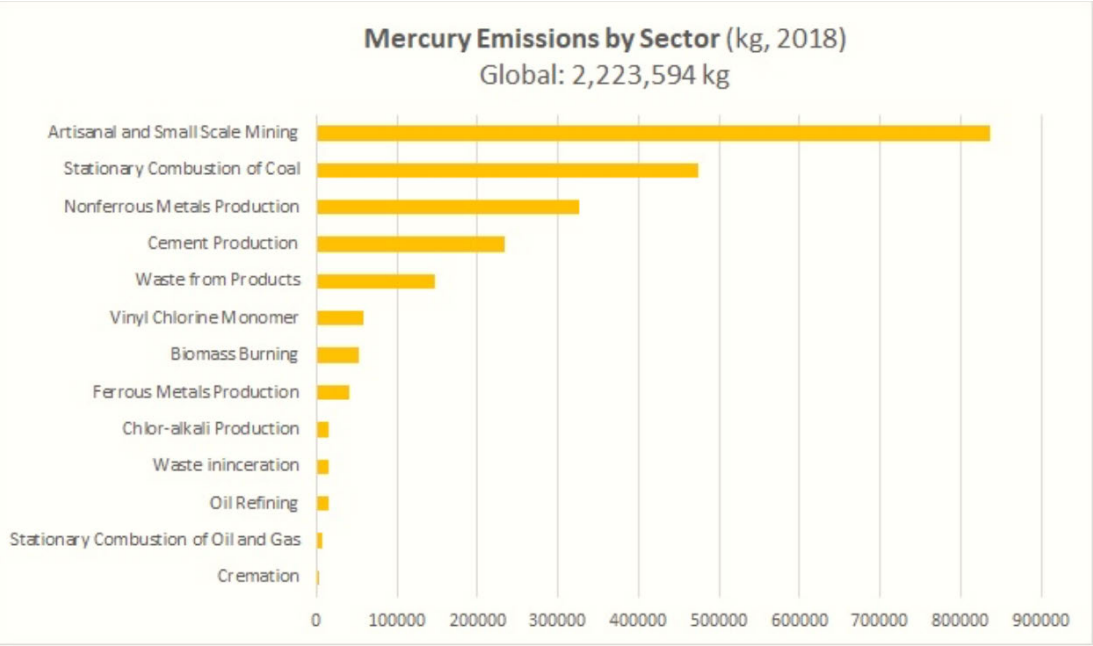

Figure 2.2: Mercury emissions by sector (United States Environmental Protection Agency, 2023)

Recent studies have shown that Mercury (Hg) emissions from anthropogenic sources such as coal combustion are approximately 473 tonnes per annum (United States Environmental Protection Agency, 2023). These are expected to increase as coal combustion increases to meet growing energy demands. Mercury is a highly toxic and harmful substance. Mercury is harmful to all living organisms as well as the environment. It can cause severe harm to humans as it is highly absorbable and causes damage to tissues and organs. Bioaccumulation of Hg as methyl-mercury occurs in aquatic ecosystems, which leads to the contamination of fish and subsequent organisms in the food chain. Mercury also contaminates soil, which leaches into water sources and can cause downstream pollution. Since Hg exists in its elemental form, it cannot be broken down to a less toxic substance; therefore, the only way to effectively remove it from the biosphere would be as deep-sea sediments or to store it in controlled landfills.

2.3. South African Mercury Emissions

South Africa produces large amounts of Hg, which is emitted during the coal combustion stage of electricity production. There is much controversy surrounding the actual amount of Hg emitted from coal-fired power stations. Table 2.1 shows some emission estimates from different sources:

Table 2.1: Estimated South African Hg emissions

Estimated Hg Emission (tonnes/year)	Reference:
9.8	Debrowski et.al, 2008
39.4	Gololo, 2015
17-23	Garnham and Langerman, 2016

South Africa has recently signed the Minamata Convention (Pmg.org.za, 2018), an international treaty which seeks "to protect human health and the environment" from mercury releases. Amongst the obligations listed in the treaty are measures to control releases. Therefore, stricter controls need to be implemented to reduce the quantity of Hg released into the atmosphere. It is necessary to explore techniques that would be commercially viable to remove mercury effectively on an industrial scale.

During the coal combustion process, Hg, amongst other pollutants, is released in the exhaust gas/flue gas. This mercury is in the form of elemental mercury (Hg^0). Due to oxidation, mercury can also be present in the form of Hg^{2+} or as particulate-bound mercury Hg(p) (Mathebula et al., 2020).

The particulate-bound mercury can be captured by Fabric Filter Plants (FFPs) or Electrostatic Precipitators (ESPs) (Garnham and Langerman, 2016). Elemental mercury (Hg^0) can be removed by catalytic conversion to Hg^{2+}, or mercury adsorption onto fly ash of mercury can be employed to remove mercury.

2.4. Mercury Removal Techniques

2.4.1. Wet Scrubbing

Elemental mercury can be removed by wet scrubbing, which converts it to water-soluble Hg^{2+}. Hg^0 can be catalytically converted to Hg^{2+} by the action of NH_3 in the presence of a Selective Catalytic Reaction (SCR) catalyst used for NOx control. The SCR catalyst promotes the conversion of Hg^0 to Hg^{2+}. Some examples of commercially used SCR catalysts are vanadium pentoxide (V_2O_5) and tungsten trioxide (WO_3).

The process is governed by the following three reactions (Madsen et al., 2012):

$$2\ HCl + Hg^0 + ½\ O_2 \leftrightarrow HgCl_2 + H_2O \quad (1)$$

$$2\ NH_3 + 3HgCl_2 \leftrightarrow N_2 + 3\ Hg^0 + 6\ HCl \quad (2)$$

$$2\ NO + 2\ NH_3 + ½\ O_2 \leftrightarrow 2\ N_2 + 3\ H_2O \quad (3)$$

Reaction 1 is the oxidation of Hg^0 by O_2 and HCl; Reaction 2 is the reduction of $HgCl_2$ with NH_3, and Reaction 3 is the DeNOx reaction.

Elemental mercury is oxidised by the halogens found in the coal gas. Since chlorine is present in the greatest concentration in coal, it is used for the oxidation of Hg^0 in the presence of oxygen, as shown by reaction 1 (Madsen et al., 2012).

The overall reaction for the Hg^0 oxidation is:

$$Hg^0 + 2\ HCl + ½\ O_2 \leftrightarrow HgCl_2 + H_2O \quad (4)$$

The overall DeNOx reaction is as follows:

$$4\ NO + 4\ NH_3 + O_2 \leftrightarrow 4\ N_2 + 6\ H_2O \quad (5)$$

The oxidation of Hg is a constructive side reaction that occurs during the NOx control process. This process is interesting since two feasible reactions occur, however the DeNOx reaction inhibits the mercury oxidation reaction.

Some factors that affect the oxidation of Hg^0 to Hg^{2+} are:

- Coal rank/type (HCl concentration)
- Operating conditions (Temperature/Pressure)
- Catalyst (Type/Geometry)

2.4.2. Adsorption by Fly Ash/Modified Fly Ash

2.4.2.1. Definition of Fly Ash

Fly Ash is a powdery residue by-product of the coal combustion process. It can be transferred by dry or wet method as illustrated by Figure 2.3.

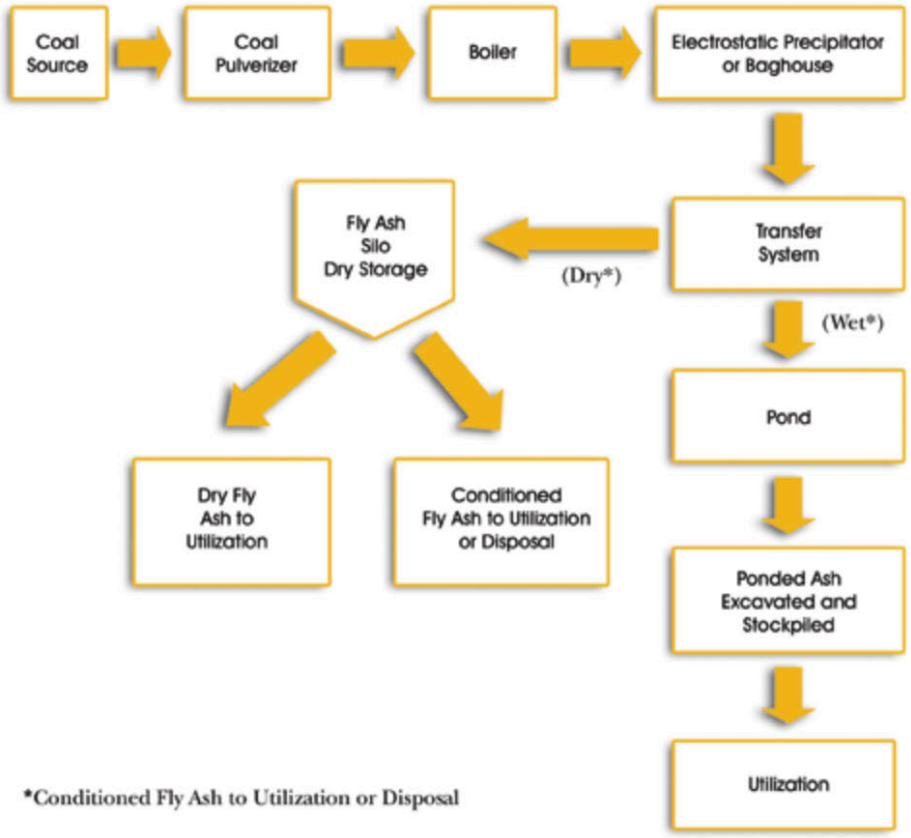

Figure 2.3: Method of transfer of fly ash (American Coal Ash Association, 2003)

2.4.2.2. Fly Ash Classification

Fly Ash can be split into two categories: cementitious or pozzolanic. It can be further classified as Class C or F (Landman, 2003). Class C has a lower calcium content and is pozzolanic, whilst Class F has a higher calcium content and exhibits both cementitious and pozzolanic properties (van Tassel, 2023). Class C has a minimum composition of 70% (SiO_2 + Al_2O_3 + Fe_2O_3), and Class F is made up of 50% (SiO_2 + Al_2O_3 + Fe_2O_3) (Korniejenko et al., 2002). Overall, fly ash composition is primarily based on the type of coal, operating conditions, power plant conditions and post-combustion technology (Risdanaren et al., 2017)

2.4.2.3. Fly Ash Structure

Fly Ash is a mixed spherically shaped particle ranging in size from 200 nm to several microns. The structure also contains cenospheres, ferrospheres, aluminosilicate spheres, plerospheres and irregular shaped carbon particles (Yadav and Fulekar, 2020).

2.5. Uses of Fly Ash (SACAA, 2023)

Fly ash can be utilised in many applications:

- **Building and Construction Industry:** It is used to produce cement and cement-based products such as grout and manufacture bricks.
- **Agricultural Industry** – Adding fly ash to soil can improve soil pH (increase alkalinity) and provide essential minerals to degraded soil (Kishor et al., 2010).
- **Mining Industry** – Can help control the effects of Acid Mine Drainage by acting as an adsorbent to adsorb heavy metals (Foundation of Water Research, 2022).
- **Power Production** – Used as an adsorbent for flue gases (SOx, NOx, CO_2 and Hg).

2.6. Fly Ash Adsorption

2.6.1. Definition of Adsorption

Adsorption is defined as the 'capability of all solid substances to attract to their surfaces molecules of gases or solutions with which they are in contact' (Britannica, 2024). Adsorption is a process whereby atoms, ions or molecules from a gas, liquid, or solid attaches to the surface of the adsorbent. This process occurs at the surface of the adsorbent. At the surface layer of the adsorbent, the particles are not in equilibrium as they are within the adsorbent; therefore, the attractive forces are unbalanced. The imbalance in the attractive forces at the surfaces allows for the adsorption of other gas, liquid, or solid particles.

Adsorption can occur by physisorption or chemisorption. Physisorption occurs when the gas attaches to a solid by weak Van De Waals forces, and during chemisorption, the gas molecules are attached to a solid by chemical bonds.

Some characteristics of the two types of adsorptions are shown in Table 2.2:

Table 2.2: Characteristics of Physisorption or Chemisorption (www.separationprocesses.com, n.d)

Physisorption	Chemisorption
1. Reversible Reaction	1. Irreversible Reaction
2. Low Specificity	2. High Specificity
3. Low Adsorption Enthalpy	3. High Adsorption Enthalpy

2.6.2. Adsorption in a Fixed Bed

A fixed bed adsorber has an immovable adsorbent bed that operates in two ways (Mostinsky, 2011):

- The adsorbent undergoes periodic adsorption-desorption reactions to regenerate and continue.
- The adsorbent bed is changed when it is spent.

Some advantages and disadvantages of operating a fixed bed adsorber include (Adsorption, Regeneration, Desorption, no date):

Advantages:

- Inexpensive to manufacture.
- Column design is simple.

Disadvantages:

- Adsorption occurs only in the current mass transfer zone; the previous mass transfer zone is spent/at equilibrium with inlet concentration, and the mass transfer zone after, although it can adsorb contaminants, will not be able to do so. If the time taken for the mass transfer zone to progress is long, this leads to a bed size increase and subsequently increases the pressure drop.
- The standard operating procedure requires that more than one adsorber be set up in parallel so that there will not be a disruption in a continuous process whilst the sorbent is regenerated or replaced. This requires the design of a system of columns, which increases the complexity of the system.
- Since adsorption is an exothermic process, it is difficult to control the temperature during thermal regeneration of the adsorbent.

2.6.2.1. Mass Transfer in a Fixed Bed Adsorber

Figure 2.4 illustrates the concentration profile as the mass transfer zone moves along the length of the adsorbent bed at four different times, namely: t_1, t_2, t_3, and t_4. Initially, the adsorbate enters the column, interacting with fresh sorbent. Adsorption occurs in the first zone until equilibrium is reached with the feed concentration. Once equilibrium is achieved, the mass transfer zone moves along the adsorbent until the adsorbate is spent.

The concentration profile shown at time t_3 indicates the breakthrough point. That is the point where the mass transfer zone reaches the end of the adsorbent bed.

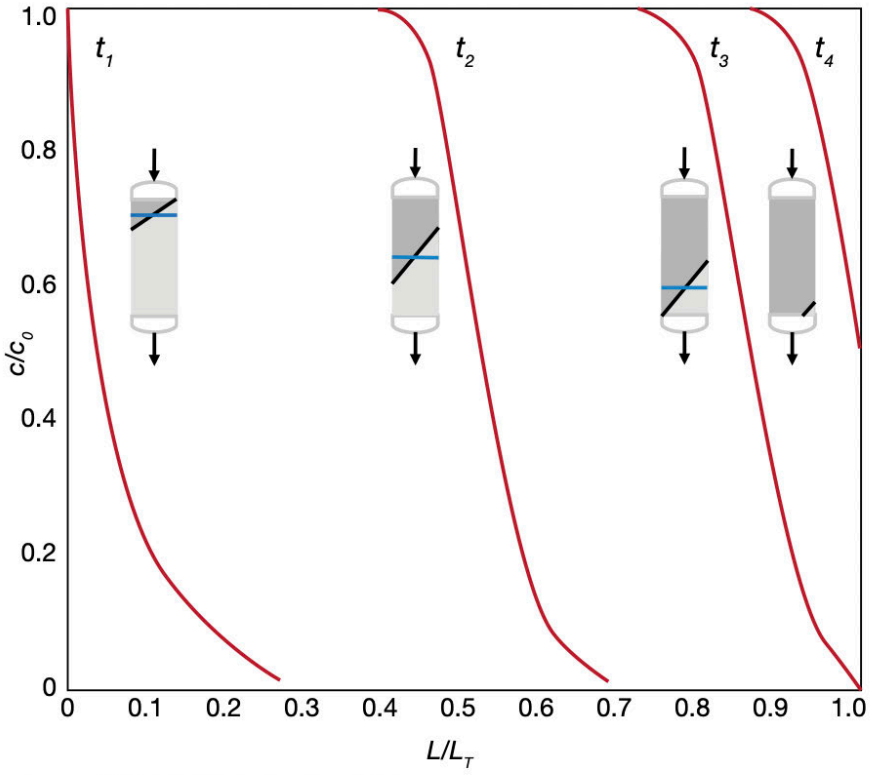

Figure 2.4: Concentration profiles at different times as mass transfer zone moves down the bed (Gabelman,2017)

2.6.2.2. Breakthrough Curves

In Figure 2.5, a breakthrough curve is illustrated. The exit adsorbate concentration is plotted as a function of time. The contaminant is adsorbed using fresh sorbent, and initially, the results show that the concentration has decreased to almost zero or zero. However, once the mass transfer zone reaches the end of the bed and the adsorbent is spent, the measured outlet concentration begins to show trace amounts of contaminant. The breakthrough point B is where the contaminant concentration begins to rise rapidly until the permissible emission value (c_{std}) is reached, and the contaminant can be released into the atmosphere or until the initial concentration c_0 is reached. A steep/vertical gradient is desired as this shows that mass transfer is instantaneous, whilst a less steep rise shows a slower mass transfer rate.

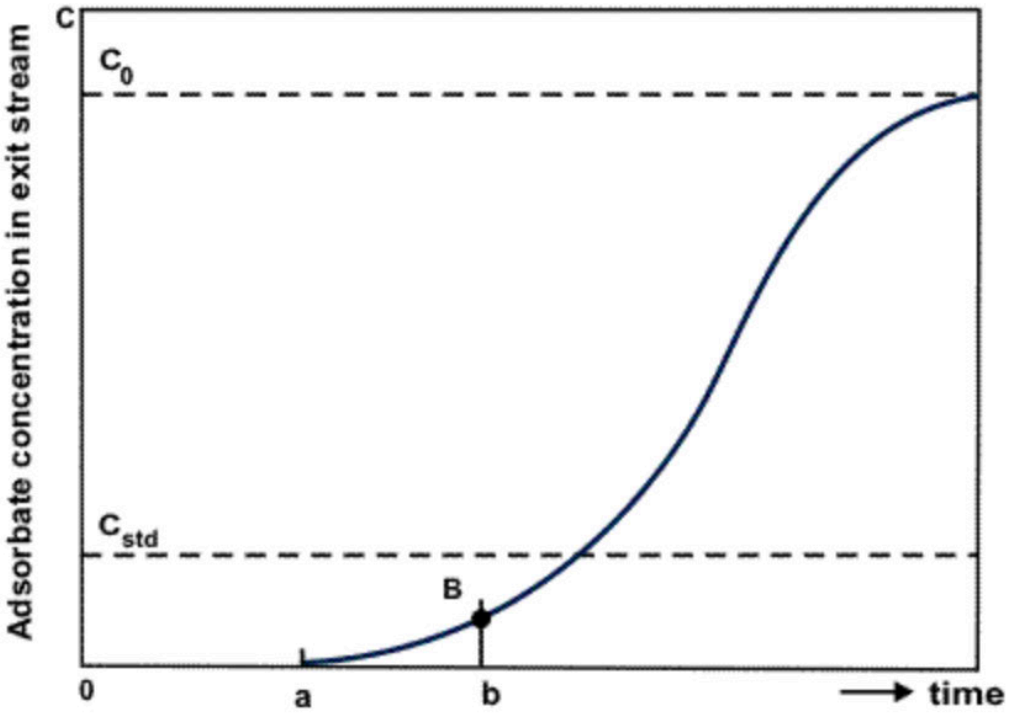

Figure 2.5: Breakthrough curve (Mostinsky, 2011)

2.7. Adsorbents

Adsorbents are specially developed solids that can adsorb large quantities of contaminants or other substances. Solid adsorbents can be classified according to their size as micropore (<20Å), mesopore (20-500 Å) or macropore (>50Å) (Seader and Henley, 2006).

For commercial applications, sorbents need to have the following properties (Seader and Henley, 2006):

- High Selectivity for a specific component.
- High Adsorption Capacity
- Good kinetic and transport properties.
- Free-flowing for ease of filling and emptying.
- High resistance to fouling to extend sorbent life.
- Low cost
- It should not promote side reactions.

2.7.1. Fly Ash as an Adsorbent

An alternate mercury removal method is the adsorption of Hg onto fly ash. Fly ash is a cheaper alternative to activated carbon, which is commonly used for mercury removal. An excess of 50 million tonnes of fly ash is produced annually in South Africa with only 10% overall utilisation (SACAA, 2024). The fly ash is a readily available by-product therefore it is recommended to use over semi-coke.

Fly ash removes mercury by adsorption (adhesion of atoms, ions, or molecules onto the surface of the adsorbent) and acts as a catalyst which promotes mercury oxidation. Studies have shown that two active sites are available on the fly ash for mercury capture. One site has a high binding/separation energy, which promotes mercury adsorption onto the fly ash, whilst the second site has a low binding energy, which serves as a catalyst for mercury oxidation (Zhao et al., 2010).

The intrinsic characteristics of fly ash, such as surface area, unburned carbon, and inorganic compounds, play an essential role in adsorption (Wang et al., 2016). High surface and small pore diameter improve Hg^0 capture. The adsorption affinity for Hg^0 and Hg^{2+} are similar, but $HgCl_2$ has a faster adsorption rate. Studies also show that Hg^0 capture increases with increased surface area of unburned carbon in ash in a linear relation (Wang et al., 2016).

The adsorption capacity of fly ash can be improved by modifying fly ash with $CuBr_2$, $CuCl_2$, and $FeCl_3$ (Xu et al., 2013) to improve Hg^0 capture. The metal chlorides act as oxidants to promote the oxidation of Hg^0 to Hg^{2+}. Operating conditions such as temperature and pH can also affect the adsorption capacity of fly ash.

2.7.2. Fly Ash Adsorption Mechanisms

The Deacon Process, Langmuir-Hinshelwood, Eley-Rideal, or Mars-Maessen mechanism describes the Adsorption of fly ash.

2.7.2.1. Deacon Process – (Over, 2013)

The 'Deacon Process' also known as gas phase oxidation of HCl. The process can be characterized by the following equation:

$$2\mathrm{HCl\,(g)} + \frac{1}{2}\mathrm{O_2\,(g)} \rightleftharpoons \mathrm{Cl_2(g)} + \mathrm{H_2O(g)} \qquad (6)$$

$$\Delta \mathrm{H_r^0} = -\frac{59\mathrm{kJ}}{\mathrm{mol}} \text{ for } \mathrm{Cl_2(300K)}$$

The Deacon Process, developed in 1868 by Henry Deacon, is a solid reaction in which Cu is chlorinated to $CuCl_2$. Then, $CuCl_2$ is re-oxidised to recover CuO, which releases Cl_2 (product) and closes the cycle. The Cl_2 is now available to react with the Hg^0. A reaction temperature of 720K is required to overcome the high activation energy for $CuCl_2$ re-oxidation. An overall conversion of only 75% is achievable due to the reaction thermodynamics. Due to the catalyst being volatile/unstable at high temperatures, this process has been discontinued for commercial use.

2.7.2.2. Langmuir – Hinshelwood Mechanism

The Langmuir-Hinshelwood reaction mechanism can be described by the following reactions (Presto and Granite, 2008):

$$\mathrm{A_{(g)}} \leftrightarrows \mathrm{A_{(ads)}} \qquad (7)$$

$$\mathrm{B_{(g)}} \leftrightarrows \mathrm{B_{(ads)}} \qquad (8)$$

$$\mathrm{A_{(ads)} + B_{(ads)} \longrightarrow AB_{(ads)}} \qquad (9)$$

$$\mathrm{AB_{(ads)}} \leftrightarrows \mathrm{AB_{(g)}} \qquad (10)$$

These chemical equations show a bimolecular interaction between two species, A and B, where A is HCl and B is HgCl (Zhao et al., No Date). The overall rate of reaction is dependent on (presto and Granite, 2008):

- Concentration of A and B.
- Adsorption equilibrium constant K_i.
- Rate constant $k_{surface}$.

Figure 2.6 shows a pictorial representation of the Langmuir-Hinshelwood Mechanism, wherein molecules A and B adsorb onto the surface, react to form a product, and then desorb from the surface (Bratan et.al., 2022).

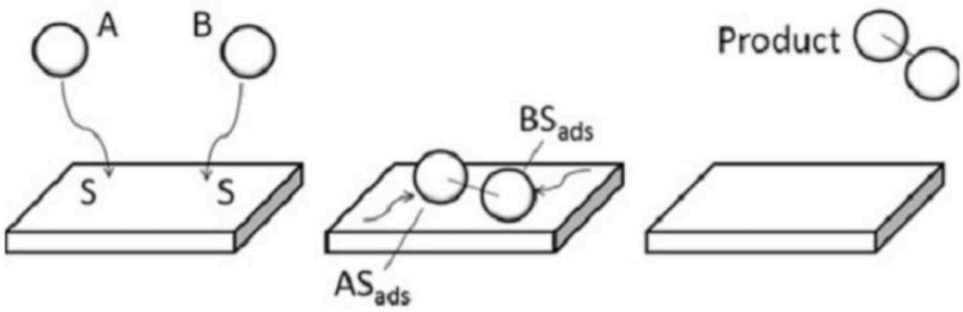

Figure 2.6: Langmuir-Hinshelwood mechanism (Bratan et.al.,2022)

2.7.2.3. Eley-Rideal Mechanism

The Eley-Rideal mechanism describes that mercury that can react in the following way, that is, a surface bound specie can react with a species directly in the gas phase (Presto and Granite, 2008).

$$A_{(g)} \leftrightarrows A_{(ads)} \quad (11)$$

$$A_{(ads)} + B_{(g)} \longrightarrow AB_{(g)} \quad (12)$$

Figure 2.7 shows where molecule A adsorbs onto the surface and then is able to react directly with molecule B in the gas B and then desorb from the surface (Bratan et al., 2022) where A is HCl, B is Hg^0 and AB is $HgCl_2$ (Zhao et al., No Date).

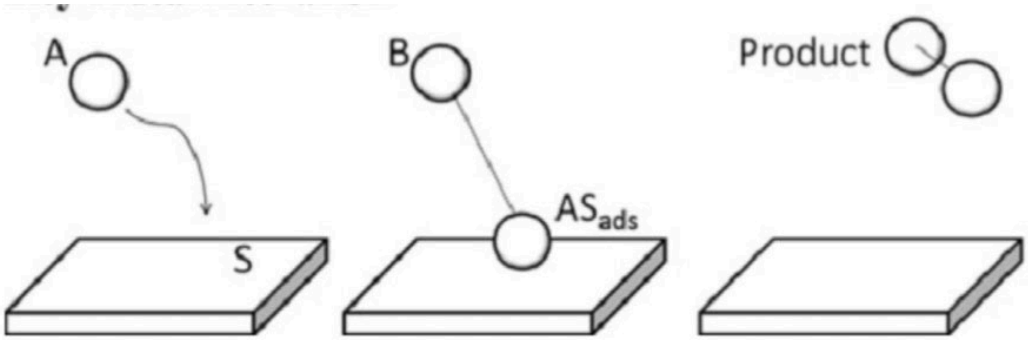

Figure 2.7: Eley-Rideal mechanism (Bratan et.al.,2022)

2.7.2.4. Mars-Maessen Mechanism

The Mars-Maessen mechanism describes the reaction of mercury with Cl_2 or O_2 from a lattice. The O_2 and Cl_2 molecules are constantly replaced in the lattice by molecules from the gas phase. Molecule A is Hg (Zhao et al., No Date). The equations below depict mercury reacting with O_2 (Bratan et al., 2022):

$$A_{(g)} \leftrightarrows A_{(ads)} \quad (13)$$

$$A_{(ads)} + M_xO_y \longrightarrow AO_{(ads)} + M_xO_{y-1} \quad (14)$$

$$M_xO_{y-1} + \frac{1}{2}O_2 \longrightarrow M_xO_y \quad (15)$$

$$AO_{(ads)} + M_xO_y \longrightarrow AM_xO_{y+1} \quad (16)$$

$$AO_{(ads)} \longrightarrow AO_{(g)} \quad (17)$$

Mercury emissions continue to pose issues to humans and the environment. Coal-fired power plants have been identified as a significant source of mercury emissions worldwide and in South Africa.

2.8. Mercury Emissions

Focus has been made on countries wherein the primary method of electricity production is via coal. The countries of India and China, which have the largest populations in the world, have experienced a significant demand for electricity. To meet the requirements for a growing economy and population coal as an energy source cannot be eradicated immediately. Other countries such as the USA or those located in the European regions have legislations which control mercury emissions. South America has moved largely to hydro, wind, and other renewable resources in recent times.

A study by Gade (2015), reveals that over 50% of mercury emissions in the USA occur from coal-fired power plants due to insufficient regulatory control measures. Because of strict control measures, sources like municipal waste combustion and medical waste incineration do not emit such large quantities of mercury into the atmosphere.

Mercury is a natural component of coal and is released during the coal combustion phase. Organic mercury is the most toxic form that is released into the atmosphere. This mercury then settles to form deposits on land and water sources, which can turn into methylmercury, which is highly toxic to humans and animals. Continued exposure to mercury can induce chronic health conditions in humans and animals.

Mercury exposure is greatest through inhalation. Effective control measures such as activated carbon injection and wet lime/limestone flue gas desulphurisation can be used to treat the coal flue gas. Mercury emissions are increasing due to increased power demand; therefore, other sustainable forms of energy production need to be used to reduce the detrimental environmental effects caused by coal-fired power stations.

The largest source of power production in India is currently coal combustion. A review of the study conducted by Joy and Qureshi in 2022 indicates that over 50% of mercury is emitted from coal-fired power plants. Due to its ability to travel great distances by air, through soil or water, it is known as a global pollutant. Since India has signed the Minamata Convention on Mercury, the country has to control and regulate mercury emissions from coal-fired power plants.

Data shows that electricity generation has increased from 800 MW in 1973 to 204080 MW in 2022 (Joy and Qureshi, 2022). The power generation demand is expected to increase by 23% by 2030. India did not have strict emission standards in place and has gradually introduced emission standards from 2015, comparable to other countries, for SO_2, NOx and Hg gases. Due to the increasing demand for energy, it is necessary to strictly enforce pollutant emission standards to reduce overall mercury emission into the atmosphere. Multipollutant systems can provide a solution for mercury control, as dedicated systems are expensive to install.

Control measures such as activated carbon injection and bromine addition can provide an immediate, cost-effective solution to adsorb mercury from coal flue gas. Renewable sources of energy must be explored to meet the current and future demand for power, and strict implementation of the emission standards must be enforced to help reduce overall mercury emissions.

China is the largest producer of mercury emissions in the world. Research conducted by Li et al. (2020), showed that since China signed the Minamata Convention on Mercury, the country has utilised three ways to reduce mercury emissions, namely:

- Small Unit Shutdowns – closure of coal-fired power plants producing < 300 MW.
- Introducing air pollution control devices to existing units.
- Upgrading power generation technology.

Results from this study (Li et al., 2020) show that overall mercury emissions were reduced by 23.51 tonnes. However, specific measures implemented only benefit large-scale operations (> 300 MW) since fitting adsorption technology to small units is costly.

Activated carbon injections are also recommended for use in reducing mercury emissions. Numerous health benefits, such as death prevention and brain function decline, were reduced. It is also shown that further health risks can be mitigated by building or moving power plants to less populated areas.

Garnham and Langerman (2016), reported a quantity of mercury emission ranging from 17- to 23 tonnes in 2015 from South African coal-fired power stations. Coal-fired power stations Matimba and Lethabo, operated by Eskom, contributed approximately 38% of total mercury emissions. Almost 90% of South Africa's electricity is produced by coal-fired power stations. South African power stations employ fabric filter plants (FFPs) and electrostatic precipitators (ESPs) as mercury emission control technology. The power stations that utilise FFPs report a significantly lower mercury emission rate than plants using ESPs. Some coal power stations also utilise a coal pre-washing treatment as a first-stage control measure.

Due to Eskom's retrofitting measures, total mercury emissions are expected to be reduced by 6% to 13%. This paper also highlights some important factors to consider when choosing Hg emission control technology. They include:

- Ability to reduce pollutants and adhere to emission standards.
- Economic feasibility of installing new technology.

It is also noted that further testing is required to obtain accurate mercury emission figures so that the effectiveness of current mercury control technology can be evaluated before new processes are implemented. A recommendation is also made to explore more sustainable renewable energy sources.

A paper by Belelie et al. (2016), highlighted the need to use different methods to quantify the actual mercury emission quantities into the atmosphere. Findings show that utilising measured and published values of Hg in coal samples from power plants could provide a more accurate account of mercury emitted into the atmosphere from coal-fired power plants in South Africa. Overall assessments show that emission control technologies achieve their purpose and that plants retrofitted with FFPs outperform those with ESPs. Changing all existing ESPs with FFPs is recommended, but it may not be economically viable due to the cost required to make the change.

Although there are many research papers available, there is a common thread that runs through them, namely:

- Coal-fired power stations are a major source of mercury emissions, especially into the atmosphere.
- The mercury emission rate has increased due to increased demand for electricity.
- Minamata Convention on Mercury has forced countries to re-evaluate their existing emission standards or create standards if they previously did not exist.
- Actual emission rates need to be quantified by alternate methods of data collection. E.g., In Chapter 2, Table 2.1 gives three different estimations for yearly South African mercury emission.
- Mercury emissions, mainly from coal-fired power plants, are not regulated due to insufficient or non-existent control measures.
- Countries with emission control technology in place have seen a reduction in overall mercury emissions.
- Power stations using FFPs show better mercury adsorption capability than those with ESPs.
- It is recommended to change all plants to FFP; however, this is a costly process, and a feasibility study should be undertaken.
- Alternate methods such as activated carbon injection, bromine addition, or using lime/limestone from the desulphurisation process can be used to remove mercury from coal flue gas. The mercury removal can occur as a part of a multipollutant removal system; however, side/competing reactions during the adsorption process could favour one pollutant over another.
- Pre-treatment, such as coal washing, can help to reduce pollutant concentration.
- Mercury as methylmercury is very toxic, and the use of control technology has lessened health issues faced by people and the environment since the emission rate is reduced.
- Future work must be focused on gradually replacing coal-fired power plants with clean, renewable energy sources.

The literature reviewed in Section 2.8 suggests the use of activated carbon injection, bromine addition or lime/limestone from the desulphurisation process to remove mercury from coal flue gas. While these methods are effective as mercury control measures, they pose a significant problem for commercial use. They are very costly and can favour one compound in a multipollutant removal system design. Due to these reasons, it is necessary to develop an inexpensive, uncomplicated, and reliable technique to remove mercury. Fly Ash/ Modified Fly Ash can be used as an adsorbent for mercury due to its structure and available active sites, which allow for Hg capture.

2.9. Effectiveness of Mercury Capture using Modified Fly Ash

Table 2.3: Fly Ash Modifiers

Author	Modification of Fly Ash using:	Experimental Outcome
Zhang et al. (2014)	$CaCl_2$, CaBr and HBr	Two samples obtained from different power plants were investigated. Results have shown that the modified fly ash has shown a greater efficiency in adsorbing mercury than the unmodified fly ash. The fly ash enhanced by HBr showed the greatest adsorption capacity. Lab analysis techniques such as SEM and BET showed that the modified fly ash had an altered structure, i.e. the pore volume, pore size and surface area had all increased.
Marczak-Grzesk et al. (2021)	Biosorbent (OT-500 or MSC-500)	Fly ash modified using biosorbent (OT-500 or MSC-500) improved the adsorption efficiency of Hg and CO_2 to 92% and 66% from 67% and 55%, respectively. The adsorption efficiency increased significantly for Hg, whilst there was a marginal increase in the efficiency for adsorbing CO_2. Fly ash samples were taken from four zones of the electrostatic precipitator. The results showed that fly ash obtained from Zone 1 and Zone 2 of the ESP had an excellent overall adsorption capacity because of the unburned carbon, halides, and metal oxides. The fly ash obtained from Zones 3 and 4 showed a distinct improvement in the adsorption capacity for mercury when compared to the unmodified fly ash. The addition of metallic ions and halogen ions from the biosorbent changed the fly ash structure by providing more active sites for mercury adsorption.

Qi et al. (2022)	Pyrite mixed with a pre-modified sulphuric acid fly ash (PY + AC-FA)	Structural imaging showed an increased surface area and pore diameter with FeS_2 dispersion. The FeS_2 provided active sites for Hg adsorption. The Hg0 was adsorbed onto the fly ash surface and then oxidised to form HgS. Results also showed that operating conditions of Reaction Temperature of 50℃, Carrier Gas flow rate of 1.0 L/min and 20 wt% loading of sulphuric acid to fly ash gave the best results of 91.92 % removal efficiency of Hg.
Gu et al. (2015)	Ammonium bromide (NH_4Br) three ways by: • Isometric impregnation • Ion exchange • Mechanochemical methods	Results show that the fly ash modified by the mechanochemical method had the greatest bromide adsorption ability. This method ensures an even distribution of bromide whilst reducing overall modified fly ash preparation time. Evenly distributed particles created a large number of active sites for mercury adsorption. The CEM fixed bed results showed that overall mercury adsorption increased with increased bromide content. Analysis using TG/DTG/MS shows that ammonia was released during the mechanochemical method. For a temperature range of 150℃ - 200℃, the released ammonia encourages the oxidation of mercury, thereby increasing the adsorption efficiency. Whilst the overall bromine concentration is low, the mechanochemical method increases the surface activity of the sorbent to increase the mercury adsorption. The experiment also shows that oxidation occurs via the Eley-Rideal mechanism.

Zhang et al. (2015)	HBr	Results showed a significant increase in adsorption capacity compared to the unmodified fly ash samples. Mercury species present when the unmodified samples were tested include $HgCl_2$ and HgS; however, when the modified fly ash samples were tested, the species present included $HgBr_2$ and HgO. This study also showed that particle size influenced the overall adsorption ability of the fly ash. Modified fly ash with a fine particle size outperformed the larger size particle to increase surface area and residence time.
Xu et al. (2012)	$CuBr_2$, $CuCl_2$ and $FeCl_3$	Fly ash modified with metallic salts such as $CuBr_2$, $CuCl_2$ and $FeCl_3$ are excellent sorbents since they increase the surface area, thereby increasing the number of active sites available for adsorption. Two components of fly ash viz; the amount of unburned carbon and the presence of metals (Ti, Si, Al, and Fe) influence the adsorption rate positively. The chlorides and bromides present in the $CuBr_2$, $CuCl_2$, and Fe_2O_3 act as oxidants to convert Hg^0 to Hg^{2+}. These experiments also investigated the effect of HCl, O_2 and SO_2 gases. Results show that whilst HCl and O_2 enhanced the adsorption of mercury, the addition of SO_2 has a negative influence on mercury adsorption since it vies for active adsorption sites.

Song et al. (2014)	Different concentrations of HBr solution	Results showed that Hg^0 adsorption capacity increases with increasing HBr concentration. Ion chromatography and thermogravimetric analysis were identified as suitable methods to quantify HBr loading on fly ash samples. Salts can be formed when HBr reacts with certain compounds present in the fly ash, which can affect the adsorption capacity and oxidising ability of the fly ash.

Table 2.4: Effect of Gas Composition

Author	Effect of Gas Composition:	Experimental Outcome
Shen et al. (2020)	SO_2, HCl and O_2	The biomass sorbent was initially modified using 1% NH4Cl to improve the adsorption capacity. The number of surface pores available and the amount of O-H functional groups increase. HCl and O_2 promote mercury oxidation by reacting with the Cl and O-H functional groups, respectively. However, the presence of SO_2 inhibits mercury oxidation because it interacts with O_2 to form SO_3, which competes for active sites that are available for adsorption. SO_2 also interacts with Hg to form $HgSO_4$, thereby hindering the oxidation of mercury.
Szeliga et al. (2022)	HCl	An activated carbon type NORIT GL5 was selected as the adsorbent. The sorbent showed a high affinity for mercury whilst also being able to adsorb HCl, acid gas and sulphur dioxides. Results showed that the rate of mercury adsorption increased significantly as the concentration of HCl increased; however, this only occurred until maximum

		efficiency was achieved. The effect of adding $Ca(OH)_2$ was also assessed, and it was found that whilst the mercury adsorption rate increased, it was marginal.
Carey et al. (1998)	SO_2 and HCl	Some observations were made, such as the adsorption capacity increased when the temperature decreased, which is consistent with a physical adsorption mechanism. Flue gas concentration influences the adsorption rate. A decrease in SO_2 and an increase in HCl concentration increases the mercury adsorption capacity. The influence of flue gas composition on elemental mercury as compared to mercuric chloride is far greater. Adding HCl (50ppm) increased the elemental mercury adsorption rate to 2500 ug/g. The presence of NOx and 50 ppm HCl decreased the elemental mercury adsorption capacity. The oxidation of elemental mercury increases the adsorption capacity. Results show that activated carbon does make a suitable sorbent, but the influence of the flue gas composition is significant to overall adsorption capacity. Additional factors to be considered are the impact on the ESPs after the carbon injection and the subsequent fly ash disposal.

Some research papers have been reviewed, as shown above, and their findings can be summarised as follows:

- Modification of fly ash is effective as it improves the overall adsorption ability.
- Fly ash can be modified by many additives such as $CaCl_2$, CaBr, HBr, $CuCl_2$, $CuBr_2$, $FeCl_3$ and biosorbent (OT-500 or MSC-500), and experiments showed that the adsorption capacity improved. However, the extent to which the efficiency improved depends on many factors.
- Fly ash composition influences the adsorption ability as samples taken from different zones in an electrostatic precipitator displayed different adsorption capacities.
- The presence of unburned carbon, metal oxides, and halides positively influences the adsorption rate.
- HBr or bromine composite seems to be the most common additive used to modify fly ash.
- The use of the mechanochemical method to modify the fly ash showed that this technique allowed for the best distribution of bromine on the surface of the fly ash. The particles were evenly distributed.
- Oxidation occurred by the Eley-Rideal mechanism for the temperature range of 150℃ - 200℃.
- An experiment also revealed that particle size influences the adsorption rate; fine particle-sized fly ash performed better.
- The influence of HCl, O_2, SO_2 and NOx gases was also investigated, and all experiments showed the same findings: the presence of HCl and O_2 increased the adsorption rate, whilst the presence of SO_2 and NOx decreased the adsorption rate. HCl and O_2 encourage mercury oxidation, but SO_2 and NOx compete with Hg for the active sites available for adsorption.
- The degree by which the reactions are influenced depends on the concentrations and combinations of the respective gases in the flue gas.

The extent of the fly ash effectiveness is dependent on the actual plant conditions where it is to be used. Since there are no fixed flue gas or fly ash compositions, it is challenging to develop a single broad-spectrum modified fly ash to fit all operating conditions.

2.10. Methods to Determine Mercury Exit Concentration

There are a few alternate methods by which mercury concentration can be measured, namely:

- Sampling Train Methods
- Dry Sorbent-Based Methods

2.10.1. Sampling Train Methods

Sampling train methods are designed to operate after the flue gas has gone through an electrostatic precipitator to remove Hg(p). Some factors that affect the data achieved from sampling train methods are (Wocken et al. 2006):

- Flue Gas Concentration
- Source
- Procedure
- Equipment

a) Ontario Hydro Method

The samples are collected isokinetically in a train consisting of eight impingers. The impingers are filled as follows (Process adapted from Keika Ventures explanation of Method D-6784):

- Impingers 1 – 3 contain 100 mL of a 1N KCl solution.
- Impinger 4 contains 100 mL of aqueous 5% HNO_3 and 10% H_2O_2 solution.
- Impingers 5 – 7 contain 100 mL of aqueous acidified $KMnO_4$ and 10% H_2SO_4.
- Impinger 8 contains 200-300 g of silica gel.
- One oversized impinger can be placed between Impingers 3 and 4 for samples with high moisture content.

After the samples are collected, the contents of impingers 1-3 and 5-7 are combined in separate vessels. For impingers, 1-3, the filter support, the back half of the filter holder, and all connecting glassware are rinsed using 0.1N HNO_3 into the vessel containing all impingers 1-3 contents. A small amount of $KMnO_4$ can be added to maintain the purple colour. Allow the solution to sit for 15 minutes, and lastly, rinse the impingers a final time with 10% HNO_3 to remove any brown deposits. Impinger 4 contents are added to the collection vessel after rinsing with 0.1N HNO_3 twice.

For impingers 5-7, the connecting glassware and impingers are rinsed twice with 0.1N HNO3 and then a third time with HNO_3 containing 10% hydroxylamine solution. The contents are added to the main collection vessel. A small amount of H_2SO_4 or $KMnO_4$ can be added to maintain the pink/purple colour.

Five fractions will be recovered from each sample. Each fraction should be analysed separately multiple times. These are analysed using cold-vapour atomic adsorption (CVAAS) or Cold-vapour atomic fluorescence (CVAFS) technique.

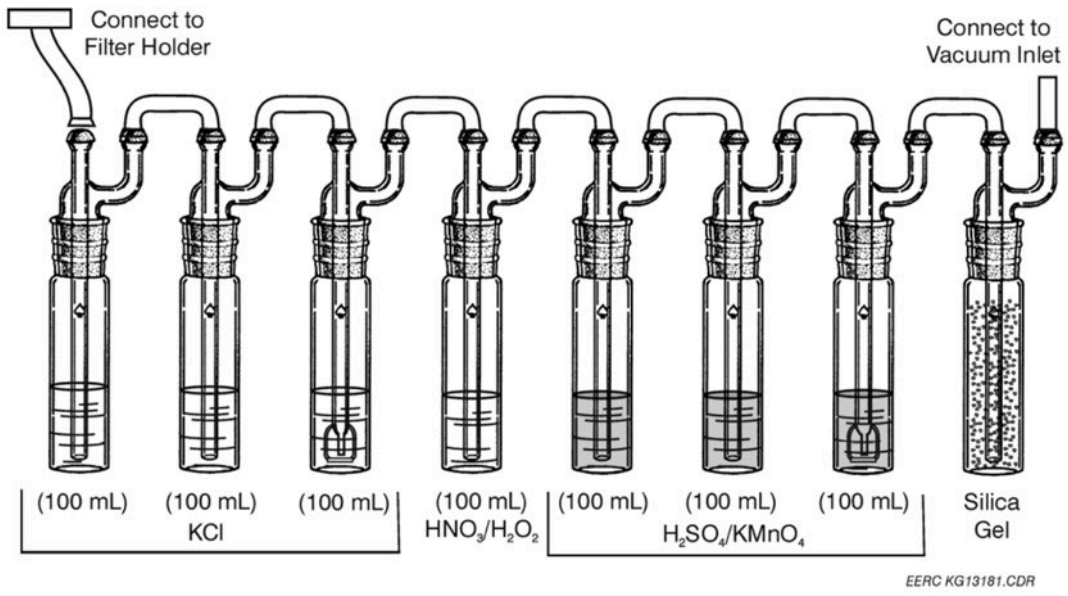

Figure 2.8: Setup of Ontario-Hydro method (Wocken et.al.,2006)

2.10.2. Dry Sorbent Method

Flue gas mercury speciation (FMSS) and Quick SEM™(QSEM) are two dry sorbent-based mercury measurement techniques. The FMSS can provide concentrations for different mercury species ($Hg^{0,}$ Hg^{2+} and $Hg_{(p)}$), but QSEM will measure the total mercury content in the flue gas stream.

a. FMSS Technique

FMSS contains three sample collection points, as illustrated in Figure 3.4. The mini quartz filter adsorbs Hg(p), whilst the KCl/Quartz and Iodated Carbon filters trap Hg^{2+} and Hg^0, respectively. After sampling, the sorbent traps undergo strong acid digestion, BrCl oxidation, aqueous $SnCl_2$ reduction and dual gold amalgamation before analysis by CVAFS is conducted (Wocken et al., 2006).

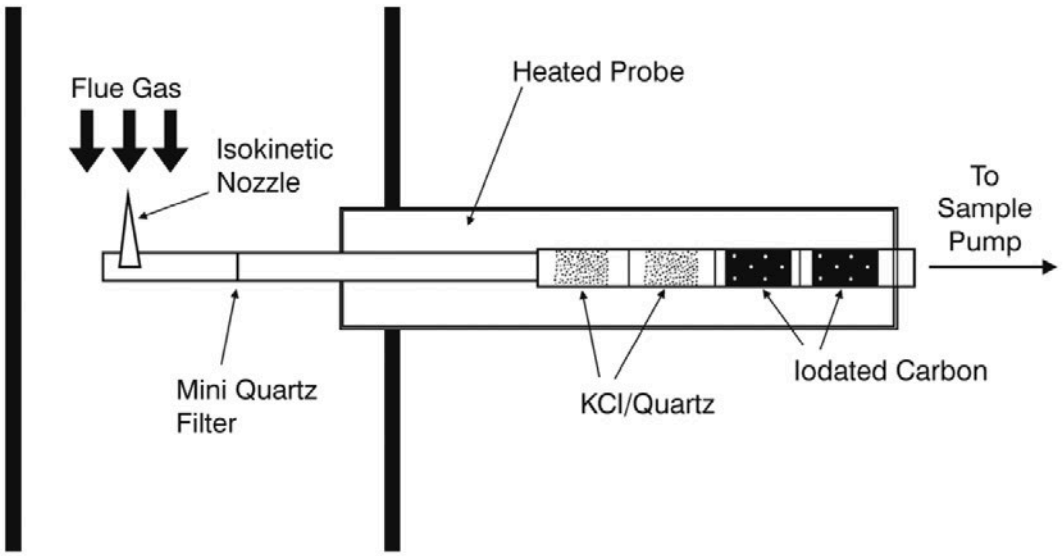

Figure 2.9: FMSS sampling method

Chapter 3
Experimental Procedure

Fly ash characterisation was undertaken by utilising FESEM/EDX analysis and measurement of pH. The mercury adsorption capacity of the unmodified fly ash samples and fly ash modified using $CuSO_4$, $ZnCl_2$, $FeCl_3$ and $CuCl_2$ was investigated using a single adsorption reactor system. This section outlines the procedure to undertake the above measurements and the required apparatus.

3.1. Fly Ash Characterisation

FESEM, in conjunction with EDX analysis and pH measurements, were utilised to characterise the two fly ash samples obtained from the Camden and Majuba power stations.

3.1.1. FESEM/EDX Analysis of Fly Ash

Field emission scanning electron microscopy (FESEM) provides an image showing a material's morphology. The method can provide information about the material's shape, size, structure and composition. Compared to SEM (scanning electron microscopy), the FESEM method can provide clearer, less distorted images at higher magnifications (PhotoMetrics, Inc., 2023).

FESEM is usually done with EDX (energy dispersive X-ray) analysis as the latter provides information about the elemental composition and chemical characterisation (Kepekçi et al., 2021).

The coal composition, degree of combustion, and rate of cooling determine the fly ash's morphology, phase, and chemical composition (Strzałkowska, 2020).

The FESEM/EDX analysis was conducted at the Microscopy and Microanalysis Unit at UKZN – Westville Campus.

3.1.2. pH Measurements

3.1.2.1. Buffering

Buffering refers to calibrating the pH meter and electrode (AWE, 2023). The pH meter and electrode were calibrated using prepared standard buffers of pH 4, pH 7 and pH 10. Initially, the electrode was calibrated using the pH 7 and pH 10 buffers since studies show that South African fly ash is alkaline due to the high concentration of CaO (Calcium oxide) present (Vadapalli et al., 2008). Standard calibration procedures recommend that the buffering be done using pH 7 and pH 10 solutions if a substance is known to be alkaline; however, the pH 4 solution can also be measured as a good practice measure (AWE, 2023). Regular calibration is necessary to ensure that accurate results are obtained.

3.1.2.2. pH Measurement of Fly Ash Samples

The pH of the fly ash samples was determined by dissolving 25 g of fly ash into 150 mL of deionised water (Risdanareni, Puspitasari and Januarti Jaya, 2017). The samples were left in the deionised water for 3 hours to allow the fly ash to leach chemicals into the solution. The pH of the two solutions was then measured using the HANNA Instruments – pH 212 Microprocessor meter. Each sample was measured thrice, and an average was obtained.

The calibration results and the pH measurements are shown in Chapter 4.

3.2. Adsorption Testing

3.2.1. Concept

A lab-scale experimental setup was developed to perform the mercury adsorption experiments using unmodified and modified fly ash samples. The experimental setup was designed to perform the following three processes: the Introduction of Mercury as Vapour into the system, Mercury Adsorption onto Fly Ash or Modified Fly Ash in the Reactor, and Determination of Exit Mercury Concentration. The experimental setup was developed to ensure that these processes occurred sequentially in a controlled manner.

3.2.2. Introduction of Mercury as a Vapour into the System

Mercury was introduced to the system through a permeation tube. The mercury contained within the permeative tube is in a liquid phase, but it needs to be converted into the vapour phase for adsorption experiments. Previous studies (Xu et al., 2012) have shown that using a U-tube placed into a heated oil bath effectively converts the liquid mercury from the permeation tube into a vapour.

3.2.2.1. Mercury Permeation Device

Mercury vapour was introduced into the experimental unit via a permeation device. A permeation tube is a device that contains a pure substance/chemical, whereby the release of the chemical occurs through the walls of the tube (Vici, 2020). The tube walls are generally manufactured using PTFE (Vici, 2020).

Some factors that affect the permeation rate include (KIN-TEK, 2021):

- Temperature.
- Permeability of the chemical compound.
- Physical properties of the material used to manufacture the permeation tube.

Table 3.1: Advantages and disadvantages of permeation tubes (KIN-TEK, 2021)

Advantages	*Disadvantages*
The tubes are small and compact which makes it easy to transport and use in a laboratory setting.	Tubes are expensive.
A precise concentration of chemical can be achieved.	Highly temperature sensitive. – Small deviations can affect the output concentrations drastically.
Tubes arrive ready to use from the manufacturer – no further assembly is required.	Limited lifespan.

Figure 3.1 shows a typical permeation tube design. The tube is normally manufactured from Teflon and contains the analyte (mercury) in the middle section.

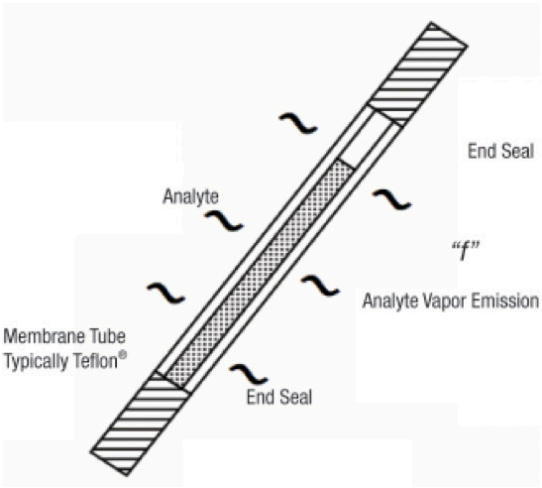

Figure 3.1: Typical permeation tube design (McKinley, 2008)

Photograph 3.1: Actual permeation tube

Photograph 3.1 shows the actual permeation tube purchased from VICI METRONICS. The tube has an outer diameter of 10 mm and a length of 53 mm.

Table 3.2 shows the approximate permeation rates that can be achieved at specific temperatures; however, the rates are not guaranteed since mercury is a volatile substance. The actual permeation rate at a specific temperature can only be determined once the permeation device has reached equilibrium in that specific environment under those operating conditions (Crowe, France, and Lewis, 2013).

Table 3.2: Permeation rates (VICI METRONICS, 2023)

Temperature (℃)	**Permeation rate (ng/min)**
30	15
35	40
40	50
45	65
50	70
60	150
70	250
80	400
90	800
100	1500

3.2.2.2 U- tube design

The U-tube which was manufactured by UKZN Pietermaritzburg Campus Glassworks is illustrated in the Figure 3.2.

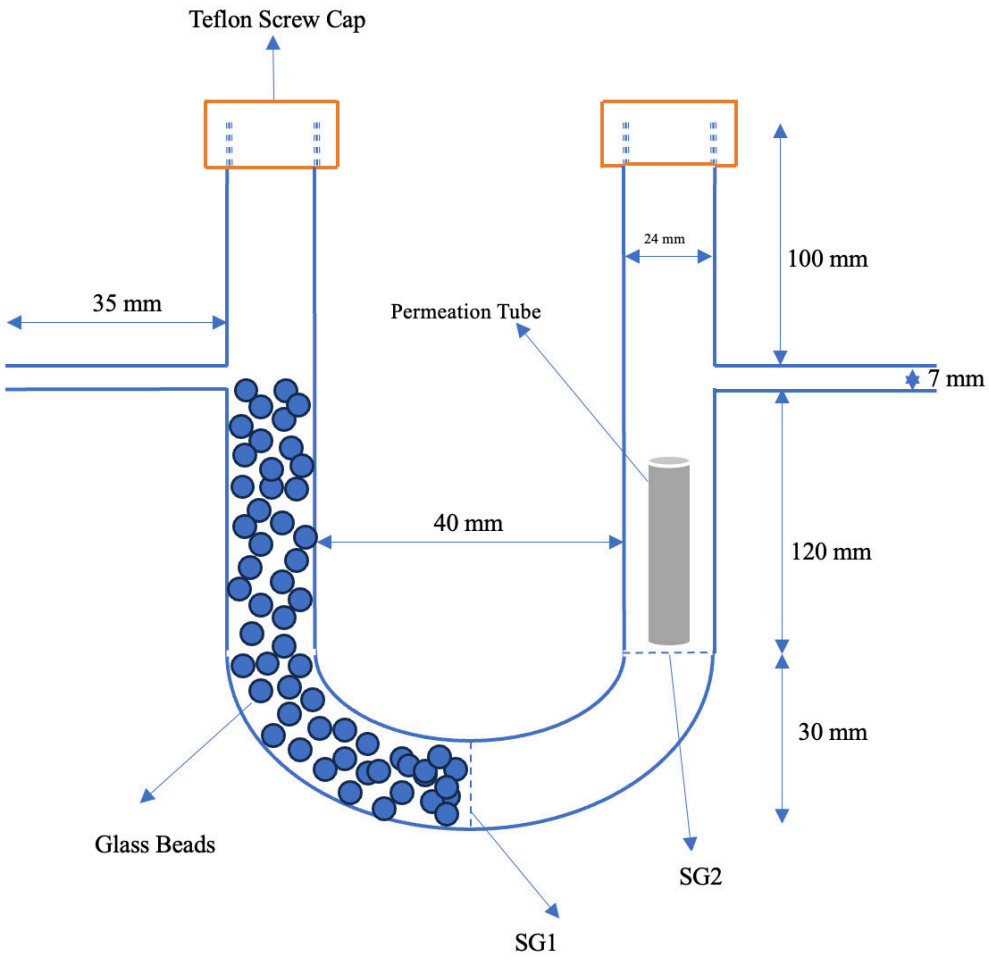

Figure 3.2: Design of the U-tube to hold the mercury permeation tube

The U-tube was designed to fit within a 2-litre glass beaker, which served as an oil bath and was manufactured using borosilicate glass. Borosilicate was used since it can withstand temperatures up to 525°C (Scientific Glass Laboratories, 2022) and has good thermal shock resistance. The tube has two side arms measuring 35 mm, allowing the U-tube to be attached to stainless steel piping via plastic tubing. Inside the tube are two sintered glass rounds, which allow the carrier gas to pass through. The first piece of sintered glass (SG1) also holds glass beads to promote heat transfer to the carrier gas.

The second piece of sintered glass (SG2) holds the permeation tube in position. The inner diameter of the tube was made to measure 24 mm. The U-tube could house the permeation tube successfully since the outer diameter was 10 mm.

The top ends of the tube are closed and have a screw design, with Teflon caps and silicon stoppers. This allows for the easy insertion and removal of the glass beads and permeation tube. The tube was designed to be fully dismantled so that all components could be soaked and cleaned to remove any residual mercury which could affect the permeation rate.

3.2.3. Mercury Adsorption onto Fly Ash or Modified Fly Ash in the Reactor

The reactor is oriented vertically and was designed to fit within a furnace with opening diameters of 24 mm at the top and bottom. It was manufactured using quartz to withstand high temperatures and damage from acidic compounds/substances. Since the reactor was manufactured from quartz, special glass to stainless steel O-ring fittings were purchased to attach the reactor to the stainless-steel tubing. Due to the narrow width and slightly odd size, special plastic (PTFE) connectors were made to cap the reactor ends before the O-ring fittings were attached to ensure proper sealing between the reactor and stainless-steel fittings.

The reactor tube has the following dimensions: an inner diameter of 10 mm, an outer diameter of 13 mm and a wall thickness of 1.95 mm. The special PTFE attachments are shown in Figure 3.3. The attachment dimensions are 13 mm outer diameter for the narrow part, which fits into the stainless-steel O-ring attachment, and 21 mm outer diameter for the larger portion, which caps the glass reactor.

The adsorption column was loaded, as shown in Photograph 3.2. At the base, a small PTFE round was inserted into the column; thereafter, a super fine stainless-steel mesh was placed on top, and glass beads were filled in. On top of the glass beads, another stainless-steel mesh was placed, and the fly ash sample was then loaded into the column using a funnel. Lastly, another stainless-steel mesh was placed before the remaining glass beads were added to the top portion of the column.

Photograph 3.2: Adsorption reactor setup

3.2.4. Method to Determine Mercury Exit Concentration

3.2.4.1. Real-Time Continuous Measurement

a. Lumex RA915+ Measurement Instrument

The exit mercury concentration was measured using the Lumex RA915+ Mercury Analyser. The analyser uses the Zeeman atomic adsorption spectrometry using high-frequency modulation of light polarisation (ZAAS-HFM) (Lumex Instruments Canada, 2015).

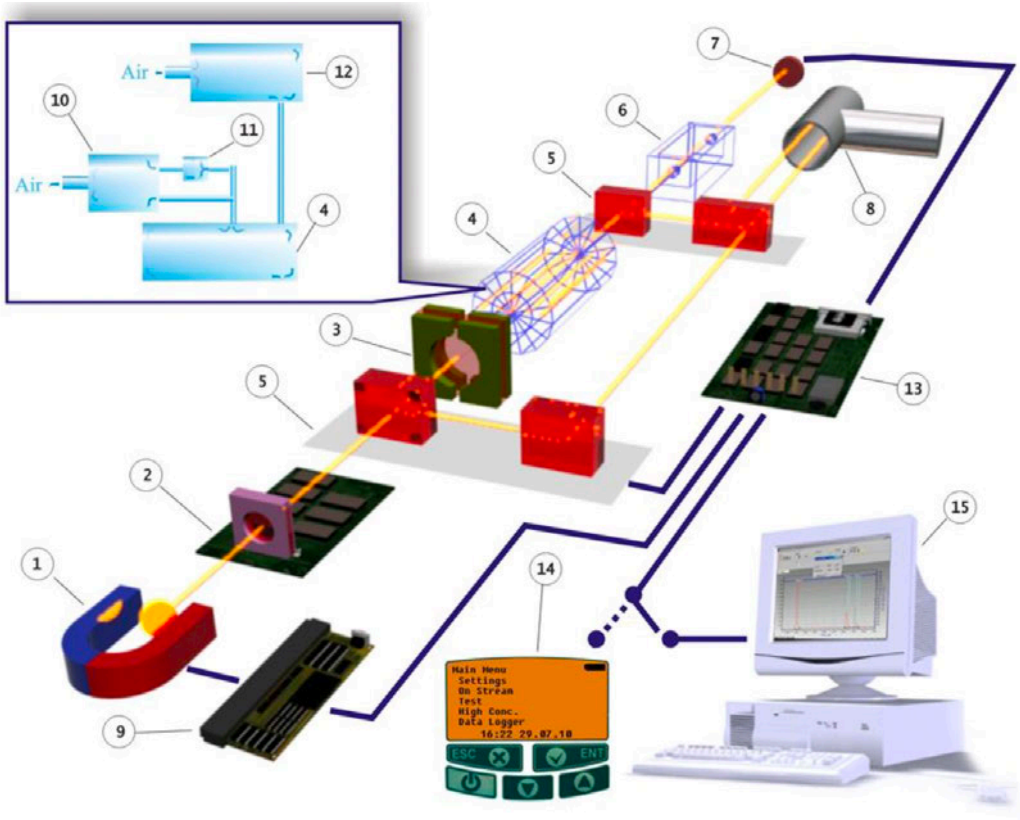

Figure 3.3: Block Diagram of Lumex RA915 mercury analyser

Method of Operation – Adapted from RA915 Operation Manual (Lumex Instruments Canada, 2015)

- Mercury EDL Lamp - situated between magnet poles.
- (9) - High-frequency generator - excites (1).
- (2) - Polarization modulator – allows lights to pass to (5) – Optical bridge – which directs light dependent on which of the three operation modes is selected.
- There are three modes of operation:
    - Multipath Cell - goes through (3) (Test mode), then enters (4) multipath test cell, then (6) single path cell and then (7) photodetector cell.
    - Single Path Cell - light only goes through (6) – (7).
    - External Cell - radiation moves through the removable optical unit of the (8) external analytical cell, then through (6) and (7).
- The photodetector signal arrives at (13) electronic signal processing unit where the signal is separated at modulation frequency to form the analytical signal.
- The information is then displayed on (14) unit display or (15) PC/Laptop.

3.3. Auxiliary Equipment

While the major components of the experimental setup have been discussed in the previous sections, other auxiliary equipment was required to conduct the adsorption experiments successfully.

3.3.1. Gas Cylinder

A gas cylinder was obtained from Air Industrial Gases, and the gas was composed of 14.5% CO_2, 79% N_2 and 6.5% O_2 to simulate a coal flue gas stream.

3.3.2. Flow Controller

Flow control was essential to maintain a constant mercury permeation rate; therefore, an Alicat flow control device was used to maintain the flow rate at 100 ml/min.

3.3.3. Hot Plate with Temperature Controller

The Stuart Hot Plate with Temperature Control (US152) was used to achieve a constant mercury permeation rate by keeping the temperature of the permeation chamber (U-tube) constant. The hot plate heated a 2lt beaker filled with Silicone Oil, which served as the bath to maintain a constant temperature for the permeation tube. A temperature control probe was placed into the silicone oil, and the temperature was set at 65℃. The hotplate also has an inbuilt stirrer function. A magnetic stirrer was placed inside the beaker to agitate the silicone oil to maintain a constant temperature in the entire beaker.

3.3.4 Furnace

A box furnace with an inbuilt temperature probe was used to heat the fly ash to the specific temperature required for the adsorption reaction. The furnace temperature was set at either (150℃ or 200℃).

3.4. Equipment Review

Number	Equipment Description	Number	Equipment Description
1	Gas Cylinder	6	U-tube
2	Regulator	7	Furnace
3	Alicat Flow Controller	8	Modified Fly Ash
4	Oil Bath	9	Reactor
5	Permeation Tube	10	Mercury Analyser

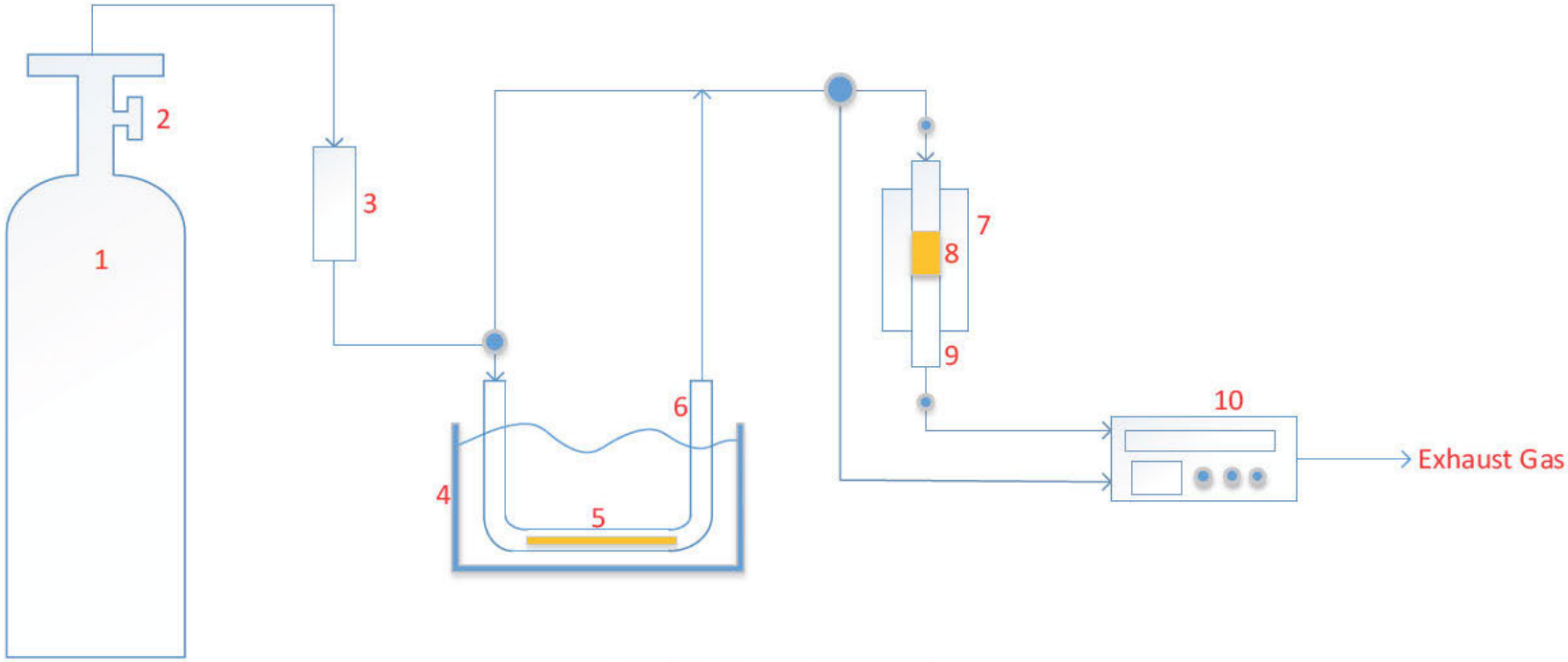

Figure 3.4: Experimental setup

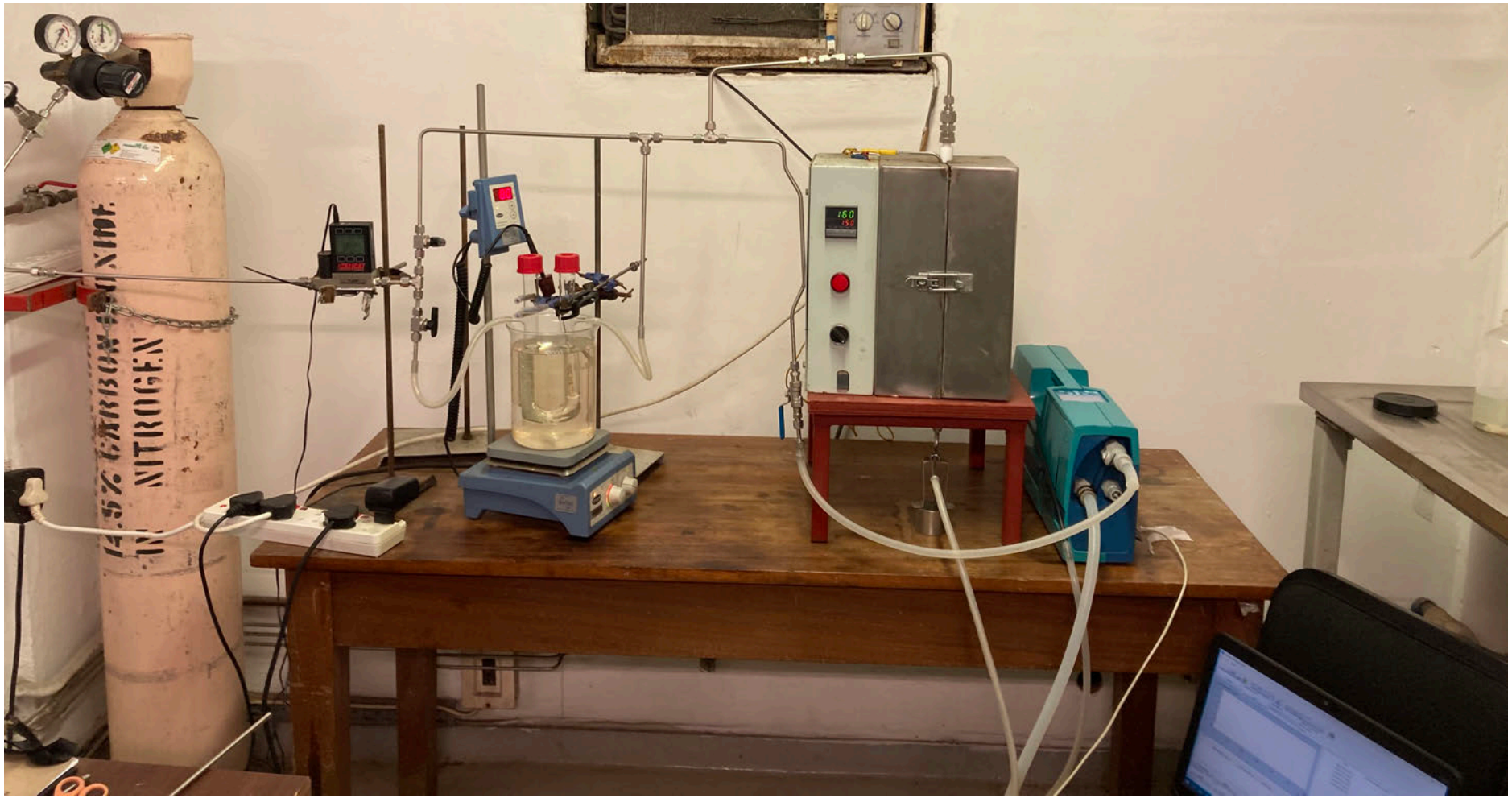

Photograph 3.3: Laboratory setup

3.5. Experimental Procedure

3.5.1. Fly Ash Preparation

Two fly ash samples were obtained from the Eskom's Camden and Majuba Power Stations in Mpumalanga. The samples were labelled as the Dark and Light samples due to their respective colours, as shown in Photographs 3.4 and 3.5.

Photograph 3.4: Dark fly ash sample obtained from Camden power station

Photograph 3.5: Light fly ash sample obtained from Majuba power station

3.5.1.1. Fly Ash Modification

The fly ash samples were modified using metallic salts: $CuSO_4$, $CuCl_2$, $FeCl_3$ and $ZnCl_2$. A 20 wt% solution was prepared by dissolving 50 g metallic salt into 250 ml of deionized water; after that, the dark and light fly ash samples (150 g) were soaked into the solutions for 24 hours at room temperature. The impregnated fly ash was filtered and dried at 90°C for 12 hours. After modification, the physical appearance of the fly ash was altered, and a colour change was observed, as shown in Photographs 3.6 – 3.13.

Photograph 3.6: Light modified with $CuCl_2$

Photograph 3.7: Dark modified with $CuCl_2$

Photograph 3.8: Light modified with $CuSO_4$

Photograph 3.9: Dark modified with $CuSO_4$

Photograph 3.10: Light modified with $ZnCl_2$

Photograph 3.11: Dark modified with $ZnCl_2$

Photograph 3.12: Light modified with $FeCl_3$

Photograph 3.13: Dark modified with $FeCl_3$

3.5.2. Preliminary Preparations

3.5.2.1. Cleaning of Piping and Glassware

All glassware and tubing was soaked overnight in a lab cleaning solution to remove any mercury residue affecting the output mercury concentration. The dish containing labware cleaning solution dissolved in warm water must be placed in a fume hood to prevent accidental inhalation of any mercury fumes that may be emitted during the cleaning process. After 12 hours, the piping and glassware should be removed, rinsed under warm water, and thoroughly dried. This process should be done at least twice a week.

3.5.2.2. Reassembly and Checking for Leaks

Once the glassware and piping have been cleaned and dried, the experimental setup should be reassembled. After reassembly, all the valves should be opened, and the system must be assessed for leaks using the Snoop liquid leak detector. Gas leaks are not favoured as they can lead to erroneous results and pose safety issues regarding emissions of hazardous carrier gas containing mercury vapour. All joints, valves and connection points were rinsed with the Snoop solution to check for bubbles forming, indicating a gas leak. If a gas leak was detected, the nut was tightened, and the joint was resprayed to check if the joint was now sealed off.

3.5.2.3. Switching on Equipment

The hotplate and furnace were switched on and set to temperatures of 65℃ and 150℃/200℃, respectively. Switch on, set up, and connect the laptop to the Lumex RA915 Mercury Analyser. The calibration sequence for the mercury analyser as described in the operation manual (Lumex Instruments Canada, 2015) should be conducted.

3.5.3. Adsorption Test

The adsorption of mercury onto fly ash/modified fly ash was done in a fixed bed quartz column within a box furnace. The furnace has a thermocouple embedded within near the reactor wall to control the temperature (150℃ or 200℃). Carrier gas, which contains 14.5% CO_2, 6.5% O_2 and 79% N_2, enters through an Alicat flow controller at 100 ml/min to maintain a constant flowrate. The gas then passes through a valve into the permeation chamber as seen in Figure 3.7, initially the gas in sent via the bypass to the mercury analyser until a stable concentration of 300 ng/m^3 is reached. Once the initial concentration is stable the reactor bypass valve is closed and the valve to the reactor is opened to allow the gas to enter the adsorption column. The exit gas then flows to the mercury analyser where the data is captured for further analysis.

3.5.3.1. Adsorption Tests at 200℃

The adsorption capacity of fly ash and modified fly samples were conducted at 200℃ and three runs were conducted on each sample namely:

Dark	Light
modified dark-$CuSO_4$	modified light-$CuSO_4$
modified dark-$ZnCl_2$	modified light-$ZnCl_2$
modified dark-$FeCl_3$	modified light-$FeCl_3$
modified dark-$CuCl_2$	modified light-$CuCl_2$

3.5.3.2. Adsorption Tests at 150℃

The tests done at 150℃ were conducted on the following two samples:

- modified dark-CuSO4
- modified light-$CuSO_4$

Chapter 4
Results

4.1. FESEM/EDX Analysis of Fly Ash

The dark and light fly ash samples were analysed by assessing different areas of the sample. The 'areas' mentioned throughout the following sections refer to different areas of the sample. The selection of these areas was done randomly multiple times to better characterise the fly ash samples.

4.1.1. Dark Fly Ash Sample Characterisation

Figure 4.1, obtained by FESEM, shows the morphology of dark fly ash area 1. The surface contains well-defined solid spherical particles of different sizes and irregularly shaped bands of particles. Figure 4.3 shows the morphology of dark fly ash area 2, where the image is magnified 3X. The surface has large, solid, well-defined spherical particles and some irregularly shaped solid particles. Figures 4.1 and 4.3 indicate the presence of cenospheres (microspheres with an outer shell and hollow inner usually made of silica or alumina). However, no plerospheres (spheres within spheres) are visible on the FESEM image.

Figure 4.5 shows the surface of dark fly ash area 3 at 5X magnification. The images in Figures 4.1 and 4.3 show that the surface looks smooth, whilst Figure 4.5 shows that the surface is rough with glass-like shards present. This is consistent with the characteristics of ferrospheres (spheres composed of thin dendrites of Fe-spinellides and ferrosilicate glass) present in the sample.

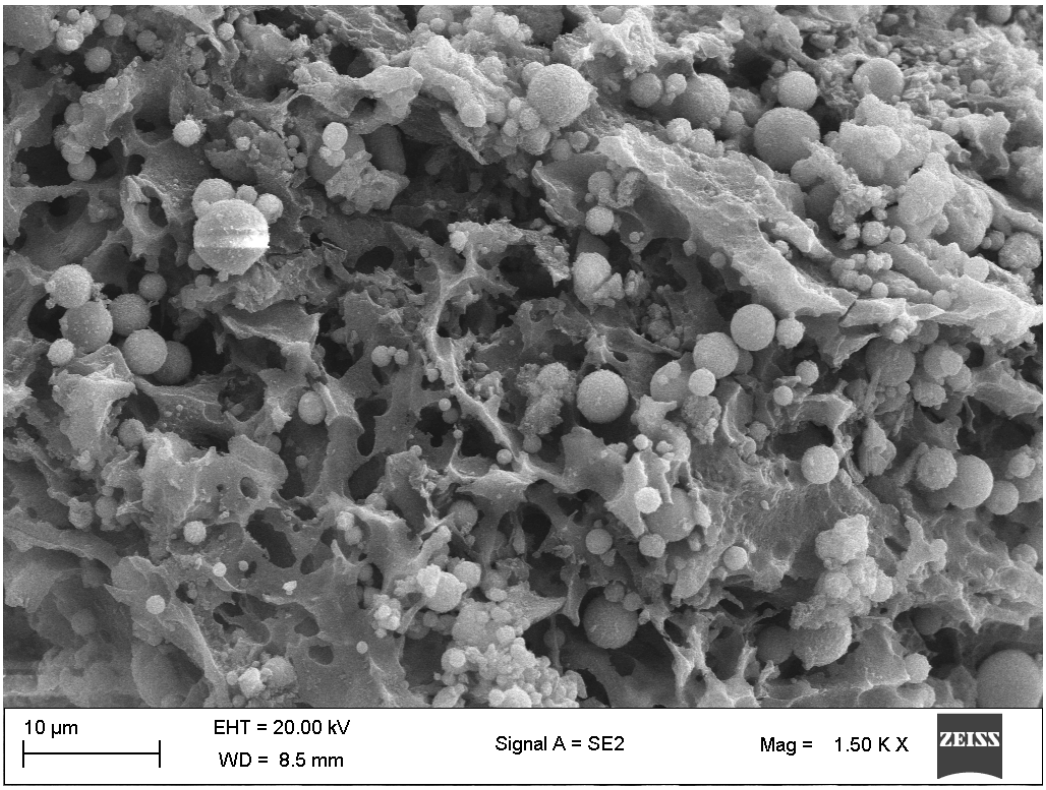

Figure 4.1: FESEM image of dark fly ash area 1 at 1.5X magnification

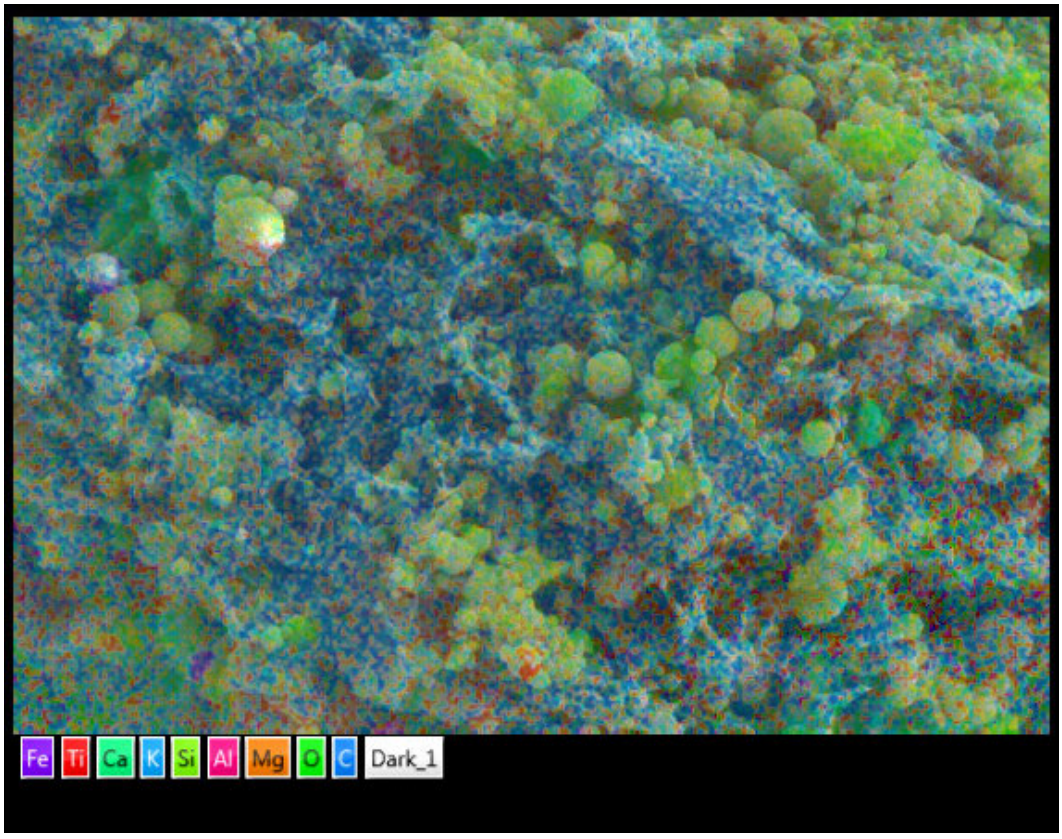

Figure 4.2: EDX composite elemental mapping of dark fly ash area 1

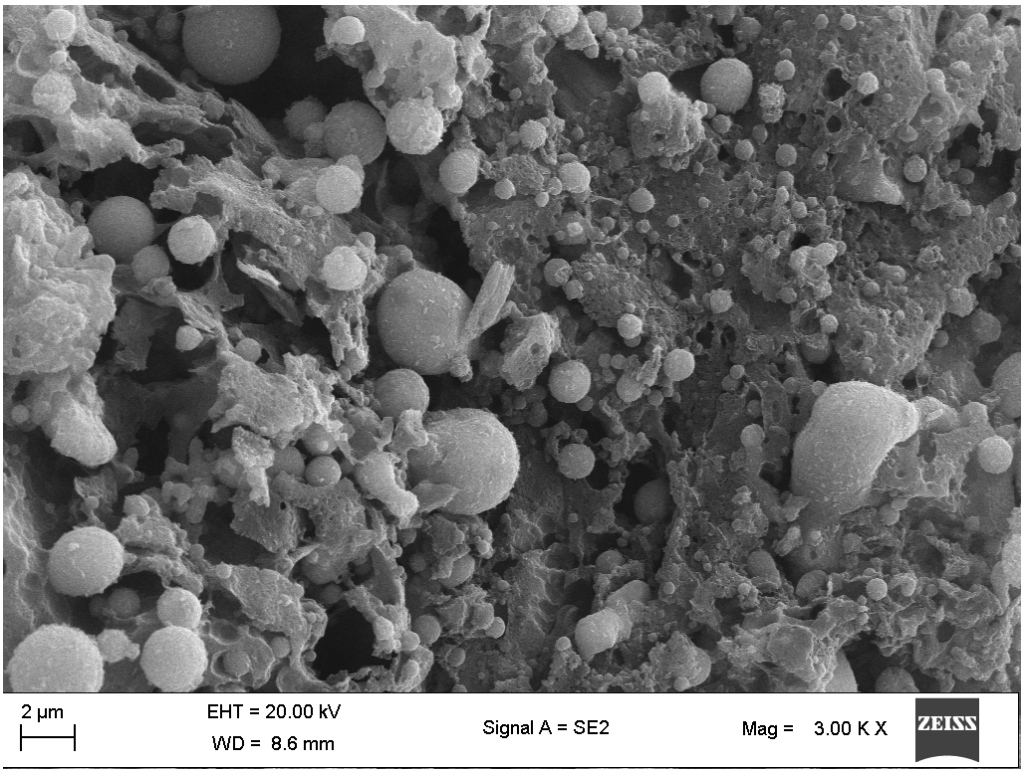

Figure 4.3: FESEM image of dark fly ash area 2 at 3.00X magnification

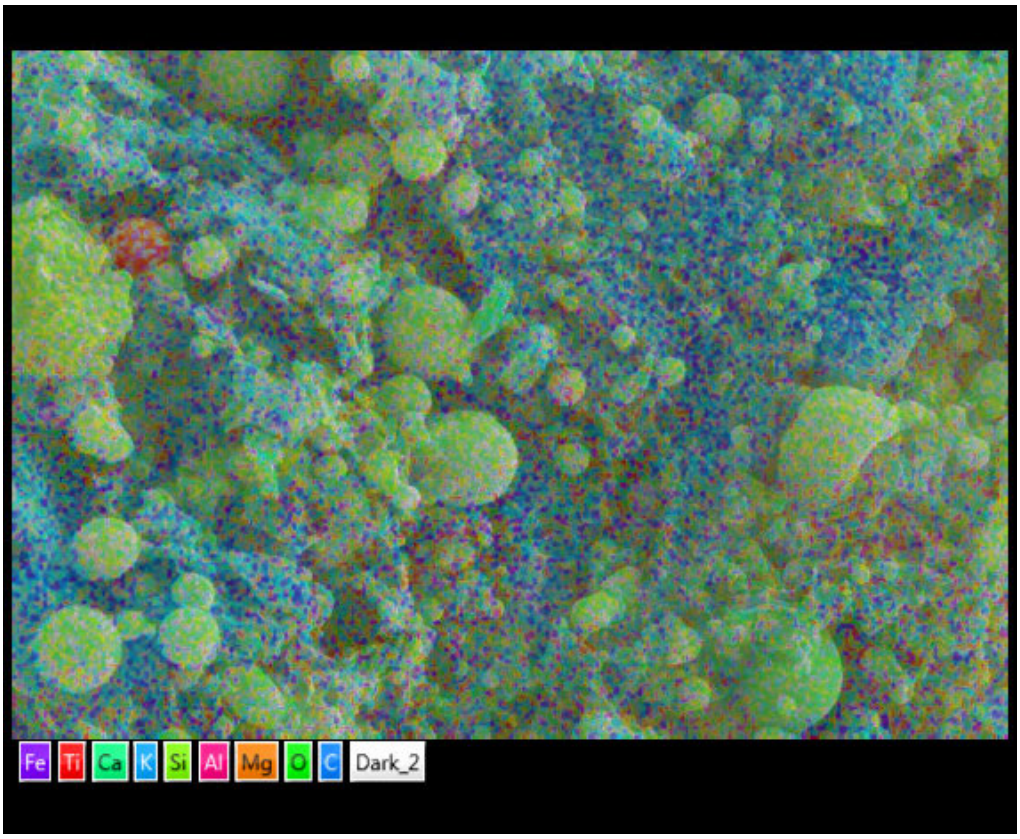

Figure 4.4: EDX composite elemental mapping of dark fly ash area 2

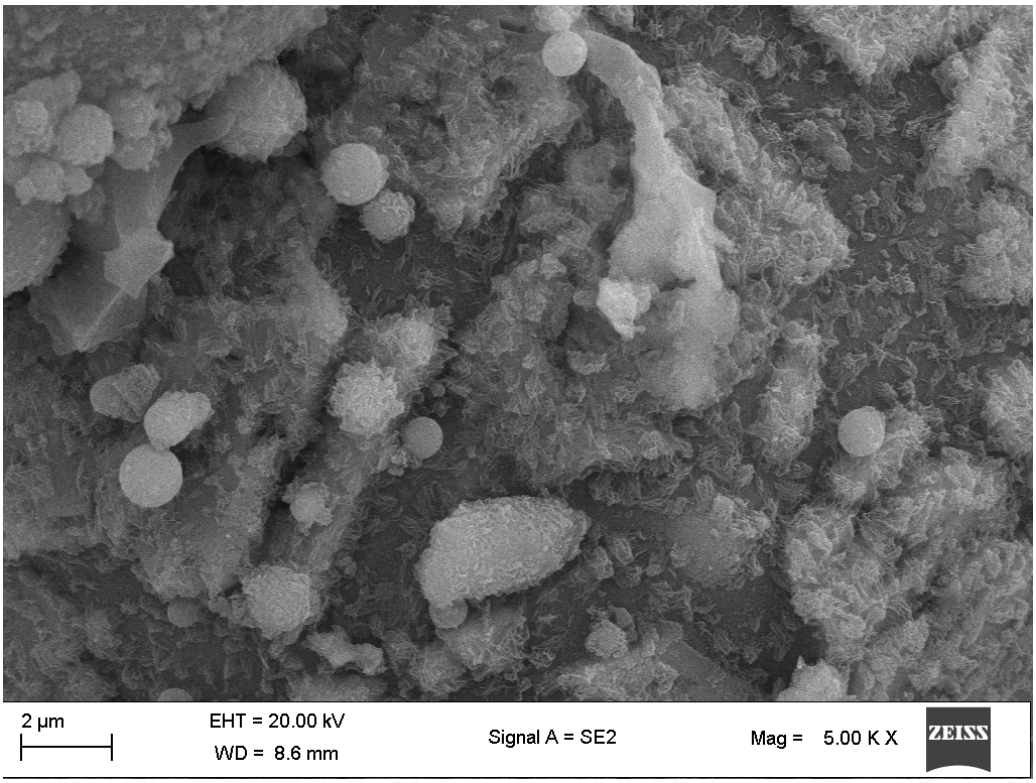

Figure 4.5: FESEM image of dark fly ash area 3 at 5.00X magnification

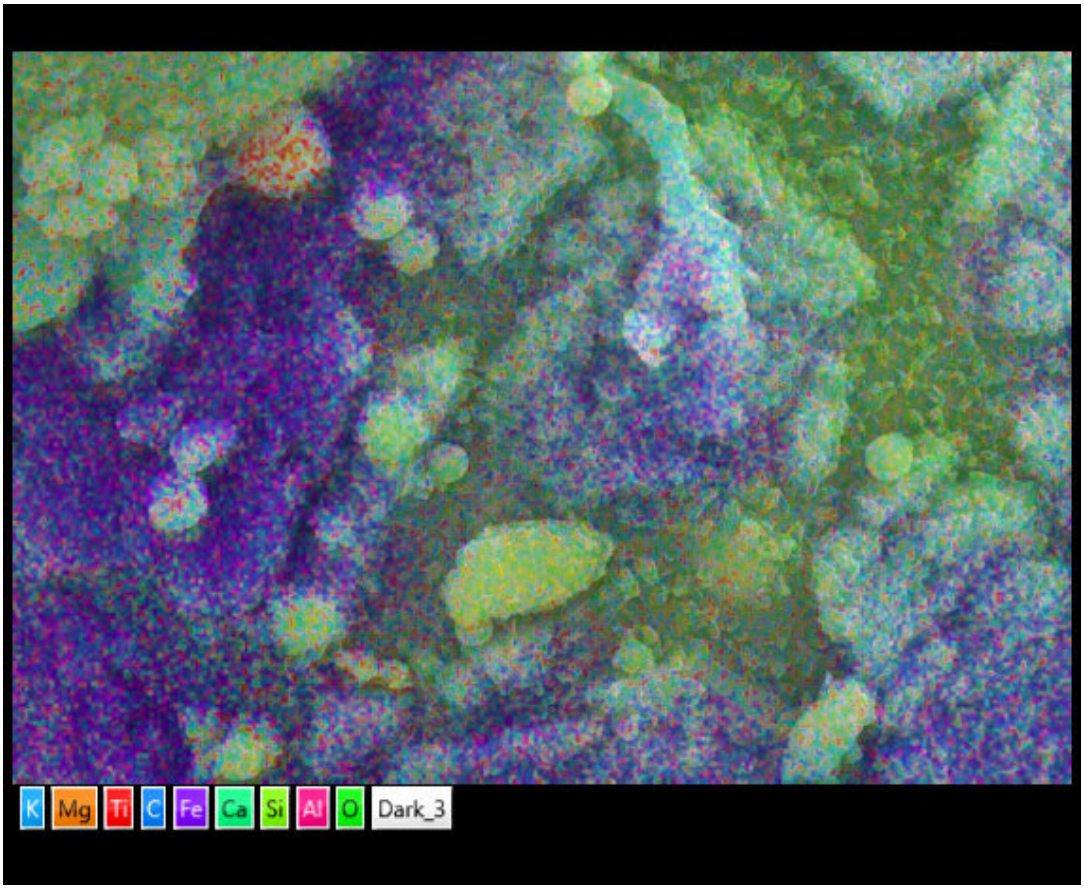

Figure 4.6: EDX composite elemental mapping of dark fly ash area 3

EDX elemental mapping indicated that the following elements are present in the dark fly ash sample: Fe, Ti, Ca, K, Si, Al, Mg, O and C. Figures 4.2, 4.4, and 4.6 show the composite of the elemental dispersion in the selected analysis area. The dispersion images can be seen in Appendix A. These images indicate how the elements are distributed in the selected analysis area.

Figure 4.2, a composite of the elemental maps, indicates the presence of large amounts of O (depicted as green spherical particles) and C (irregular blue bands). Si and Al are also dispersed throughout dark fly ash area 1.

Figure 4.4, which displays the composite elemental map for dark fly ash area 2, again shows the presence of O (green spherical particles) and C (blue irregularly shaped bands). Al and Si are also present in significant amounts compared to other elements.

Figure 4.6, displaying the elemental map for dark ash 3, differs significantly from the previous two maps. A significant amount of Fe is attached to an O particle with Si and Al dispersed throughout the area. C is also present but only as a tiny band on the top right of the image.

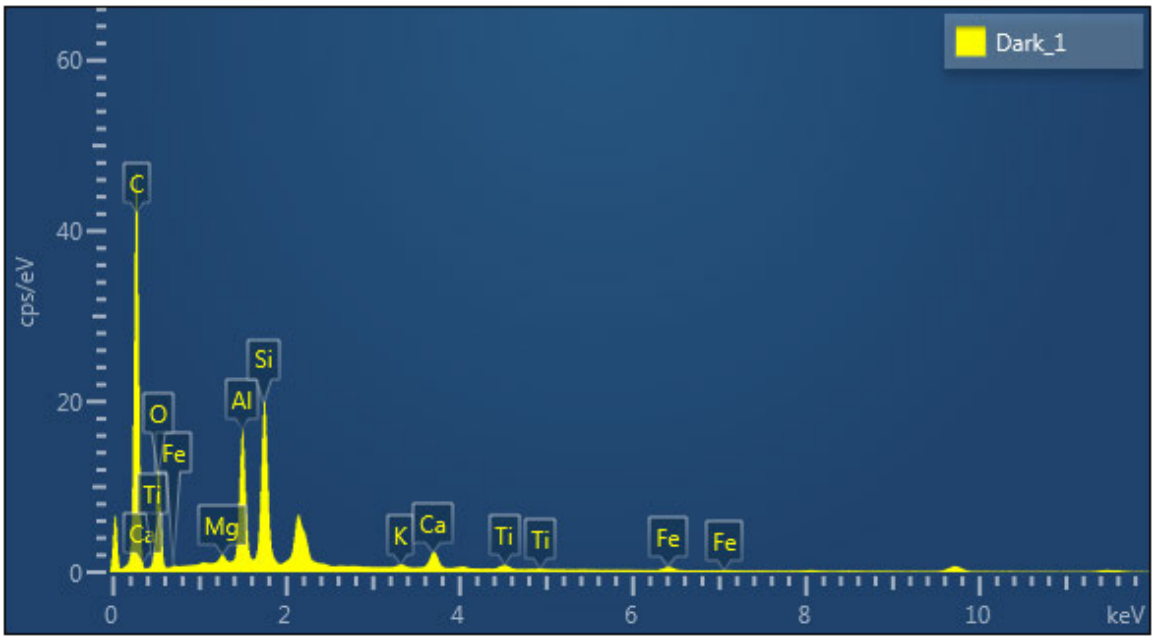

Figure 4.7: EDX spectrum for dark fly ash area 1

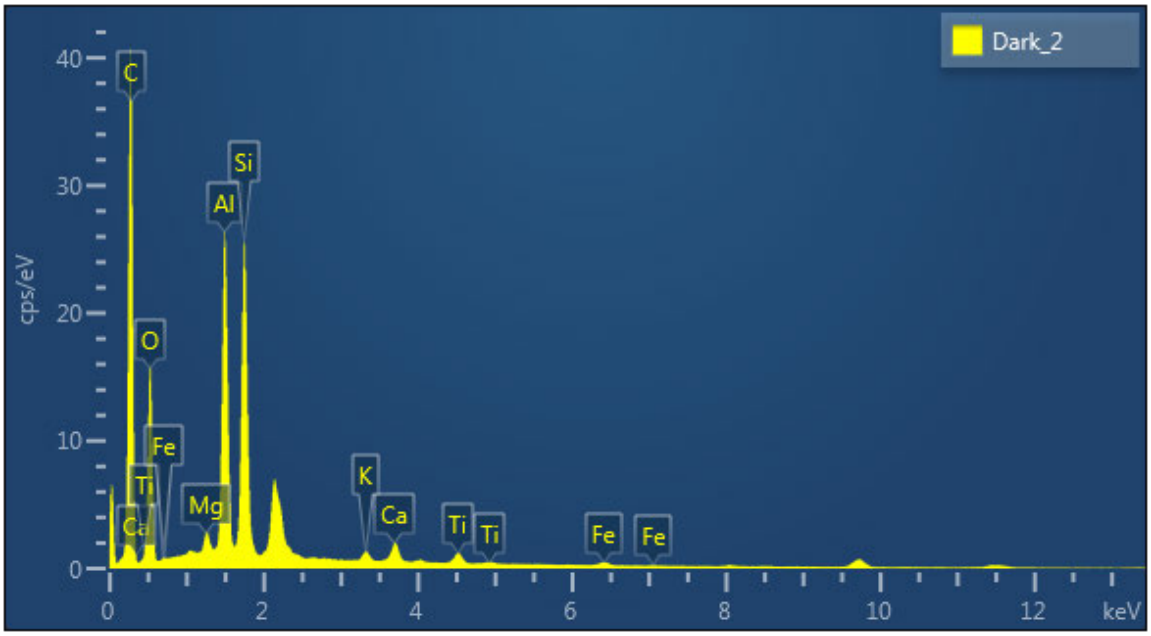

Figure 4.8: EDX spectrum for dark fly ash area 2

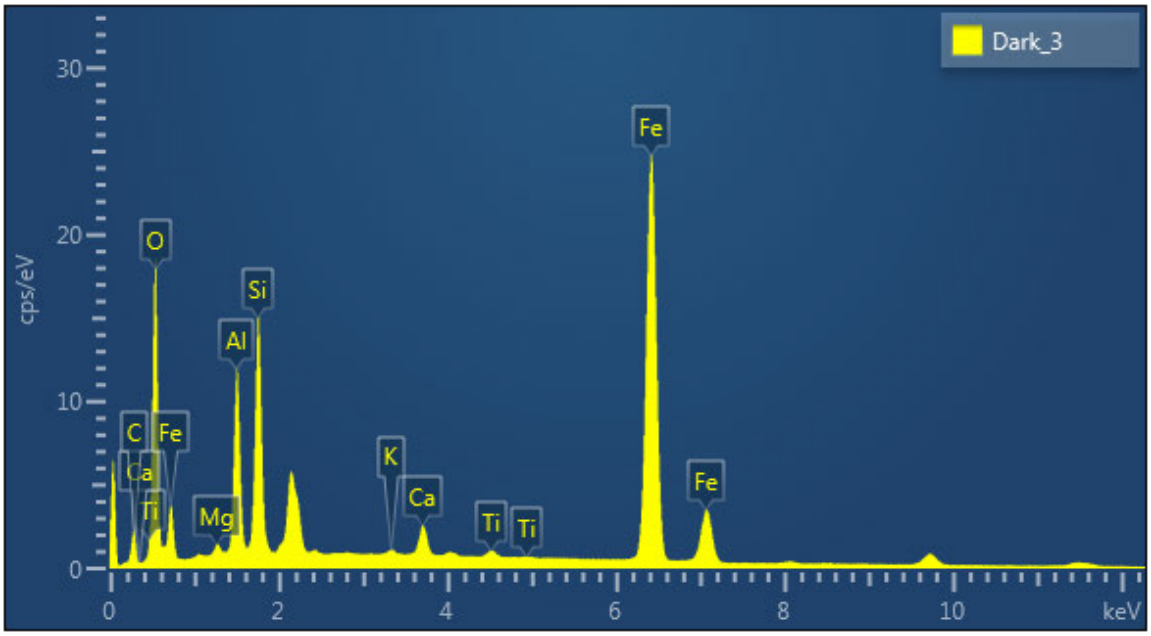

Figure 4.9: EDX spectrum for dark fly ash area 3

Figures 4.7, 4.8 and 4.9 show the spectra for dark fly ash areas 1, 2 and 3, respectively. The peak intensity for C, O, Si, Al, and Fe are the highest, which shows that the concentration of these elements is highest for the dark fly ash sample. Table 4.1 shows the weight percentage of each element in the dark sample.

Table 4.1: Elemental weight percent for dark fly ash sample

Area	Wt %								
	C	O	Mg	Al	Si	K	Ca	Ti	Fe
1	67.22	23.04	0.24	3.51	4.26	0.13	0.82	0.29	0.49
2	61.81	25.99	0.37	5.19	5.11	0.25	0.55	0.45	0.27
3	10.89	25.16	0.47	6.51	7.52	0.16	1.26	0.38	47.66

4.1.2. Light Fly Ash Characterisation

Figure 4.10, obtained by FESEM, shows the morphology of light fly ash area 1. The surface contains well-defined solid spherical particles of different sizes and irregularly shaped bands of particles. Figure 4.12 shows the morphology of light fly ash area 2, where the image is magnified 1.5X. The surface has large, solid, well-defined spherical particles, irregularly shaped solid particles, and some very large, elongated particles. Figures 4.10 and 4.12 have cenospheres present but no plerospheres visible on the FESEM image.

Figure 4.14 shows the surface of light fly ash area 3 at 2.5X magnification. The images in Figures 4.10 and 4.14 also show particles that are rough with glass-like shards present. These particles are characteristically defined as ferrospheres.

Figure 4.11, a composite of the elemental maps, indicates the presence of significant amounts of O (depicted as green spherical particles), C (irregular blue bands) and Fe (patches of purple). Si and Al are also dispersed throughout light fly ash area 1.

Figure 4.13, which displays the composite elemental map for light fly ash area 2, again shows the presence of O (green spherical particles), C (irregularly blue bands), and Fe (patches of purple). Al and Si are also present in significant amounts compared to other elements.

Figure 4.15 displays the elemental map for light fly ash 3, which differs from the previous two maps. A significant amount of Fe is attached to an O particle with Si and Al dispersed throughout the area. C is also present in a few small areas within the analysed area.

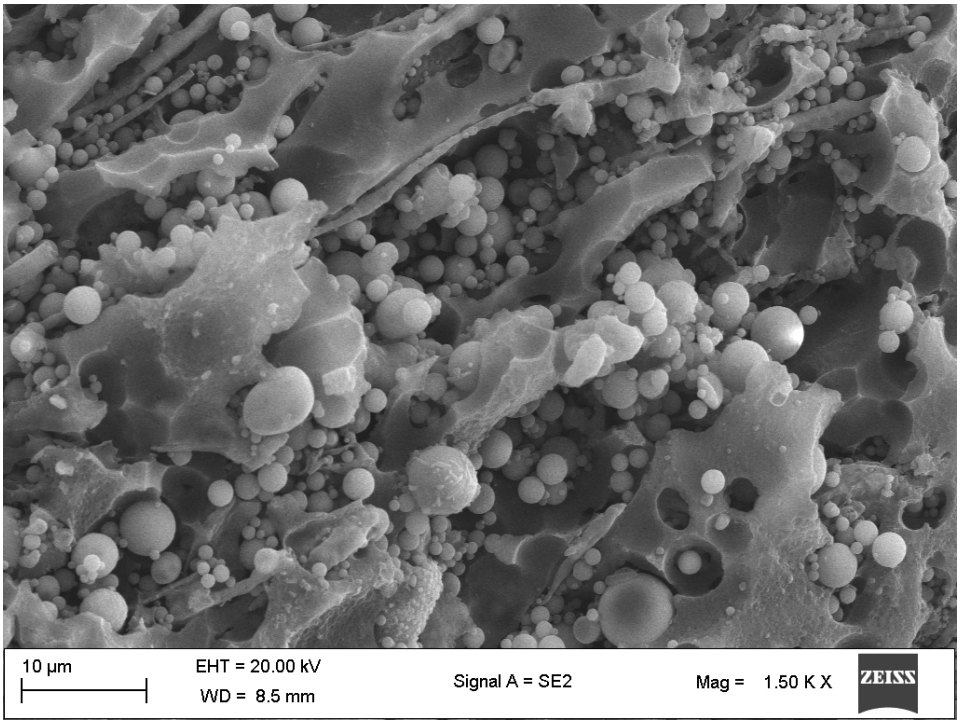

Figure 4.10: FESEM image of light fly ash area 1 at 1.5X magnification

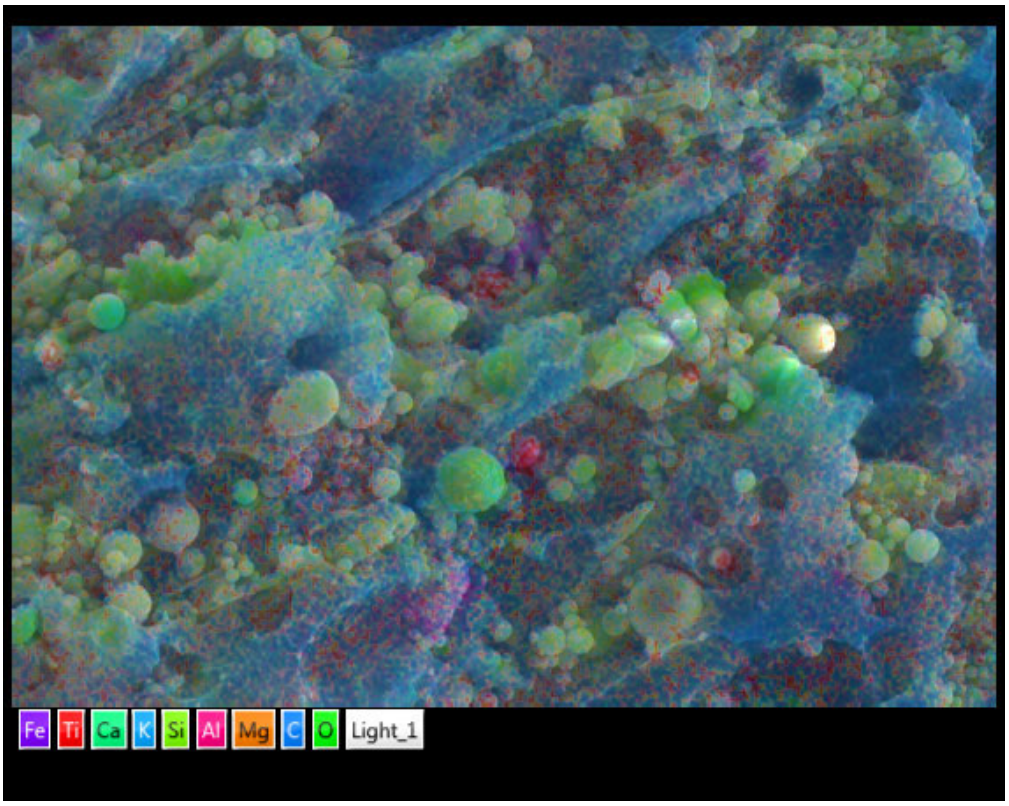

Figure 4.11: EDX composite elemental mapping of light fly ash area 1

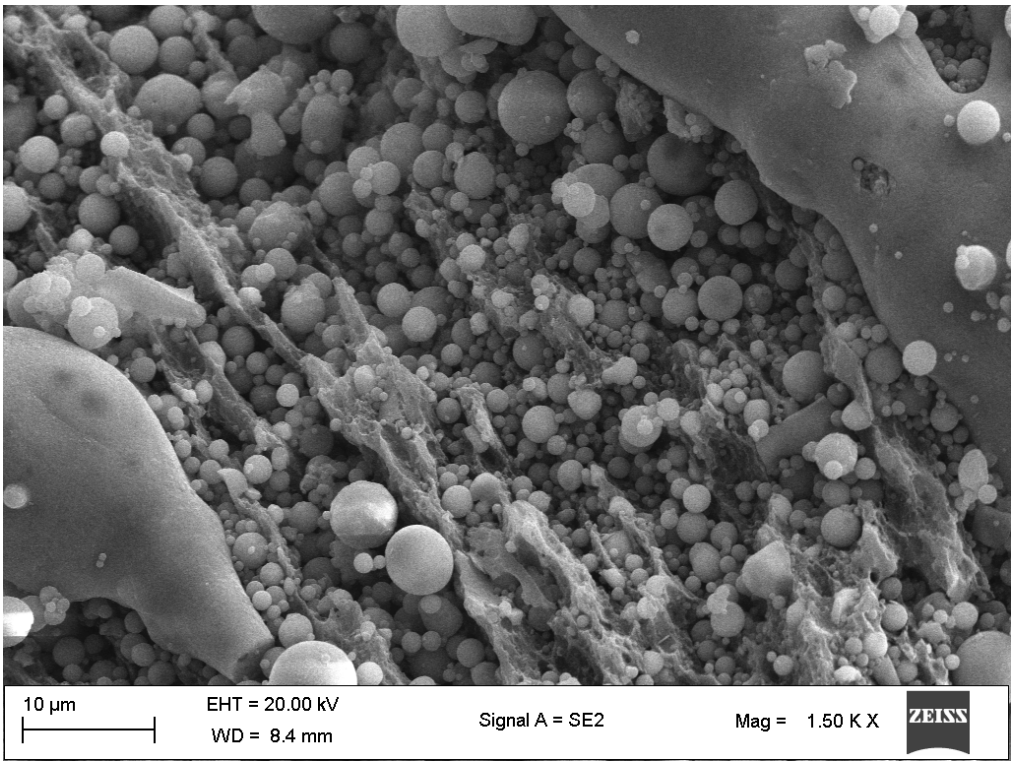

Figure 4.12: FESEM image of light fly ash area 2 at 1.5X magnification

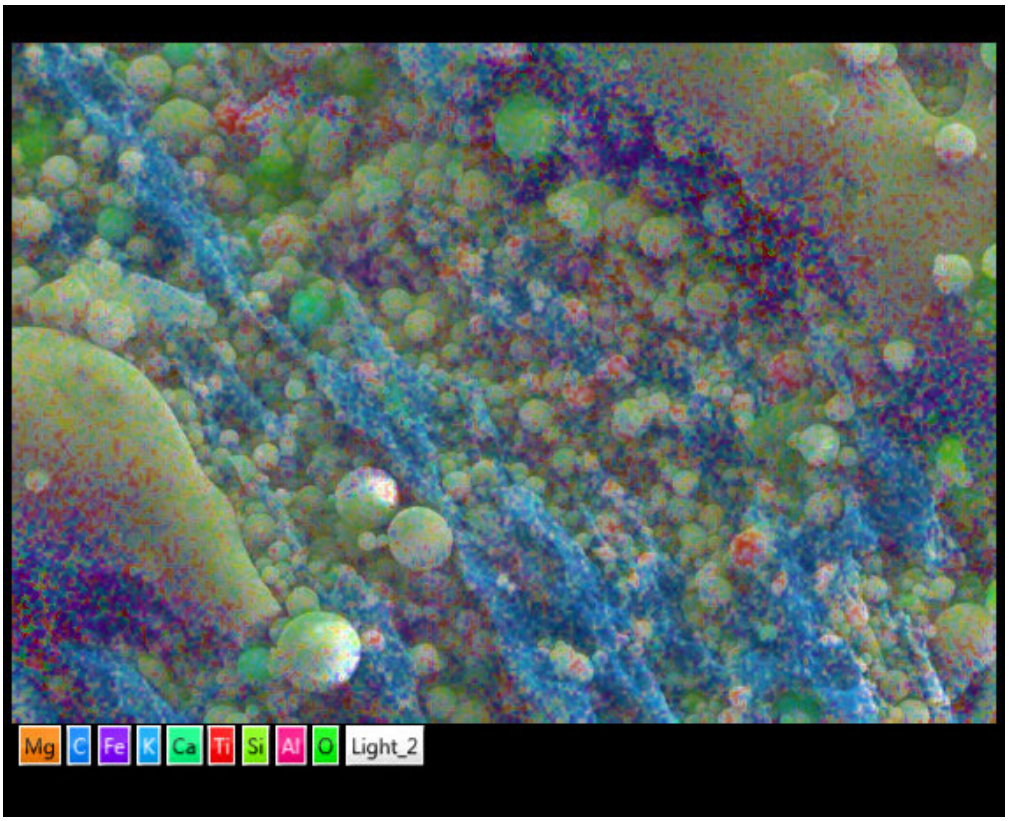

Figure 4.13: EDX composite elemental mapping of light fly ash area 2

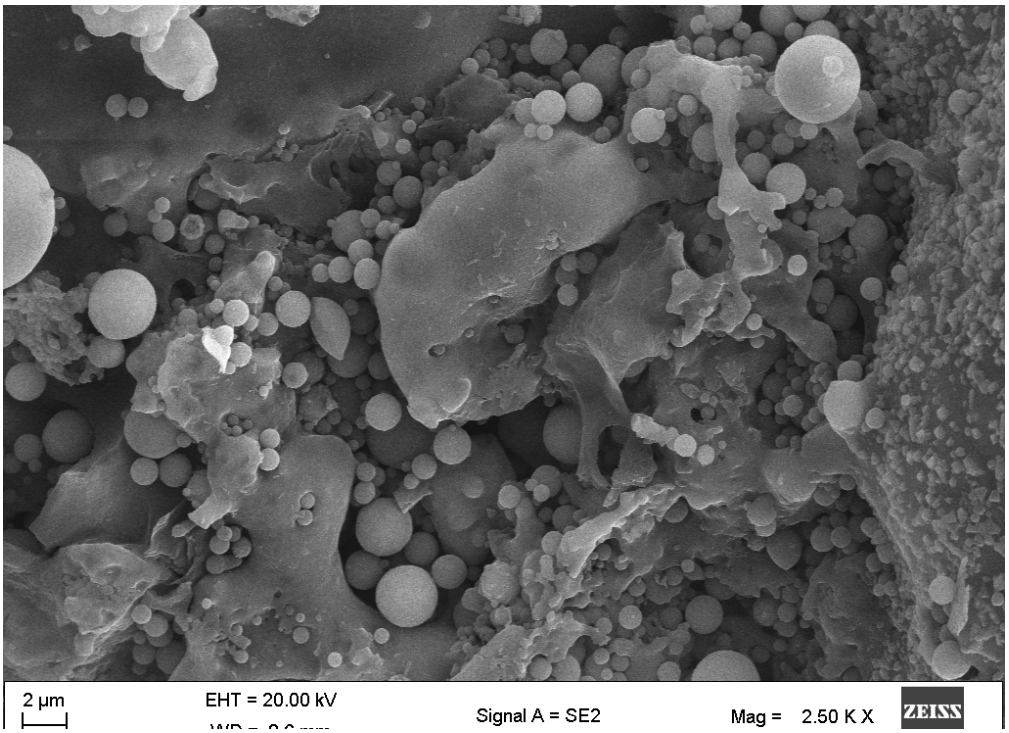

Figure 4.14: FESEM image of light fly ash area 1 at 2.5X magnification

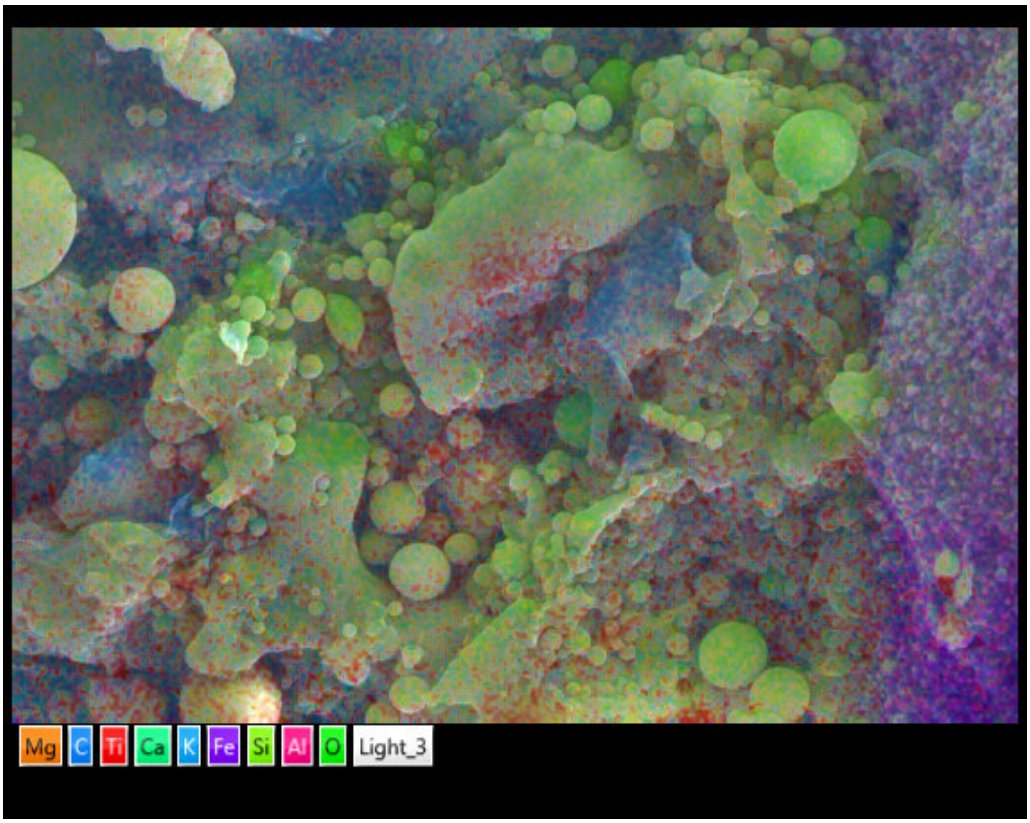

Figure 4.15: EDX composite elemental mapping of light fly ash area 3

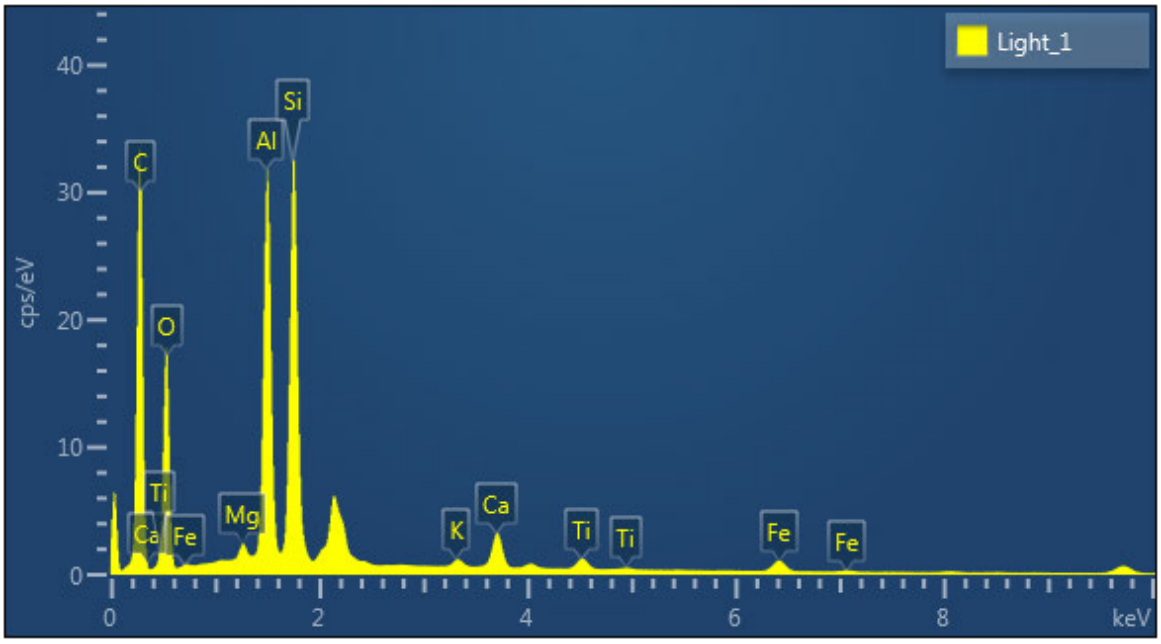

Figure 4.16: EDX spectrum for light fly ash area 1

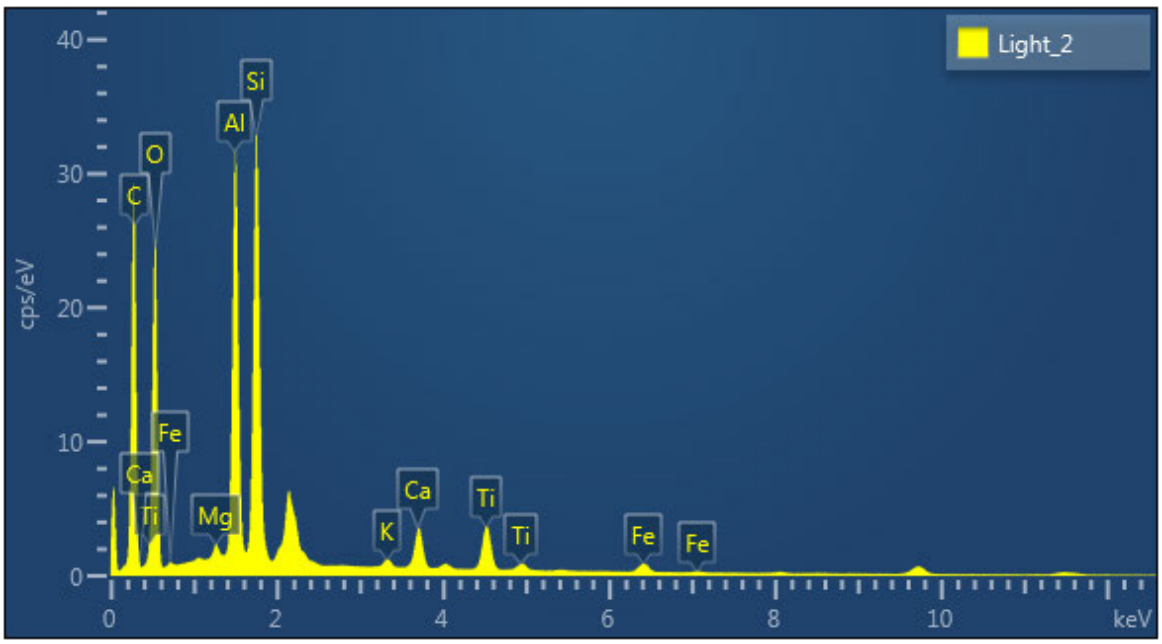

Figure 4.17: EDX spectrum for light fly ash area 2

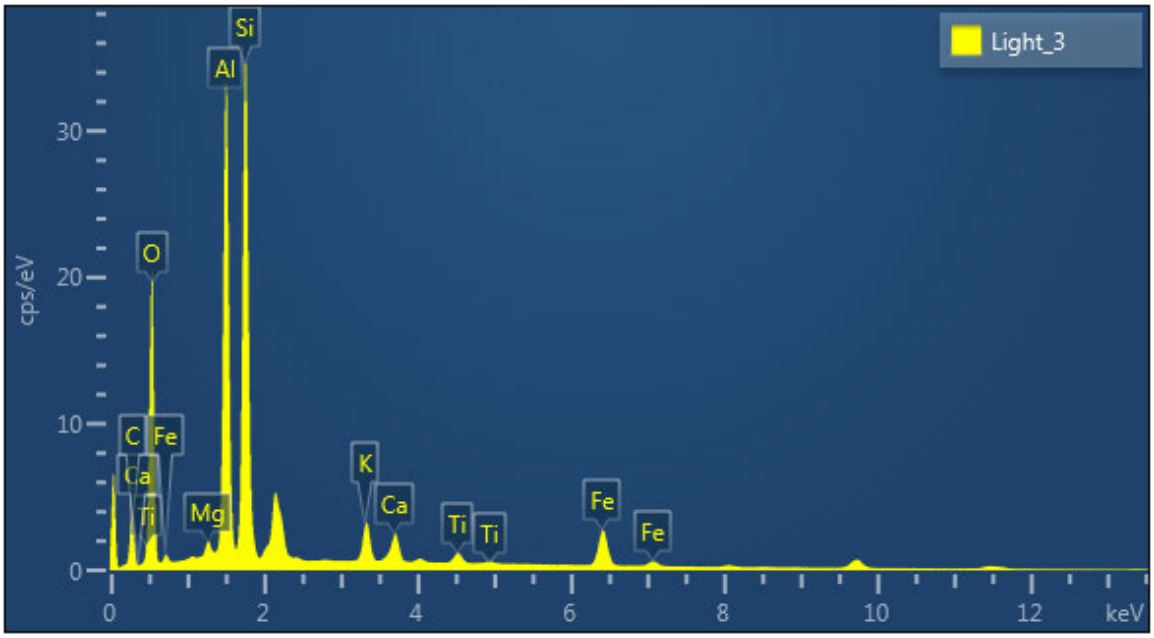

Figure 4.18: EDX spectrum for light fly ash area 3

Figures 4.16, 4.17 and 4.18 show the spectra for light fly ash areas 1, 2 and 3, respectively. The peak intensity for C, O, Si, Al, and Fe are the highest, which shows that the concentration of these elements is highest for the light fly ash sample. The intensity of the Si and Al peaks are similar for light fly ash areas 1, 2 and 3.

Table 4.2 shows the weight percentages of the elements in the light fly ash sample.

Table 4.2: Elemental weight percent for light fly ash sample

Area	Wt %								
	C	**O**	**Mg**	**Al**	**Si**	**K**	**Ca**	**Ti**	**Fe**
1	57.26	27.14	0.27	6.17	6.58	0.19	1.03	0.46	0.91
2	49.62	33.86	0.23	6.07	6.49	0.19	1.09	1.77	0.66
3	22.57	39.82	0.45	13.11	15.23	1.78	1.41	0.72	4.91

Fly ash comprises compounds such as C, SiO_2, Al_2O_3, Fe_2O_3, CaO, TiO_2, K_2O and others (Xu et. al., 2012). The presence of unburned carbon, Fe_2O_3, SiO_2 and Al_2O_3 positively influences the adsorption of mercury (Wang et al., 2015). The above results from EDX analysis show that C, Fe, Si and Al are present in significant quantities for the dark and light fly ash samples. The fly ash's porous structure containing unburned carbon enhances mercury adsorption and oxidation. The presence of O from the metallic oxides promotes the mercury adsorption reaction.

The FESEM images also show the structure of the fly ash, which contains cenospheres and ferrospheres, which are beneficial for mercury adsorption. Yang et al. (2017) investigated the capacity of magnetospheres/ferrospheres from fly ash on mercury adsorption. Whilst temperature influenced the reaction, the Hg^0 removal capacity increased with increasing Fe content. The addition of HF (hydrogen fluoride) has the ability to remove the glass shards on the ferrosphere to expose the active Fe for Hg^0 adsorption. The capacity for Hg^0 adsorption increased with the increase in available Fe active sites for adsorption. Since both the dark and light ash samples are rich in these elements, both fly ashes were tested during the adsorption reaction.

4.2. pH Measurements

Figure 4.19 shows the calibration curve for the prepared standard buffers of pH 4, pH 7 and pH 10. The best fit straight line gives an R^2 value equal to one, which indicates that the measured data perfectly fits the modelled data.

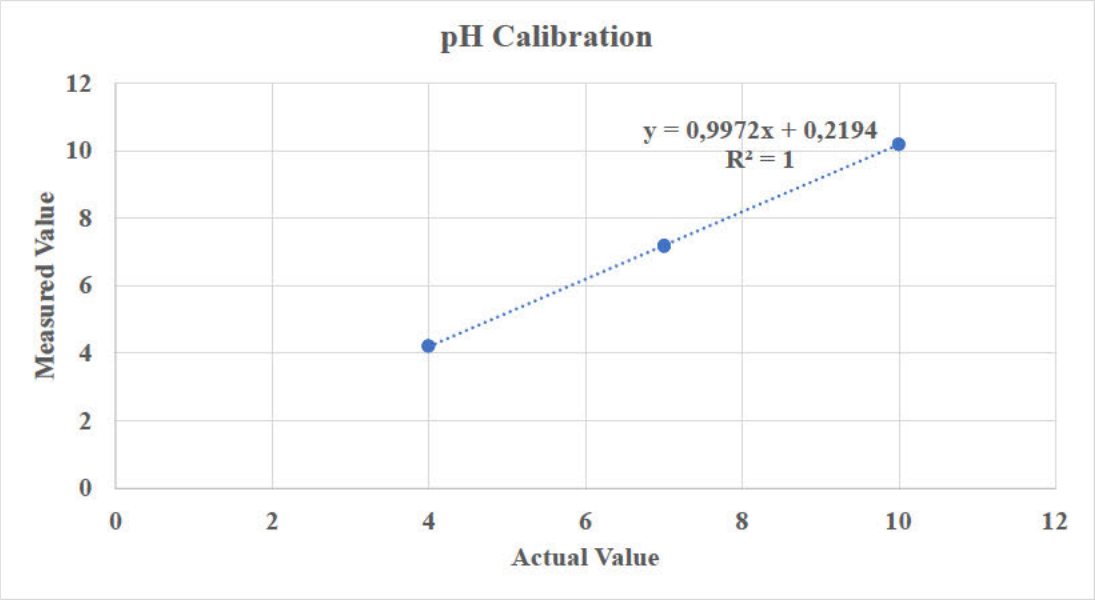

Figure 4.19: Calibration graph for pH 212 Microprocessor pH meter

pH indicates whether a substance is an acid or a base. The range of 0 – 7 indicates an acid, 8 – 14 indicates a base, whilst a reading of 7 is neutral (Water Science School, 2019). A substance with more H+ ions is acidic, while a substance with more OH- ions is basic. Fly ash can be classified as either acidic (pH 1.2 – pH 7), mildly alkaline (pH 8 – pH 9) or strongly alkaline (pH 11 – pH 13) (Bhatt et al., 2019). The pH was measured for dark fly ash and light fly ash samples, as shown in Figures 4.20 and 4.21, respectively. The average pH for the dark fly was 8.62, whilst the light fly ash pH was 10.35. The dark fly ash sample can then be classified as mildly alkaline, whilst the light fly ash sample can be classified as having mild-strong alkalinity.

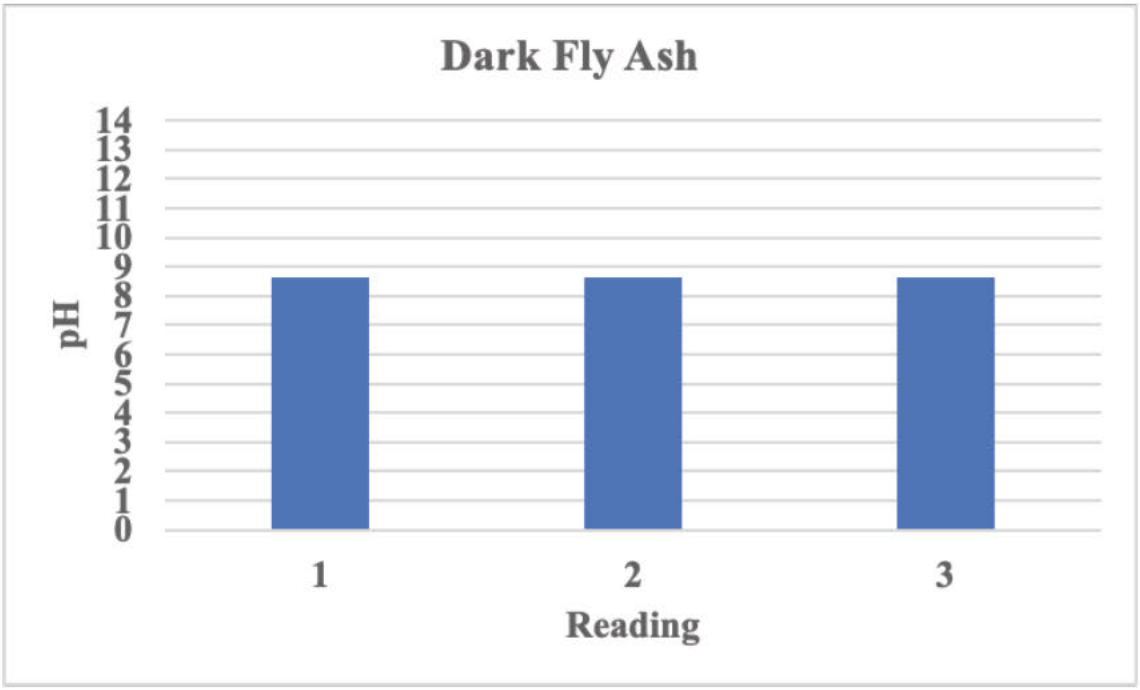

Figure 4.20: pH measurement for dark fly ash

Figure 4.21: pH measurement for light fly ash

4.3. Adsorption Tests

The adsorption tests were conducted to assess the performance of the fly ash and modified fly ash samples. Two fly ash samples obtained from Majuba and Camden power stations were modified using metallic salts such as $CuCl_2$, $FeCl_3$, $ZnCl_2$ and $CuSO_4$ to determine the effect of the modification on the fly ash's adsorption capacity. The adsorption tests were also used to assess the differences/similarities in the performance of fly ash samples from different power stations. The fly ash samples were modified using a 20 wt% solution of the metallic salts. Adsorption tests were undertaken at temperatures of 150°C and 200°C. The temperatures of 150°C and 200°C were selected based on experimental results obtained by Xu et al. (2012) and Gu et al. (2015). Experiments conducted by Xu et al. (2012) showed that mercury adsorption was greatest at 150°C whilst results obtained by Gu et al. (2015) showed that a temperature range of 150°C - 200°C encouraged mercury oxidation.

The efficiency curves were determined using the formula (Xu et al., 2012):

$$\eta = \left(\frac{C_0 - C}{C_0}\right) \times 100$$

where C_0 is the initial concentration (ng/m^3)

C is the concentration at time (t) (ng/m^3)

The dark and light fly ash samples (obtained from different power stations) were tested since the characterisation by FESEM/EDX showed that both samples had similar morphology and chemical composition. The pH values obtained for the dark and light fly ash samples also show that both are alkaline.

4.3.1 Adsorption Tests for Dark Fly Ash and Modified Dark Fly Ash Samples at 200°C.

The adsorption tests were conducted at 200°C, with a carrier gas flowrate of 100 sccm and a mercury permeation rate of 300 ng/m^3. Three experimental runs were performed for each sample. David et al. (2007) indicates that the amount of CO_2 in the flue gas generated by coal-fired power stations can range from between 3% – 15% and that a typical flue gas composition can be 13% CO_2, 5% O_2 and 82% N_2.

Using those values, the carrier gas composition for the adsorption tests was set to contain 79% N_2, 14.5% CO_2 and 6% O_2 to simulate the composition of the flue gas stream from a coal-fired power station. Concentration readings were set to be taken every 15 s on the Lumex RA 915 Mercury Analyser.

Figure 4.22 – figure 4.24 shows the adsorption curves for the dark fly ash sample; the adsorption process is quick, as seen by the gradient of the adsorption curve. It takes 3 – 3.5 minutes for the concentration to drop to 0 ng/m^3 from an initial 300 ng/m^3 concentration. While the time taken to drop to 0 ng/m^3 varies between 3.08 and 3.66 mins, the trajectory of the adsorption curve is the same for each of the experimental runs conducted. The quick reduction in the mercury concentration could be consistent with the physisorption mechanism.

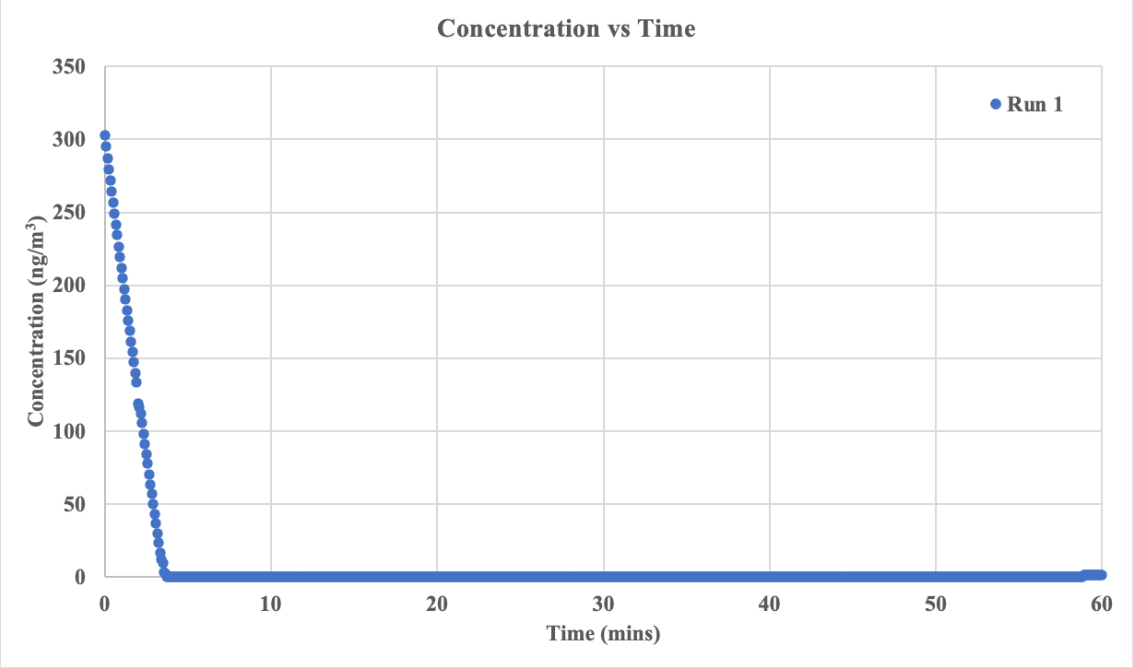

Figure 4.22: Run 1 of Hg adsorption curve at 200℃ for dark fly ash sample

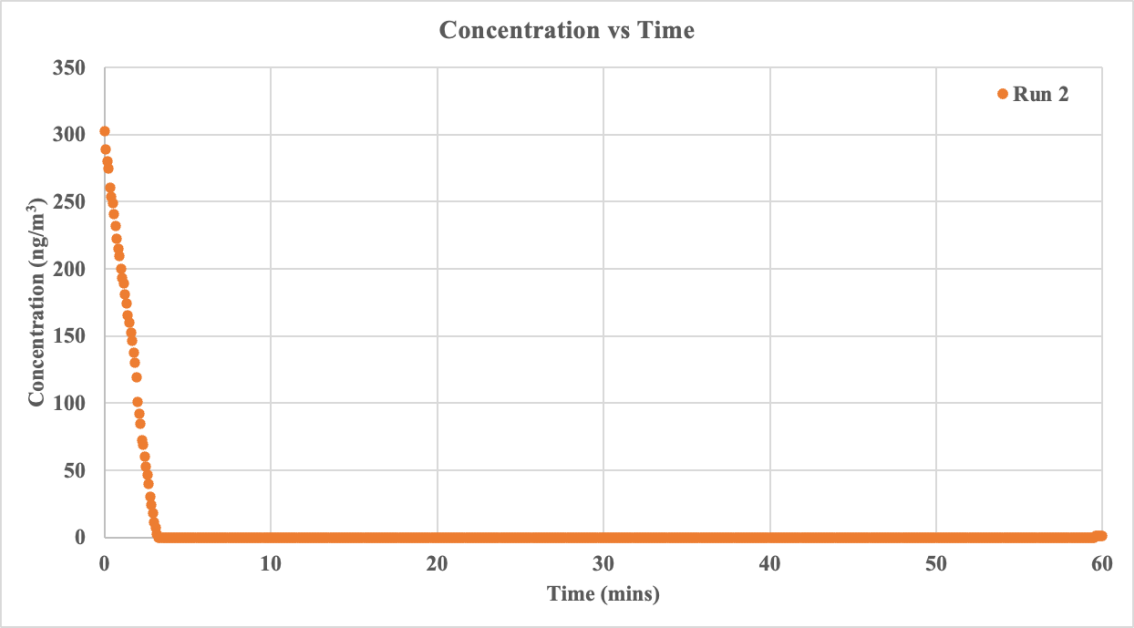

Figure 4.23: Run 2 of Hg adsorption curve at 200℃ for dark fly ash sample

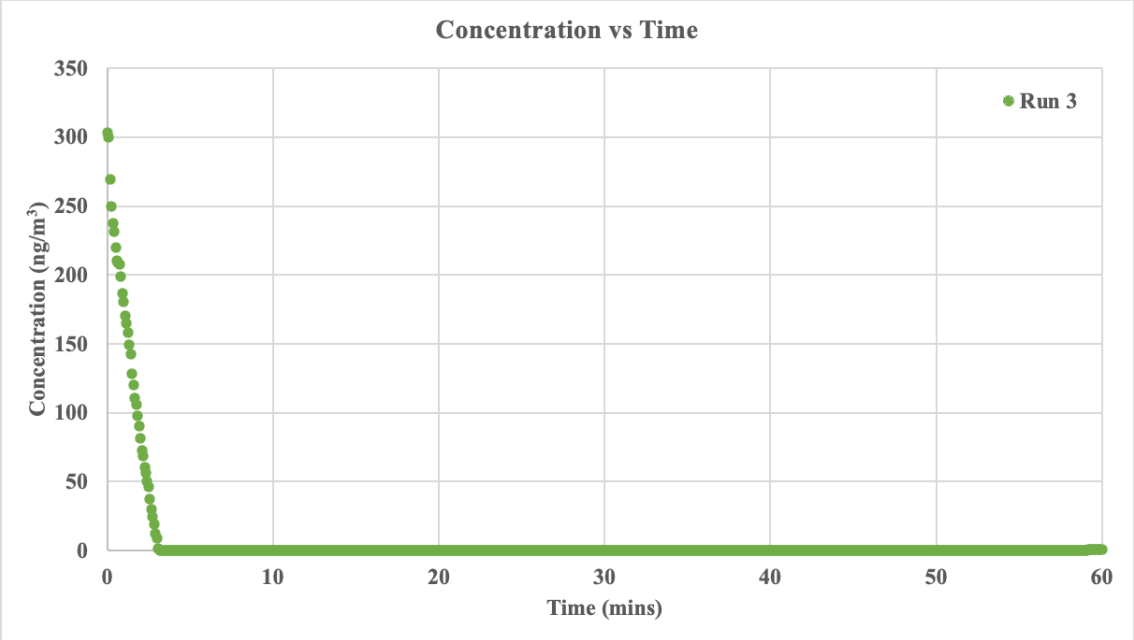

Figure 4.24: Run 3 of Hg adsorption curve at 200℃ for dark fly ash sample

Figure 4.25 – figure 4.27 shows the adsorption efficiency curves for the dark fly ash sample; the sample shows 100% adsorption until 58.91 mins for run 1, 59.53 mins for run 2 and 59.17 mins for run 3, where there is a slight decline to 99%. However, a breakthrough was not achieved in 1 hour. The decline in efficiency is gradual and not rapid, as seen by the values in Appendix B.

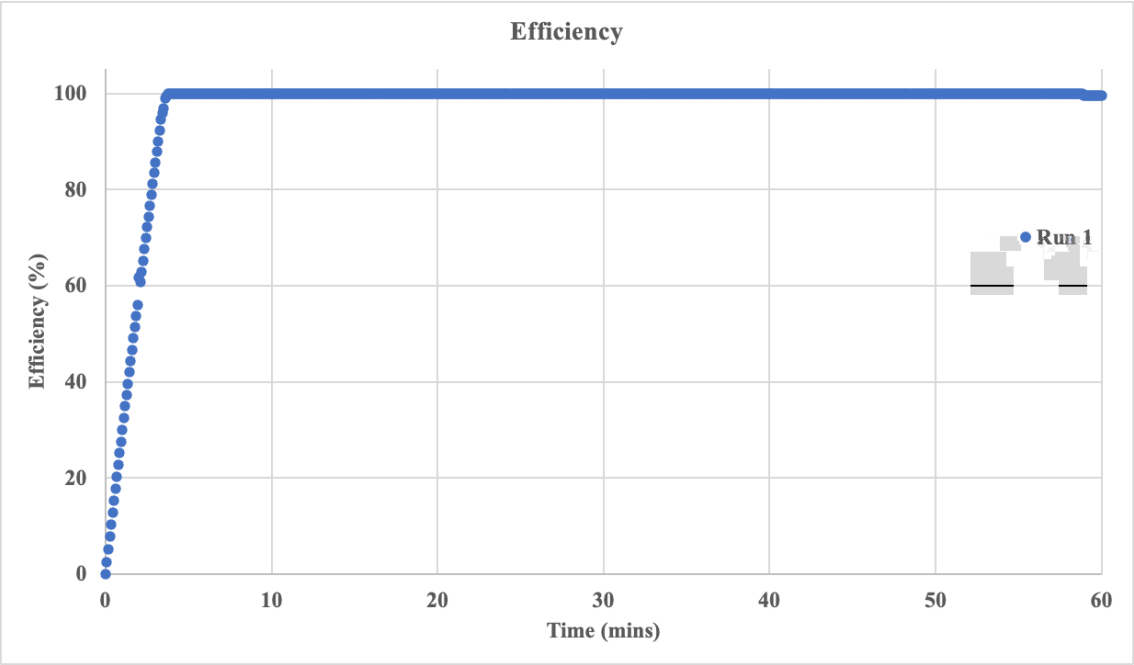

Figure 4.25: Run 1 of Hg adsorption efficiency curve at 200℃ for dark fly ash

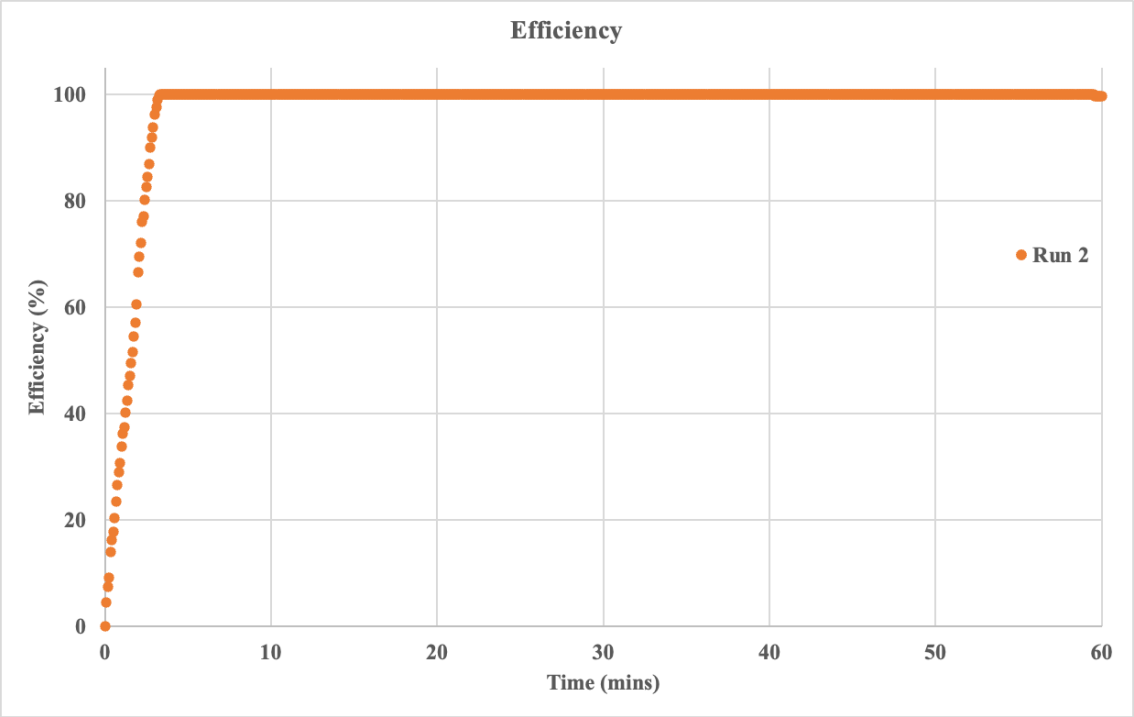

Figure 4.26: Run 2 of Hg adsorption efficiency curve at 200℃ for dark fly ash

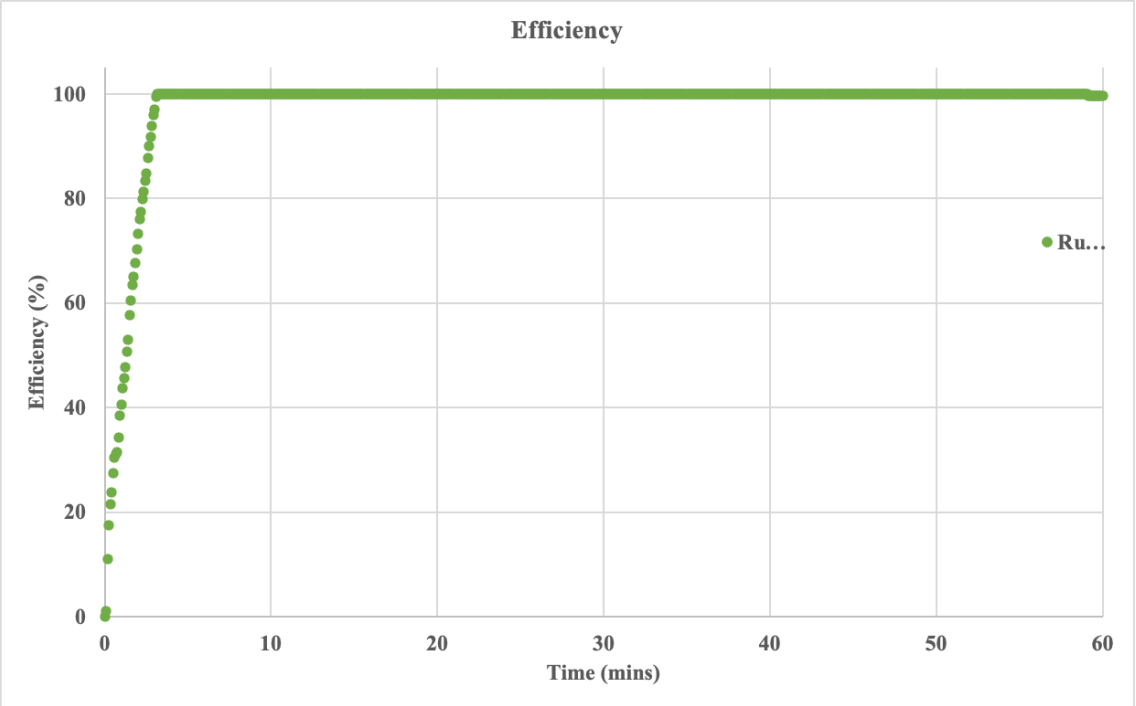

Figure 4.27: Run 3 of Hg adsorption efficiency curve at 200℃ for dark fly ash

An assessment of figures 4.28 – 4.30, which shows the adsorption of mercury with the modified dark-$CuSO_4$ fly ash sample, shows that the rate at which the adsorption occurs slows down very slightly as compared with unmodified dark fly ash sample, with the time taken to reduce to mercury concentration to 0 ng/m^3 varies between 3.5 – 5 minutes. The graphs also have a slight curve and are less linear than the unmodified dark sample. The efficiency curves in figures 4.31 – 4.33 also show that 100% of mercury is adsorbed until around 59 mins; at this point, efficiency gradually declines to 99%. Breakthrough was not achieved in the duration during which the experiment was conducted.

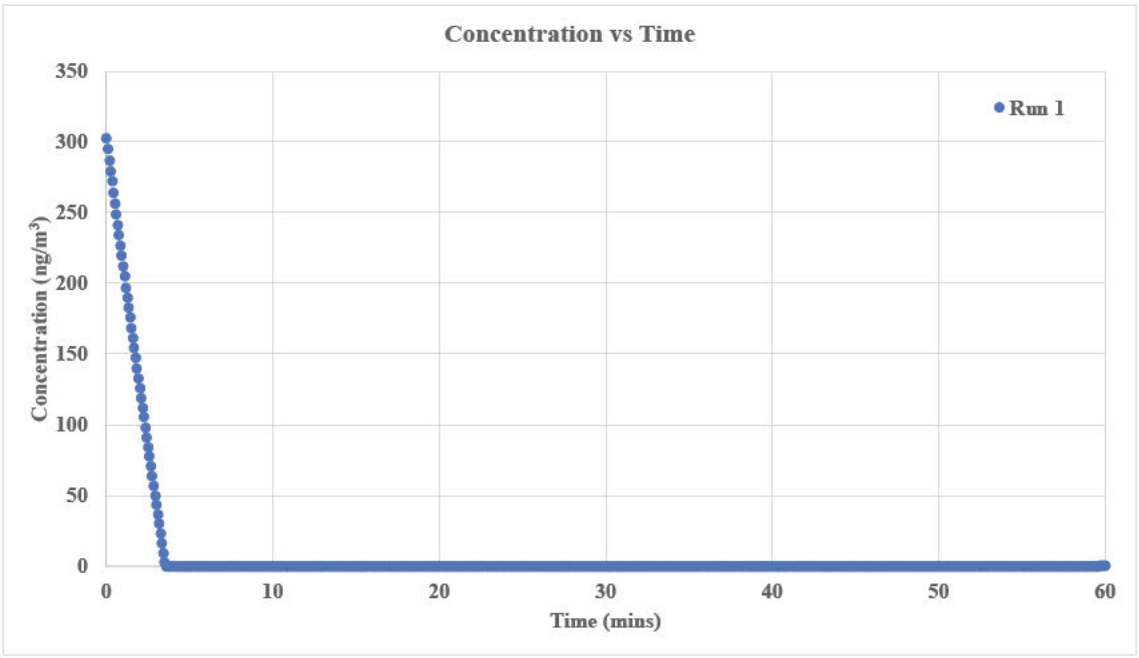

Figure 4.28: Run 1 Hg adsorption curve at 200℃ for modified dark-$CuSO_4$ fly ash sample.

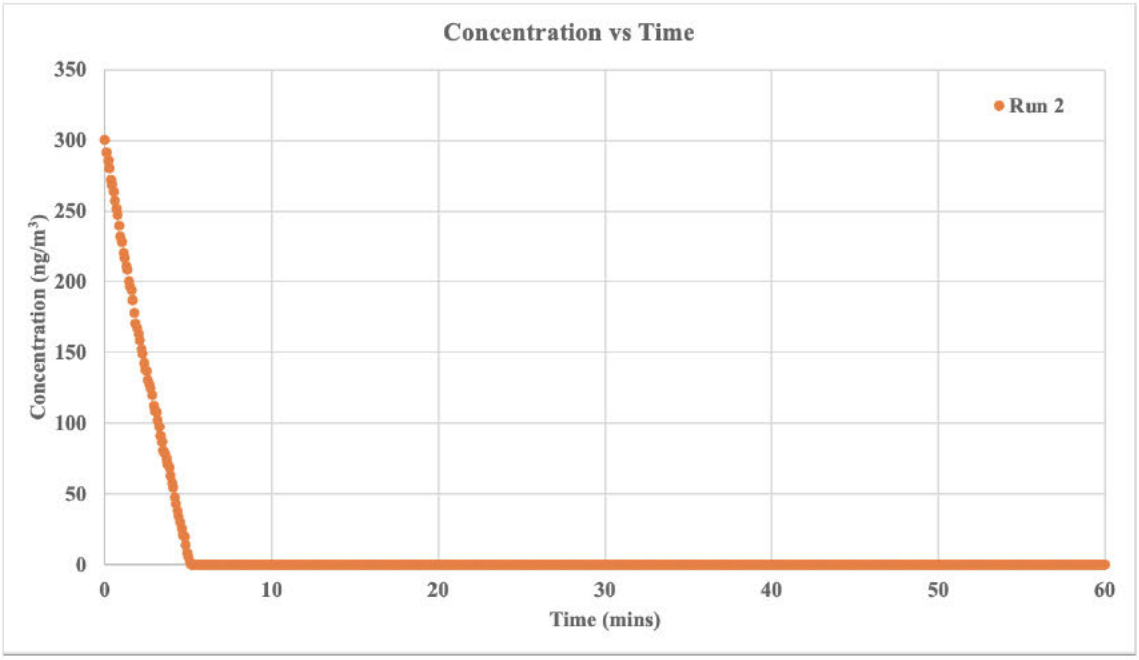

Figure 4.29: Run 2 Hg adsorption curve at 200℃ for modified dark-$CuSO_4$ fly ash sample

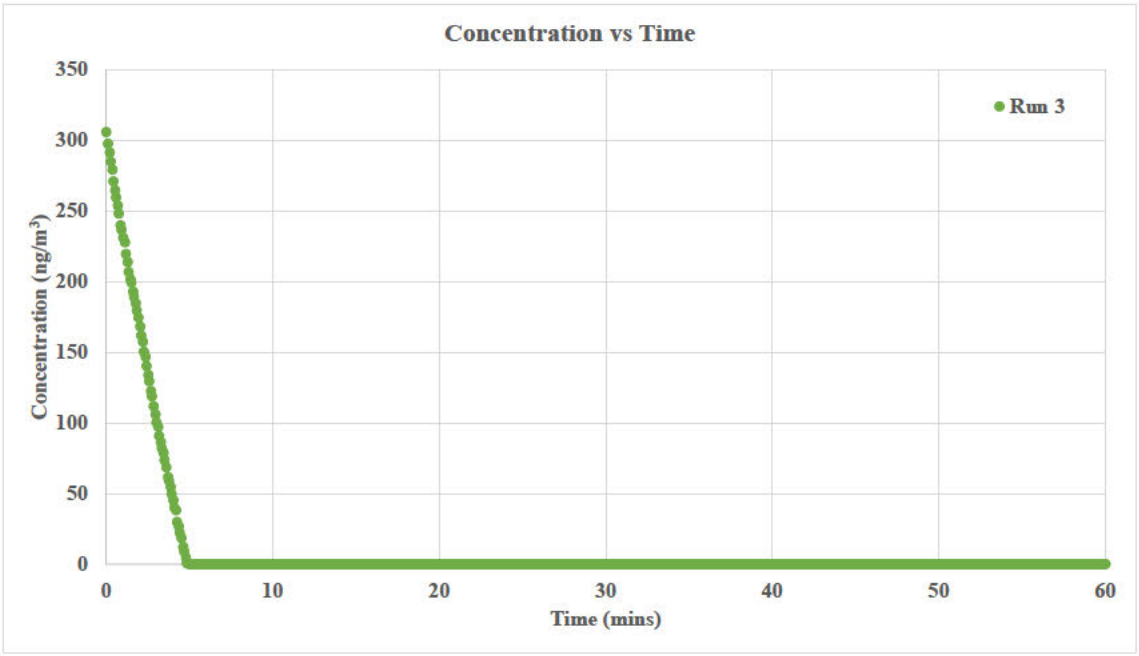

Figure 4.30: Run 3 Hg adsorption curve at 200℃ for modified dark-$CuSO_4$ fly ash sample

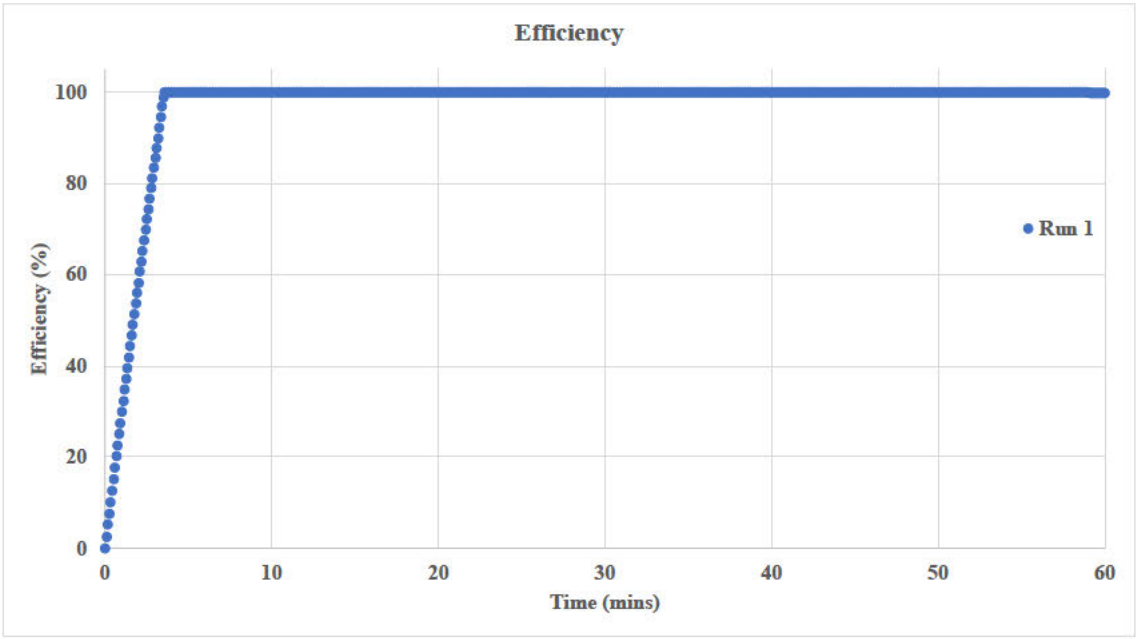

Figure 4.31: Run 1 of Hg adsorption efficiency curve at 200℃ for modified dark-$CuSO_4$ fly ash sample

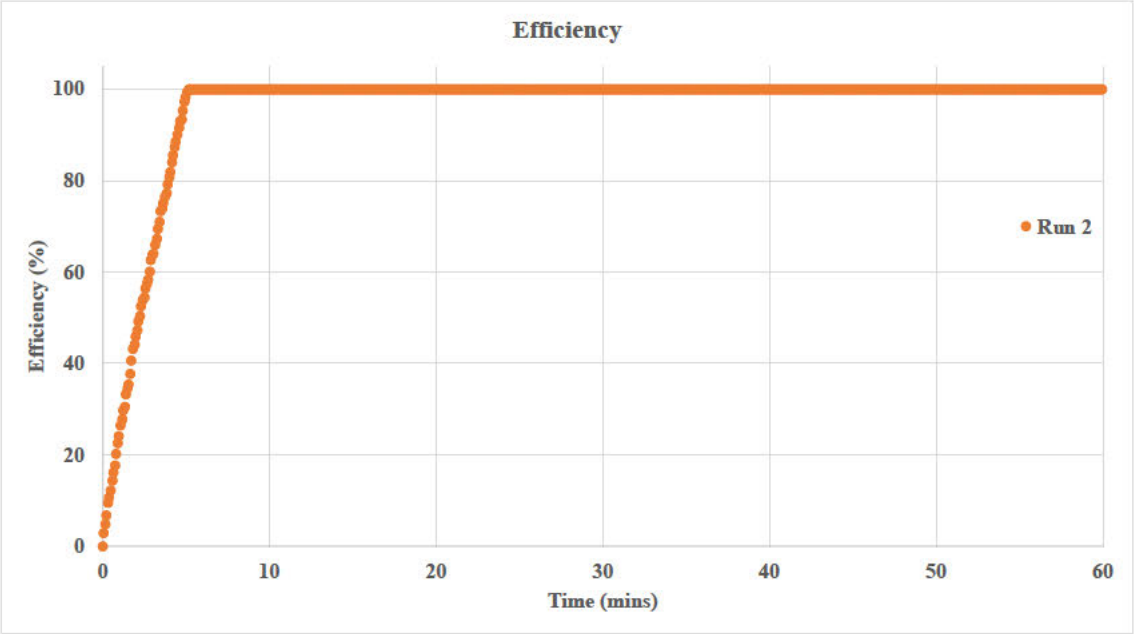

Figure 4.32: Run 2 of Hg adsorption efficiency curve at 200℃ for modified dark-$CuSO_4$ fly ash sample

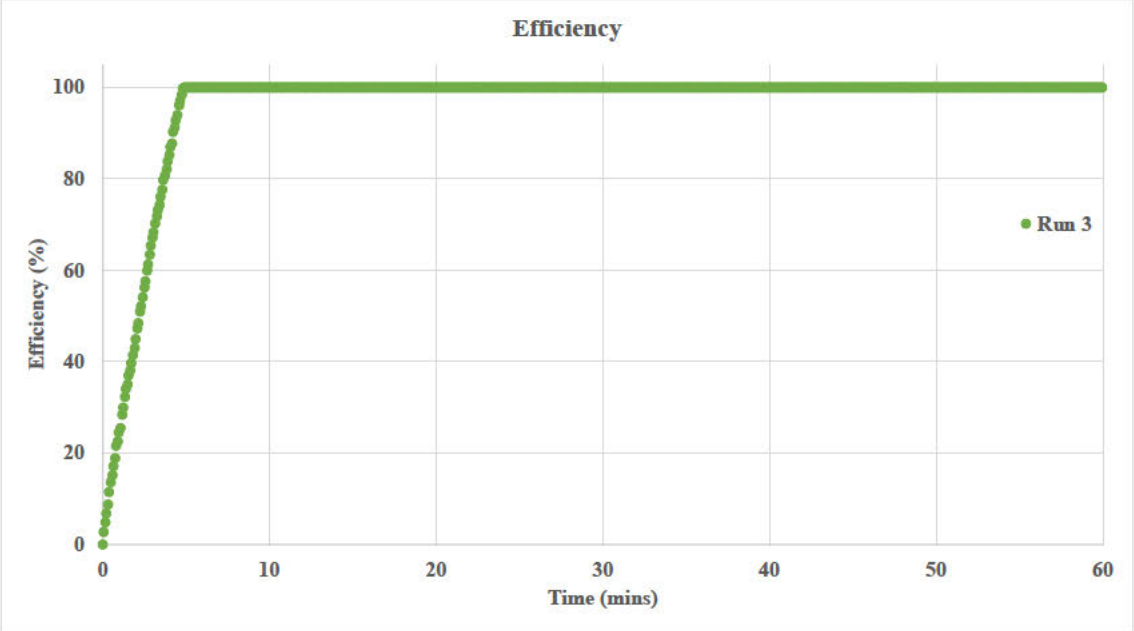

Figure 4.33: Run 3 of Hg adsorption efficiency curve at 200℃ for modified dark-$CuSO_4$ fly ash sample

An assessment of figures 4.34 – 4.36, which shows the adsorption of mercury with the modified dark-$ZnCl_2$ fly ash sample, shows that the rate at which the adsorption occurs is slower than the adsorption with dark and modified $CuSO_4$ fly ash samples, where the time taken to reduce to mercury concentration to 0 ng/m^3 varies between 6 – 7 minutes. The graphs also have a visible curve with a more gradual decrease in concentration compared to the dark and modified $CuSO_4$ fly ash samples. The efficiency curves in figures 4.37 – 4.39 also show that 100% of mercury is adsorbed until around 59 mins; at this point, efficiency gradually declines to 99%. Breakthrough was not achieved in the duration during which the experiment was conducted.

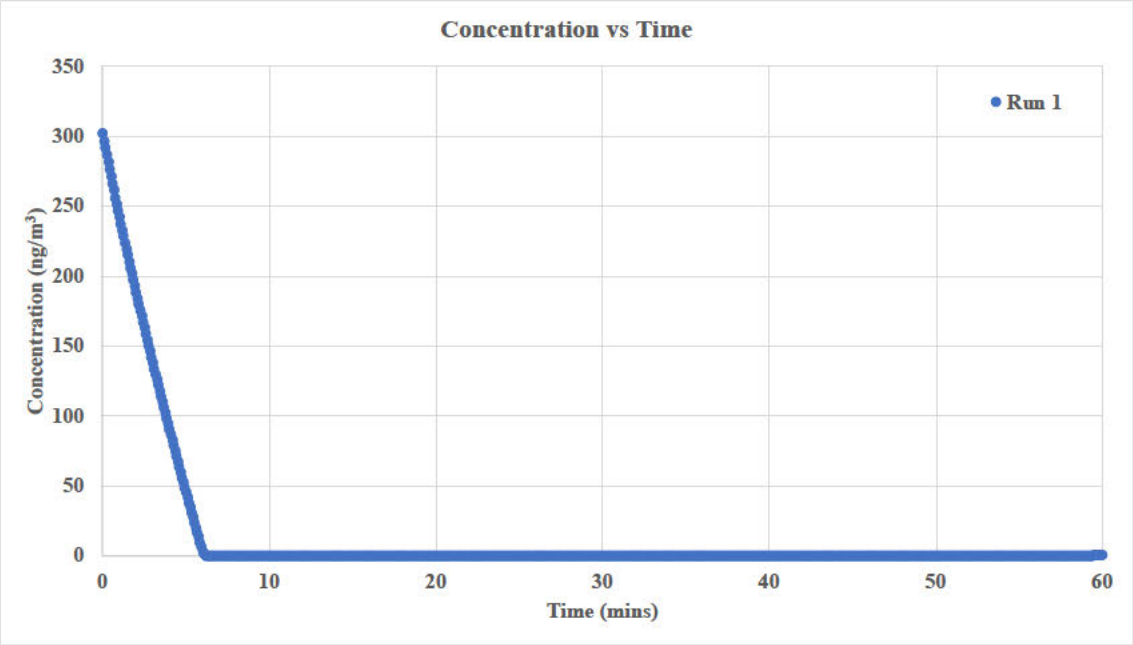

Figure 4.34: Run 1 of Hg adsorption curve at 200°C for modified dark-$ZnCl_2$ fly ash sample.

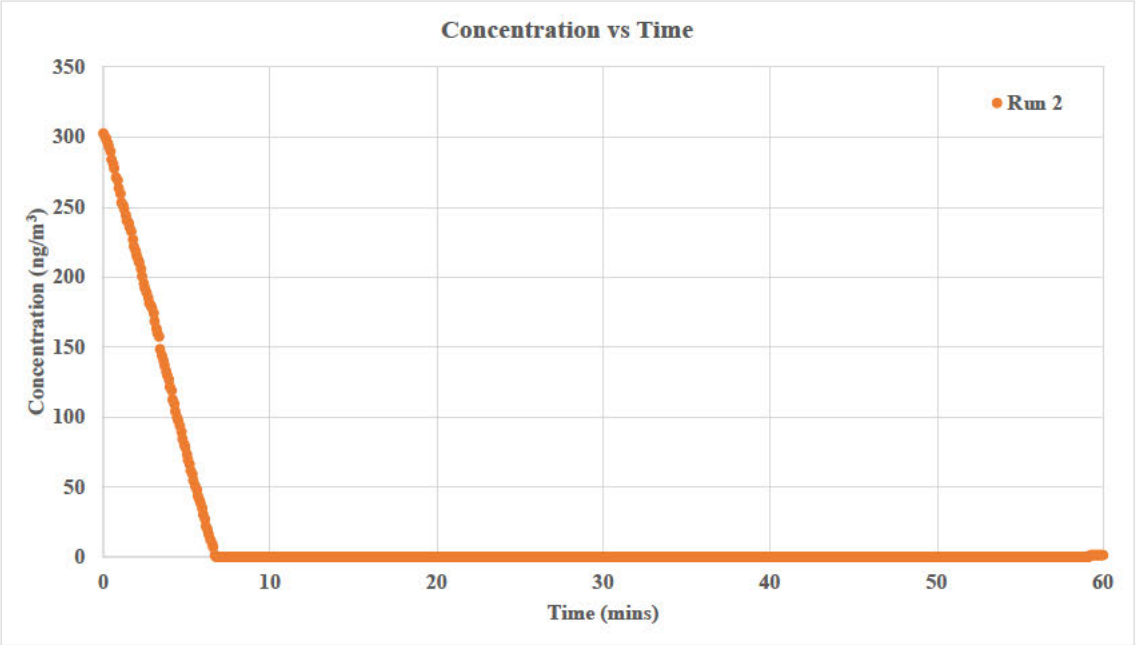

Figure 4.35: Run 2 of Hg breakthrough curve at 200°C for modified dark-$ZnCl_2$ fly ash sample.

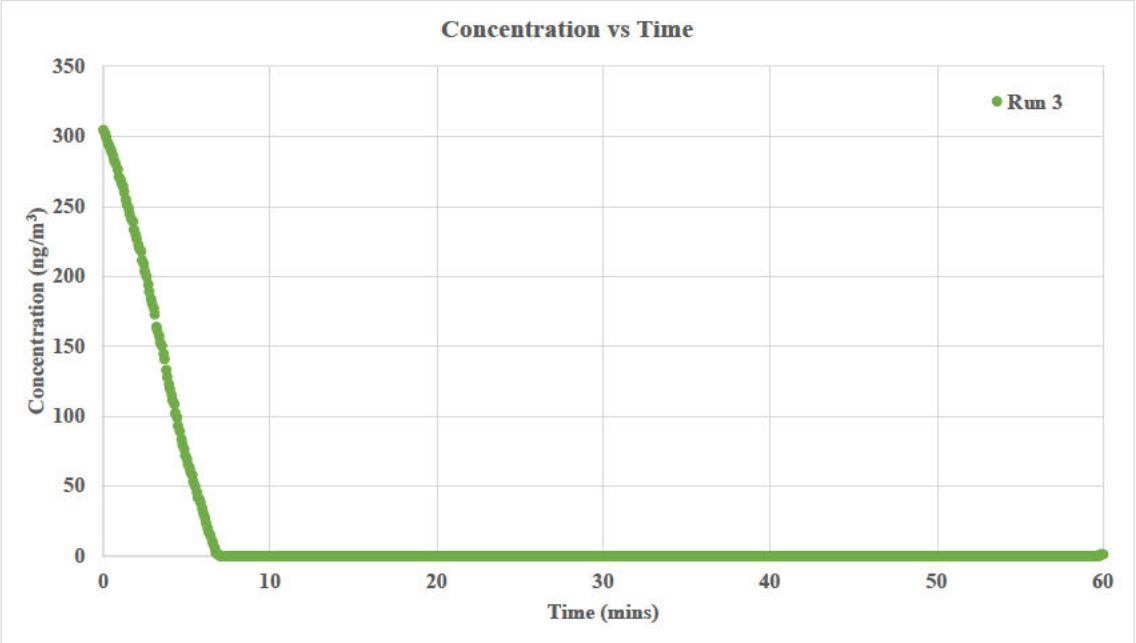

Figure 4.36: Run 3 of Hg breakthrough curve at 200°C for modified dark-$ZnCl_2$ fly ash sample.

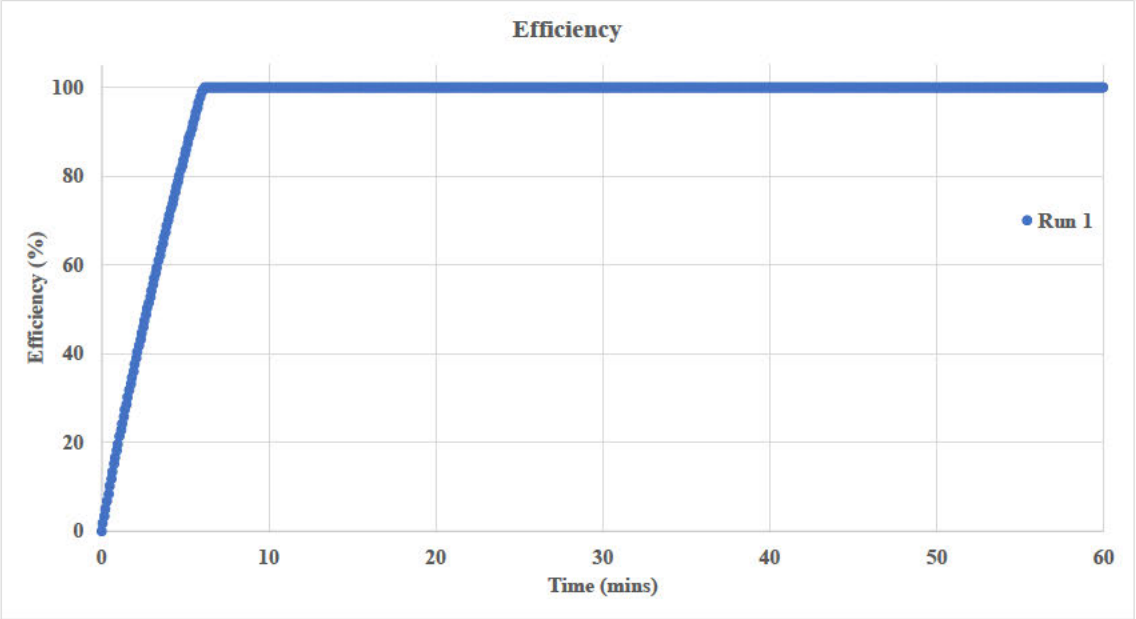

Figure 4.37: Run 1 of Hg adsorption efficiency curve at 200℃ for modified dark-$ZnCl_2$ fly ash sample.

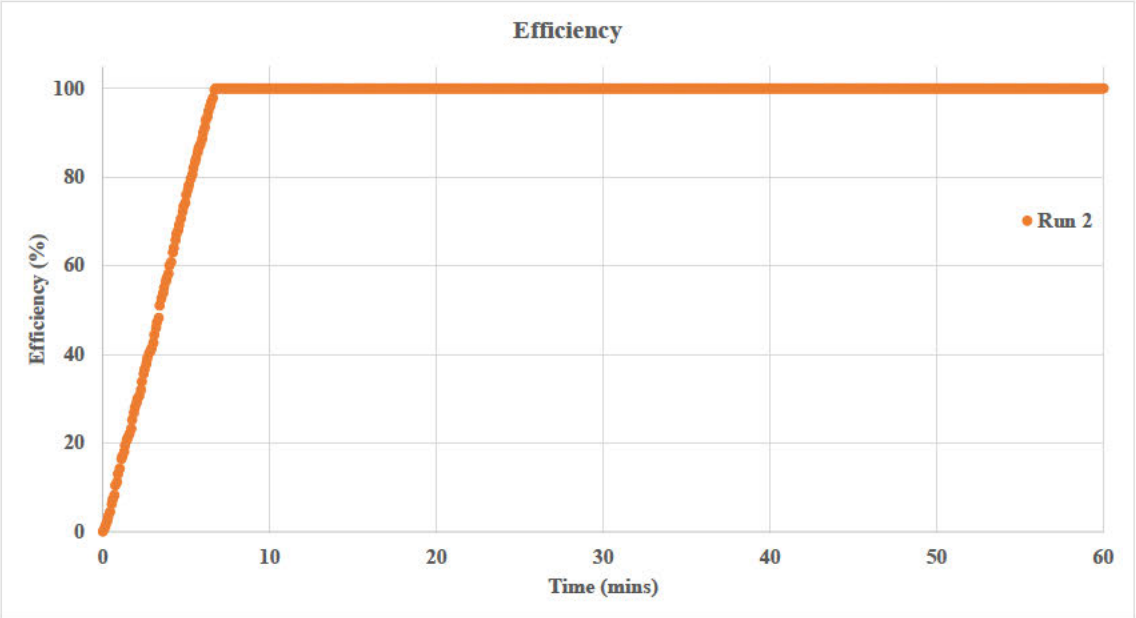

Figure 4.38: Run 2 of Hg adsorption efficiency curve at 200℃ for modified dark-$ZnCl_2$ fly ash sample.

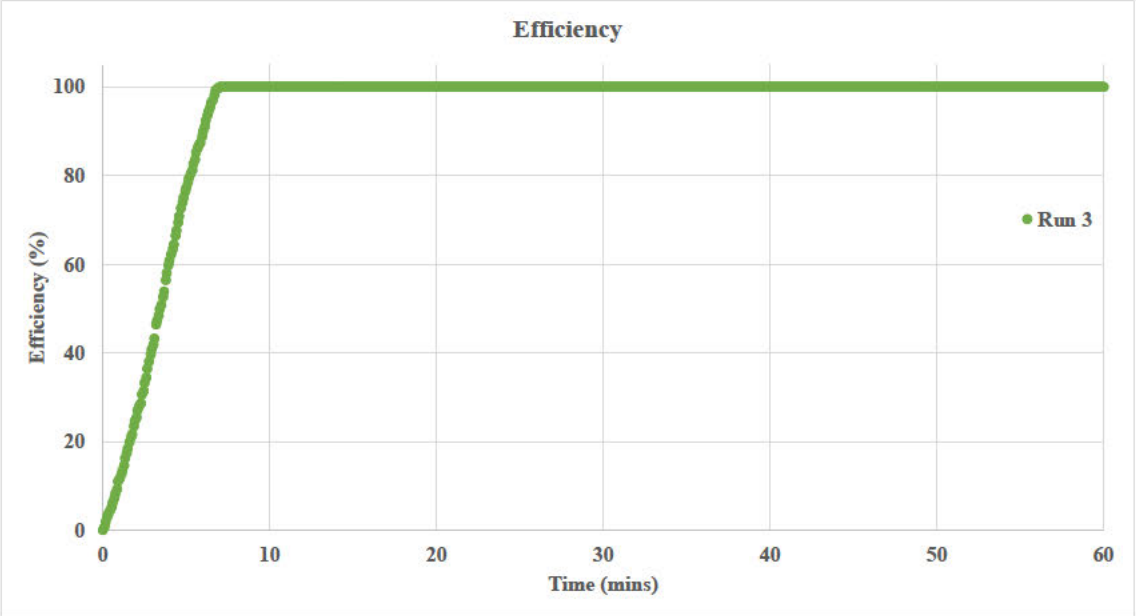

Figure 4.39: Run 3 of Hg adsorption efficiency curve at 200℃ for modified dark-$ZnCl_2$ fly ash sample.

Figures 4.40 – 4.42, which show the adsorption of mercury with the modified dark-$FeCl_3$ fly ash sample, show that the rate at which the adsorption occurs is significantly slower than any of the other samples that were tested, where the time taken to reduce to mercury concentration to 0 ng/m^3 varies between 20 – 21 minutes. The graphs also have a distinct curve, showing that the adsorption occurs gradually compared to the quick decrease in the other fly ash samples. The efficiency curves in figures 4.43 – 4.45 also show that 100% of mercury is adsorbed for the duration of the experiment (1 hour). Breakthrough was not achieved in the duration during which the experiment was conducted.

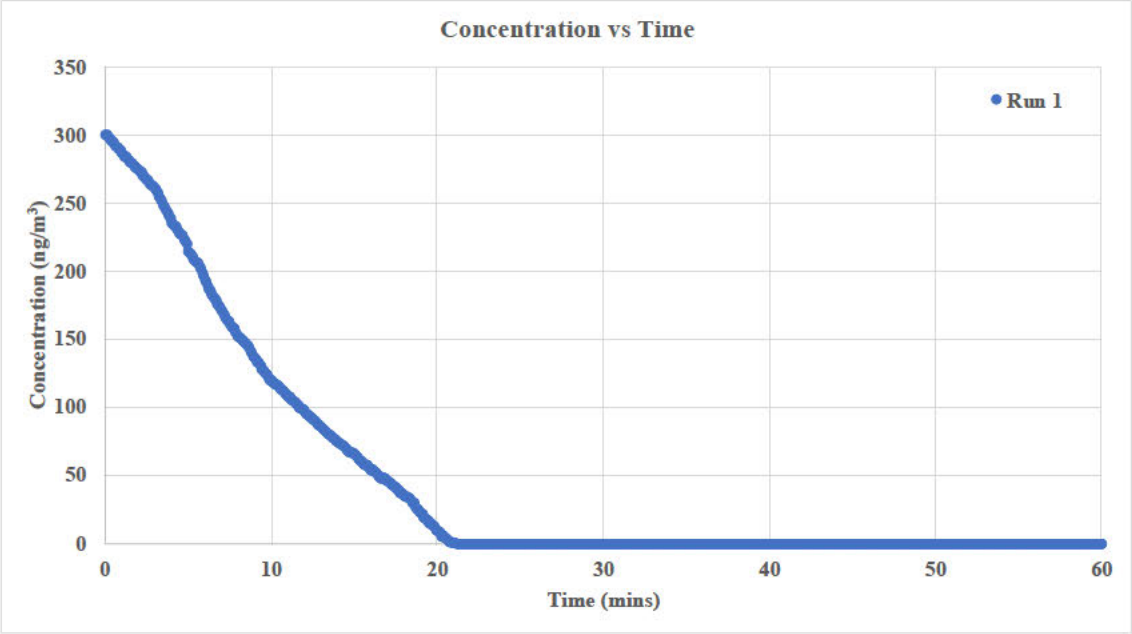

Figure 4.40: Run 1 of Hg adsorption curve at 200℃ for modified dark-$FeCl_3$ fly ash sample.

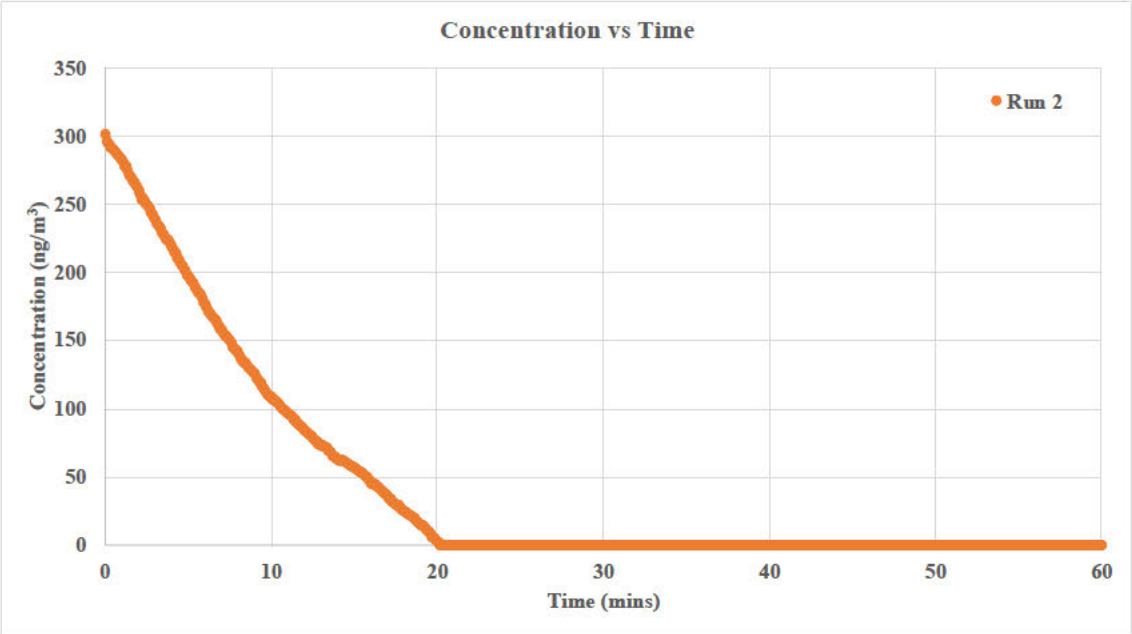

Figure 4.41: Run 2 of Hg adsorption curve at 200℃ for modified dark-$FeCl_3$ fly ash sample.

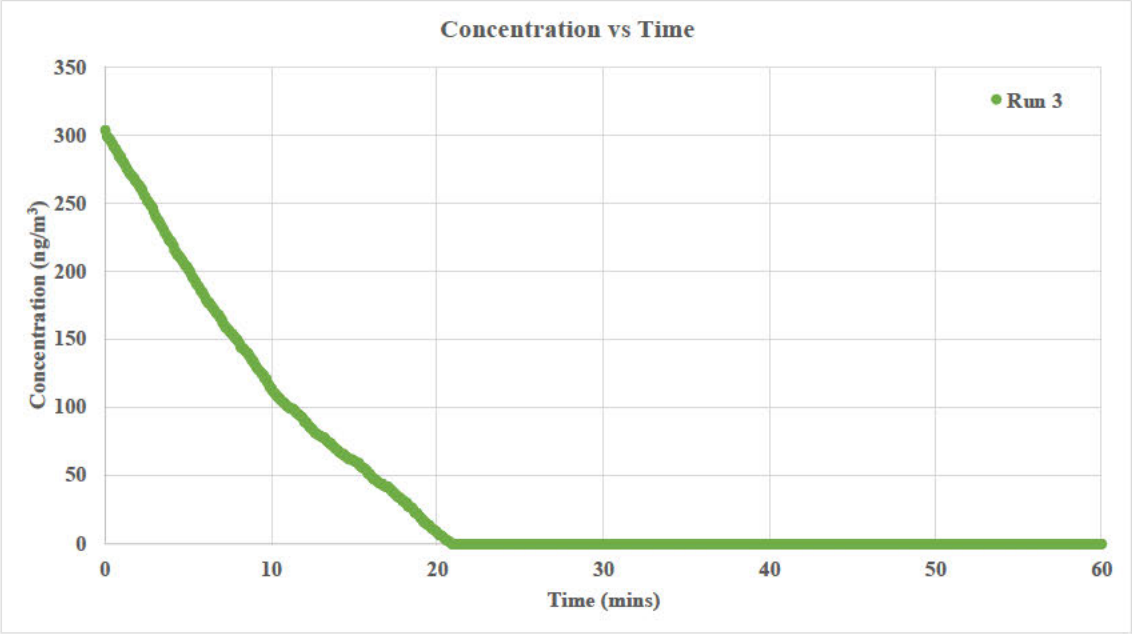

Figure 4.42: Run 3 of Hg adsorption curve at 200℃ for modified dark-$FeCl_3$ fly ash sample.

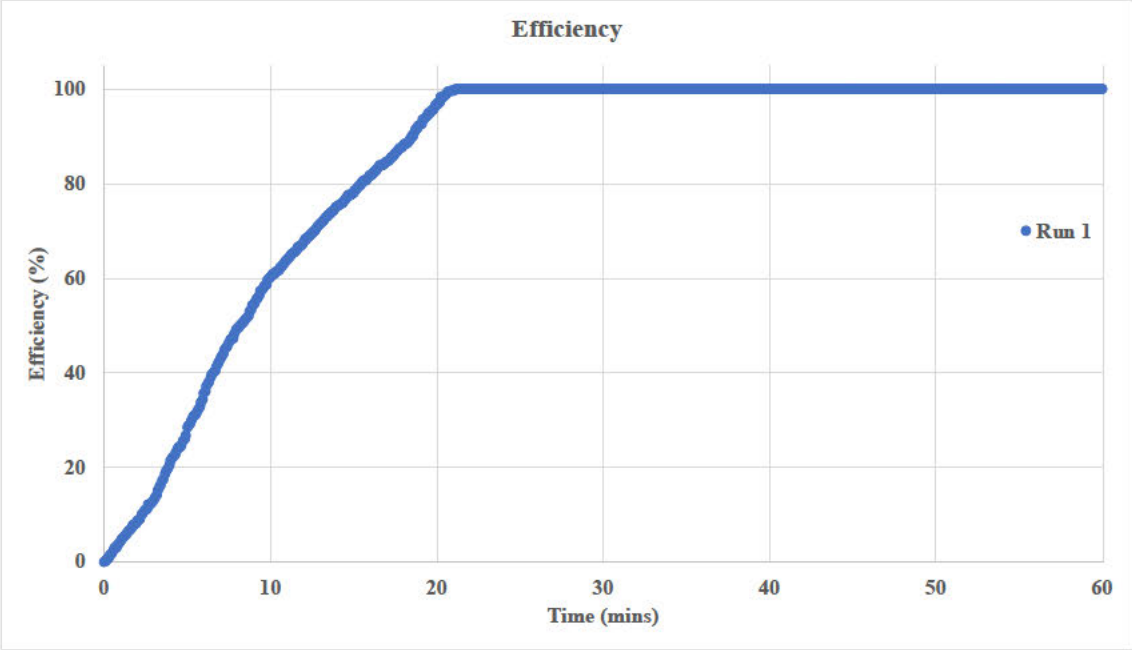

Figure 4.43: Run 1 of Hg adsorption efficiency curve at 200℃ for modified dark-$FeCl_3$ fly ash sample.

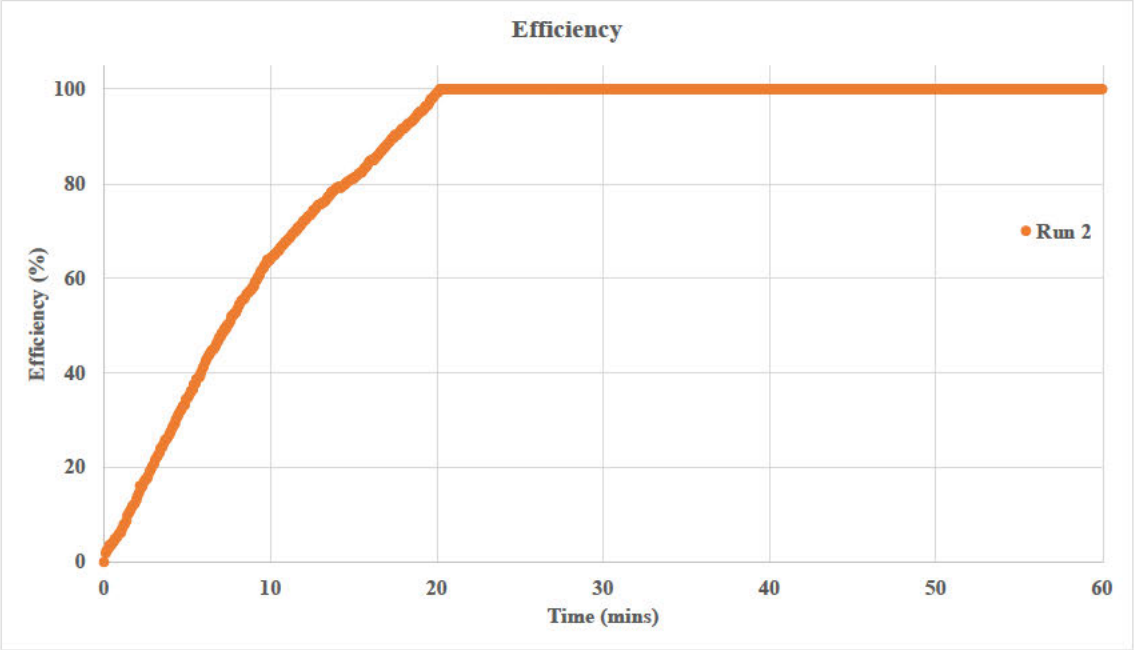

Figure 4.44: Run 2 of Hg adsorption efficiency curve at 200℃ for modified dark-$FeCl_3$ fly ash sample.

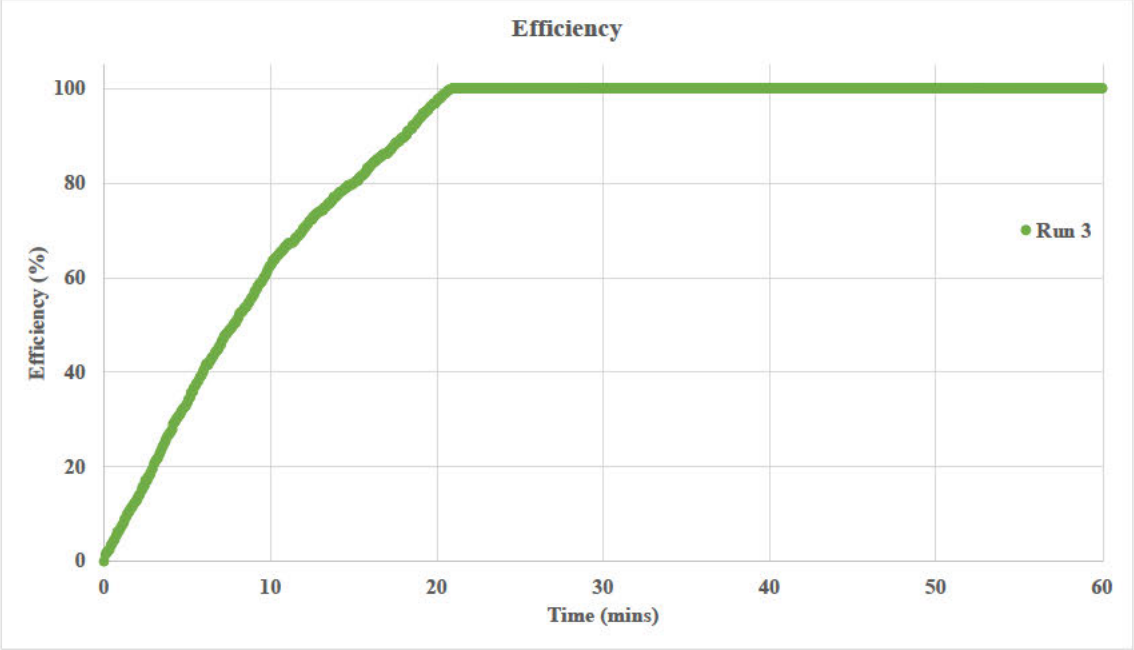

Figure 4.45: Run 3 of Hg adsorption efficiency curve at 200℃ for modified dark-$FeCl_3$ fly ash sample.

An assessment of figures 4.46 – 4.48, which shows the adsorption of mercury with the modified dark-$CuCl_2$ fly ash sample, shows that the rate at which the adsorption occurs is slower than the adsorption with dark, modified $CuSO_4$ and modified $ZnCl_2$ fly ash samples, where the time taken to reduce to mercury concentration to 0 ng/m^3 varies between 9.5 – 12 minutes. The adsorption rate is quicker than the modified dark $FeCl_3$ sample. The graphs also have a visible curve with a more gradual decrease in concentration compared to the dark, modified dark $CuSO_4$ and modified dark $ZnCl_2$ fly ash samples. The efficiency curves in figures 4.49 – 4.51 also show that 100% of mercury is adsorbed for the duration of the experiment (1 hour). Breakthrough was not achieved in the duration during which the experiment was conducted.

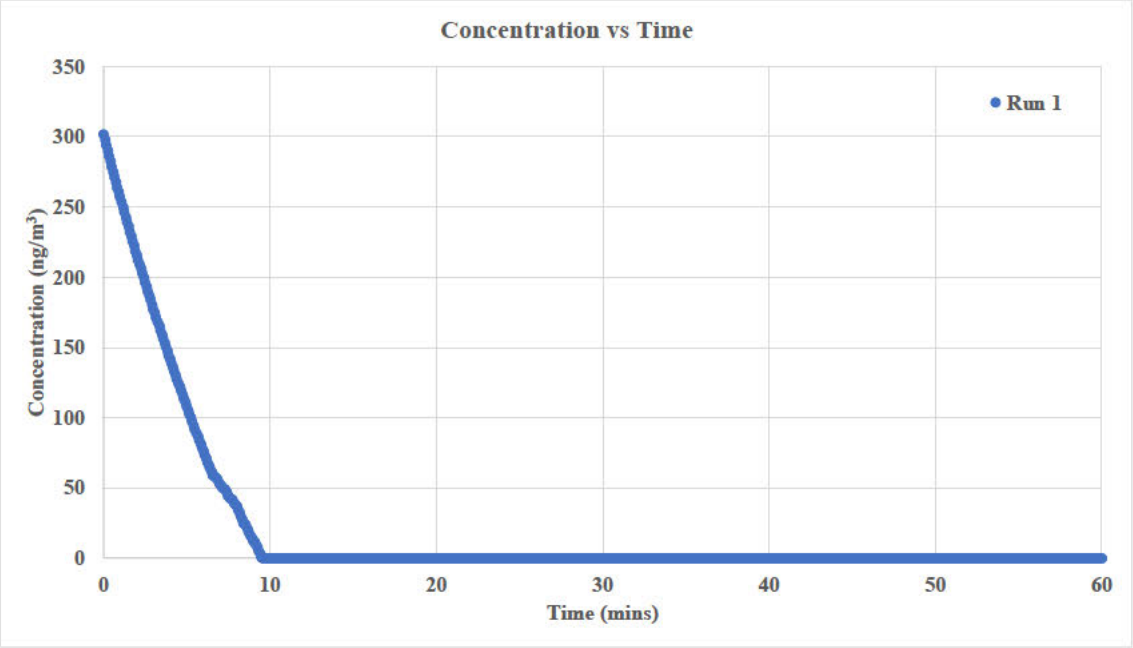

Figure 4.46: Run 1 of Hg adsorption curve at 200℃ for modified dark-$CuCl_2$ fly ash sample.

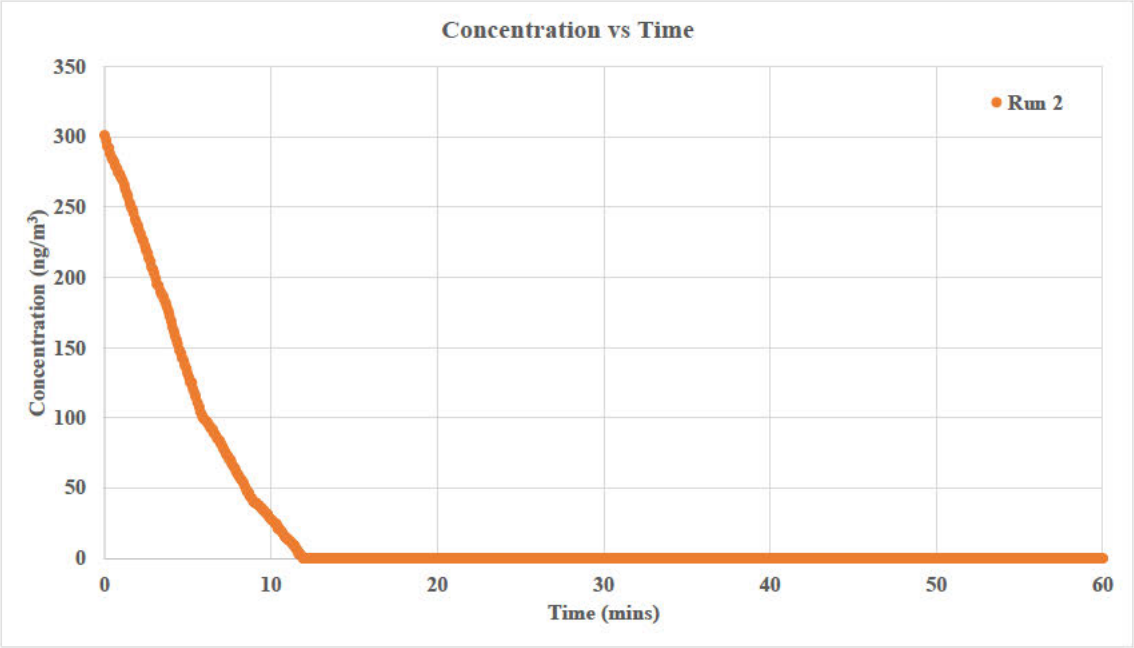

Figure 4.47: Run 2 of Hg adsorption curve at 200℃ for modified dark-$CuCl_2$ fly ash sample

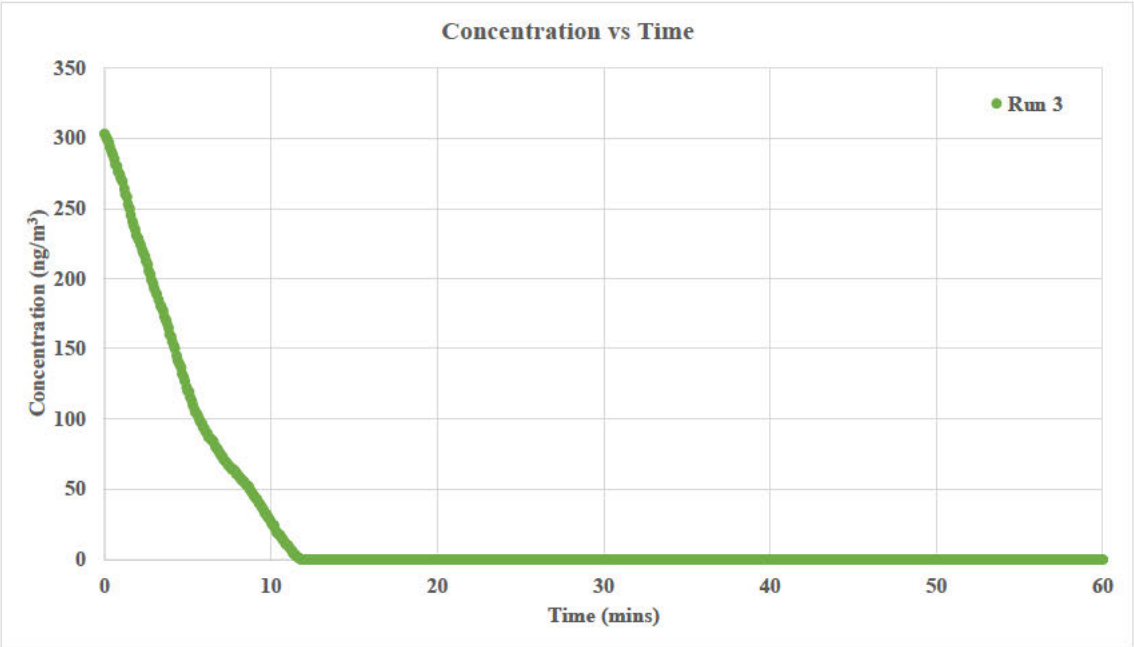

Figure 4.48: Run 3 of Hg adsorption curve at 200℃ for modified dark-$CuCl_2$ fly ash sample

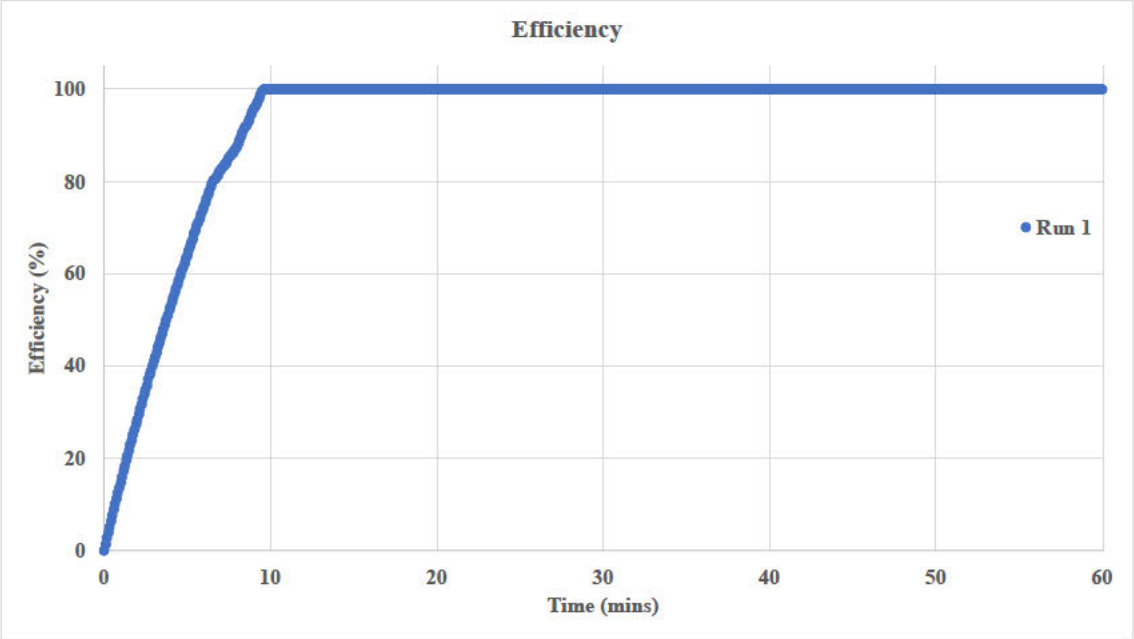

Figure 4.49: Run 1 of Hg adsorption efficiency curve at 200℃ for dark-$CuCl_2$ fly ash sample

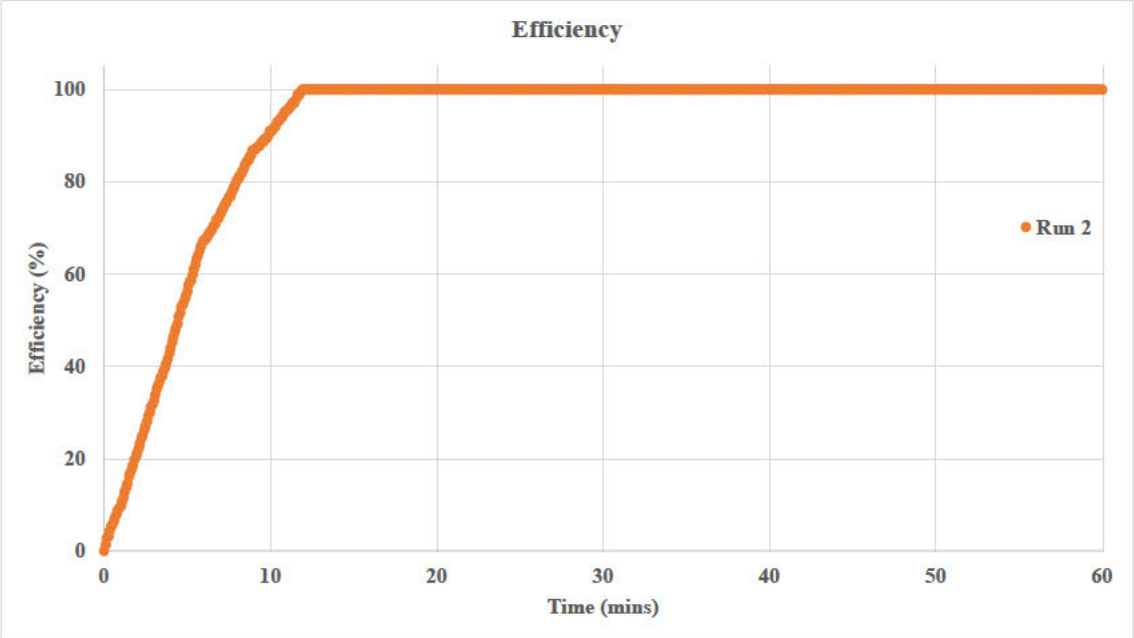

Figure 4.50: Run 2 of Hg adsorption efficiency curve at 200℃ for dark-$CuCl_2$ fly ash sample

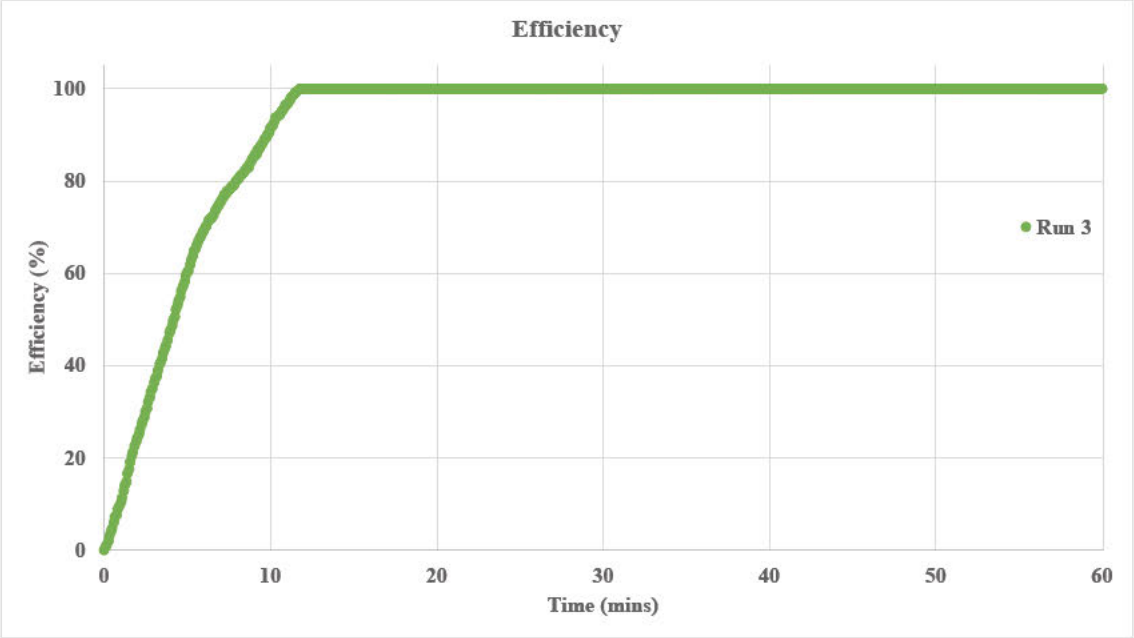

Figure 4.51: Run 3 of Hg adsorption efficiency curve at 200℃ for dark-$CuCl_2$ fly ash sample

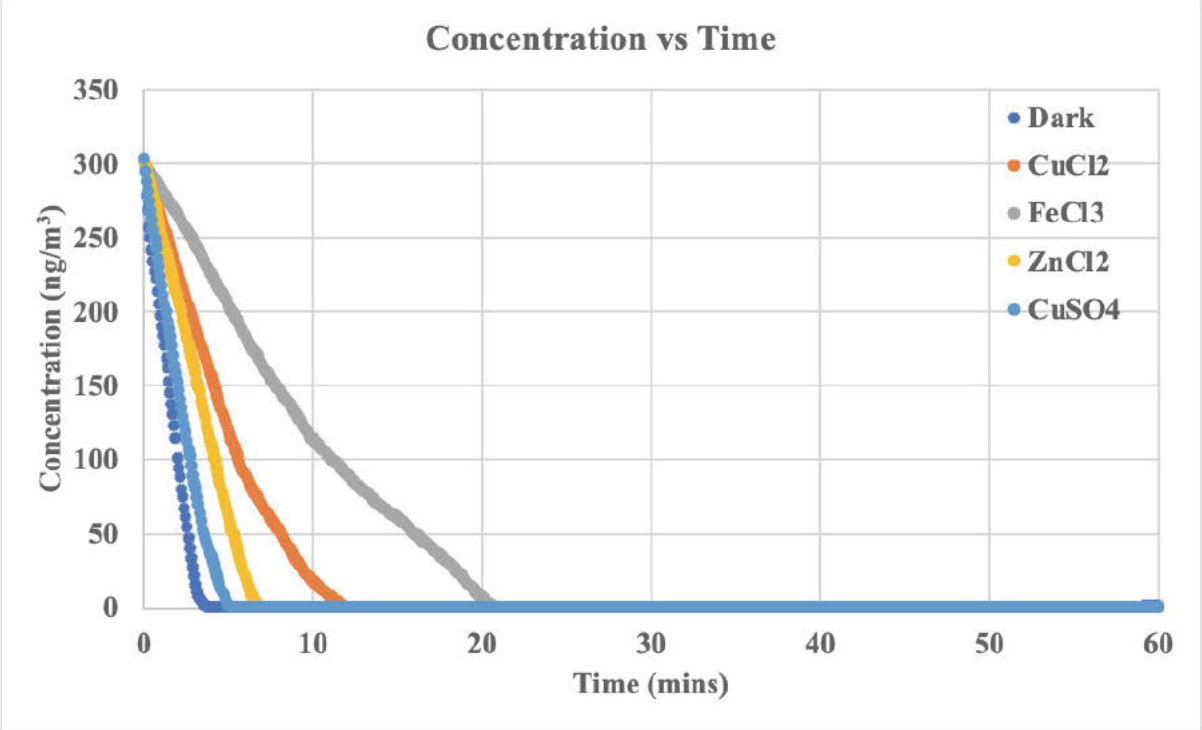

Figure 4.52: Cumulative Hg adsorption curve at 200℃ for dark and modified dark fly ash samples

4.3.2 Adsorption Tests for Light Fly Ash and Modified Light Fly Ash Samples at 200℃.

Figure 4.53 – figure 4.55 shows the adsorption curves for the light fly ash sample, the adsorption process is quick as seen by the gradient of the adsorption curve. It takes 4 - 5 minutes for the concentration to drop to 0 ng/m^3 from an initial 300 ng/m^3 concentration. Whilst the time taken to drop to 0 ng/m^3 varies, the trajectory of the adsorption curve is the same for each of the experimental runs conducted. The quick reduction in the mercury concentration could be consistent with the physisorption mechanism. Figure 4.56 – figure 4.58 shows the adsorption efficiency curves for the light fly ash sample; the sample shows 100% adsorption until 57.83 mins for run 1, 59.25 mins for run 2 and 58.67 mins for run 3, where there is a slight decline to 99%. However, a breakthrough was not achieved in 1 hour. The decline in efficiency is gradual and not rapid, as seen by the values in Appendix B.

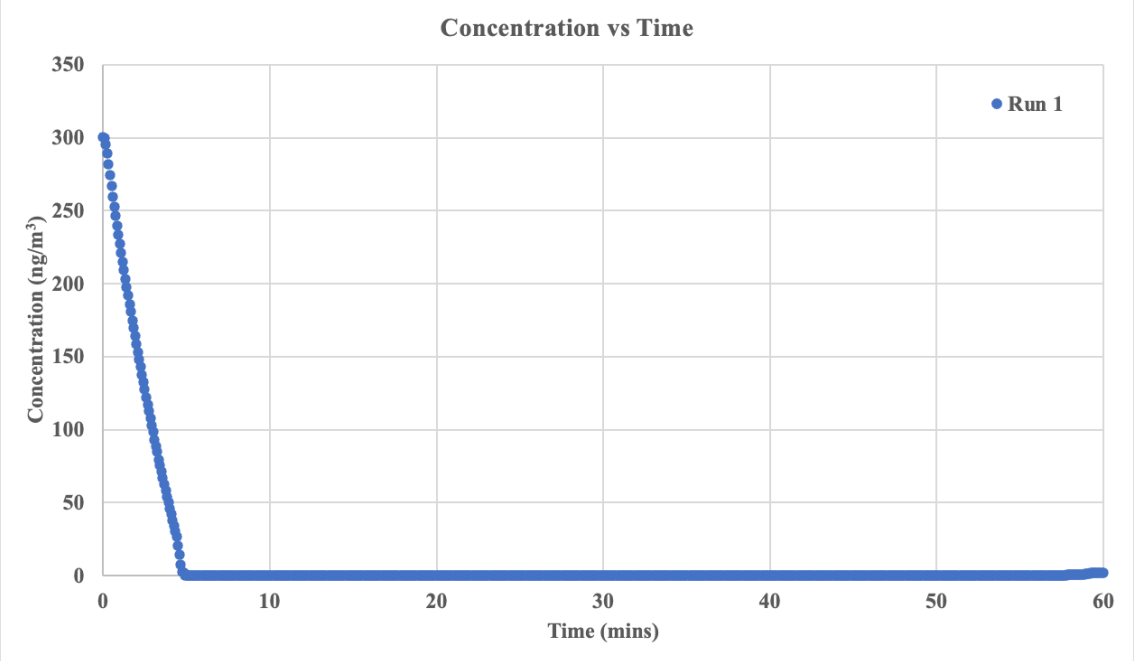

Figure 4.53: Run 1 of Hg adsorption curve at 200℃ for light fly ash sample

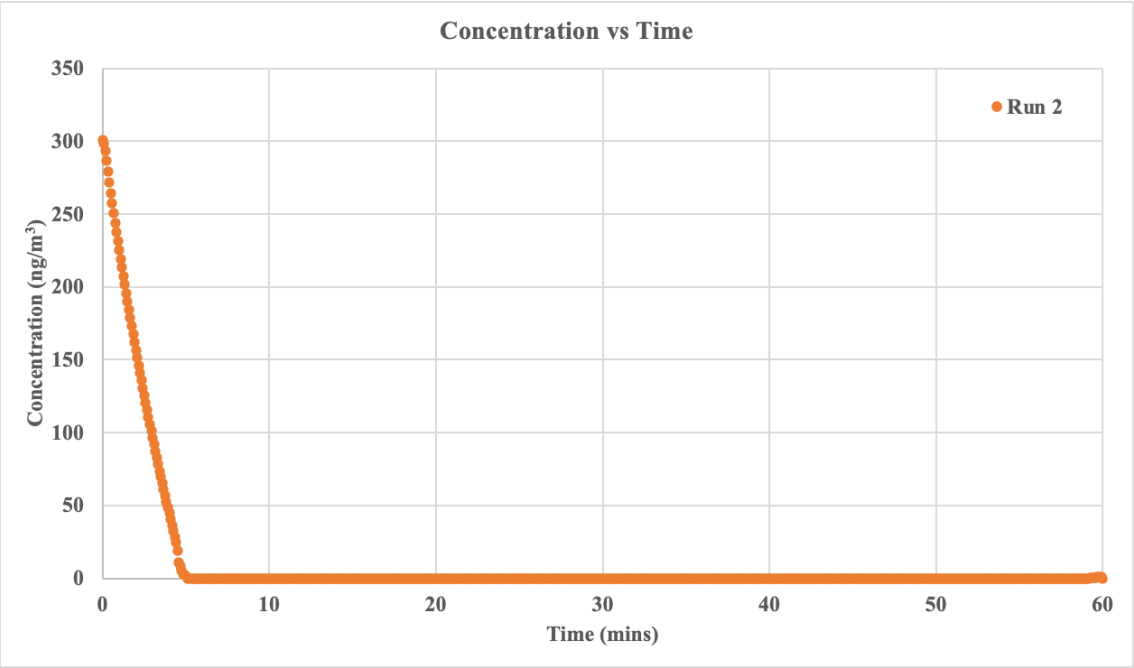

Figure 4.54: Run 2 of Hg adsorption curve at 200℃ for light fly ash sample

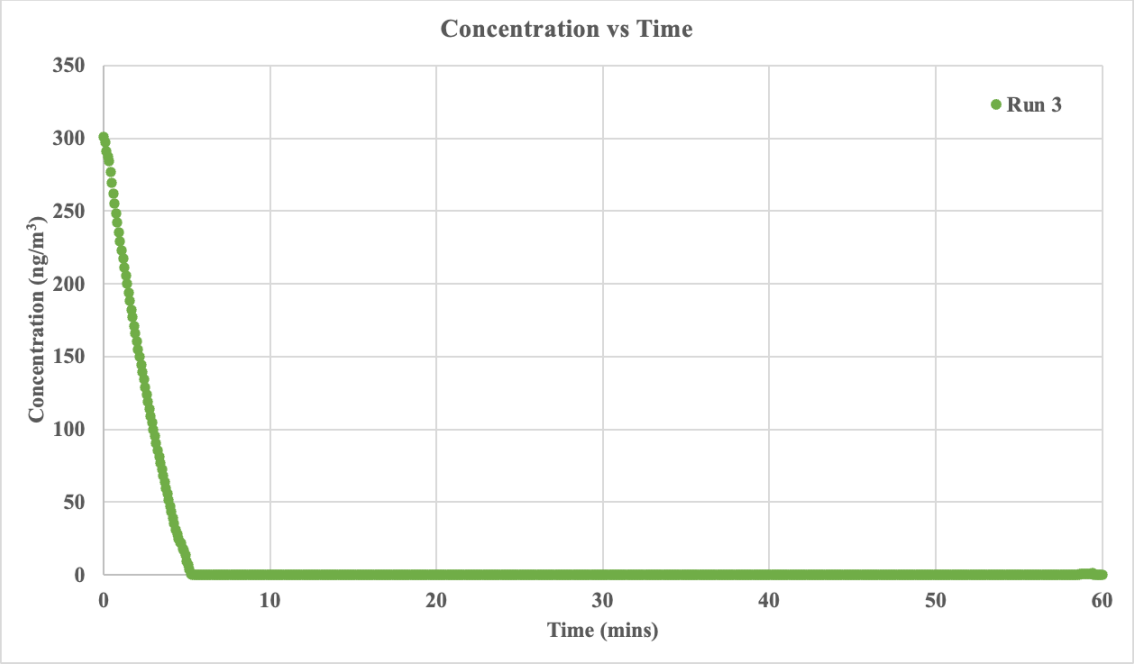

Figure 4.55: Run 3 of Hg adsorption curve at 200℃ for light fly ash sample

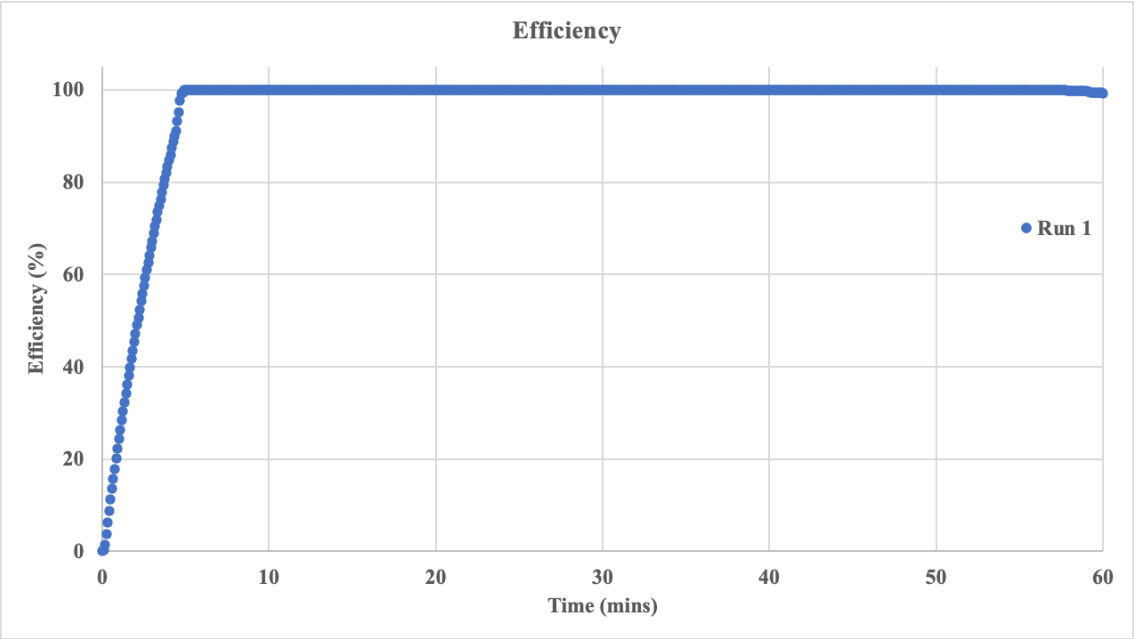

Figure 4.56: Run 1 of Hg adsorption efficiency curve at 200℃ for light fly ash

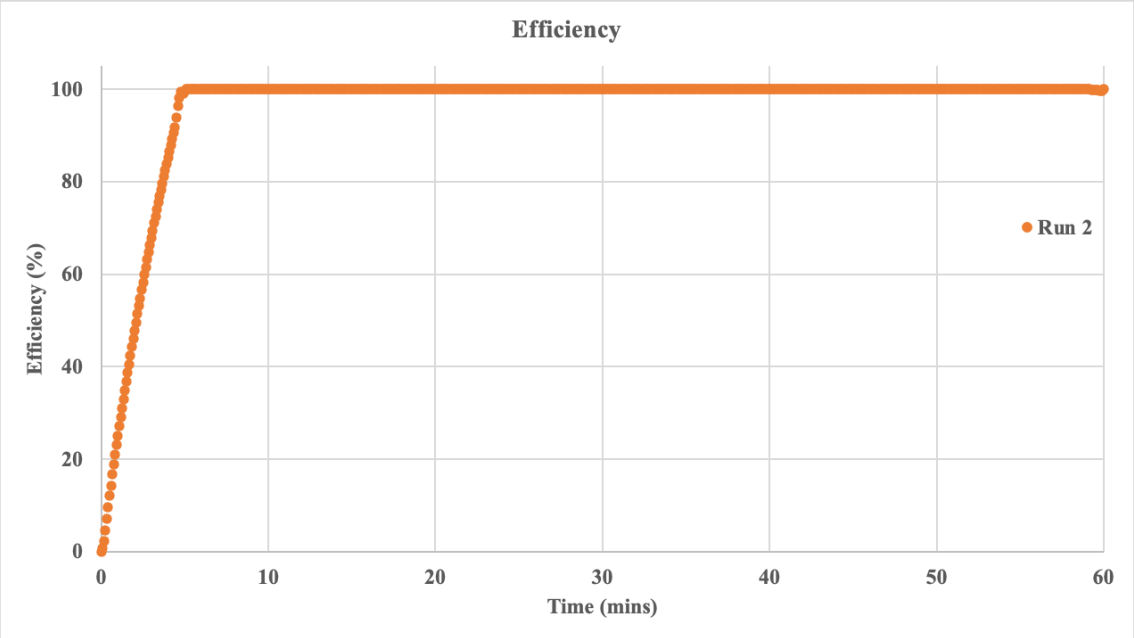

Figure 4.57: Run 2 of Hg adsorption efficiency curve at 200℃ for light fly ash

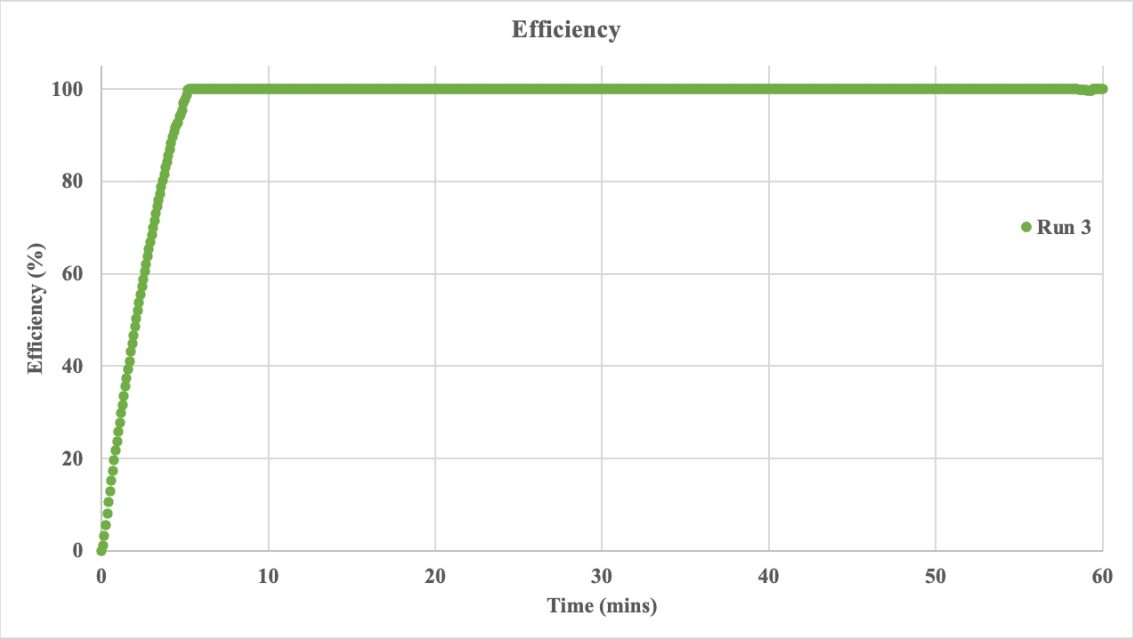

Figure 4.58: Run 3 of Hg adsorption efficiency curve at 200℃ for light fly ash

An assessment of figures 4.59 – 4.61, which shows the adsorption of mercury with the modified light-CuSO4 fly ash sample, shows that the rate at which the adsorption occurs slows down very slightly as compared with unmodified light fly ash sample, with the time taken to reduce to mercury concentration to 0 ng/m3 varies between 5 - 6 minutes. The graphs also have a slight curve and are less linear than the unmodified light sample. The decrease in the mercury is a more gradual process. The efficiency curves in figures 4.62 – 4.64 also show that 100% of mercury is adsorbed until around 58 mins; at this point, efficiency gradually declines to 99%. Breakthrough was not achieved in the duration during which the experiment was conducted.

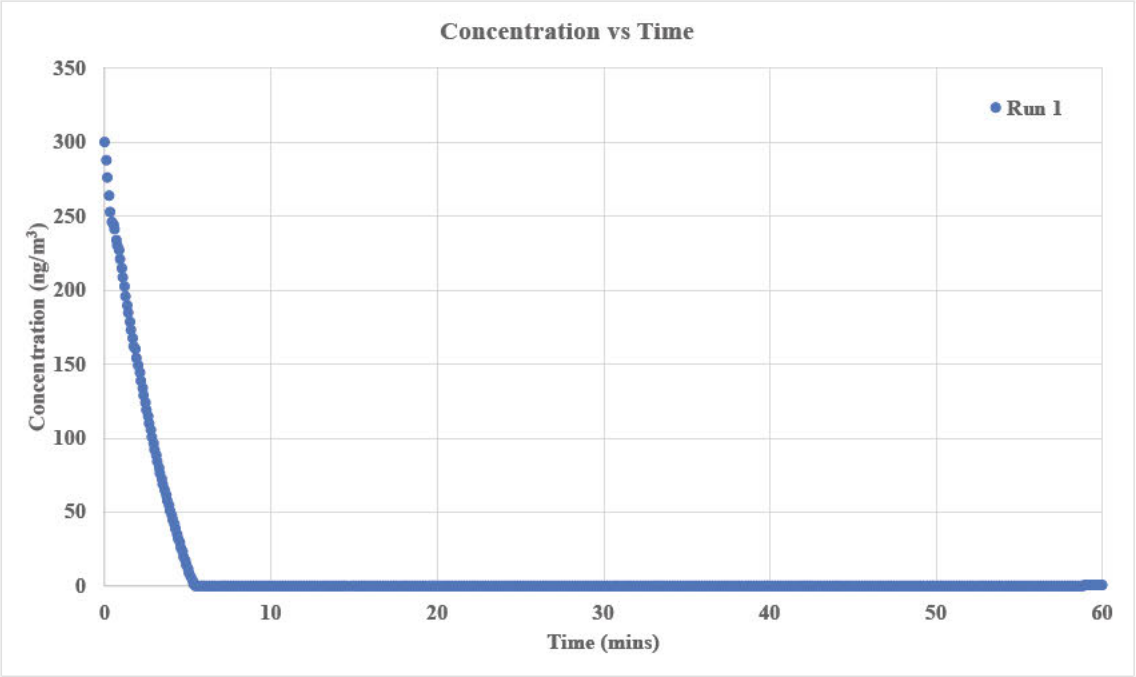

Figure 4.59: Run 1 Hg adsorption curve at 200℃ for modified light-$CuSO_4$ fly ash sample.

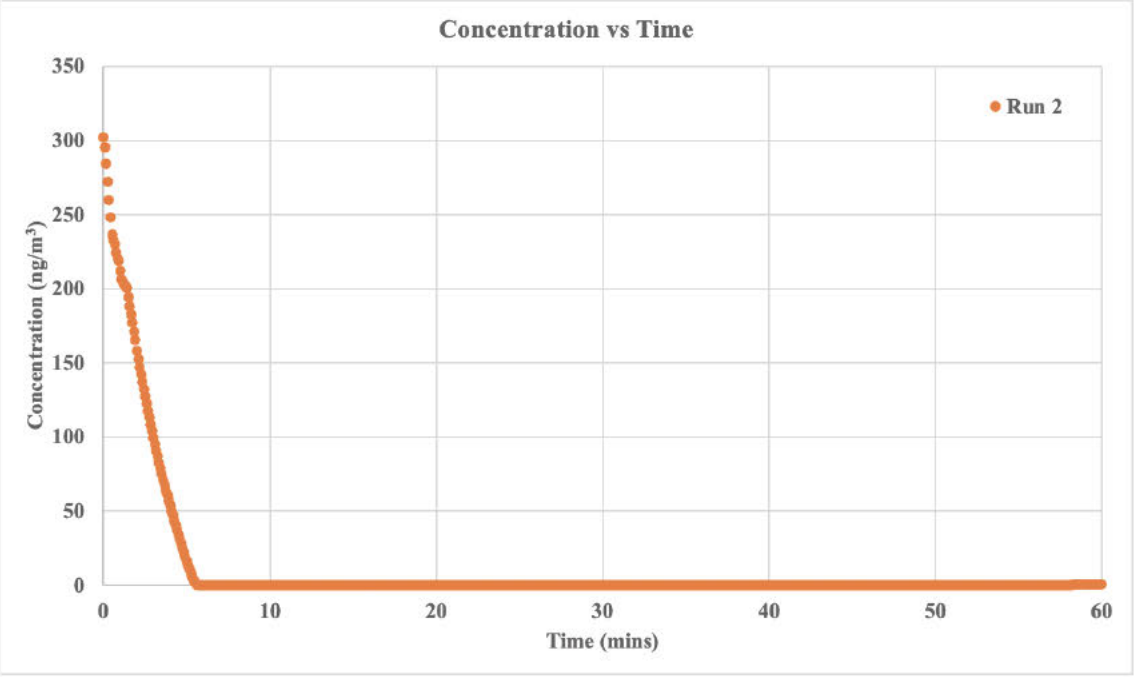

Figure 4.60: Run 2 Hg adsorption curve at 200℃ for modified light-$CuSO_4$ fly ash sample.

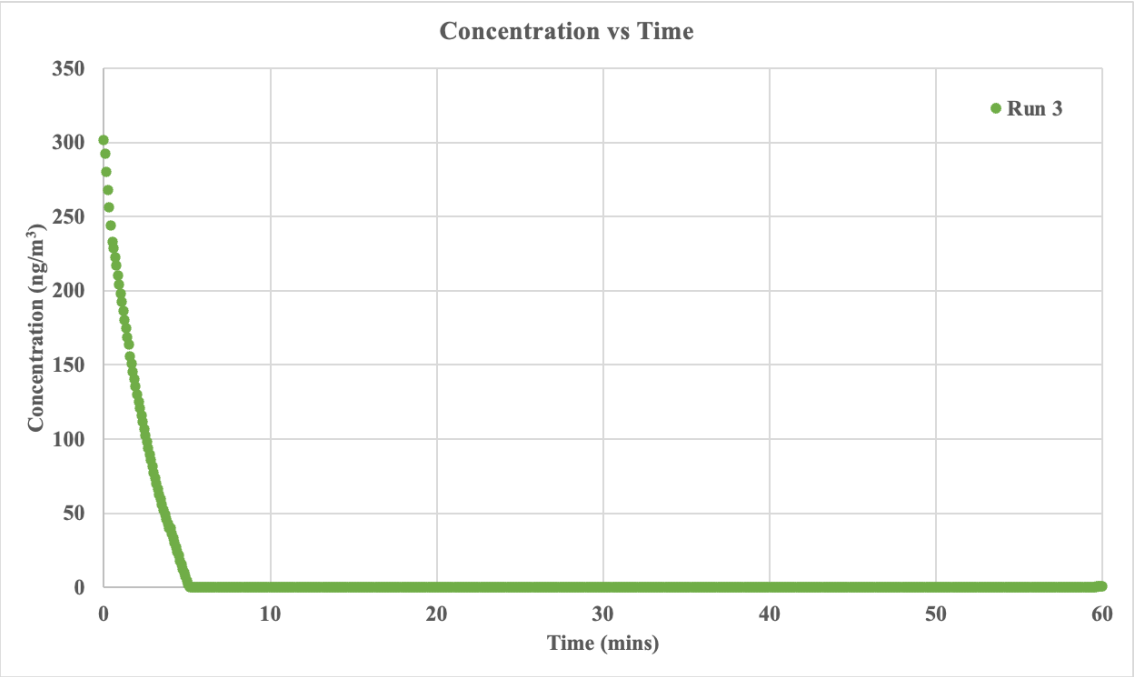

Figure 4.61: Run 3 Hg adsorption curve at 200℃ for modified light-$CuSO_4$ fly ash sample.

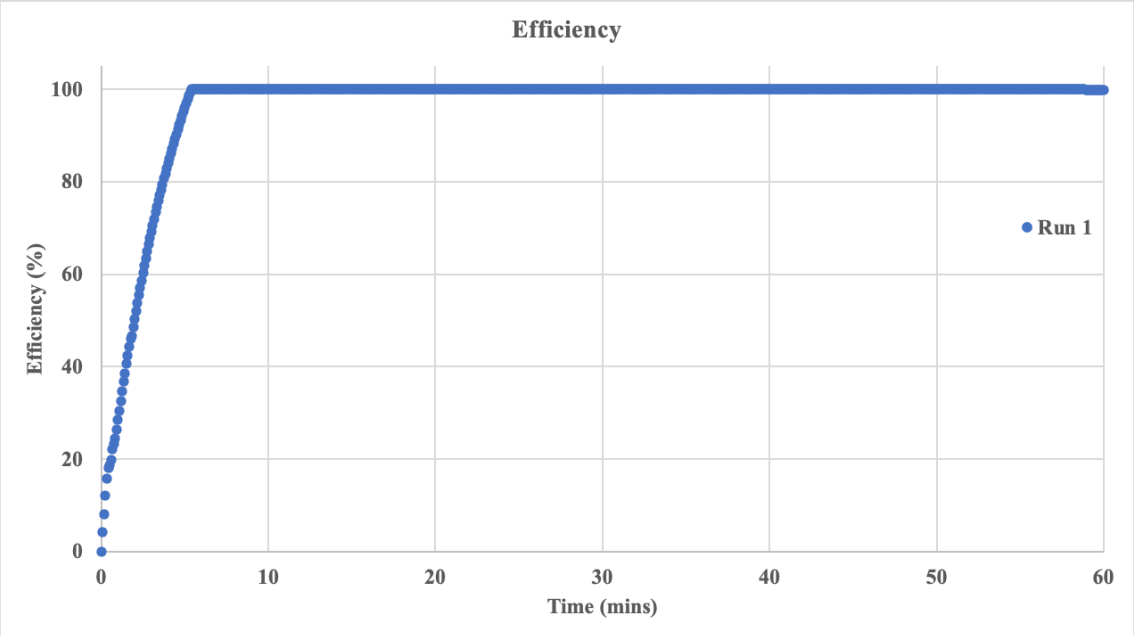

Figure 4.62: Run 1 of Hg adsorption efficiency curve at 200℃ for modified light-$CuSO_4$ fly ash sample

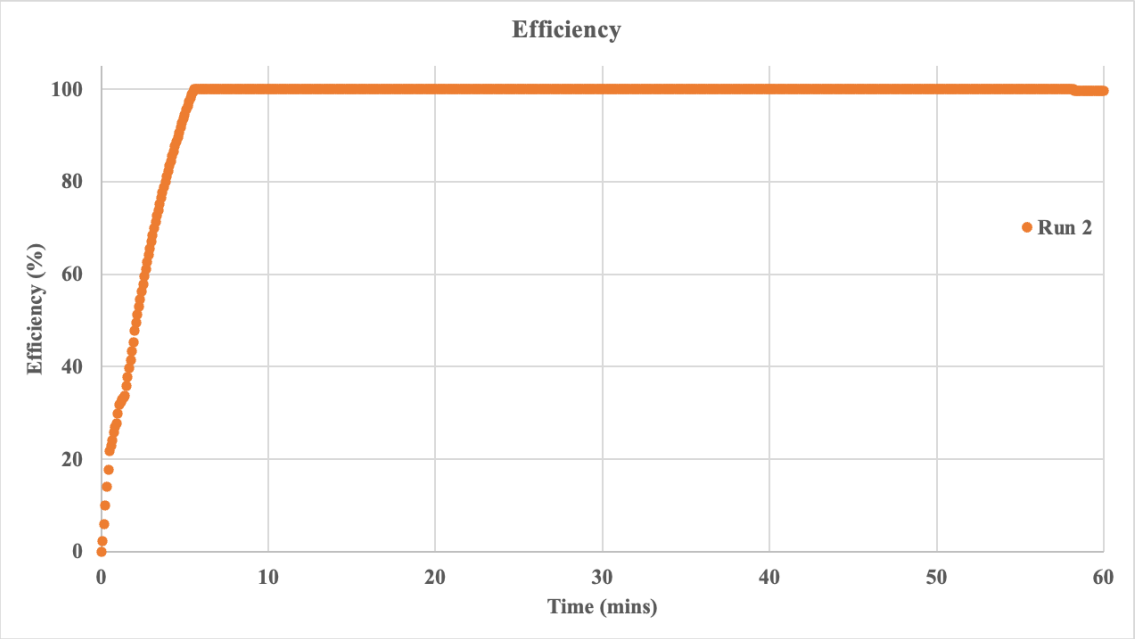

Figure 4.63: Run 2 of Hg adsorption efficiency curve at 200℃ for modified light-$CuSO_4$ fly ash sample

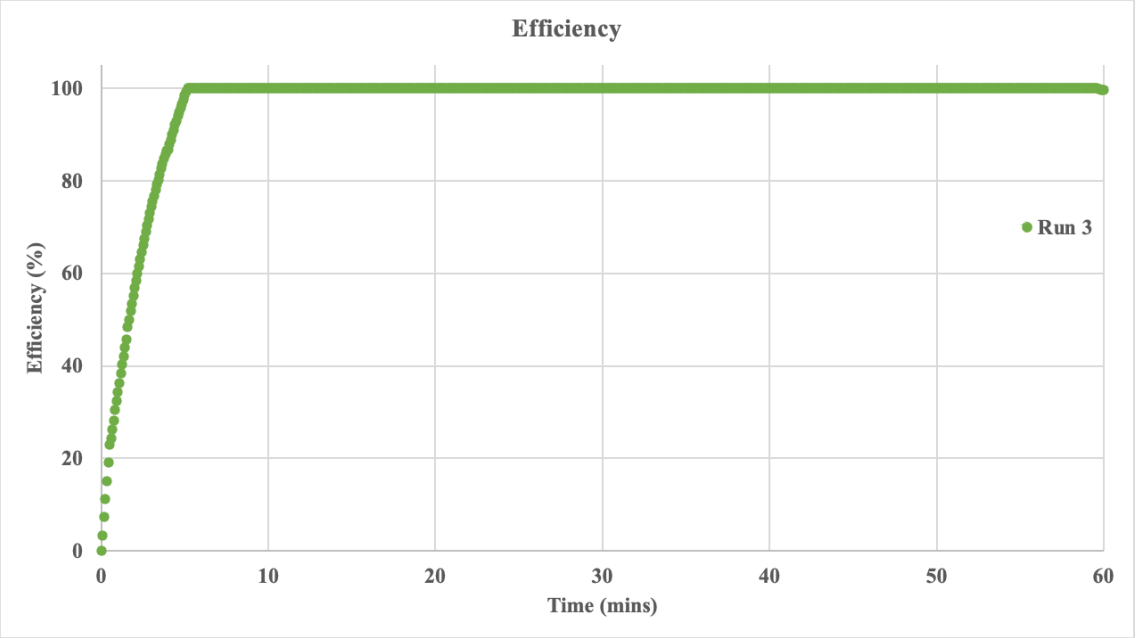

Figure 4.64: Run 3 of Hg adsorption efficiency curve at 200℃ for modified light-$CuSO_4$ fly ash sample

Figures 4.65 – 4.67, which show the adsorption of mercury with the modified dark-$ZnCl_2$ fly ash sample, show that the rate at which the adsorption occurs is slower than the adsorption with dark and modified $CuSO_4$ fly ash samples, where the time taken to reduce to mercury concentration to 0 ng/m^3 varies between 5 – 8 minutes. The graphs also have a visible curve with a more gradual decrease in concentration compared to the dark and modified $CuSO_4$ fly ash samples. The efficiency curves in figures 4.68 – 4.70 also show that 100% of mercury is adsorbed until around 59 mins, where there is a gradual decline in the efficiency to 99%. Breakthrough was not achieved in the duration during which the experiment was conducted.

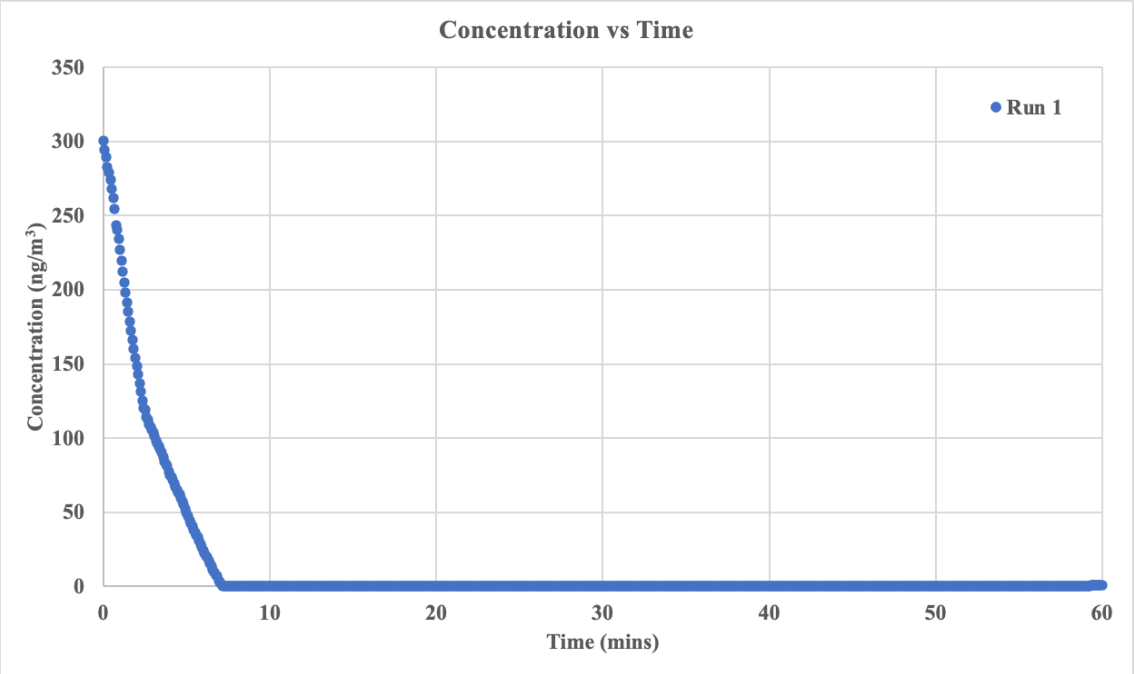

Figure 4.65: Run 1 of Hg adsorption curve at 200°C for modified light-$ZnCl_2$ fly ash sample.

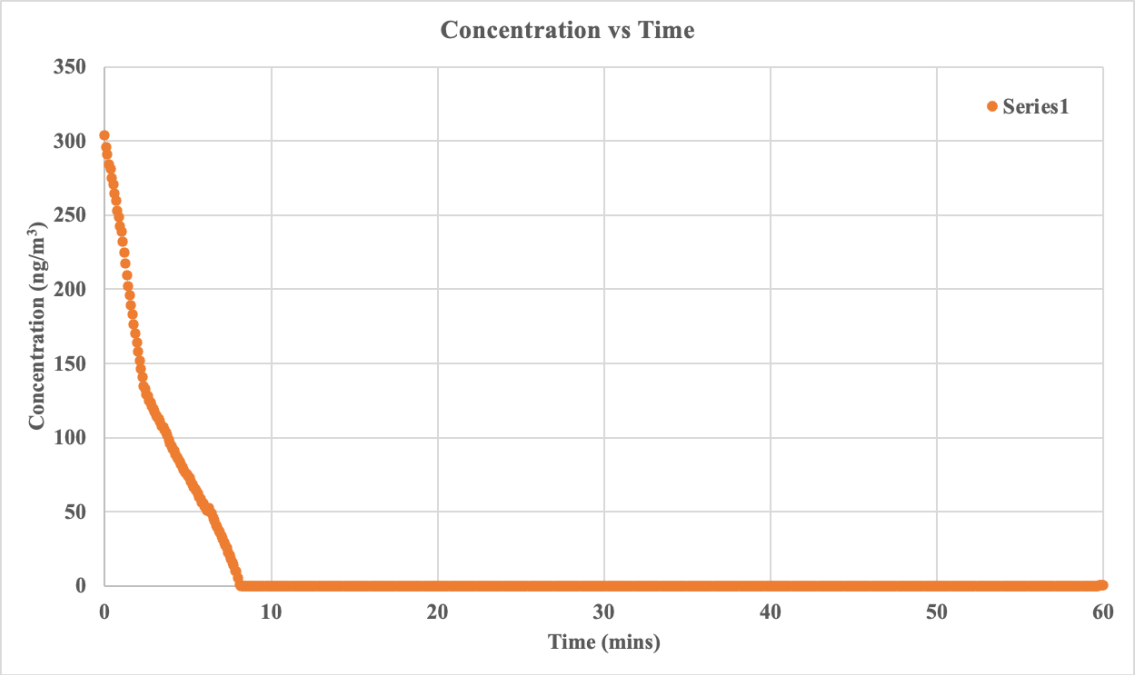

Figure 4.66: Run 2 of Hg adsorption curve at 200°C for modified light-$ZnCl_2$ fly ash sample.

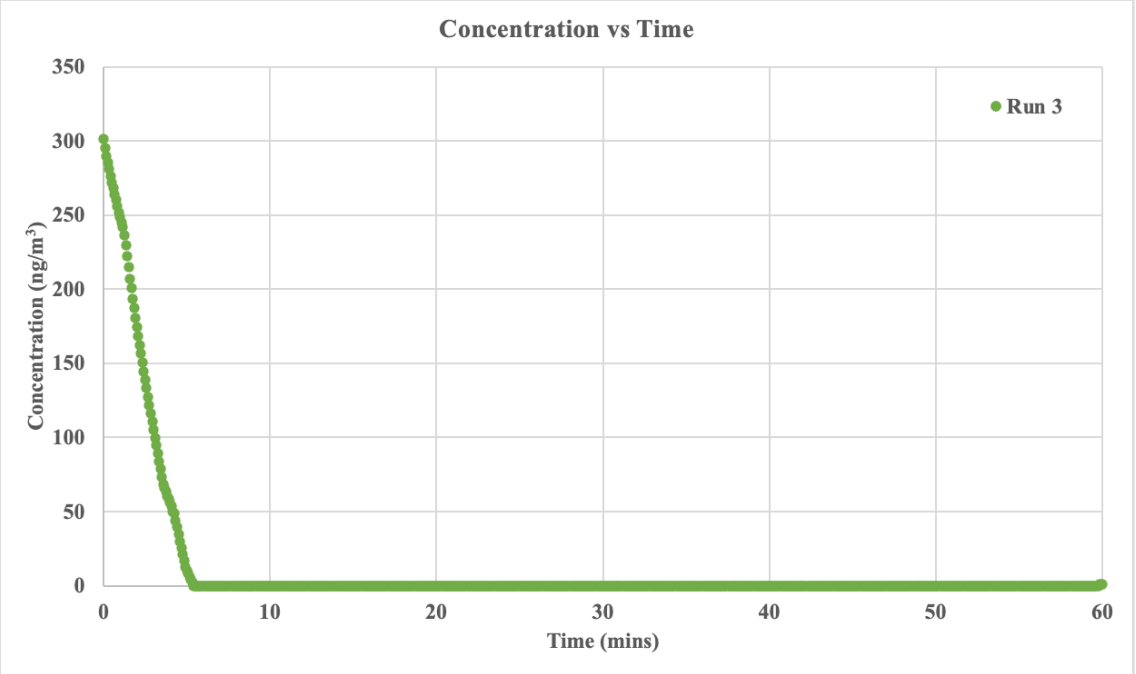

Figure 4.67: Run 3 of Hg adsorption curve at 200°C for modified light-$ZnCl_2$ fly ash sample.

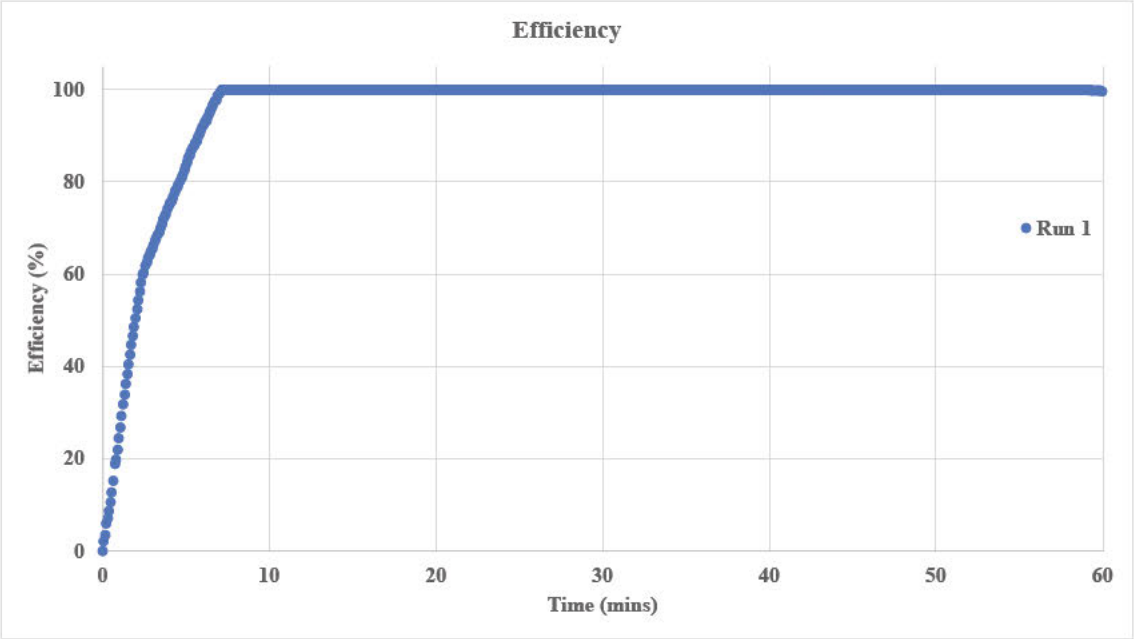

Figure 4.68: Run 1 of Hg adsorption efficiency curve at 200℃ for modified light-$ZnCl_2$ fly ash sample.

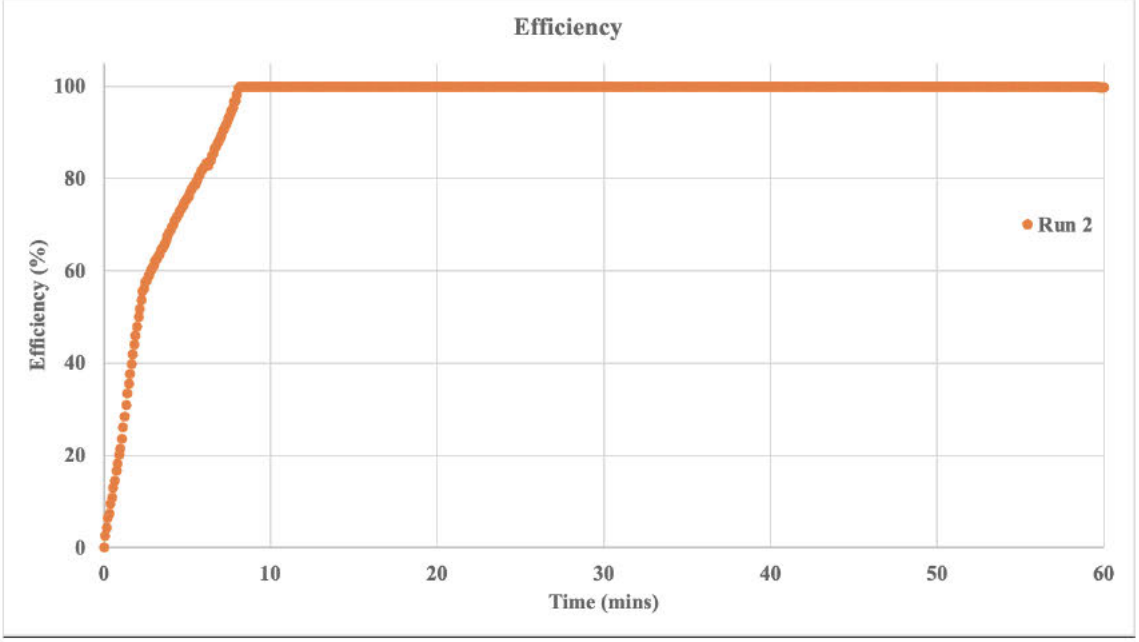

Figure 4.69: Run 2 of Hg adsorption efficiency curve at 200℃ for modified light-$ZnCl_2$ fly ash sample.

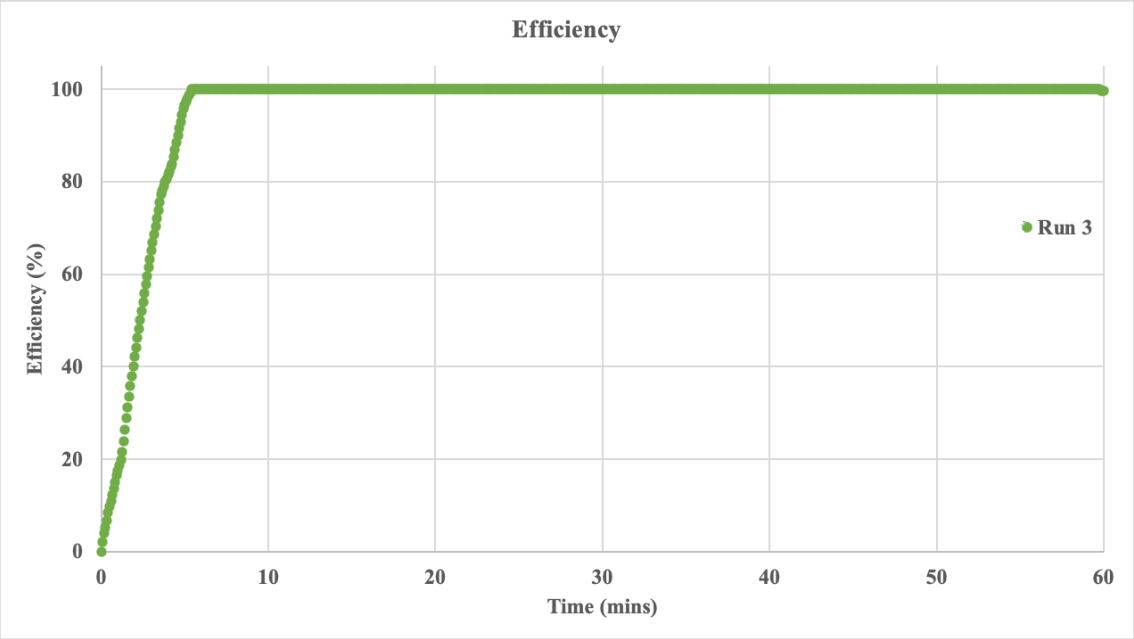

Figure 4.70: Run 1 of Hg adsorption efficiency curve at 200℃ for modified light-$ZnCl_2$ fly ash sample.

Figures 4.71 – 4.73, which show the adsorption of mercury with the modified dark-$FeCl_3$ fly ash sample, show that the rate at which the adsorption occurs is significantly slower than any of the other samples that were tested, where the time taken to reduce to mercury concentration to 0 ng/m3 varies between 22 – 24 minutes. The graphs also have a distinct curve, showing that the adsorption occurs gradually compared to the quick decrease in the other fly ash samples. The efficiency curves in Figures 4.74 – 4.76 also show that 100% of mercury is adsorbed for the duration of the experiment (1 hour). Breakthrough was not achieved in the duration during which the experiment was conducted.

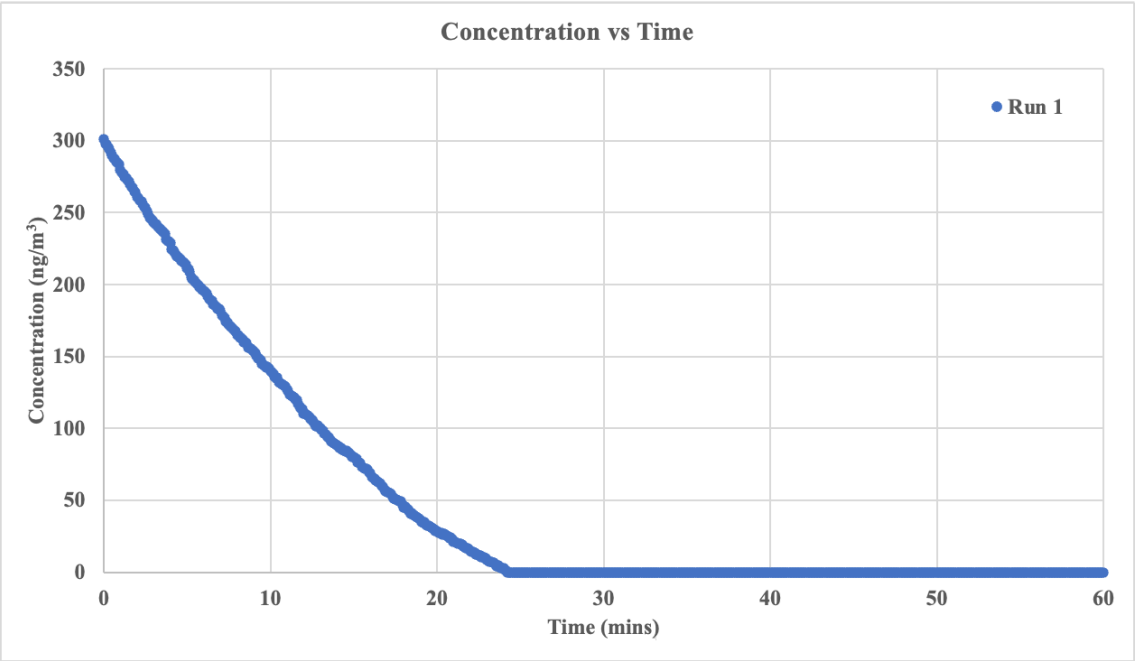

Figure 4.71: Run 1 of Hg adsorption curve at 200℃ for modified light-$FeCl_3$ fly ash sample.

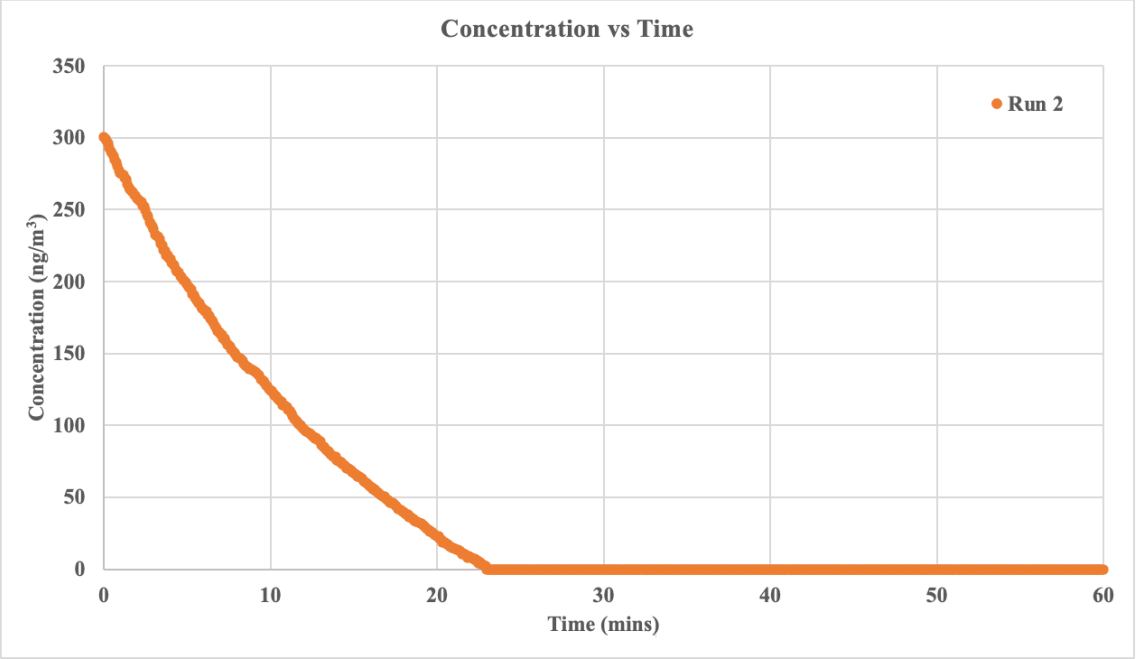

Figure 4.72: Run 2 of Hg adsorption curve at 200℃ for modified light-$FeCl_3$ fly ash sample.

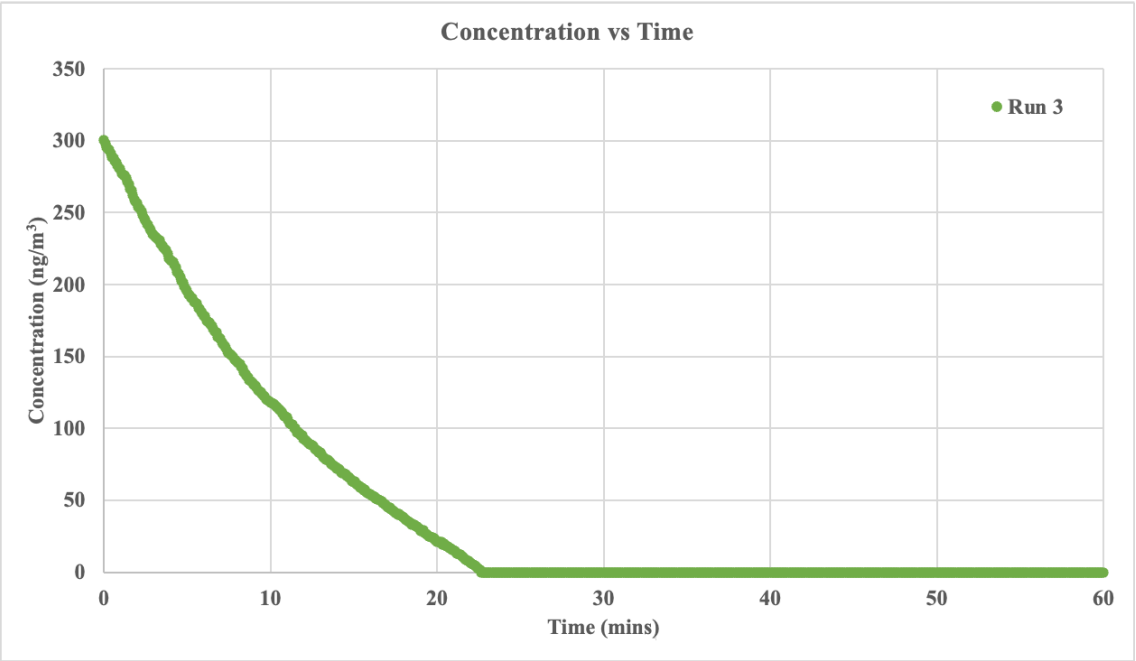

Figure 4.73: Run 3 of Hg adsorption curve at 200℃ for modified light-$FeCl_3$ fly ash sample.

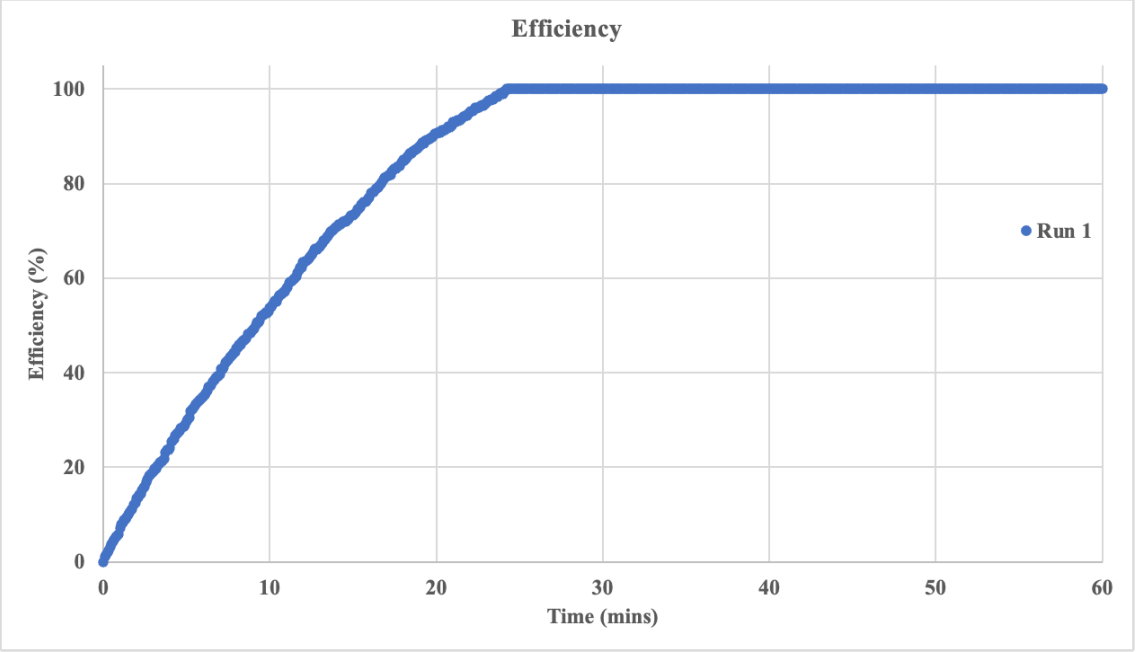

Figure 4.74: Run 1 of Hg adsorption efficiency curve at 200℃ for modified light-$FeCl_3$ fly ash sample.

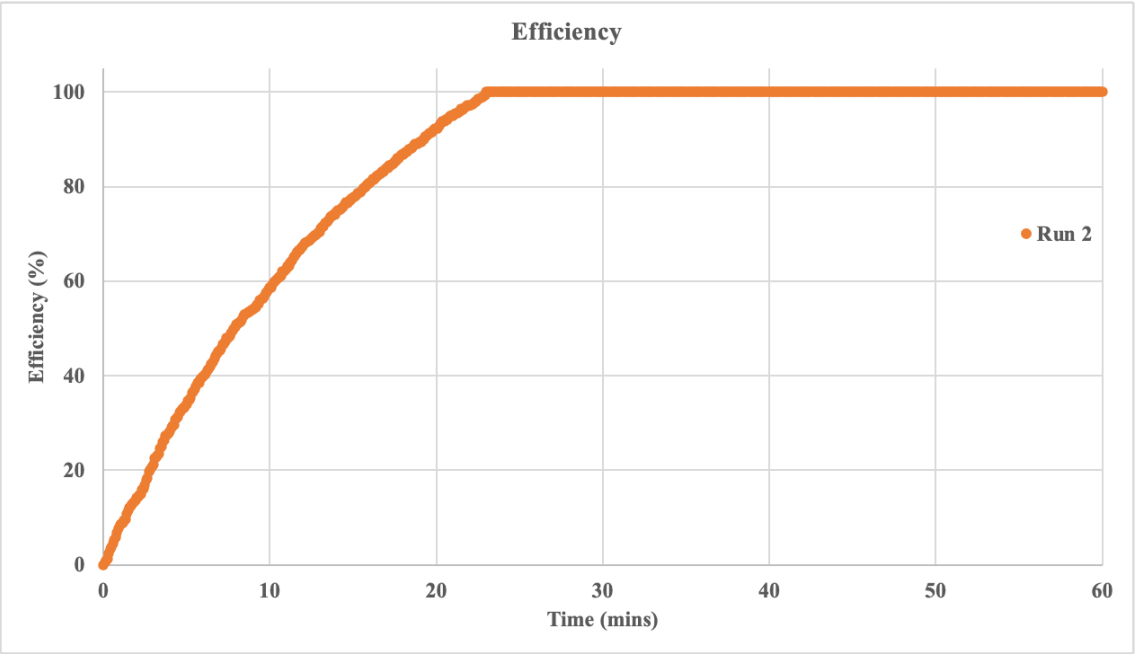

Figure 4.75: Run 2 of Hg adsorption efficiency curve at 200℃ for modified light-$FeCl_3$ fly ash sample.

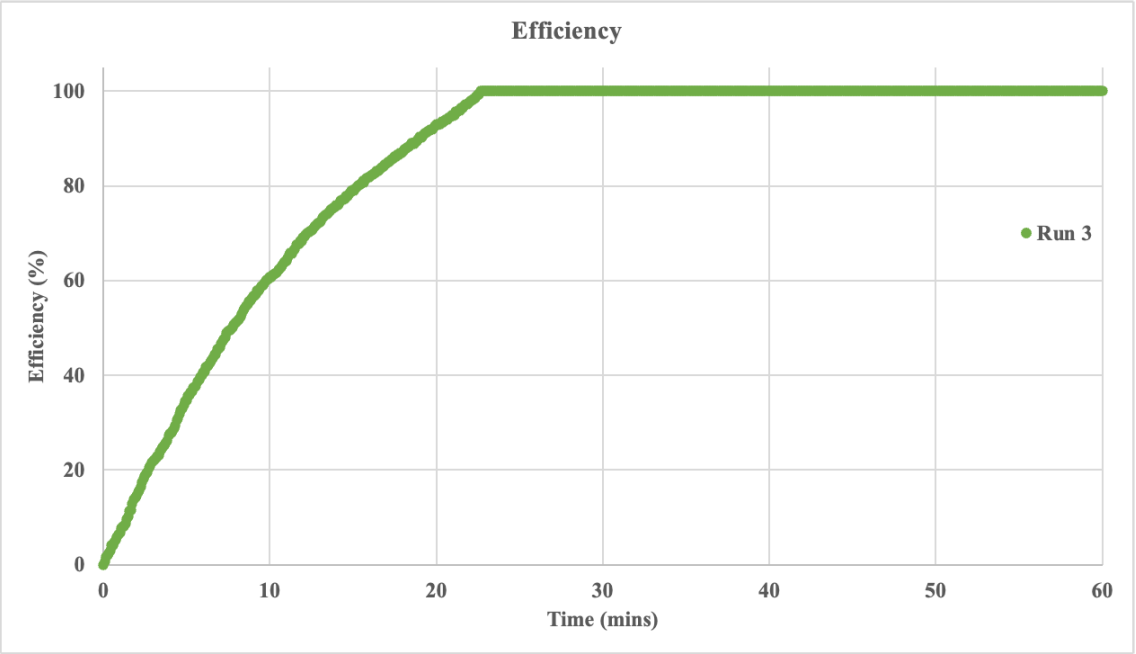

Figure 4.76: Run 3 of Hg adsorption efficiency curve at 200℃ for modified light-$FeCl_3$ fly ash sample.

An assessment of figures 4.77 – 4.79, which shows the adsorption of mercury with the modified dark-$CuCl_2$ fly ash sample, shows that the rate at which the adsorption occurs is slower than the adsorption with dark, modified $CuSO_4$ and modified $ZnCl_2$ fly ash samples, where the time taken to reduce to mercury concentration to 0 ng/m3 varies between 15 – 16 minutes. The adsorption rate is quicker than the modified dark $FeCl_3$ sample. The graphs also have a visible curve with a more gradual decrease in concentration compared to the dark, modified dark $CuSO_4$ and modified dark $ZnCl_2$ fly ash samples. The efficiency curves in figures 4.80 – 4.83 also show that 100% of mercury is adsorbed for the duration of the experiment (1 hour). Breakthrough was not achieved in the duration during which the experiment was conducted.

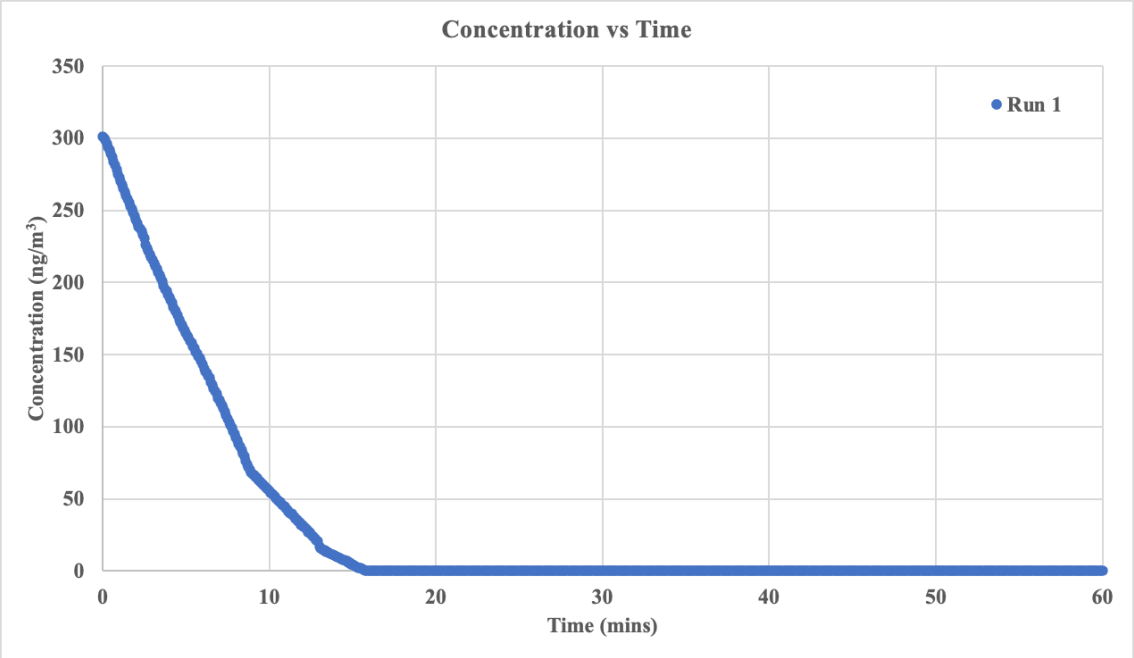

Figure 4.77: Run 1 of Hg adsorption curve at 200℃ for modified light-$CuCl_2$ fly ash sample.

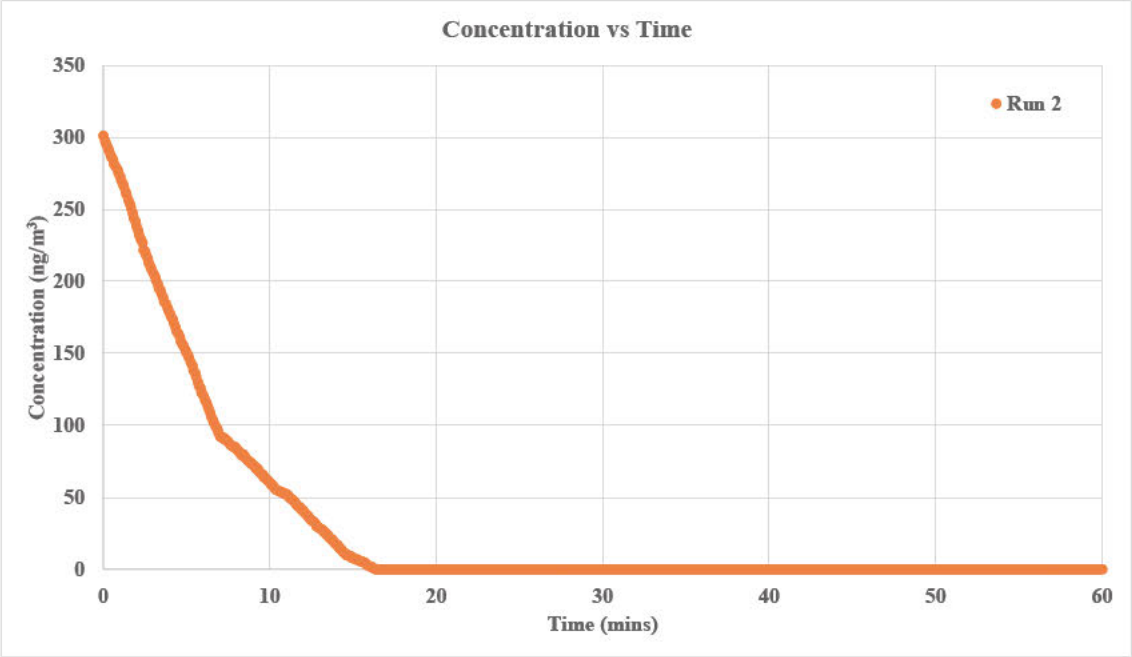

Figure 4.78: Run 2 of Hg adsorption curve at 200℃ for modified light-$CuCl_2$ fly ash sample.

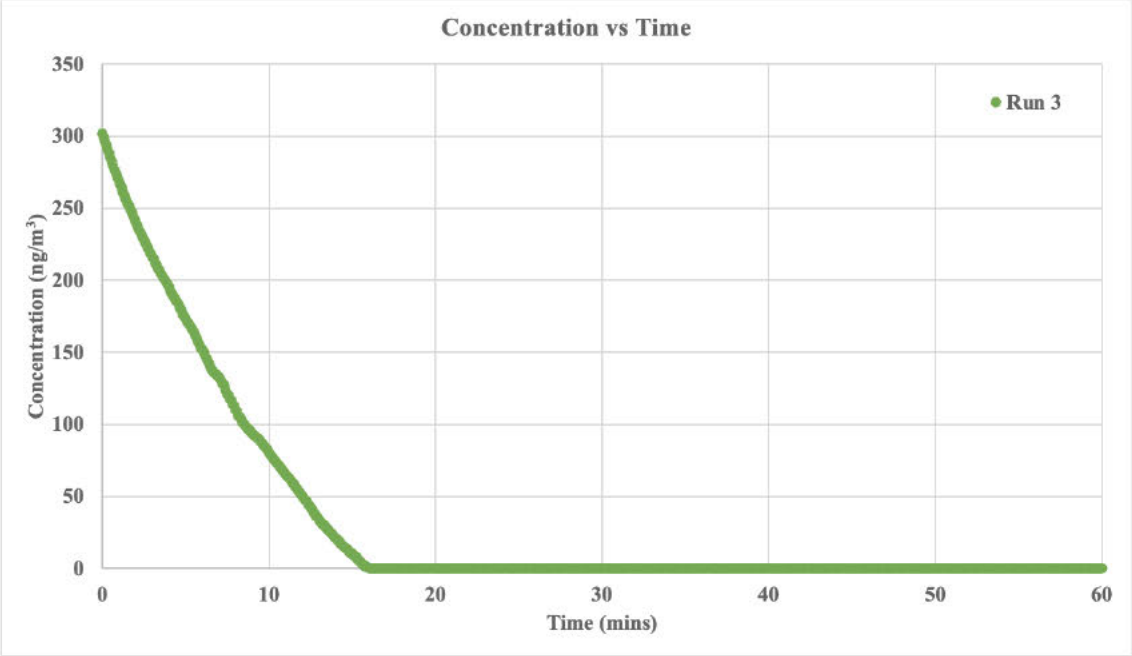

Figure 4.79: Run 3 of Hg adsorption curve at 200℃ for modified light-$CuCl_2$ fly ash sample.

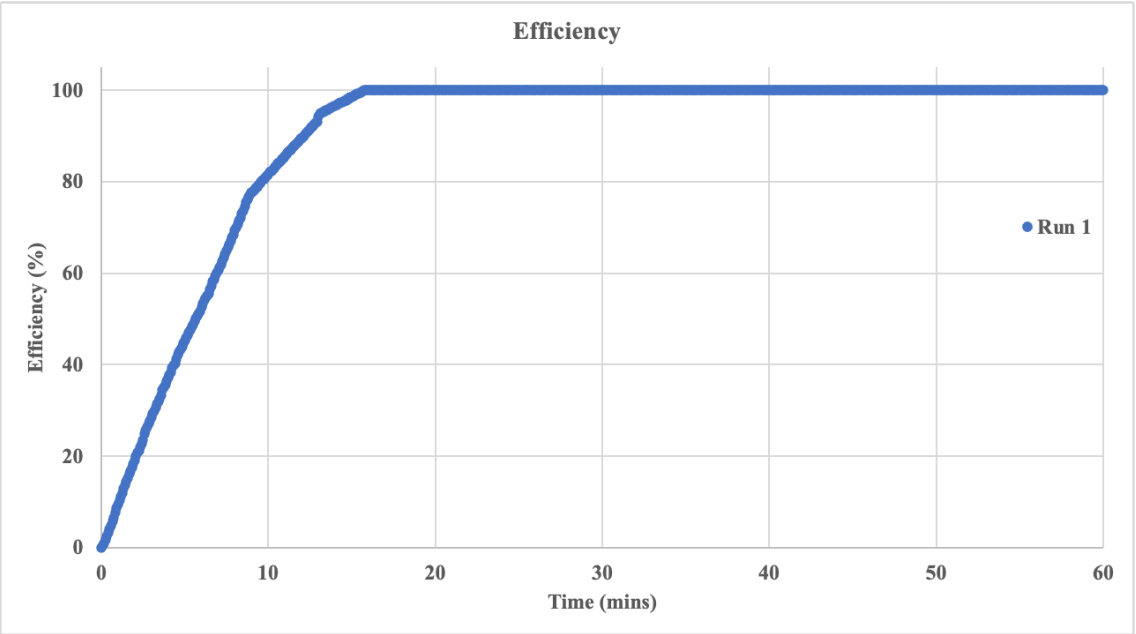

Figure 4.80: Run 1 of Hg adsorption efficiency curve at 200℃ for light-$CuCl_2$ fly ash sample

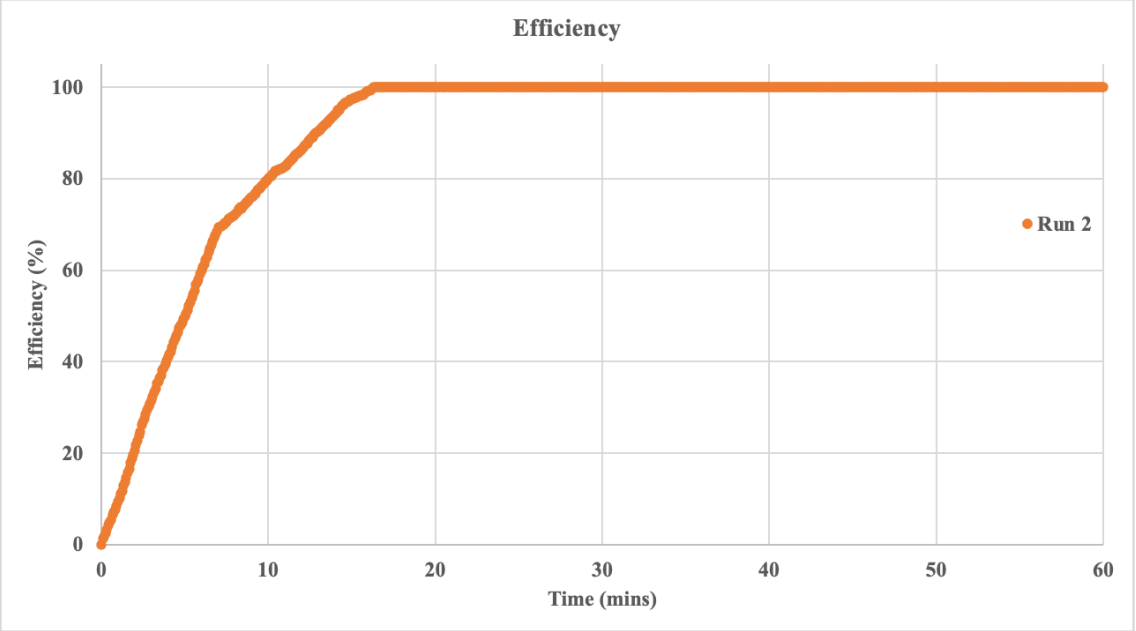

Figure 4.81: Run 2 of Hg adsorption efficiency curve at 200℃ for light-$CuCl_2$ fly ash sample

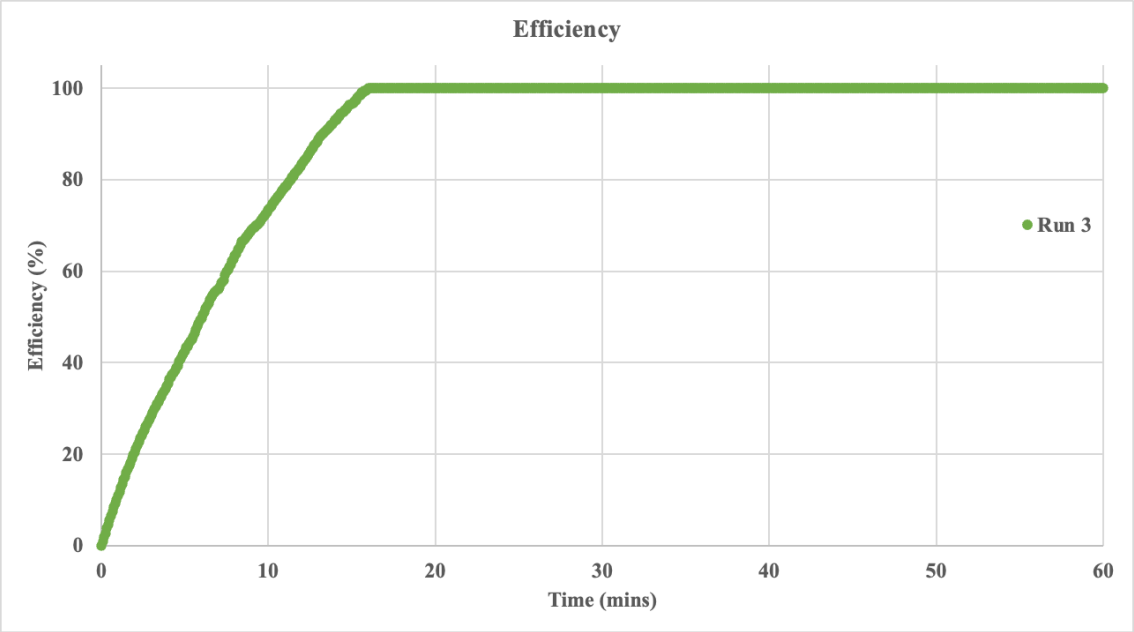

Figure 4.82: Run 3 of Hg adsorption efficiency curve at 200℃ for light-$CuCl_2$ fly ash sample

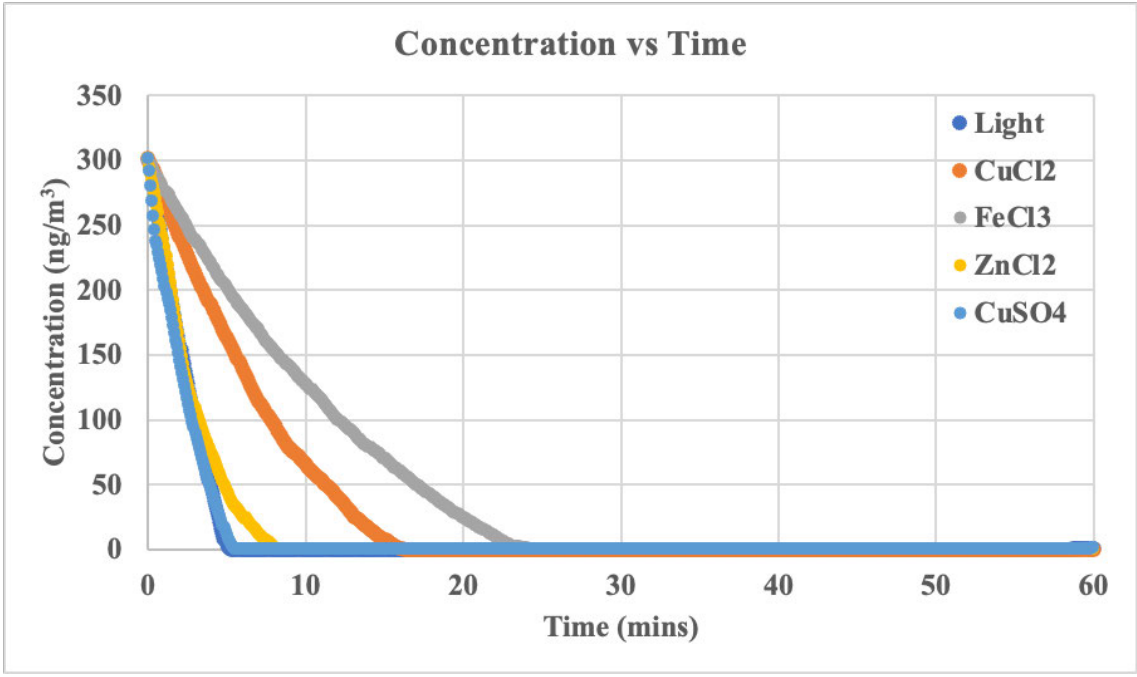

Figure 4.83: Cumulative Hg adsorption curve at 200℃ for light and modified light fly ash samples

4.3.3 Adsorption Tests for Dark Fly Ash and Modified Dark Fly Ash Samples at 150℃

Figure 4.84 – figure 4.85 shows the adsorption curves for the modified dark-$CuSO_4$ fly ash sample, the adsorption process is quick as seen by the gradient of the adsorption curve. It takes 3 - 4 minutes for the concentration to drop to 0 ng/m^3 from an initial 300 ng/m^3 concentration. Whilst the time taken to drop to 0 ng/m^3 varies, the trajectory of the adsorption curve is the same for each of the experimental runs conducted. The quick reduction in the mercury concentration could be consistent with the physisorption mechanism. Figure 4.86 – figure 4.87 shows the adsorption efficiency curves for the light fly ash sample; the sample shows 100% adsorption until 58.83 mins for run 1 and 59.25 mins for run 2 where there is a slight decline to 99%. However, a breakthrough was not achieved in 1 hour.

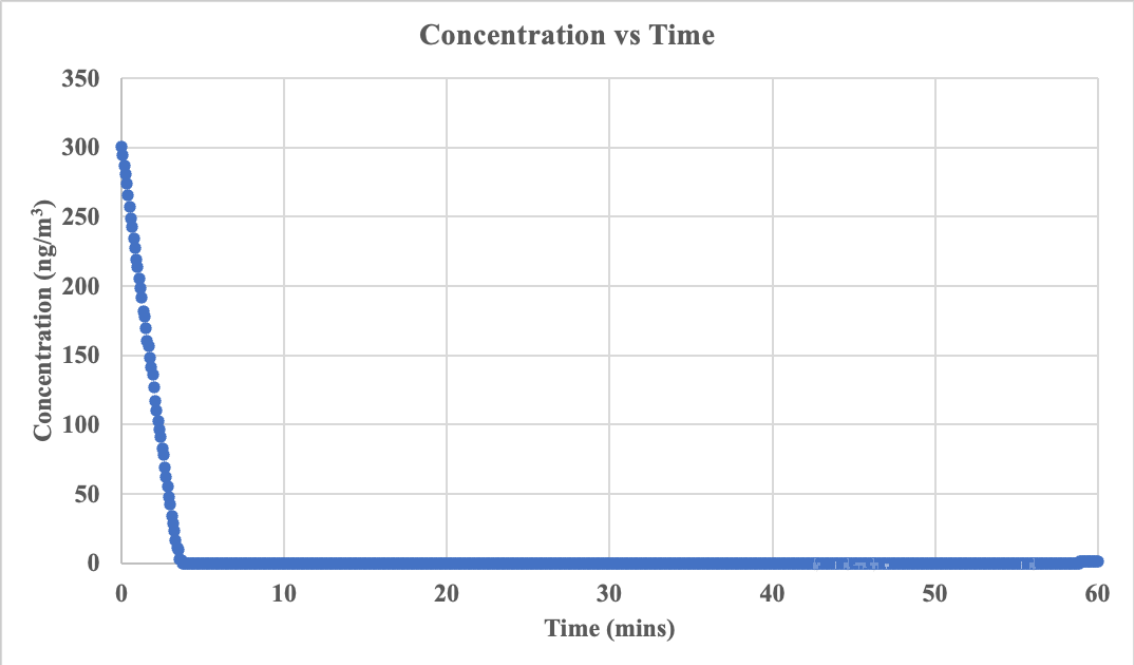

Figure 4.84: Run 1 Hg adsorption curve at 150℃ for modified dark-$CuSO_4$ fly ash sample.

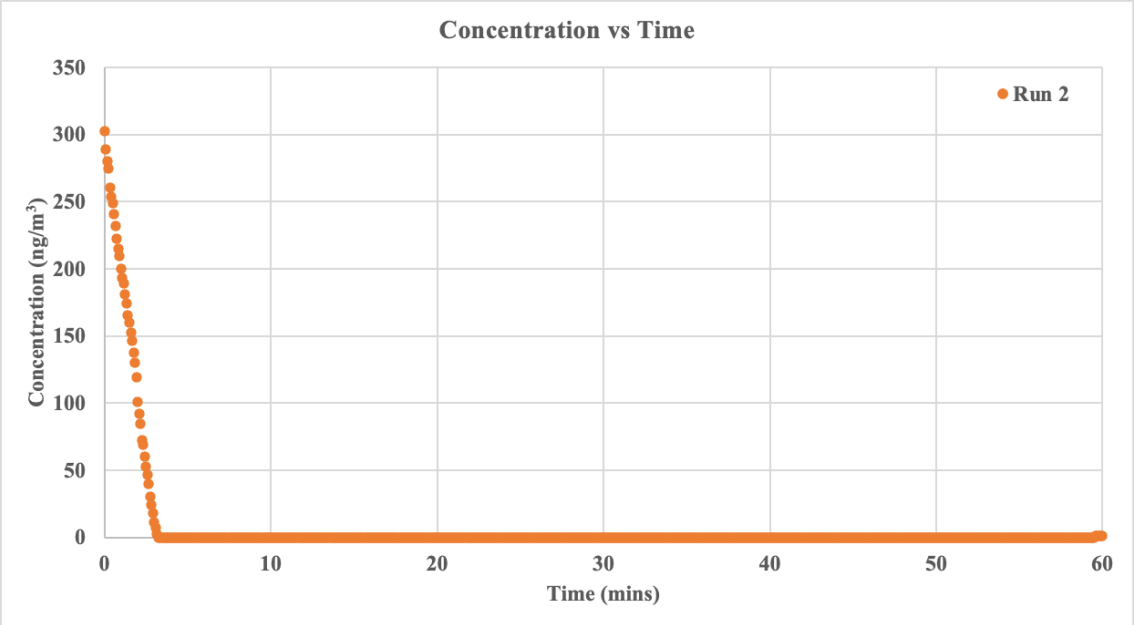

Figure 4.85: Run 2 Hg adsorption curve at 150℃ for modified dark-$CuSO_4$ fly ash sample.

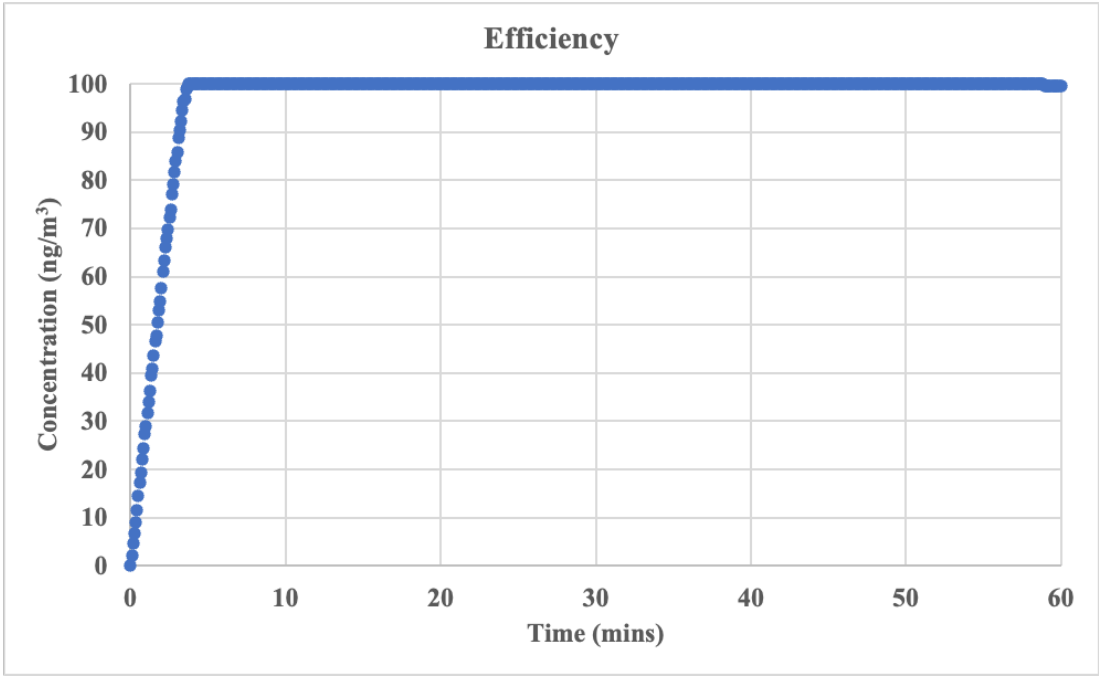

Figure 4.86: Run 2 of Hg adsorption efficiency curve at 150℃ for modified dark-$CuSO_4$ fly ash sample

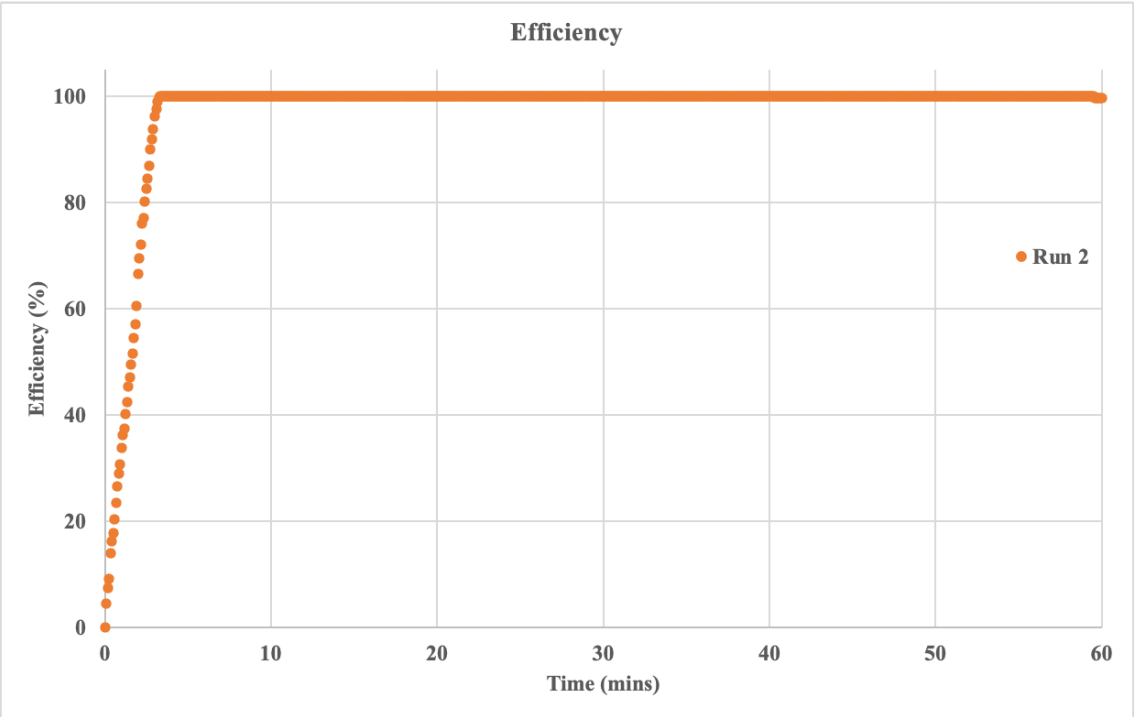

Figure 4.87: Run 2 of Hg adsorption efficiency curve at 150℃ for modified dark-$CuSO_4$ fly ash sample

4.3.4 Adsorption Tests for Light Fly Ash and Modified Light Fly Ash Samples at 150°C

Figure 4.88 – figure 4.89 shows the adsorption curves for the modified light-$CuSO_4$ fly ash sample, the adsorption process is quick as seen by the gradient of the adsorption curve. It takes 3 - 4 minutes for the concentration to drop to 0 ng/m^3 from an initial 300 ng/m^3 concentration. Figure 4.90 – figure 4.91 shows the adsorption efficiency curves for the light fly ash sample; the sample shows 100% adsorption until 57.83 mins for run 1 and 58 mins for run 2 where there is a slight decline to 99%. However, a breakthrough was not achieved in 1 hour. The decline in efficiency is gradual and not rapid, as seen by the values in Appendix B.

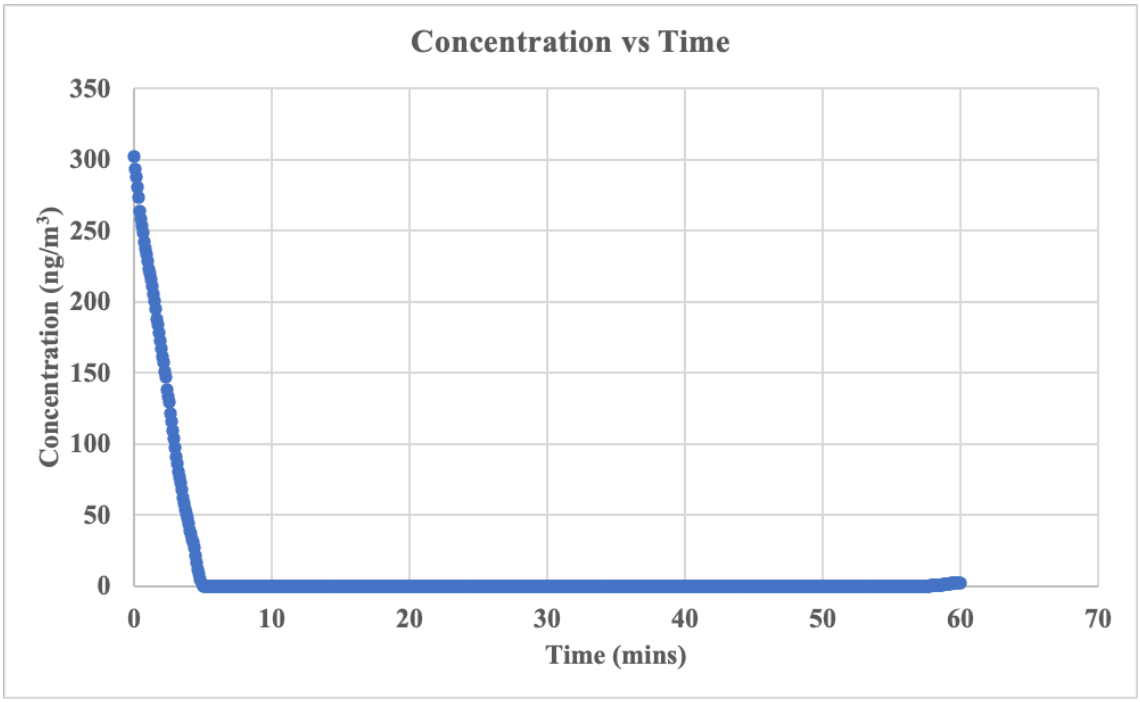

Figure 4.88: Run 1 Hg adsorption curve at 150℃ for modified light-$CuSO_4$ fly ash sample

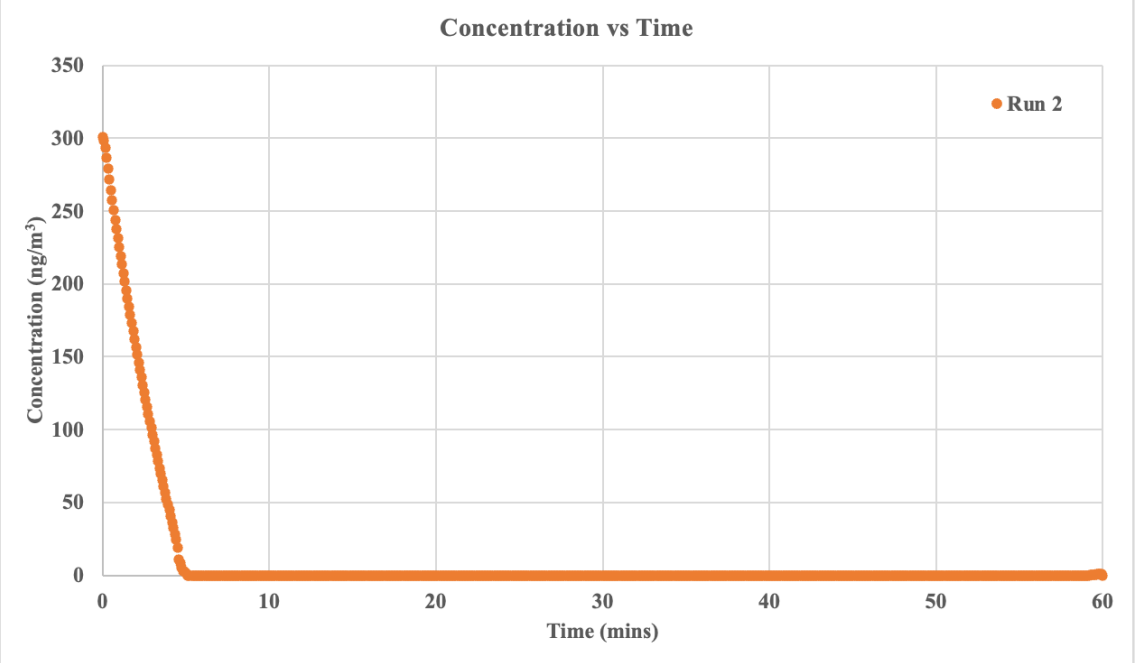

Figure 4.89: Run 1 Hg adsorption curve at 150℃ for modified light-$CuSO_4$ fly ash sample.

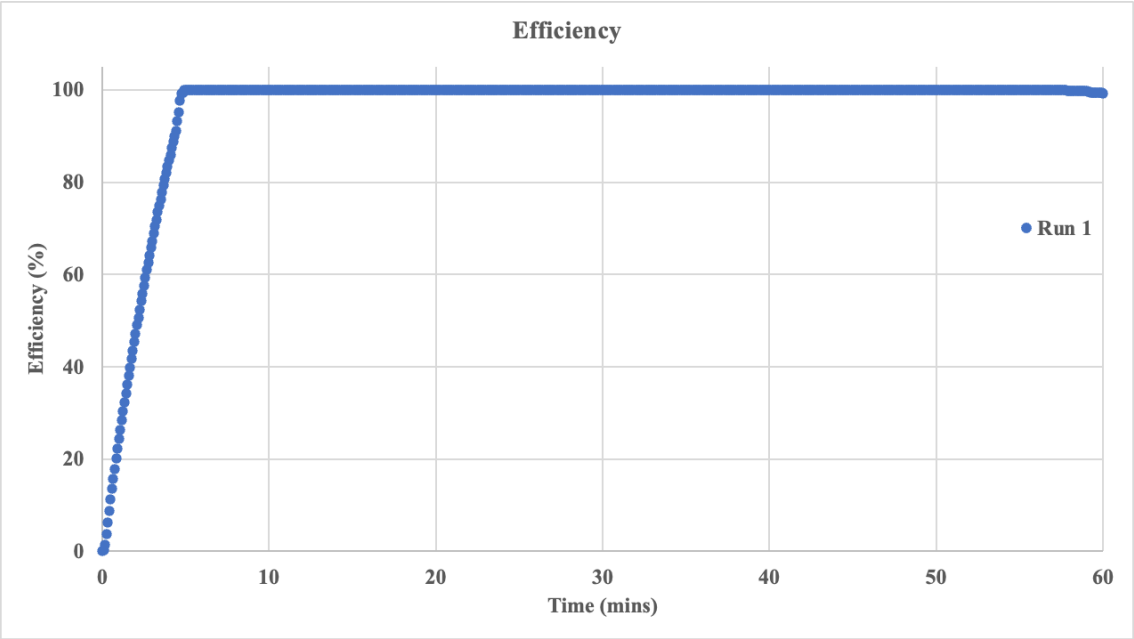

Figure 4.90: Run 1 of Hg adsorption efficiency curve at 150℃ for modified light-$CuSO_4$ fly ash sample

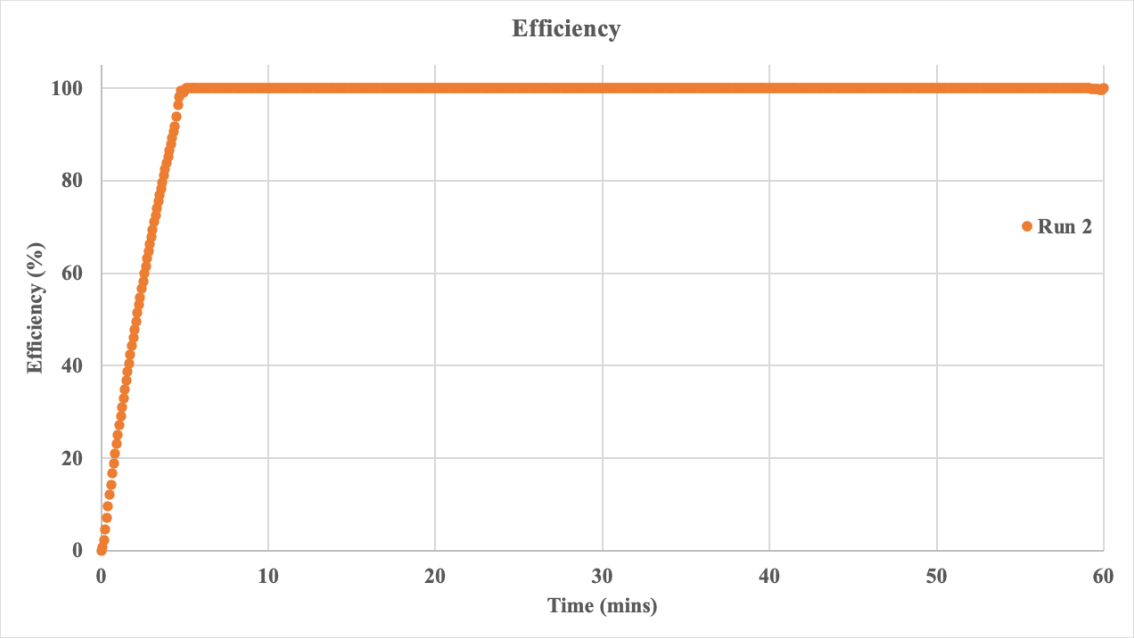

Figure 4.91: Run 2 of Hg adsorption efficiency curve at 150℃ for modified light-$CuSO_4$ fly ash sample

4.4 Evaluation of Current Emission Control Technology, Integration of Proposed Mercury Adsorption onto Fly Ash Process, Costing and Environmental Impact Assessment

Eskom currently has 15 coal-fired powered plants in operation. The power plants are listed below in order of largest to smallest installed capacity (Generation Division, 2021):

Table 4.3: Installed Electricity Generation Capacity for Eskom's Coal-Fired Power Stations (Eskom, 2023)

Power Station	Installed Capacity (MW)
Medupi	4764
Kendal	4116
Majuba	4110
Matimba	3990
Lethabo	3708
Tutuka	3654
Matla	3600
Duvha	3000
Kriel	3000
Kusile	2397
Arnot	2220
Hendrina	1723
Camden	1561
Grootvlei	1180
Komati	Decommissioned – October 2022

The generation capacity indicates the amounts of pollutants that can be emitted. The higher the generation capacity, the greater the production of possible pollutants such as PM, SO_2, NOx and Hg. Power stations with a higher generation capacity need better emission control technology installed to meet minimum emission limits due to the large throughput of coal.

In addition to the 15 coal-fired power stations, 14 peaking power stations are in operation to supplement the power generated from base stations (coal and nuclear), especially during breakdown periods or when demand is high. These peaking power stations, which can be classified as gas turbine stations, hydroelectric, hydro pumped storage or wind generation, are shown in Figure 4.92. The peaking power stations have their own control technology and emission standards to abide by and will not be explored further for this project.

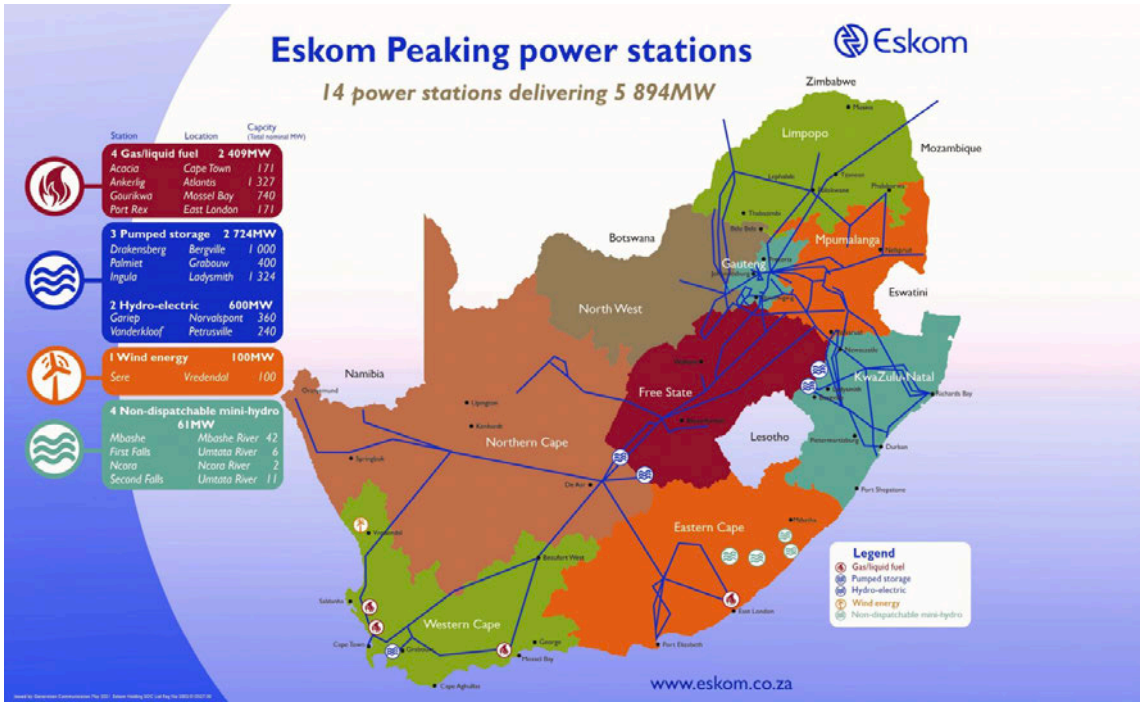

Figure 4.92: Eskom's peaking power stations – alternative power generation methods (Eskom, n.d.)

4.4.1 Status of Eskom's Coal Fired Power Stations

Eskom's power stations can be classified as follows (Patel,2012). The tentative decommissioning dates are stated in Table 4.4.

Table 4.4: Eskom Decommissioning Schedule (Patel, 2012)

Category	Power Station	Scheduled Decommissioning
Oldest	Camden	2025-2028
	Hendrina	2030-2036
	Arnot	2031-2039
	Komati	2022
	Grootvlei	2021-2023
	Kriel	2036-2039
Older	Duvha	2040-2044
	Matla	2039-2043
Midlife	Kendal	2048-2053
	Lethabo	2045-2050
	Majuba	2046-2051
	Matimba	2047-2051
	Tutuka	2045-2050
New	Kusile	2069
	Medupi	2065

Eskom had applied to bypass government pollution regulations for PM, SO_2 and NOx from the coal-fired power stations. Out of the 15 operational power stations, six (Camden, Hendrina, Arnot, Komati, Grootvlei and Kriel) were granted the allowance provided that a detailed decommissioning plan was available by November 2022 and that the stations were decommissioned by 31 March 2030 (Eskom, n.d.). Whilst Komati has since been fully decommissioned as scheduled by October 2022, the decommissioning of the other five power stations has been delayed due to the demand for power in South Africa.

The ruling has also stated that the other seven power stations (Duvha, Matla, Kendal, Lethabo, Majuba, Matimba and Tutuka) will not be granted any leniency for PM, SO_2 and NOx emissions and must follow the minimum emission standards until they are decommissioned as per the schedule set out by Eskom (Eskom, n.d.).

Whilst Kusile has a wet FGD control system, the Medupi power station, which has a planned installation of a wet FGD system, must comply with the pollution emission control limits in the interim (Eskom, n.d.).

Figure 4.93 illustrates the years left until the proposed decommissioning of the coal-fired power stations is scheduled. Komati has been decommissioned since October 2022, and Grootvlei was scheduled for decommissioning in 2023. Assessing the lifespan based on the upper limit for decommissioning year, 11 power stations have over 15 years more of run time. While older power stations have a limited lifespan, the remaining power stations must have effective emission control technology installed to meet emission limits for PM, SO2, NOx, and Hg. An assessment needs to be made regarding which power stations would be most suitable and feasible to retrofit with control technology; otherwise, more renewable sources of energy would have to be explored. The data required to produce Figure 4.93 was obtained from Patel (2012).

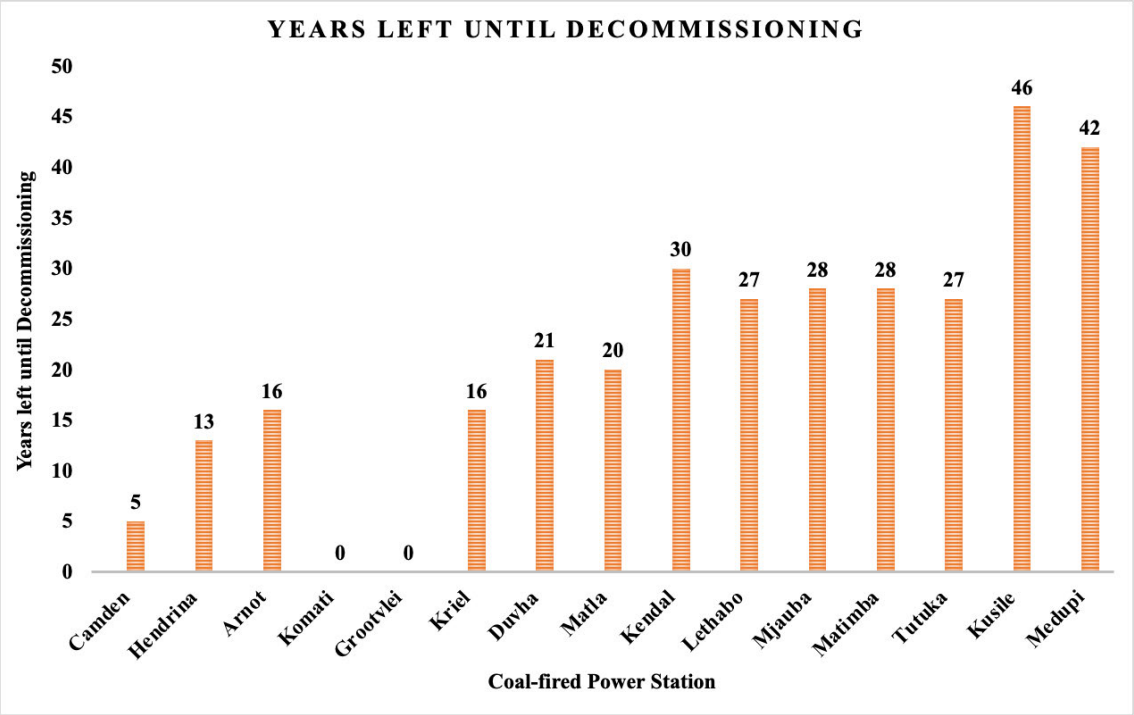

Figure 4.93: Years left until decommissioning.

4.4.2 Emission Control Measures

Table 4.5 shows a comparison of the information collected by Garnham & Langerman (2016) and the current information available from Eskom's Atmospheric Emission License (AEL) (2023) report listing the emission control technology in operation at Eskom's coal-fired power stations then and now.

Table 4.5: Comparison between older and current emission control technology installed at Eskom's power stations.

Power Station	Emission Control Technology – Garnham & Langerman (2016)	Emission Control Technology – AEL Reports 2023
Medupi	FFP's	FFP's
Kendal	ESP+SO_3	ESP+SO_3
Majuba	FFP's	FFP's
Matimba	ESP+SO_3	ESP+SO_3
Lethabo	ESP+SO_3	ESP+SO_3
Tutuka	ESP	ESP
Matla	ESP+SO_3	ESP
Duvha	FFP's & ESP+SO_3	FFP's & ESP+SO_3
Kriel	ESP+SO_3	ESP
Kusile	FFP's & wet FGD	FFP's, LNB and wet FGD
Arnot	FFP's	FFP's
Hendrina	FFP's	FFP's
Camden	FFP's	FFP's
Grootvlei	FFP's & ESP+SO_3	FFP's & ESP+SO_3
Komati	ESP+SO_3	Decommissioned – October 2022

Key: ESP+SO_3 – Electrostatic Precipitator with SO3 flue gas conditioning, FFP's – Fabric Filter Plants and FGD – Flue gas Desulphurisation

The information displayed in Table 4.5 shows that no significant changes have been made to the emission control technology operating at the coal-fired power stations from 2016 – 2023. There are plans to build a FGD system at Medupi as it is a new build with a lifespan going up to 2065. Except for Kusile and Medupi, Eskom's power stations only have emission control technology installed to remove particulate matter.

Table 4.6: Summary of Eskom's Planned Retrofits and Essential Retrofit to meet Emission Limits (Eskom Air Quality Improvement Plan, 2023)

Power Station	Planned Retrofits	Required Retrofits to meet Minimum Emission Limits
Medupi	FGD	-
Kendal	HFT, ESP+SO_3 Plant, DHP refurbishment and FGD	-
Majuba	LNB	FGD
Matimba	HFT, ESP+SO_3 Plant, DHP refurbishment and FGD	-
Lethabo	HFT, ESP+SO_3 Plant Upgrade, DHP refurbishment	LNB AND FGD
Tutuka	FFP and LNB	FGD
Matla	HFT, ESP Upgrade and LNB	FGD
Duvha	HFT, ESP+SO_3 Plant, DHP refurbishment	LNB AND FGD
Kriel	FFP's	LNB and FGD
Kusile		
Arnot		LNB Optimisation and FGD
Hendrina		LNB and FGD
Camden		LNB Optimisation and FGD
Grootvlei	FFP's	LNB Optimisation and FGD
Komati		Decommissioned – October 2022

Key: ESP+SO_3 – Electrostatic Precipitator with SO_3 flue gas conditioning, FFP's – Fabric Filter Plants, FGD – Flue Gas Desulphurisation, LNB- Low NOx Burner, HFT – High Frequency Transformer and DHP – Dust Handling Plant

Table 4.6 shows Eskom's plans to retrofit emission control technology to the coal-fired power stations and the necessary emission control technology required to adhere to minimum emission limits for PM, SO_2 and NOx. The information presented in Table 4. shows that a significant amount of work needs to be done to meet the world standards in controlling emissions. While the ESP+SO_3 or FFP may remove Hg in particulate form, there is no other control technology in place currently to remove mercury as Hg^0 and Hg^{2+}, and there are no plans to install emission technology in the future.

4.4.3 Evaluation of Current Control Technology

Eskom's current control technology consists of the older ESP+SO_3 systems, the upgraded FFP systems, advanced flue gas desulphurisation units and low NO_x burners.

4.4.3.1 ESP+SO_3 Control Technology

An ESP (Electrostatic Precipitator) is utilised to capture particulate matter, such as fly ash, in coal-fired power stations as a pollution control measure. ESPs are installed as a part of the emission control system to clean flue gas before it is released into the atmosphere. In coal-fired power stations, ESPs are installed between the furnace and the induced draught fan, as illustrated by Figure 4.94.

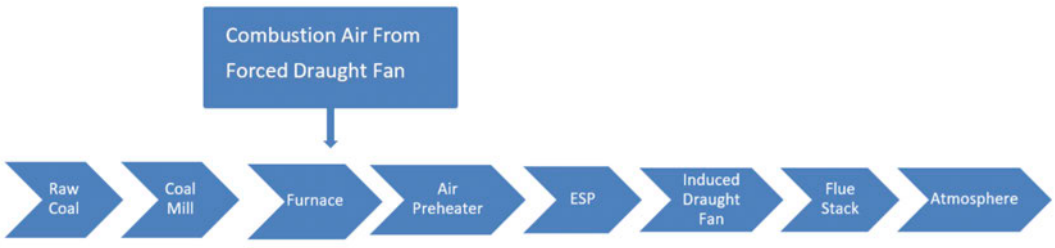

Figure 4.94: Coal fired plant process flow diagram (saVRee, n.d.)

A dry ESP system charges fly ash particles and then utilises a strong electric field in the flue gas stream to remove the ash particles (BABCOCK & WILCOX, n.d.). Once the ash has been collected in a sufficiently thick layer, it can be removed as a sheet by mechanically striking the plates (BABCOCK & WILCOX, n.d.). The ash should be allowed to collect in a thick enough layer to prevent re-entry into the flue gas stream (BABCOCK & WILCOX, n.d.).

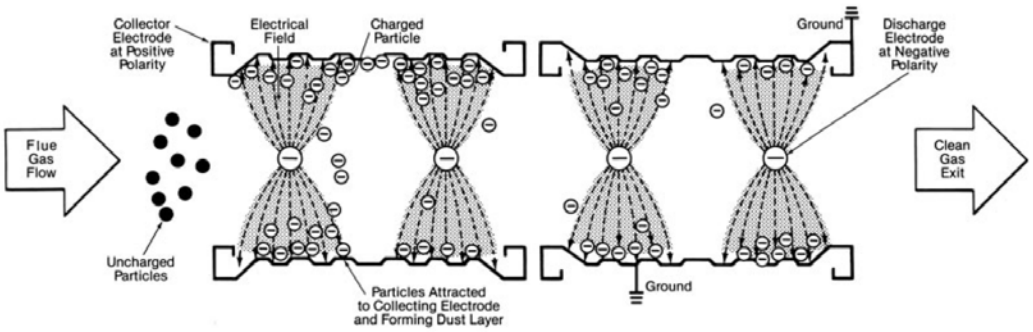

Figure 4.95: ESP process arrangement (BABCOCK & WILCOX, n.d.)

Adding SO_3 into the flue gas stream improves the efficiency of ESP as it reduces the fly ash resistivity and enhances overall capture. The SO_3 required for the flue gas conditioning is produced by the catalytical conversion of SO_2, which is produced by the combustion of elemental sulphur (www.ftek.com, n.d.).

4.4.3.2 Fabric Filter Plants

There are three types of fabric filter plants, namely, pulse jet, reverse gas and shake-deflate (Miller, 2005). The FFPs can be distinguished by the type of cleaning mechanism and the A/C ratio (air to cloth ratio) (Miller, 2005).

Eskom's power stations have pulse jet FFPs installed (Eskom, 2021). A pulse jet fabric filter is a self-cleaning dry filtration system which uses compressed air to remove particulate matter and dust from the filter media (CPE Filters, 2020). The fly ash is collected on the outer surface of the filter and forms a sheet/cake, which is periodically sent to the hopper for removal at a timed interval or when the pressure drop is at a specific value (CPE Filters, 2020).

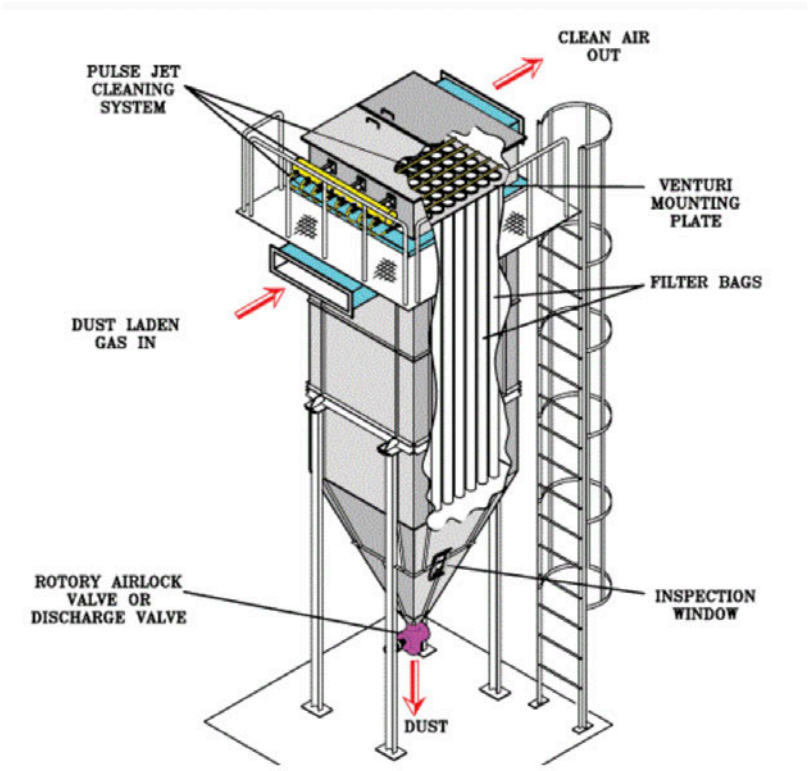

Figure 4.96: Pulse jet fabric filter (Filson, 2020)

Eskom has converted most of the older ESP+SO_3 systems to FFPs because the FFPs have a greater removal efficiency (99.9%) as compared to the ESPs (98% - 99%) (Martech JSC, 2023). The FFPs are more cost-effective as the operating cost is limited to compressed air for the pulse jets. Maintenance is required for the fabric filter bags, while the ESPs require significant electricity to operate. There are many mechanical parts which undergo wear and tear and need regular maintenance or replacement (Martech JSC, 2023).

Whilst some plants have transitioned to full FFPs, some are upgrading the existing ESP technology and running a combination of FFPs and ESPs, as shown in Table 4.6. The transition is slow but is an eventual necessity to achieve higher efficiency for particulate capture and lower operating and maintenance costs.

4.4.3.3 Wet Flue Gas Desulphurisation (FGD) systems

The wet FGD unit at Kusile operates as follows: the sulphur dioxide-containing flue gas enters the unit and gravitates upwards, where it reacts with the limestone slurry spray at the top of the unit. The limestone slurry absorbs the SO_2 to form $CaSO_3$-$1/2H_2O$ (calcium sulphite hemihydrate). This product is then washed down to the bottom of the unit, where air is added to oxidise the $CaSO_3$-$1/2H_2O$ to form $CaSO_3$-$2H_2O$ (Gypsum) (Pillay and Moodley, 2012). This is a continuous process where the limestone slurry is constantly pumped to the top of the unit until the solid concentration at the bottom of the unit reaches 15% (Pillay & Moodley, 2012). A stream is then bled off and sent to the dewatering unit, where the gypsum and water are separated.

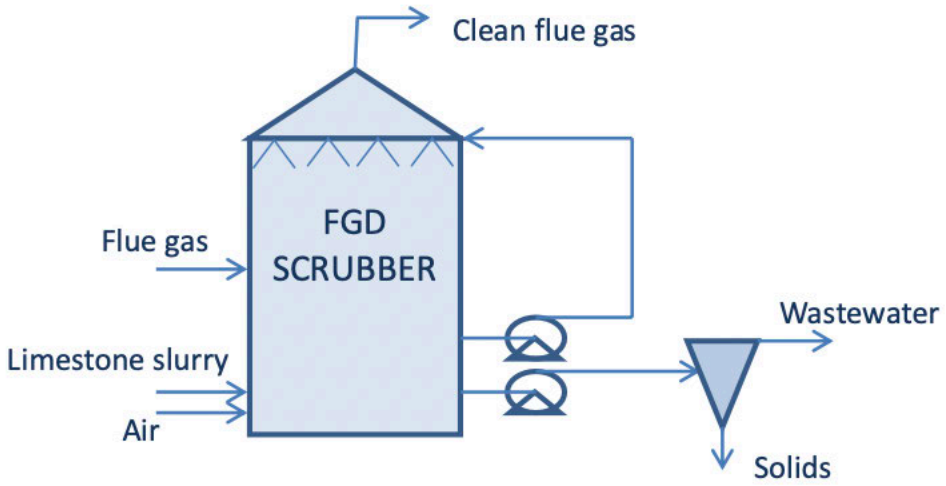

Figure 4.97: Schematic of FGD process (Pillay & Moodley, 2012)

4.4.3.4 Low NO_x Burners

Low NOx burners are manufactured to reduce the amount of NOx formed by controlling the ratio of air to coal mixing. The aim is to create a larger, more branched flame to reduce the peak flame temperature (Ruichang, 2019). The low NOx burner is effective in reducing the emission of NOx (nitrogen oxides) and CO (carbon monoxide) (Ecostar Combustion Systems, 2023)

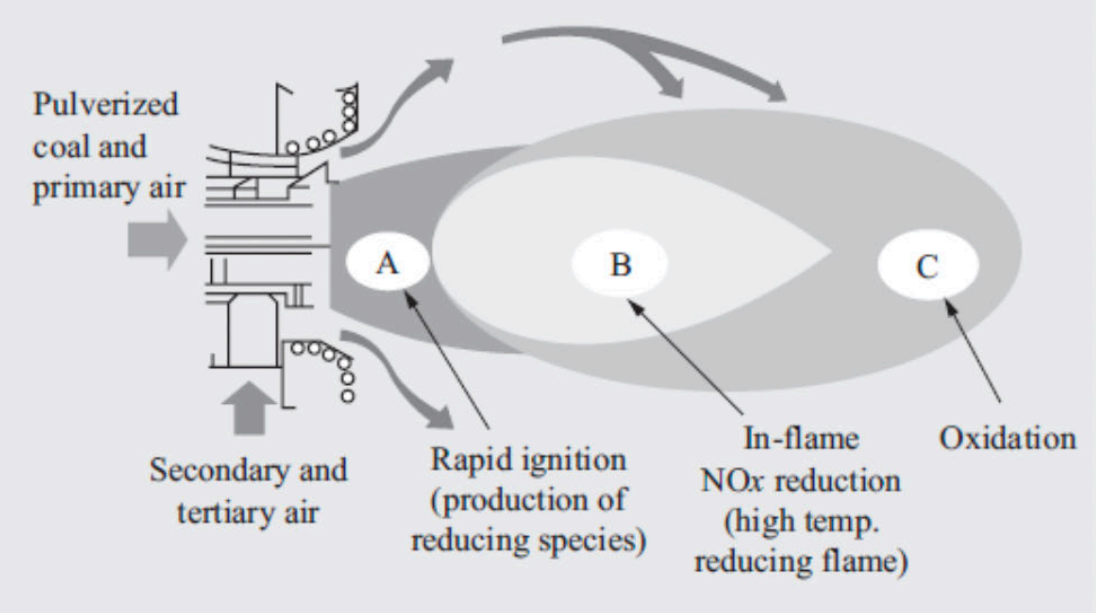

Figure 4.98: Burning mechanism of a low NOx burner (van der Merwe et.al., 2018)

4.5 Integration of Adsorption by Fly ash/Modified Fly Ash into existing Processes

Upon evaluation of the emission control technology currently in use at Eskom's power stations and the proposed installation of new emission control technology, the process of utilising fly ash/modified fly ash as an adsorbent to remove Hg^0 can be integrated in either of two ways:

- As an independent Hg, only removal is done by using an adsorption system.
- As a part of a sequential pollutant removal system.

The incorporation into an existing plant, ease of building and feasibility are factors that must be considered when deciding which option would work best.

4.5.1 Single Pollutant Adsorption Unit

A single pollutant removal unit can be added to the process line as mercury removal is an end-stage process that can be located after the FFPs or the wet FGD system before the stack. The mercury adsorption by fly ash/modified fly ash process can be operated independently. The system can be designed as follows (Adapted from Figure 9-17 – Peavy, Rowe and Tchobanoglous (1985)) for a two-unit fixed-bed adsorber.

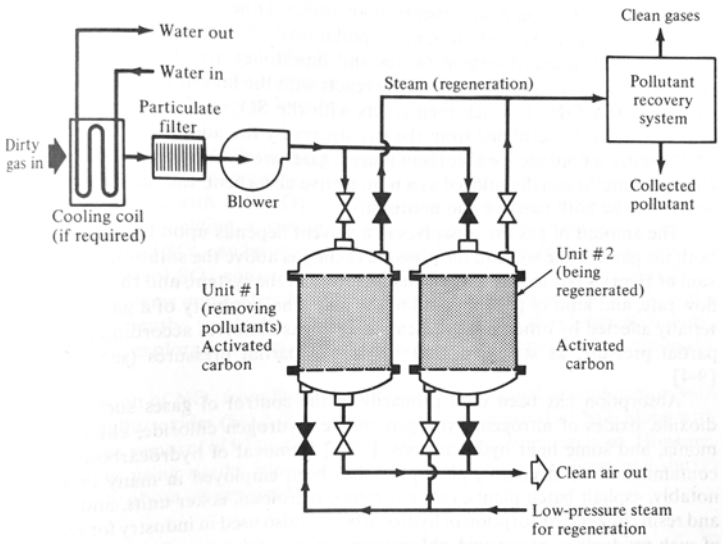

Figure 4.99: Two-unit fixed bed adsorber (Peavy, Rowe and Tchobanoglous, 1985)

The fly ash/ modified fly ash can be used in a two-unit fixed bed adsorption system, as illustrated by Figure 4.99. Suppose the method of adsorption is due to physisorption. In that case, the sorbent can be regenerated using steam, but if the adsorption mechanism occurs via chemisorption, the spent adsorbent must be removed and fresh adsorbent must be loaded again. Many factors will determine the adsorption efficiency of the fly ash/modified fly ash, such as other pollutants in the stream or the flue gas composition.

4.5.2 Sequential Pollutant Removal Systems

The UNEP (United Nations Environmental Program) (2011) has developed a POG (Process Optimization Guidance) to assist with the best possible options for Hg capture in a sequential pollutant removal system. The POG uses a decision tree to select an 'optimum mercury control strategy by analysing other pollutants, namely SO2, NOx and PM' (UNEP, 2011). Figure 4. shows the decision tree developed by UNEP. Using the information from Eskom's power stations, a path can be developed to indicate the method that should include the fly ash/modified fly ash as an adsorbent to the system. There are some limitations to the decision tree in that it is very specific to the particular types of emission control technology for each pollutant, e.g., the only type of NOx removal technology considered is the SCR process, whilst Eskom uses Low NOx burners to reduce the NOx emissions.

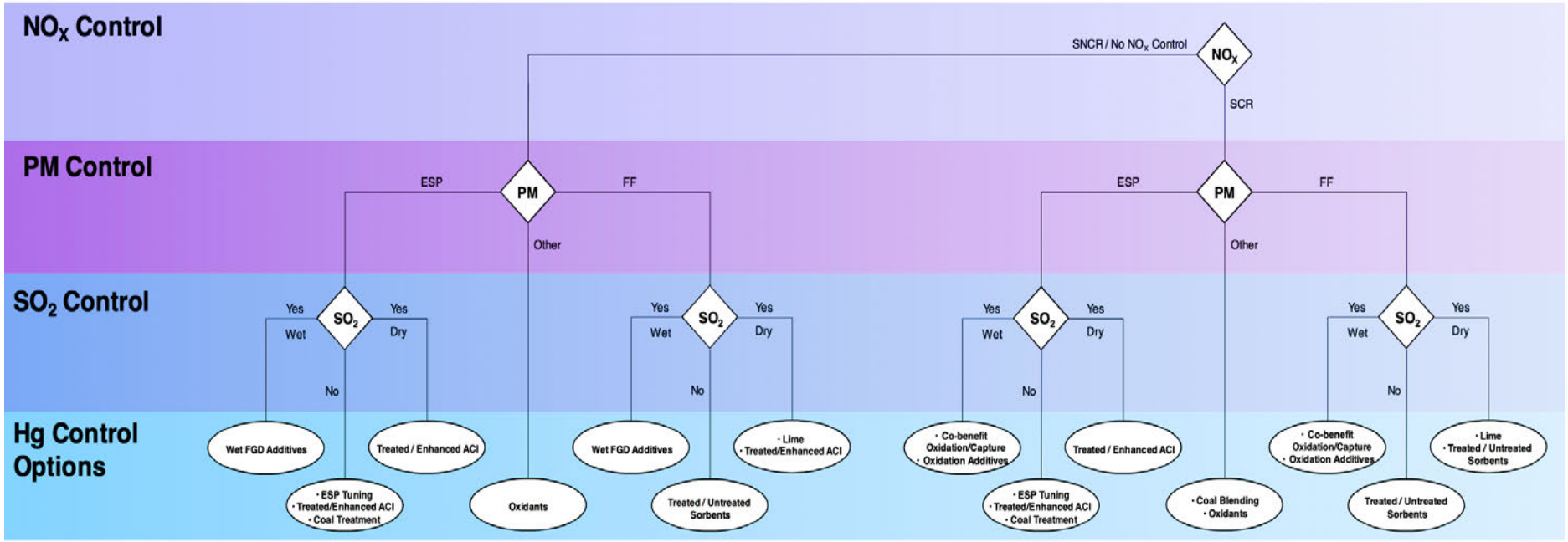

Figure 4.100: Decision tree for mercury control options (UNEP, 2011)

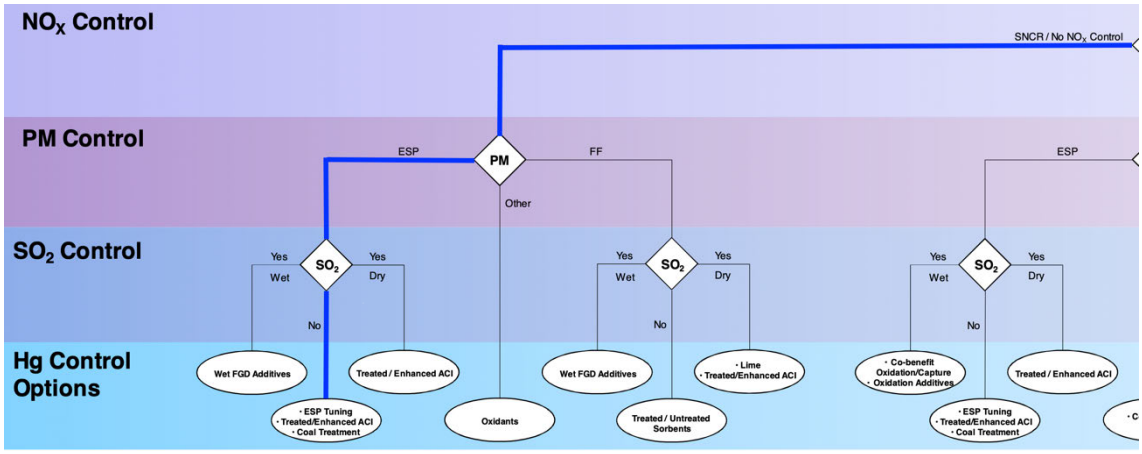

Figure 4.101: Decision tree path for Eskom's power stations which have ESP+SO_3 emission technology installed (UNEP, 2011)

Eskom's power stations (Kendal, Matimba, Lethabo, Tutuka, Matla, Duvha (partly), Kriel and Grootvlei (partly)) have ESP+SO_3 (Electrostatic precipitators with SO_3 flue gas conditioning) emission control systems installed. In following the decision tree branches, there is no SCR control, with ESP control technology and no SO_2 control technology; therefore, the decision tree recommends ESP tuning, treated/enhanced ACI (activated carbon injection) or coal treatment as the best mercury removal technique.

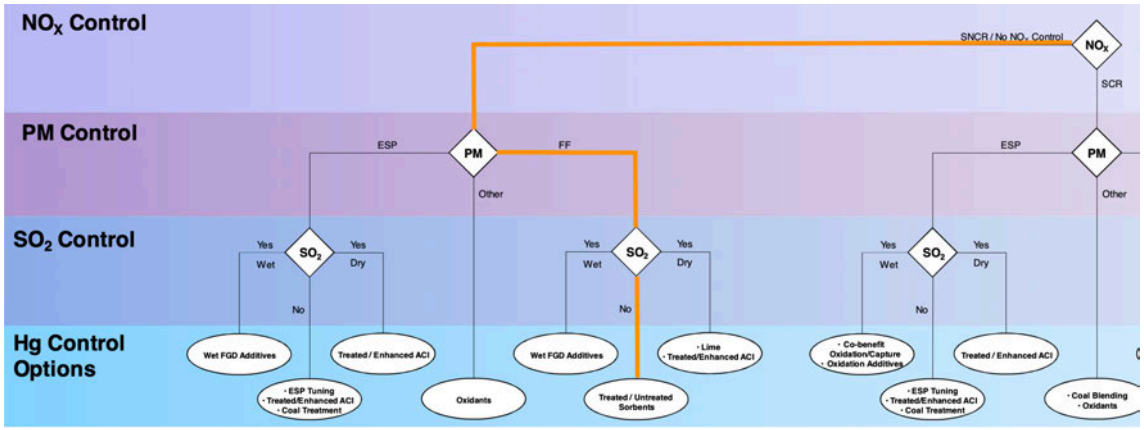

Figure 4.102: Decision tree path for Eskom's power stations which have FFP emission technology installed (UNEP, 2011)

Eskom's Arnot, Hendrina, Camden, and Medupi power stations employ FFPs as pollution emission control technology. By following the branches of the decision tree, there is no SCR control for NOx emission control, but to control particulate matter, there is FFP, and for SO_2, there is no control; therefore, the recommended mercury adsorption technique is via treated or untreated sorbents.

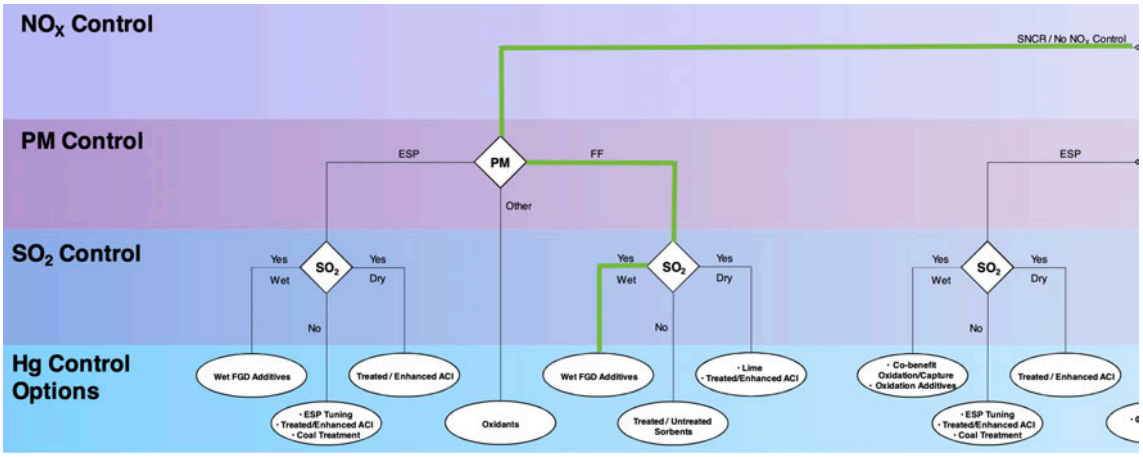

Figure 4.103: Decision tree path for Eskom's power stations which have FFP's and wet FGD emission technology installed (UNEP, 2011)

Eskom's Kusile and Medupi power stations are the only two with wet FGD technology installed. In following the branches of the decision tree, there is no SCR control, with FFP control technology for particulate and for SO_2 control, a wet FGD system is in use; therefore, the decision tree recommends wet FGD additives as the method for mercury adsorption.

4.6. Cost

Emission control technology such as ESPs, FFPs, wet FGD systems and low NOx burners are costly. They are highly specialised devices that must be constructed from materials that can withstand the effects of the pollutants. The equipment also has high maintenance and costs due to the excessive wear and tear experienced by regular contact with pollutants/hazardous materials, which are often corrosive.

The total cost from Eskom to meet emission standards is estimated to be over R300 billion, and the consequence of meeting these requirements will eventually filter down to the consumer as there would be an approximately 10% hike in the electricity tariff (South African Government, 2021).

4.7. Environmental Impact Evaluation

The previous section shows the results obtained from the adsorption testing and the subsequent utilisation in a single control system or as a part of multipollutant technology systems. Whilst it was established by the adsorption testing, which showed that the unmodified/modified fly ash was effective in adsorbing mercury from a simulated flue gas stream, it is also necessary to conduct a post-control evaluation of the process, especially regarding the potential environmental impact that it causes.

The waste materials of interest for post-control evaluation are:

Fly ash laden with Hg (Dark and Light samples).
Fly ash modified with $CuSO_4$ laden with Hg.
Fly ash modified with $ZnCl_2$ laden with Hg.
Fly ash modified with $FeCl_3$ laden with Hg.
Fly ash modified with $CuCl_2$ laden with Hg.

4.7.1. Fly Ash

The definition of fly ash, according to the South African Bureau of Standards, is: “a powdery residue obtained by the separation of solids from flue gas during the combustion of coal.” (SABS, 2002) (Heyns and Hassan, n.d). Fly ash composition and characterisation are influenced by the composition of the origin coal and additives utilised during the pre-washing and post-combustion stages as well as the pollution control technologies employed by the power stations, e.g., Hg, SO_2 or CO_2 adsorption using fly ash (American Coal Association, 2003).

According to the National Environmental Waste Act – (NEM: WA) (2008), fly ash is classified as a hazardous waste substance in South Africa (Department of Environmental Affairs, 2012). Hazardous waste can be defined as follows according to the NEM: WA: “Any waste that contains organic or inorganic elements or compounds that may, owing to the inherent physical, chemical, or toxicological characteristics of that waste, have a detrimental impact on health and environment. (DFFE – Waste Management, 2023).

Fly ash is classified in level 1 as hazardous waste, level 2 as major waste type – HW 14 and level 3 as specific waste type 01 – Fly Ash (Department of Environmental Affairs, 2012). Fly ash is classified as a hazardous material since it can contain organic pollutants and toxic metals such as Selenium, Arsenic, Boron, Vanadium, Aluminium, Lead, Mercury, Chromium, Uranium and Thorium in trace amounts (Jambhulkar, Shaikh, and Kumar, 2018).

Fly ash can also be classified as an air pollutant since it is composed of very fine, light particles which can become airborne during windy conditions. This is especially prevalent when fly ash is disposed of in dry landfill sites. Prolonged exposure of humans to these particles, primarily via inhalation, can cause respiratory diseases. The fly ash can also accumulate over time in areas close to power stations, and when the ash is exposed to rain, leaching of contaminants can occur into the ground.

The other method of fly ash disposal is in wet ponds where the ash slurry is transferred to specially designed ponds, allowing the water to drain out or evaporate slowly and the fly ash to remain (Mohanty et al., 2020). Whilst this provides a solution for power stations to store fly ash, it can cause significant environmental problems as the water exposed to the fly ash can adsorb the pollutants, which can leach into the ground (Energy Education, n.d). This can contaminate groundwater sources and harm humans and animals if the water is consumed. The water runoff can also contaminate other water bodies (rivers/lakes), harming aquatic plants and animals.

Since fly ash is considered a hazardous material, the necessary measures must be implemented to handle the output from Eskom’s power stations, which are some of the largest fly ash producers.

4.7.2. Mercury

Mercury is a silver, odourless, liquid chemical with a boiling point 356.72°C (ThermoFisher Scientific, 2021). In South Africa, mercury and its associated waste are classified in level 1 as hazardous waste, level 2 as major waste type – HW 02 and level 3 as specific waste type 02 – Solid waste containing mercury according to the NEM: WA (2008) (Department of Environmental Affairs, 2012). Since the adsorption process utilised fly ash to capture Hg from the coal flue gas stream, the material obtained would be a solid waste containing mercury, classified under the above category in the NEM: WA (2008).

Mercury poses a severe risk when discharged into the atmosphere as the gaseous or particulate matter can travel vast distances. The mercury, which eventually settles onto the ground, can be washed into water bodies by rain. Inorganic elemental mercury and organic methylmercury can have atmospheric lifespans of up to 2 years and decades, respectively (New Hampshire Department of Environmental Services). Mercury released from anthropogenic and natural sources does not degrade; it is merely transferred between locations in a cycle, where it is eventually stored in sediment or deep sea deposits before it enters the cycle again.

Studies conducted by Driscoll et al. (2013) indicate that mercury sources, the interaction of mercury in the air-land-water body cycle, its subsequent formation of methyl mercury, and the Hg emission control policies are all integrated. This study also says that the mercury released into the atmosphere as Hg^0 and Hg^{2+} does not directly threaten human and animal organisms. The actual threat occurs when the Hg^{2+} is converted to methyl mercury (CH_3Hg) in water bodies such as oceans and rivers. Methyl mercury can also seep into the ground and affect terrestrial organisms.

The greatest mercury bioaccumulation occurs in aquatic organisms; therefore, exposure is highest when humans eat fish and other aquatic animals. A study by van Rooyen et al. (2023) investigated the effects of atmospheric transport of Hg. Results showed mercury was found in the sediments, macroinvertebrates and fish. The apex predator in this ecosystem was found to contain the largest amount of mercury, thereby suggesting that biomagnification had occurred in the food chain where the largest predator was consuming all the mercury that was previously consumed by all its predecessors in the food chain. This is consistent with previous studies

indicating that mercury does not degrade, accumulates, and is transferred from one location to another.

An article by Paul Tolmè (2012) highlighted the danger of "atmospheric deposition" of mercury. Areas situated downwind of coal-burning epicentres are experiencing the harmful effects of mercury poisoning. The mercury contaminates water sources and sources, poisoning fish and other aquatic animals in those ecosystems. Research has shown that the birds consuming fish and other species from these contaminated water sources produce fewer offspring. Methylmercury is affecting reproduction rates. Wetland birds are especially susceptible to methylmercury poisoning since fish and other aquatic species are their primary food sources. The mercury bioaccumulates in the aquatic species (fish, frogs, insects and spiders). Besides birds, the bats in these ecosystems are also susceptible to mercury poisoning.

4.7.3. Copper Sulphate - $CuSO_4$

Copper II sulphate ($CuSO_4$) is a metallic salt highly soluble in water. It is classified as hazardous when ingested, during eye contact, and when released into the aquatic environment (CARLROTH, 2021). In South Africa, solid material containing sulphur is classified in level 1 as hazardous waste, level 2 as primary waste type – HW 09 and level 3 as specific waste type 02 – Solids containing halogens and or sulphur according to the NEM: WA (2008) (Department of Environmental Affairs, 2012).

$CuSO_4$ can be utilised as an aquatic herbicide to treat algae blooms. However, it is only a short-term solution (Beem, 2019). When the algae die, it releases phosphorus, which releases light into the water for the algae to bloom (Beem, 2019). The accumulation of these toxins caused by $CuSO_4$ sinks and phosphorus can enhance the algae bloom, creating a bigger problem (ATS Senior Editor, 2016).

$CuSO_4$ also poses another major environmental problem since it is non-biodegradable, accumulates over time in aquatics sources, and can poison beneficial organisms present in aquatic environments (ATS Senior Editor, 2016).

$CuSO_4$ is also highly toxic to aquatic species. A study by Tavares-Das (2021) investigates the effect of $CuSO_4$ in water bodies. The results show that water quality also impacts the toxicity of $CuSO_4$ to fish species. Extended exposure to $CuSO_4$ can lead to mortality, and sublethal exposure can cause an array of health complications, such as changes in behaviour, feeding, growth, O_2 consumption and damage to vital organs (Tavares-Das, 2021). The study also shows that $CuSO_4$ in controlled doses is beneficial in treating ectoparasites in farmed fish.

The effects of $CuSO_4$ are not limited to the natural environment but also to the built environment, as the $CuSO_4$ solution is highly corrosive to iron, galvanised iron and steel (Clarkson, 2001). Equipment and components must be manufactured using corrosion-resistant materials, which are costlier.

$CuSO_4$ is highly toxic to humans when absorbed through the skin and if ingested accidentally. It can cause itchiness and pain when adsorbed via the skin and, if ingested, can cause pain, nausea, diarrhoea and death in some instances in significant quantities consumed ((ATS Senior Editor, 2016).

4.7.4. Zinc chloride – $ZnCl_2$

Zinc chloride is a white, crystalline solid highly soluble in water. In South Africa, solid material containing sulphur is classified in level 1 as hazardous waste, level 2 as major waste type – HW 09 and level 3 as specific waste type 02 – Solids containing halogens and or sulphur according to the NEM: WA (2008) (Department of Environmental Affairs, 2012).

$ZnCl_2$ is a white crystalline powder highly soluble in water (CAMACHEM, n.d). Information presented by CAMACHEM (n.d.) indicates that $ZnCl_2$ is highly corrosive when ingested or during skin/eye contact. When ingested, it can cause gastric burns, breathing problems, and, in severe cases, pancreatic damage on contact; it can cause burns to the eyes and skin.

The $ZnCl_2$ is highly toxic to aquatic animals and should not be exposed to water bodies (rivers, lakes and oceans) (ILO and WHO, 2021). A study conducted by Küçükoglu, Melek and Bįnokay (2013) investigated the effects of exposing Zebrafish embryos to 5 different concentrations of $ZnCl_2$ solution, and it was observed that the hatchlings that did survive hatched later than usual whilst the remainder died in the embryo stage. The hatchlings were born with deformities caused by exposure to $ZnCl_2$. The results obtained from the study indicate that $ZnCl_2$ could be classified as a teratogen.

4.7.5. Ferric chloride - $FeCl_3$

Ferric chloride is a brown-orange solid that is slightly soluble in water (PubChem, 2024). In South Africa, solid material containing sulphur is classified in level 1 as hazardous waste, level 2 as major waste type – HW 09 and level 3 as specific waste type 02 – Solids containing halogens and or sulphur according to the NEM: WA (2008) (Department of Environmental Affairs, 2012).

The information presented by AQUASAN (2021) highlights the detrimental effects of ferric chloride. It is a highly corrosive material, and due care should be taken when manufacturing equipment and piping that can withstand the chemical's effects. It can also cause chemical burns when exposed to the skin and eyes. $FeCl_3$ is also highly toxic to aquatic life and should not be allowed to enter water sources like rivers, lakes and oceans.

A study conducted by Sotero-Santo, Rocha and Povinelli (2007) on three aquatic organisms exposed to $FeCl_3$ sludge showed that continued exposure caused the emergence of a chronic condition affecting the fertility of the D. similis organism. Increased amounts of the sludge released into the water decreased the water quality by increasing the sediment, turbidity, conductivity, chemical oxygen demand (COD) and hardness (Sotero-Santo, Rocha and Povinelli, 2007).

4.7.6. Copper chloride - $CuCl_2$

Copper chloride *is* a blue-green solid which is completely soluble in water. In South Africa, solid material containing sulphur is classified in level 1 as hazardous waste, level 2 as major waste type – HW 09 and level 3 as specific waste type 02 – Solids containing halogens and or sulphur according to the NEM: WA (2008) (Department of Environmental Affairs, 2012). $CuCl_2$ is classified as a corrosive, toxic (ingestion and skin/eye contact) substance which is also toxic to the aquatic environment (CARLROTH, 2022)

4.8. Eskom – Ash Handling

Since the chemicals utilised during the adsorption testing are all classified as hazardous according to the NEM: WA (2008), the protocol of handling hazardous must be followed to ensure safe transport and disposal of the waste materials.

Eskom's coal-fired power stations utilise approximately 109 million tonnes of coal for electricity generation per annum, of which 2.6 million tonnes of ash is produced, constituting 85 % fly ash and 15% bottom ash (Eskom, 2021).

The ash is transported to designated sites called ash dumps/slurry dams and used as mine backfill for open-cast coal mines. Over time, the ash dumps are rehabilitated by depositing soil and sediment and eventually revegetating the area with plants, flowers, and trees (Eskom, 2021). The ash has also been sold to other industries for the manufacture of brick, the production of cement, road construction and as a soil conditioner under the recently proclaimed Waste Legislation, which allows for the bypassing of the NEM: WA (2008) under certain conditions (Eskom, 2019).

4.8.1. South African Ash Classification

South African fly ash can be classified according to criteria shown in Table 4.7 and Table 4.8. Data presented by Reynolds-Clausen and Singh (2019) indicate that fly ash collected from coal-fired power stations can be classified as Type 3: Low Risk. According to SANS – South African National Standard -10234 is classified as Class 12 – Ecotoxic waste (Golder Associates, 2012).

Table 4.7: Criteria and risk level (Reynolds-Clausen and Singh, 2019)

Criteria	Risk Level	Description of Risk associated with Disposal to Landfill
LC > LCT2, or TC > TCT2	Type 1: High Risk	Considered high risk waste with a very high potential for contaminant release. Requires very high level of control and ongoing management to protect health and the environment
LC > LCT 1 and <LCT 2 or TC > TCT 1 and < TCT 2	Type 2: Moderate Risk	Considered moderate risk waste with high potential for contaminant release. Requires high level of control and ongoing management to protect health and the environment
LC > LCT 0 and < LCT 1 or TC > TCT 0 and < TCT 1	Type 3: Low Risk	Considered low risk waste with some potential for contaminant release. Requires proper control and ongoing management to protect health and the environment
LC < LCT 0 or TC < TCT 0	Type 4: Very Low Risk	Very low risk waste with low potential for contaminant release. Requires some level of control and ongoing management to protect health and the environment

TC – Total concentration

LC – Leachable concentration

Table 4.8: Permissible levels in waste (Reynolds-Clausen and Singh, 2019)

Contaminants in Waste	TCT0 mg/kg	TCT1 mg/kg	TCT2 mg/kg	LCT0 mg/l	LCT1 mg/l	LCT2 mg/l
Metal Ion Contaminants						
As, Arsenic	5.8	500	2000	0.01	0.5	1
B, Boron	150	15 000	60 000	0.5	25	50
Ba, Barium	62.5	6 250	25 000	0.7	35	70
Cd, Cadmium	7.5	260	1 040	0.005	0.25	0.5
Co, Cobalt	50	5 000	20 000	0.5	25	50
$Cr_{Total,}$ Chromium Total	46 000	800 000	N/A	0.1	5	10
Cr(VI), Chromium (VI)	6.5	500	2 000	0.05	2.5	5
Cu, Copper	16	19 500	78 000	1	50	100
Hg, Mercury	0.93	160	640	0.001	0.05	0.1
Mn, Manganese	1 000	25 000	100 000	0.4	20	40
Mo, Molybdenum	40	1 000	4 000	0.07	3.5	7
Ni, Nickel	91	10 600	42 400	0.07	3.5	7
Pb, Lead	20	1 900	7 600	0.01	0.5	1
Sb, Antimony	10	75	300	0.01	0.5	1
Se, Selenium	10	50	200	0.01	0.5	1
V, Vanadium	150	2 680	10 720	0.1	5	10
Zn, Zinc	240	160 000	640 000	3	150	300
Inorganic Anions						
TDS	N/A	N/A	N/A	1 100	12 500	25 000
Chloride	N/A	N/A	N/A	300	15 000	30 000
Sulphate	N/A	N/A	N/A	250	12 500	25 000
NO_3 as N, Nitrate-N	N/A	N/A	N/A	11	550	1 100
CN^- (total), Cyanide Total	14	10 500	42 000	0.07	3.5	7

Chapter 5
Discussion

5.1. Fly Ash Characterisation

FESEM/EDX analysis and pH measurement techniques characterised the two unmodified fly ash samples. The FESEM/EDX results showed that the compositions of the two unmodified fly ash samples were similar. The fly ashes contained significant amounts of C, Fe, Si and Al, which are beneficial to mercury adsorption. pH measurements indicated that the dark fly ash had an average pH of 8.62, and the pH of light fly ash was 10.35. South African fly ash has a normal pH averaging about 11.5, which decreases to 8.5 over time (Reynold-Clausen and Singh, 2019). The range of the pH values obtained from the pH measurements for the two fly ash samples agrees with the literature value. Fly ash, which is alkaline in nature, like South African fly ash, with a pH of 10, can adsorb CO_2, and the pH can be reduced to 8-9 (Roy and Burger, 2011). The dark fly ash already has a pH of 8.62, which could indicate that it was an older fly ash sample, whilst the pH of the light fly ash is 10.35, indicating a 'fresh' fly ash sample.

5.2. Adsorption Tests

5.2.1. Adsorption Tests at 200℃

Ten different fly ash samples were tested by placing 2.5 g of adsorbent into a reactor and exposing it to 300 ng/m^3 of Hg in carrier gas with a flowrate of 100 ml/min. The dark and light original and modified fly ash samples ($CuCl_2$, $FeCl_3$, $ZnCl_2$ and $CuSO_4$) show excellent adsorption capacity for elemental mercury (Hg^0). The ten fly ash samples exposed to Hg^0 laden simulated flue gas stream containing (N_2, O_2 and CO_2) could effectively adsorb the mercury out of the flue gas stream. The graphs show the reactor exit concentration measured for one hour. The modified space time was determined by using the formular $\tau = \frac{V}{V_0}$ where V – reactor volume and V_0 – volumetric flowrate and was calculated to be 25000 $\frac{mg}{ml/min}$.

The results corroborate similar previous experiments conducted by Xu et al. (2012), which also investigated the ability to utilise fly ash as an absorbent and the subsequent effects of modifying fly ash. Similarly, the modified space time was also determined for Xu et al. (2012) and was calculated to be only 200 $\frac{mg}{ml/min}$. Since the space time velocity is so much greater than Xu et al. (2012) breakthrough would not be achieved in one hour. The residence time is significantly shorter than Xu et al hence it will take a very long time to reach saturation. Xu et al (2012) conducted experiments for three hours and $CuCl_2$ and $FeCl_3$ modified samples had still not achieved breakthrough.

Whilst the results from Xu et al. show that fly ash/modified fly ash does work effectively as an adsorbent, the experiments were conducted in an inert environment with only N_2 being used as the carrier gas. The effects of additional compounds such as HCl, O_2 and SO_2 were investigated separately. The effect of the addition of CO_2 into the system was not investigated.

It was also imperative to test the fly ash's ability to adsorb the mercury from a simulated flue gas stream containing compounds such as CO_2. It is a significant component of the flue gas stream and can make up almost 15% of the composition.

Fly ash can adsorb heavy metals and compounds such as CO_2, SO_2 and NOx from gas streams, which makes it a desirable, cheap adsorbent material. Since it has an affinity for many substances, it is essential to test the ability of the fly ash to adsorb the desired substance (Hg^0) from a stream containing CO_2, which can also be adsorbed onto the fly ash and compete for active sites.

Work done by Marczak-Grzesk et al. (2021) shows that fly ash/modified fly ash has excellent adsorption capabilities for both Hg^0 and CO_2. The experiments highlighted fly ash's ability as an adsorbent for Hg^0 and CO_2 when modified using a commercial biosorbent (OT-500 or MSC-500). The efficiency for Hg^0 adsorption increased significantly, but there was only a slight increase in efficiency for CO_2.

Zhou et al. (2021) investigated the effects of mercury adsorption in the presence of CO and CO_2. Results show that the presence of CO_2 inhibits mercury adsorption (Hg^0). The presence of the functional group's lactone, carboxyl and hydroxyl could improve the adsorption of CO_2, thereby competing with the Hg0 for active sites available for physical adsorption (Zhou et al., 2021).

The results obtained from the adsorption tests, as shown in the figures in Chapter 4, show that the original/modified dark and light fly ash samples display good adsorption ability for mercury despite the flue gas stream containing 14.5% CO_2. The original dark, light and modified dark-$CuSO_4$, light $CuSO_4$, dark-$ZnCl_2$ and light-$ZnCl_2$ fly ash samples show good adsorption capacity until around 58 minutes when a gradual decline to 99% efficiency is observed. The fly ash samples modified with $CuCl_2$ and $FeCl_3$ show excellent adsorption capacity for mercury (Hg^0), with the efficiency remaining at 100% for the duration of the experiment.

The 6% O_2 present in the carrier gas stream has a positive effect and enhances the adsorption ability of the fly ash/modified fly ash. Previous studies conducted by Xu et al. (2021) and Shen et al. (2020), amongst others, show that the presence of O_2 enhances mercury adsorption as it promotes mercury oxidation by increasing the presence of the O-H functional group.

The fly ash samples modified with $CuCl_2$ and $FeCl_3$ have the best adsorption capacity due to the presence of the Cl ion. The elemental mercury reacts with the Cl to form $HgCl_2$. Due to the presence of Cl_2 from the metallic salts and O_2 in the carrier gas, it can be suggested that the mercury oxidation occurs via the Mars-Maessen mechanism described by equations 13 - 17. Previous studies by Xu et al. (2021) and Lim et al. (2020) show that whilst $FeCl_3$ and $CuCl_2$ are very good adsorbents, $CuCl_2$ is better, as shown by the efficiency tests performed in these studies.

The results shown in the figures above do show that both the $FeCl_3$ and $CuCl_2$ samples displayed 100% effectiveness in adsorbing mercury for the duration of the experiment; however, in the adsorption curves, the time taken to reduce the mercury concentration to 0 ng/m3 is far more significant for the $FeCl_3$ modified fly ash whilst compared to the $CuCl_2$ modified fly ash. The time taken for the $FeCl_3$-modified dark and light samples is 21 and 24 minutes, respectively, whilst the time taken for the $CuCl_2$-modified dark and light samples is 12 and 16 minutes, respectively.

In the $FeCl_3$ and $CuCl_2$ modified fly ash samples the adsorption reaction is mainly chemisorption based therefore the initial period shown on these graphs can represent the induction period for the sorbent during which the mass transfer from the bulk to the surface is overcome and the sites are activated and begin adsorbing mercury. The induction period in descending order for the samples are as follows $FeCl_3$, $CuCl_2$, $ZnCl_2$, $CuSO_4$ and original dark/light fly ash.

Figures 4.52 and 4.83 show the average cumulative adsorption curves for the original/modified dark and light fly ash samples. These graphs show that the corresponding dark and light fly ash samples behave similarly in the time it takes to reduce the mercury concentration to 0 ng/m3 and the trajectory. The original dark and light samples modified dark $CuSO_4$, light $CuSO_4$, dark-ZnCl2, and light-ZnCl2 fly ash samples, which all behave similarly and decline to an efficiency of 99% around 58 minutes. The $CuCl_2$ and $FeCl_3$ modified samples also behave similarly to the dark and light fly ash samples. While the adsorption curves are similar, it can be observed that the light fly ash samples take a longer time to decrease the mercury concentration to 0 ng/m3. The similarity is that the adsorption mechanism of both the dark and light fly ashes is beneficial since, in a full-scale working scenario, it would be possible for each power station to utilise fly ash present on the plant instead of needing to purchase fly ash from other sources thereby decreasing/avoiding a base material cost.

Whilst CO_2 was not a component of interest in this thesis, it does have a direct influence on mercury adsorption in real plant operations. To assess the influence of CO_2 on the adsorption of mercury using fly ash the carrier gas contained 13 % CO_2 where the normal plant flue gas contains a maximum amount of 15% CO_2. The experiments were successful despite the high concentration of CO_2 present in the carrier gas. It would not be recommended to have a separate system designed to remove CO_2 due to the increased operating costs. It would be preferable to remove the CO_2 as a co-benefit of the fly ash adsorption. It is also recommended that future experiments also measure the exit concentration of CO_2 to fully assess the quantity of CO_2 is adsorbed versus mercury.

5.2.2. Adsorption Tests at 150℃

The modified dark and light $CuSO_4$ showed no significant difference to the experiments conducted at 200℃. The graphs did decrease to 0 ng/m^3 slight quicker than the experiment done at 200℃ but still maintained the same trajectory as before.

5.3. Evaluation of Current Emission Control Technology, Integration of Proposed Mercury Adsorption onto Fly Ash Process, Costing and Environmental Impact Assessment

It is extremely costly to retrofit power stations with emission control technology; cost estimation from Eskom is over R300 billion to overhaul all the coal-fired power stations. Figure 4.93 provides a graphical representation of the estimated years until the decommissioning of Eskom's coal-fired power stations. The power stations should be evaluated to determine the most suitable candidates for installing emission control technology. For example, power stations with less than ten years of lifespan should not be considered since installing equipment for such a short time is too expensive. Another factor that should be considered is the generational output of the plant. It is not economically feasible to retrofit plants with a low generational output. Li et al. (2020) describes that one of China's mitigation methods is to shut down small units with a generational capacity of less than 300 MW.

South Africa's power stations, apart from Kusile and Medupi, which have wet FGD technology, only have emission control technology installed to reduce particulate matter. The proposed method of utilising fly as an adsorbent can be implemented in two ways: as a single pollutant adsorption unit or as a part of a sequential pollutant removal system. The sequential pollutant system is more appealing since a co-benefit can exist. If the fly ash is introduced into the wet FGD, there will be a co-benefit of SO_2 adsorption. The sequential pollutant adsorption system is favoured over single pollutant adsorption unit because multiple pollutants would be removed simultaneously. The sequential removal system is more cost effective and economically viable as compared to building separate units to remove pollutants in isolation.

While the fly ash works well as an adsorbent, the environmental impact of implementing the process should also be considered. Fly ash, mercury and the modifiers $CuSO_4$, $ZnCl_2$, $FeCl_3$ and $CuCl_2$ are classified as hazardous substances according to the NEM: WA (2008). Extra measures need to be implemented when handling these materials.

Fly ash can be useful under normal circumstances since it can be classified as Type 3: Low-Risk material, according to Table 4.7. However, when it is used as an adsorbent, the classification will change since heavy metals' total and leachable concentrations will increase.

Currently, Eskom disposes run of mill fly ash in 'ash dumps' where the ground is prepared by installing special liners and membranes to prevent contamination of the soil and ground water. A continuous water spray keeps the ash mounds moist to suppress the fly ash from being carried away in the wind. Eskom also has water management systems in place to handle the clean and contaminated water which are transferred to separate water storage dams. The 'clean' water is water that has not been in contact with the fly ash and is the surface runoff from the rehabilitated areas. The contaminated water is from ash runoff, seepage and plant effluent which can be recycled and used to keep the ash mounds moist. The overall aim is to rehabilitate the ash storage areas by gradually filling in topsoil and indigenous vegetation.

Whilst Eskom has procedures in place to handle the fly ash, special precautions need to be undertaken when handling the mercury laden fly ash. The liner (thicker and more durable) and membrane system should be developed to handle more corrosive materials and extra layers should be incorporated to prevent ground and water contamination. The mercury laden fly ash should be transported and stored in a special demarcated area separate from the run of mill fly ash. A separate drainage system must be designed to allow water to flow into a different water dam. This water could be recycled to keep the ash mounds moist.

Overall, the modified fly ash performs better and has a higher capacity to adsorb the mercury whilst the unmodified fly ash would require more frequent replacement in the system as the adsorption capacity is lower. However, the unmodified fly ash poses a lower environmental risk as there are no added metallic salts which can leach and contaminate water and ground sources. It would be cheaper to utilise the unmodified fly ash as the extra processes of modifying the fly ash using the metallic salts is now removed from the manufacturing and

operating costs. The cost of purchasing the metallic salts is also removed from the running costs.

The mercury present in coal fly ash is chemically stable (Date et al., 2020) and does not require further intervention since it can be stored safely in a demarcated landfill. However, regular monitoring and maintenance of the site should be done to prevent any environmental issues.

Chapter 6
Conclusions and Recommendations

6.1. Conclusions

Whilst the world is transitioning to renewable forms of energy some of the countries with the largest populations such as China and India are experiencing an economic boom which translates to increased energy requirements. These countries primarily use coal as a form of energy production will continue to do so for the next foreseeable future. For countries such as India, China and South Africa amongst others who are primary coal users the demand far outweighs the need to stop using coal as a fuel source. Many countries and continents such as USA, Europe and South America have made great strides in transitioning to renewable energy sources and possibly in the next few decades the use of coal will decline gradually as a primary energy source in the rest of the world also.

The aim of the project was successful as unmodified and modified fly ash displayed excellent adsorption capacity for mercury from a simulated flue gas stream. The high value of the space time velocity indicates that whilst the experiment was only conducted for one hour it has the capacity to continue for a much longer time until the sorbent is spent. The experiment conducted by Xu et al. (2012) only has a space velocity of 200 mg/L/min and was still operating at almost 100% efficiency for the modified $CuCl_2$ sample by the same measure this experiment will take many hours until the sorbent achieves breakthrough. The experiments worked successfully at temperatures of 150℃ and 200℃. This corroborates results from literature (Xu et al. (2012) and Gu et al. (2015)). The experiments can be conducted within the temperature range of 150℃ - 200℃ which will be beneficial to incorporate as a part of a sequential pollutant removal system.

$FeCl_3$ and $CuCl_2$ modified fly ash samples had longer induction times initially but are still exhibiting 100% efficiency after 1 hour whilst the original dark and light, $CuSO_4$ and $ZnCl_2$ modified samples which had shorter induction times are experiencing a decline in adsorption efficiency.

Modification of fly ash is effective to reduce the overall quantity required however the cost increases significantly for the consumables (metallic salts) and operation. Overall, from a cost perspective the modification would not be advantageous. Special consideration also should be given to the potential environmental impacts that could be caused by modifying the fly ash. It is a trade-off that needs to be considered carefully before implementation.

Due to the high cost associated with installing and maintaining emission control technology a specific criterion must be employed to determine which power-stations are best suited to have this equipment installed. Extra precautions must be taken when utilising the fly ash as an adsorbent due to the environmental hazards associated with running the process.

6.2. Recommendations

Due to the high cost associated with retrofitting power stations with emission control technology further experiments should be done to assess the ability of the fly ash to adsorb SO_2, CO_2 and Hg. Multiple measurements should be conducted simultaneously of the different gas concentrations to observe the behaviour of the fly ash and its affinity to adsorb the multiple pollutants and ascertain if the adsorption rate is equal for each the pollutants or one/two are favoured over the others.

Chapter 7
References

American Coal Ash Association (2003) 'Fly ash facts for highway engineers' [online] Available at: https://www.fhwa.dot.gov/pavement/recycling/fafacts.pdf

AQUASAN (2021). 'Ferric chloride risks and alternatives' [online] Available at: https://aquasan.ca/articles/ferric-chloride-risks-and-alternatives/

ATS Senior Editor (2016). '10 Reasons not to use copper sulfate for water treatment. [online] ATS Innova Water Treatment | Wastewater Treatment | Clean Water Chemistry Available at: https://atsinnovawatertreatment.com/blog/avoid-copper-sulfate-water-treatment/

AWE (2023) 'How to buffer or calibrate a pH electrode and pH instrument?' [online] Available at: https://www.awe-ltd.co.uk/knowledge-base/ph/how-to-buffer-a-ph-electrode.html

BABCOCK & WILCOX. (n.d.) Basics of Electrostatic Precipitator (ESP) Operation. Available at: https://www.babcock.com/home/about/resources/learning-center/basic-esp-operation#:~:text=A%20dry%20electrostatic%20precipitator%20(ESP,to%20collect%20and%20remove%20them.

Bhatt, A., Priyadarshini. S., Acharath Mohanakrishnan, A., Abri, A., Sattler, M. and Techpaphawit, S. (2019). 'Physical, chemical, and geotechnical properties of coal fly ash: A global review'. *Case Studies in Construction Materials,* [online] 11, p.e00263. Available at: https://www.google.com/search?client=safari&rls=en&q=.+https://doi.org/10.3390/app8071116&ie=UTF-8&oe=UTF-8

Beem, M., (2019). 'Copper sulphate an often overused chemical in pond management'. *Oklahama State University.* [online] extension.okstate.edu/ Available at: https://extension.okstate.edu/fact-sheets/copper-sulfate-an-often-overused-chemical-in-pond-management.html

Belelie, M., Piketh, S.J., Burger R.P., Venter, A.D. and Keir J.N. (2016) 'Mercury emissions from the power sector in South Africa' Available at: https://www.researchgate.net/publication/375422999_Mercury_emissions_from_the_power_sector_in_South_Africa

Blythe, G. (2014), 'Mercury capture in wet flue gas desulfurization', in Granite. E.J., Pennline, H.W., Senior, C. (ed.) Mercury Control: for Coal-Derived Gas Streams

Bratan, V., Vasile, A., Chesler, P. and Hornoiu, C. (2022) 'Insights into the redox and structural properties of CoOx and MnOx: fundamental factors affecting the catalytic performance in the oxidation process of VOCs' *Catalysts,* 12(10), p.1134 Available at: https://www.mdpi.com/2073-4344/12/10/1134

Britannica (2024), 'Adsorption surface phenomenon' Available at: https://www.britannica.com/science/adsorption

CAMACHEM (n.d.). 'High-quality chemical and reagents for sale' Camachem. [online] Available at: https://camachem.com/en/blog/post/Zinc-Chloride-hazards-and-safety

CARLROTH (2021). 'Copper(II) sulphate pentahydrate' [online] Available at: https://www.carlroth.com/medias/SDB-P025-GB-EN.pdf?context=bWFzdGVyfHNlY3VyaXR5RGF0YXNoZWV0c3wyODY1ODN8YXBwbGljYXRpb24vcGRmfHNlY3VyaXR5RGF0YXNoZWV0cy9oMTUvaGNhLzkwNDYxOTczMDUzNzQucGRmfDY5M2EwMTAyMTQ0NGUzOWMwMGEyZDljMDViZDU5MWY0MDU1ZTFlNjUxNGU4ZmE4YjIxOTcwMDI5MjgzZmYyZGI

CARLROTH (2022). 'Copper II chloride dihydrate' [online] Available at: https://www.carlroth.com/medias/SDB-2623-GB-EN.pdf?context=bWFzdGVyfHNlY3VyaXR5RGF0YXNoZWV0c3wzMjEwMjV8YXBwbGljYXRpb24vcGRmfHNlY3VyaXR5RGF0YXNoZWV0cy9oMTUvaGNiLzkwNjIwODg0NzQ2NTQucGRmfDFiOWZhMGZiMjk4MWU2YjBjYmVhMmZkYTk2N2E2NGQ3Nzc2NjFhZWQxMzdkNDY5NGRjMGFiNDc5MmQ4N2RjM2I

CPE Filters (2020). Pulse Jet Bag Filter: Pulse Jet Baghouses & How They Work [online] CPE Filters Inc Available at: https://cpef.com/blog/what-is-a-pulse-jet-bag-filter/

Department of Environmental Affairs (2012). 'National environmental waste act, 2008' *Department of Environmental Affairs – Government Notice – Act 59 of 2008* [online] Available at: https://www.gov.za/sites/default/files/gcis_document/201409/35583rg9801gon625.pdf

Ecostar Combustion Systems (2023). What is Low NOx Burner and What Does Low NOx Emission Mean?|Ecostar [online] Available at: https://www.ecostar.com.tr/en/corporate/media/ecoblog/what-is-a-low-nox-burner-and-what-does-low-nox-emission-mean#:~:text=A%20Low%20NOx%20burner%20offers,and%20carbon%20monoxide%20(CO)

David, E., Stanciu, V., Sandru, C., Armeanu, A. and Niculescu, V. (2007). 'Exhaust gas treatment technologies for pollutant emission abatement from fossil fuel power plants. *Sustainable Development and Planning III.* Available at:https://doi.org/10.2495/sdp070882.

Driscoll, C.T., Mason, R.P., Chan, H.M., Jacob, D.J. and Pirrone, N. (2013). 'Mercury as a global pollutant: sources, pathways, and effects' Environmental Science & Technology, [online] 47(10), pp.4967-4983. Available at: https://doi.org/10.1021/es305071v

Energy Education (n.d) 'Fly ash' [online] Available at: https://energyeducation.ca/encyclopedia/Fly_ash

Eskom Air Quality Improvement Plan (2023) [online] Available at: https://cer.org.za/wp-content/uploads/2016/05/Record-13.3-pg-37-48.pdf

Eskom (2021). 'Ash management in Eskom' [online] Available at: https://www.eskom.co.za/wp-content/uploads/2021/08/CO-0004-Ash-Management-Rev-15.pdf

Eskom (2023), 'Atmospheric Emission License (AEL) reports' Available at: https://www.eskom.co.za/dataportal/emissions/ael/

Eskom (2019) ‘Beneficiation of Eskom ash’ [online] Available at: https://www.eskom.co.za/wp-content/uploads/2021/03/ENV0009BeneficiationEskomAshRev1.pdf

Eskom (2021). Coal fired power station – Eskom Available at: https://www.eskom.co.za/eskom-divisions/gx/coal-fired-power-stations/

ESKOM – DECOMMISSIONING/END OF LIFE DATES & MES APPLICATIONS PER COAL-FIRED POWER STATION Available at: https://cer.org.za/wp-content/uploads/2022/02/Annexure-A1_Summary-Table.pdf

Eskom. (n.d.). Peaking power stations Available at: https://www.eskom.co.za/eskom-divisions/gx/peaking-power-stations/

Eskom.co.za. (2016). *Understanding Electricity*. [online] Available at: http://www.eskom.co.za/AboutElectricity/ElectricityTechnologies/Pages/Understanding_Electricity.aspx [Accessed 2 Jan. 2019].

Filtration, F. (2020). Pulse Jet Bag Filters: The Ultimate FAQ Guide [online] Filson Filter. Available at: https://www.filsonfilters.com/pulse-jet-bag-filters/

Gableman, A. (2017) ‘Adsorption basics: part 1’ [online] Available at: https://www.aiche.org/sites/default/files/docs/pages/adsorption_basics_part_1.pdf

Gade, D. (2015) ‘Mercury emission from coal-fired powerplants’ [online] Available at: https://digitalcommons.wku.edu/cgi/viewcontent.cgi?article=1000&context=pubh_560

Garnham, B.L. (2016). Mercury emissions from South Africa’s coal-fired power stations. Clean Air Journal, 26(2), pp. 14-20 Available at: http://dx.doi.org/10.17159/2410-972X/2016/v26n2a8

Ge, J.C., Yoon, S.K. and Choi, N.J. (2018). ‘Application of fly ash as an adsorbent for removal of air and water pollutants’. *Applied Sciences,* [online] 8(7), p.1116 Available at: https://doi.org/10.3390/app8071116&ie=UTF-8&oe=UTF-8

Generation Division. (2021). Generation plant mix Available at: https://www.eskom.co.za/wp-content/uploads/2022/03/GX-0001-Generation-Plant-Mix-Rev-25.docx.pdf

Granite, E.J. and Presto, A.A. (2008) 'Comment on the role of SO2 for elemental mercury removal from coal combustion flue gas by activated carbon' *Energy & Fuels,* 22(5), pp.3557-3558. Available at: DOI: 10.1595/147106708X319256

Greenfacts.org. (2019). *Scientific Facts on Mercury*. [online] Available at: https://www.greenfacts.org/en/mercury/mercury-1.htm#2 [Accessed 18 December 2018].

Gu, Y., Zhang, Y., Lin, L., Xu, H., Orndorff, W. and Pan, W-P. (2015) 'Evaluation of elemental mercury adsorption by fly ash modified with ammonium bromide.' *Journal of Thermal Analysis and Calorimetry,* 119(3), pp.1663-1672 Available at: https://doi.org/10.1007/s10973-014-4376-0

Heyns, M.W. and Hassan, M. M. (n.d.) 'South Africa class f fly ash for roads: physical and chemical analysis' [online] Available at: https://journals.co.za/doi/pdf/10.10520/EJC150370

ILO and WHO (2021). 'ICSC 1064 – zinc chloride' [online] Available at: https://www.ilo.org/dyn/icsc/showcard.display?p_lang=en&p_card_id=1064&p_version=2

Jambhulkar, H.P., Shaikh, S.M.S. and Kumar, M.S (2018) 'Fly ash toxicity, emerging issues and possible implications for its exploitation in agriculture; Indian scenario: a review' *Chemosphere,* 213, pp.333-344. Available at: https://doi: 10.1016/j.chemosphere.2018.09.045

Joy, A., and Qureshi, A. (2022) 'Reducing mercury emissions from coal-fired power plants in India: possibilities and challenges' *Ambio* Available at: https://www.ncbi.nlm.nih.gov/pmc/articles/PMC9666568/

Keika Ventures (n.d.) 'Method D-6784 standard test method for elemental, oxidised, particle-bound, and total mercury in flue gas generated from coal-fired stationary sources (Ontario Hydro Method) [online] Available at:

https://www.keikaventures.com/analyticalmethod.php?m=1724#:~:text=Standard%20Test%20Method%20for%20Elemental,from%20coal%2Dfired%20stationary%20sources

Küçükoglu, M., Seçil Binokay, U. and Boga Pekmezekmek, A. (2013). 'The effects of zinc chloride during early embryonic development in zebrafish (Brachdanio rerio)' *Turkish Journal of Biology.* [online] Available at: https://doi.org/10.3906/biy-1203-27

Li, J., Zhou, S., Wei, W., Qi, J., Li, Y., Chen, B., Zhang, N., Guan, D., Qian, H., Wu, X., Miao, J., Chen, L., Feng, K. and Liang, S. (2020). 'China's retrofitting measures in coal-fired power plants bring significant mercury related health benefit. *One Earth,* [online] 3(6), pp.777-787 Available at: https://doi.org/10.1016/j.oneear.2020.11.012

Madsen, K., Thogersen, J., Frandsen, F. and Jensen, A. (2012). Mercury oxidation over selective catalytic reduction (SCR) catalysts. In: *Power-Gen Europe*. [online] Denmark: Haldor Topsøe, pp.1-14. Available at: https://www.topsoe.com/sites/default/files/mercury_oxidation_over_scr_catalysts.ashx_.pdf

Marczak-Grzesik, M., Piersa, P., Karczewski, M., Szufa, S., Ünyay, H., Kędzierska-Sar, A. and Bochenek P. (2021) 'Modified fly ash-based adsorbents (MFA) for mercury and carbon dioxide removal from coal-fired flue gases. *Energies,* 14(21), pp.7101-7101. Available at: https://doi.org/10.3390/ en14217101

Martech JSC. (2023). Why Electrostatic Precipitators (ESPs) are being replaced by Bag Filter? [online] Available at: https://www.linkedin.com/pulse/why-electrostatic-precipitators-eps-being-replaced-bag-filter#:~:text=ESPs%20operates%20best%20with%20very%20large%20airflow&text=However%2C%20now%2C%20bag%20filter%20technology,only%2098%25%2D99%25%20efficiency

McKinley (2008) 'Permeation tubes: a simple path to very complex gas mixtures' [online] Available at: https://kin-tek.com/wp-content/uploads/2015/12/Gases-Instruments-Jan-2008.pdf

Merriam-Webster (2024), 'Methylmercury' [online] Available: https://www.merriamwebster.com/dictionary/methylmercury

Miller, B.G. (2005). Emissions Control Strategies for Power Plants. Coal Energy Systems, pp.283-392. Available at: https://doi.org/10.1016/B978-012497451-7/50006-1.

Mohanty, J.K., Guru, S.R., Dash, P. and Pradhan, P.K. (2020) 'Fly ash management and condition monitoring of ash pond' *Earth Systems and Environment* Available at: https://doi.org/10.1007/s41748-020-00163-9

Mostinsky, I.L. (2011). 'Adsorption' [online] Begel House Inc Available at: https://www.thermopedia.com/content/292/

Neto, V., Raulino, G., Freire, P., Silva, M. and do Nascimento, R., (2013). 'Equilibrium and kinetic studies in adsorption of toxic metal ions for wastewater treatment' in Naushad, M., and Alotman, Z.A., (ed.) *A Book on Ion Exchange and Solvent Extraction* pp. 145-182 available at: https://www.researchgate.net/publication/286266905_Equilibrium_and_kinetic_studies_in_adsorption_of_toxic_metal_ions_for_wastewater_treatment/citation/download

New Hampshire Department of Environmental Services (2019) 'Mercury: sources, transport deposition and impacts. [online] Available at: https://www.des.nh.gov/sites/g/files/ehbemt341/files/documents/2020-01/ard-28.pdf

Over, H. (2013) 'Atomic scale insights into electrochemical versus gas phase oxidation of HCl over RuO2-based catalysts: a comparative review' *Electrochimica,* 93, pp.314-333. Available at: http://dx.doi.org/10.1016/j.electacta.2012.12.099

Patel, E.M. (2012), Practical considerations in the implementations of emissions reduction solutions at Eskom's coal fired power plant. Available at: https://www.energy.gov.za/files/4thEUSouthAfricaCleanCoalWorkingGroup/Practical%20Considerations%20in%20the%20Implementation%20of%20Emissions%20Reduction%20Solutions%20in%20SA%20Coal%20Fired%20Power%20Plant%20Final.pdf

Peavy, H.S., Rowe, D.R. and Tchobanoglous, G. (1985). Environmental engineering. New York: Mcgraw-Hill.

Pillay, L., Moodley, N. (2012), 'Kusile power station flue gas desulplhurization waste water treatment plant' [online] Available at: https://www.google.com/url?sa=t&rct=j&q=&esrc=s&source=web&cd=&ved=2ahUKEwi_387U55mEAxVuSUEAHWKcDTkQFnoECBQQAQ&url=https%3A%2F%2Fwisa.org.za%2Fwp-content%2Fuploads%2F2018%2F12%2FWISA2012-P091.pdf&usg=AOvVaw2HRJU76epnIQ1BXAPYEEEA&opi=89978449

Pmg.org.za. (2018). *NEMLA Bill: deliberations; Minamata Convention on Mercury | PMG*. [online] Available at: https://pmg.org.za/committee-meeting/26633/ [Accessed 22 December 2018].

PubChem (2024). 'Ferric chloride' [online] Available at: https://pubchem.ncbi.nlm.nih.gov/compound/Ferric-Chloride#section=GHS-Classification

Ravi Bhardwaj, Xihua Chen & Radisav D. Vidic, (2009), Impact of Fly Ash Composition on Mercury Speciation in Simulated Flue Gas, Journal of the Air & Waste Management Association, 59:11, 1331-1338

Reynolds-Clausen, K. and Singh, N. (2019). 'South Africa's power producer's revised coal ash strategy and implementation progress' *Coal Combustion and Gasification Products,* 11(1), pp. 10-17. Available at: https://doi.org/10.4177/CCGP-D-18-00015.1

Risdanareni, P., Puspitasari, P. and Januarti Jaya, E. (2017) 'Chemical and physical characterization of fly ash as geopolymer material' *MATEC Web of Conferences,* 97, p.01031 Available at: https://www.matec-conferences.org/articles/matecconf/pdf/2017/11/matecconf_etic2017_01031.pdf

Roy, W. and Berger, P, (2011) 'Geochemical controls of coal fly ash leachate pH' *Coal Combustion and Gasification Products'* 3. Pp. 63-66 Available at: https://www.researchgate.net/publication/276230163_Geochemical_Controls_of_Coal_Fly_AshLeachate_pH#:~:text=When%20coal%20fly%20ash%20is,because%20of%20geochemical%20buffering%20reactions

Ruichang (2019). Ultra Low NOx Burner Is Good Product to Reduce NOx Emission In Industry [online] Ruichang Available at : https://burnertec.com/ultra-low-nox-burner-everything-you-should-know/

saVRee (n.d.). Electrostatic Precipitator (ESP) Explained – saVRee Available at: https://savree.com/en/encyclopedia/electrostatic-precipitator-esp

Seader, J.D. and Henley, E.J. (2006). Separation process principles. New York, N.Y. John Wiley & Sons, Inc.

Shen, H., Wang, H., Shen, C., Wu, J., Zhu, Y., Shi, W., Zhand, X. and Ying, Z (2020). 'Effect of atmosphere of SO_2 co-existed with oxidizing gas on mercury removal under oxy-fuel condition. *Chemosphere,* 259, pp.127525-127525 Available at: https://doi.org/10.1016/j.chemosphere.2020.127525

Sotero-Santos, R.B., Rocha, O. and Povinelli, J. (2007). 'Toxicity of ferric chloride sludge to aquatic organisms. *Chemosphere*, 68(4), pp. 628-636 Available at: https://aquasan.ca/articles/ferric-chloride-risks-and-alternatives/

South African Coal Association (2024), 'Ash Benefits & Uses' Available at: https://www.sacaa.co.za/about-us/ash-benefits-uses

South African Government (2021), 'Eskom receives DFFE's decisions on minimum emissions standard' Available at: https://www.gov.za/news/media-statements/eskom-receives-dffe's-decisions-minimum-emissions-standard-15-dec-2021

Tavares-Dias, M.(2021). 'Toxic, physiological, histomorphological, growth performance and antiparasitic effects of copper sulphate in fish aquaculture. *Aquaculture,* 535, p.736350. Available at: https://doi.org/10.1016/j.aquaculture.2021.736350

ThermoFisher Scientific (2021) 'Mercury' [online] Available at: https://www.fishersci.com/store/msds?partNumber=M1416LB&productDescription=MERCURY+MTL+INST+GRD+REAG+6LB&vendorId=VN00033897&countryCode=US&langua g

Tolmé, P. (2012) ‘Mercury’s harmful effects’ [online] National Wildlife Federation. Available at: https://www.nwf.org/Magazines/National-Wildlife/2013/DecJan/Conservation/Mercury-and-Wildlife

UNEP (2011), ‘Process optimization guidance for reducing mercury emissions from coal combustion power plants. [online] Available: https://wedocs.unep.org/bitstream/handle/20.500.11822/11418/POG_FINAL_2011_edited_07_Jan_2011.pdf?sequence=1&isAllowed=y

Vadapalli, V.R.K., Klink, M.J., Etchebers, O., Petrik, L.F., Gitari, W., White, R.A., Key, D. and Iwuoha, E. (2008). ‘Neutralization of acid mine drainage using fly ash, and strength development of the resulting solid residues. *South African Journal of Science,* [online] 104(7-8), pp.317-322. Available at: http://www.scielo.org.za/scielo.php?script=sci_arttext&pid=S0038-23532008000400017#:~:text=Combustion%20of%20South%20African%20coal,for%20remediation%20of%20acidic%20soils

van der Merwe, J.C., Sukdeo, P., Peta, S. and Smit, D.,(2017) Eskom low NOx burner combustion simulation experience – A low NOx burner design case study Available at: https://www.researchgate.net/publication/329443440_ESKOM_Low_NOx_burner_combustion_simulation_experience_-_A_Low_NOx_burner_design_case_study

van Rooyen, D., Erasmus, J.H., Gerber, R., Nachev M., Sures, B., Wepener, V. and Smit N.J. (2023) ‘Bioaccumulation and trophic transfer of total mercury through the aquatic food webs of an Africa sub-tropical wetland system’ *Science of The Total Environment’* 889, pp.164210-164210 Available at: https://doi.org/10.1016/j.scitotenv.2023.164210

Wang, F., Wang, S.-M., Meng, Y., Zhang, L. and Hao, J. (2016). ‘Mechanisms and roles of fly ash compositions on the adsorption and oxidation of mercury in flue gas from coal combustion. *Science Direct,* 163, pp.232-239. Available at: https://doi.org/10.1016/j.fuel.2015.09.065

www.ftek.com (n.d). Flue Gas Conditioning – Fuel Tech Inc
Available at: https://www.ftek.com/en-US/products/productssubapc/fgc

www.separationprocesses.com (n.d.). 'Adsorption – fixed bed adsorption, desorption & regeneration. [online] Available at: http://www.separationprocesses.com/Adsorption/AD_Chp02b.htm

Xu, W., Wang, H., Zhu, T., Kuang, J. and Jing, P. (2013) 'Mercury removal from coal combustion flue gas by modified fly ash. *Journal of Environmental Sciences,* 25(2), pp.393-398. Available at https://doi.org/10.1016/S1001-0742(12)60065-5

Zhang, Y., Duan, W., Liu, Z. and Cao, Y. (2014) . 'Effects of modified fly ash on mercury adsorption ability in an entrained flow reactor. *Fuel*, 128 pp.274-280 Available at: https://www.sciencedirect.com/science/article/abs/pii/S0016236114002506

Zhang, Y., Zhao, L., Guo, R., Song, N., Wang, J., Cao, Y., Orndorff, W. and Pan, W (2015). 'Mercury adsorption characteristics of HBr-modified fly ash in an entrained flow reactor. *Journal of Environmental Sciences,* [online] 33, pp.156-162. Available at: (https://www.sciencedirect.com/science/article/pii/S1001074215001461)

Zhao, L., Li, C., Zhang, X., Zeng, G., Zhang, J. and Xie, Y. (2015) 'A review of elemental mercury from coal-fired flue gas with selective catalytic reduction catalysts. *Catalysis Science & Technology,* 5(7), pp. 3459-3472.

Zhao, Y., Zhang J., Liu, J., Diaz-Somoano, M., Martinez-Tarazona, R.M. and Zheng, C. (2010). 'Study on mechanism of mercury oxidation by fly ash from coal combustion. *Chinese Science Bulletin,* 55(2). Pp. 163-167. Available at: https://www.researchgate.net/publication/225342682_Study_on_mechanism_of_mercury_oxidation_by_fly_ash_from_coal_combustion/citation/download

Appendices

Appendix A: XRD Elemental Dispersion Maps

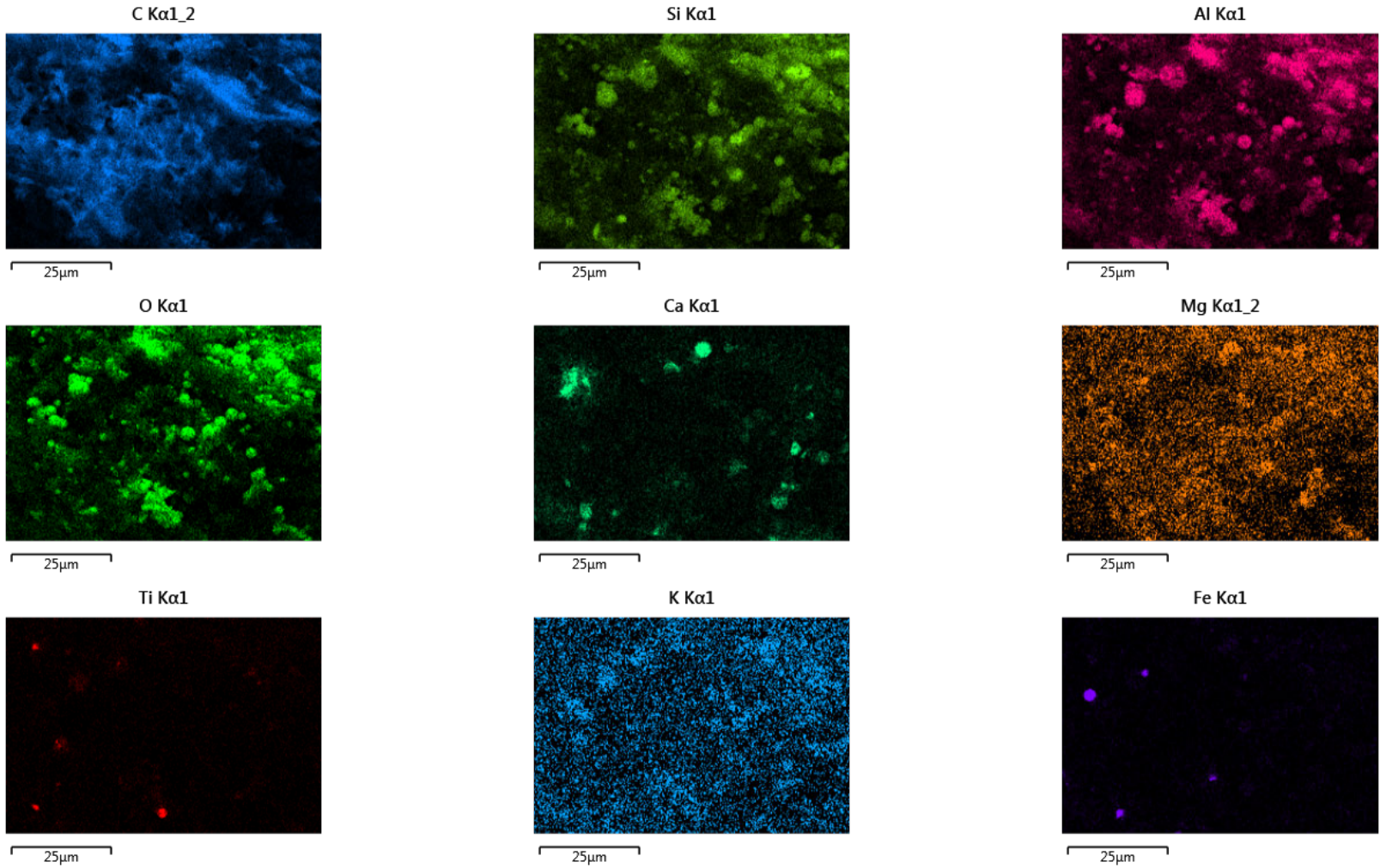

Figure A.1: Elemental dispersion maps for dark fly ash area 1

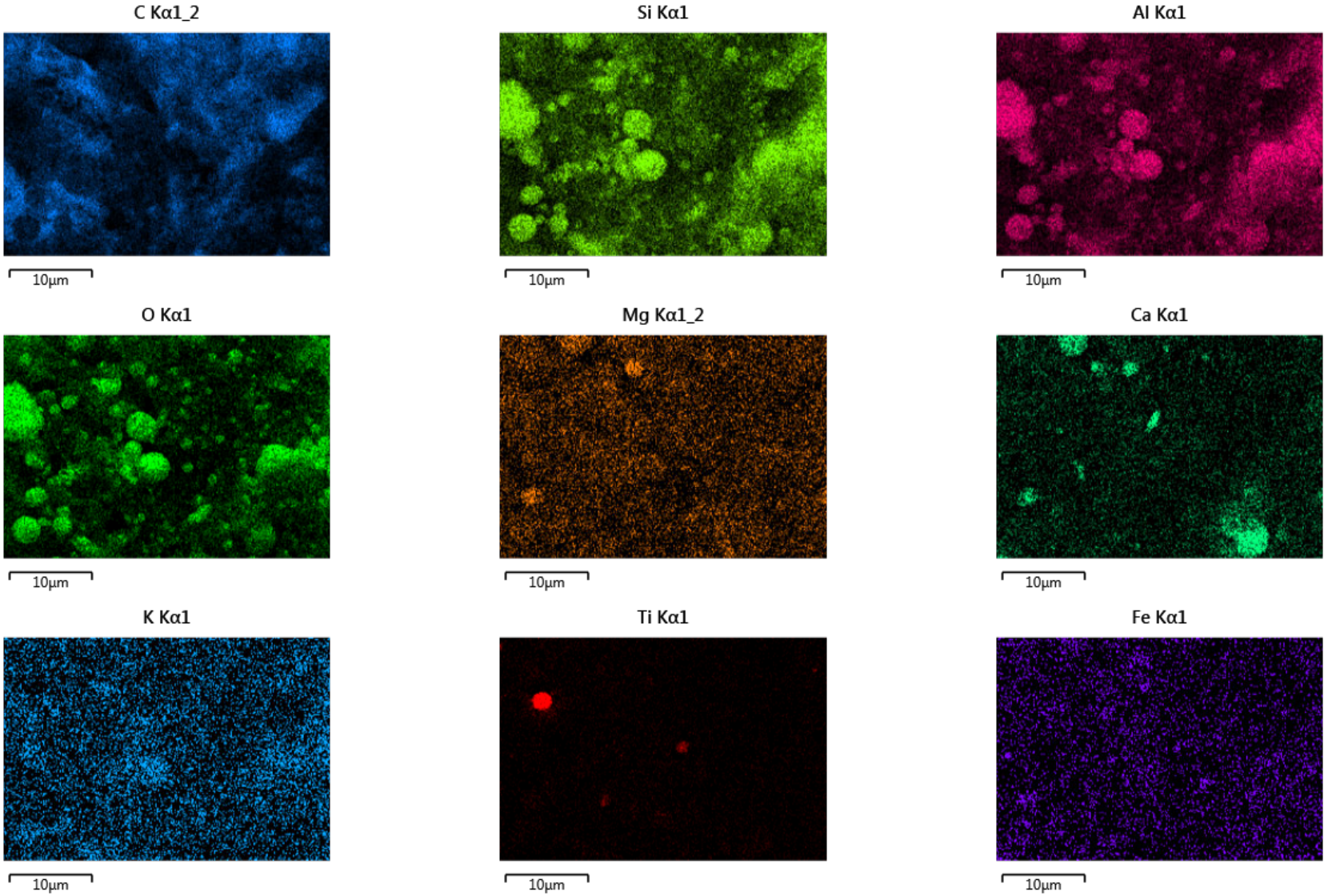

Figure A.2: Elemental dispersion maps for dark fly ash area 2

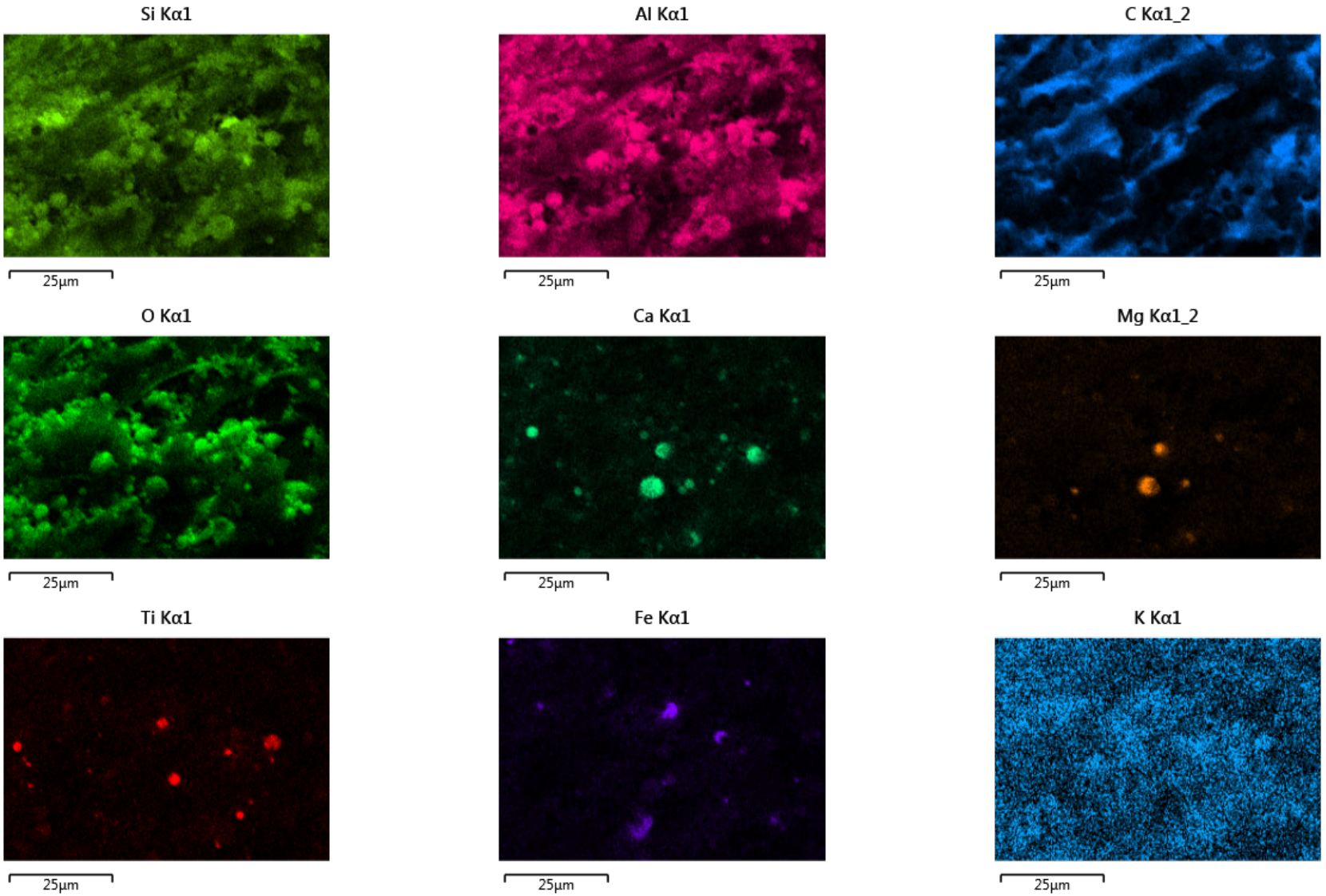

Figure A.3: Elemental dispersion maps for light fly ash area 1

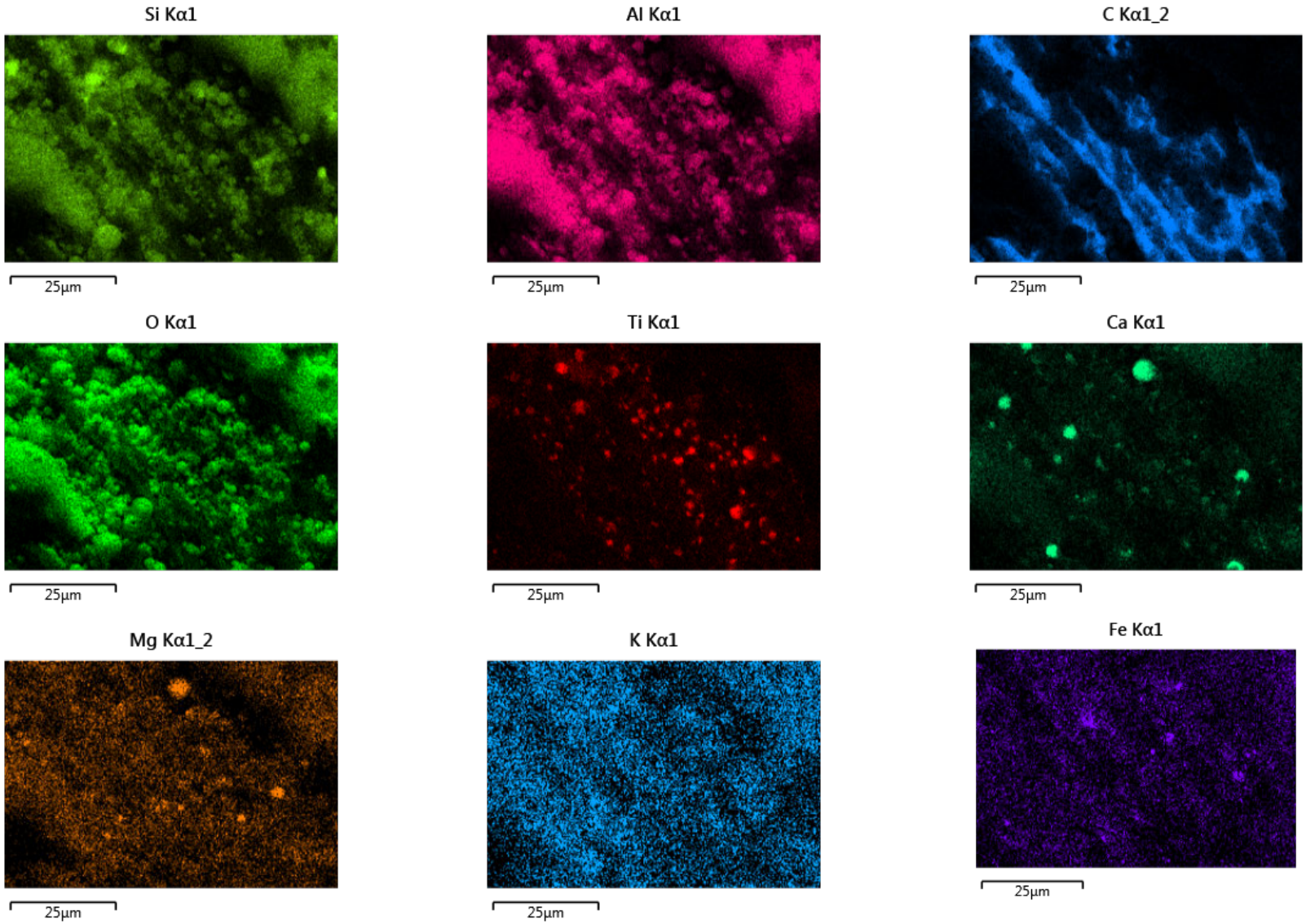

Figure A.4: Elemental dispersion maps for light fly ash area 2

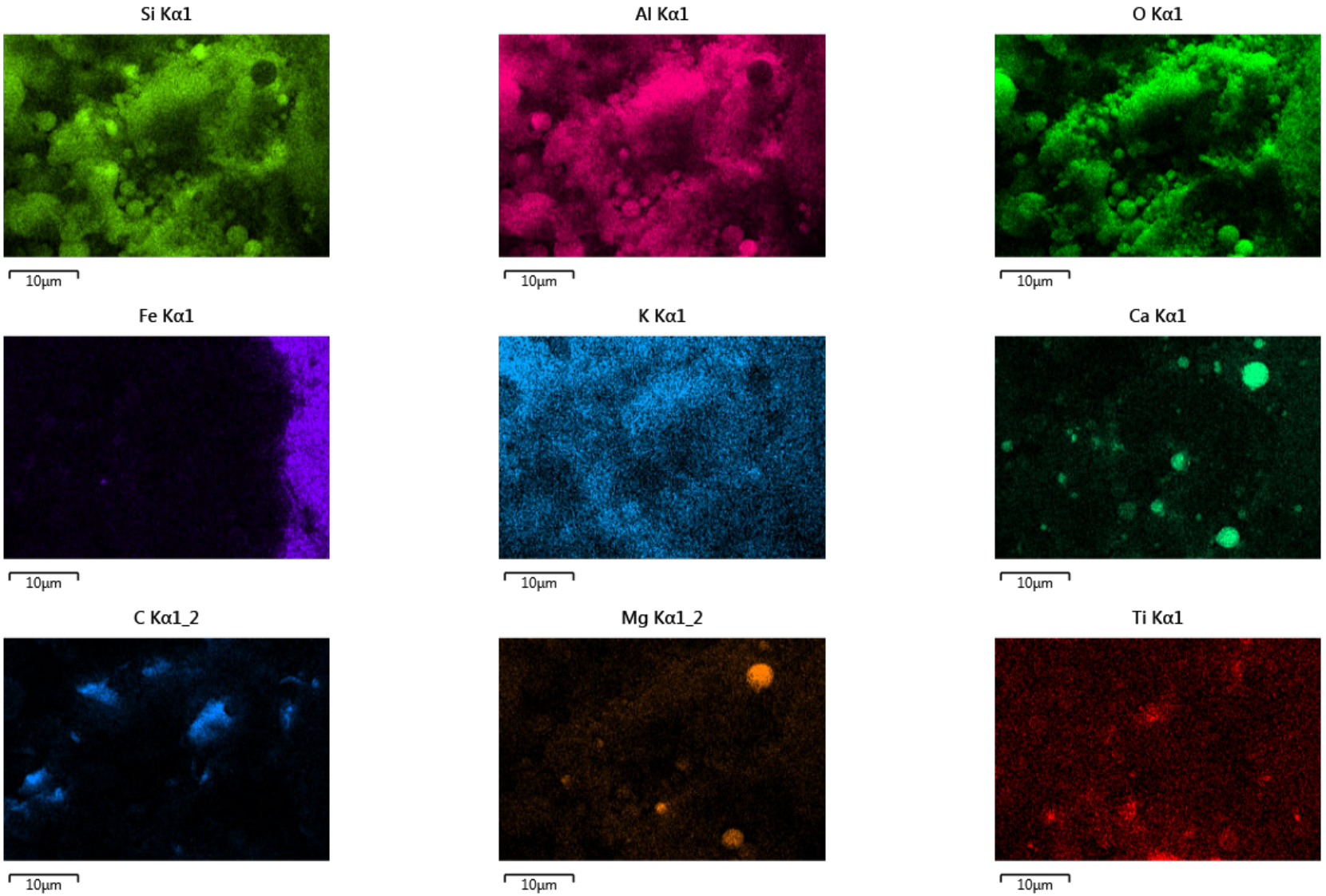

Figure A.5: Elemental dispersion maps for light fly ash area 3

Appendix B

Raw Data

Table B.1: Raw data at 200℃ for dark fly ash sample

Time (mins)	Run 1	Run 2	Run 3
0.00	303.01	302.76	303.15
0.08	295.38	289.10	299.74
0.17	287.23	280.06	269.55
0.25	279.65	274.93	249.90
0.33	272.10	260.28	237.70
0.42	264.35	253.49	231.22
0.50	256.70	248.62	219.95
0.58	249.17	240.97	210.70
0.67	241.58	231.78	208.69
0.75	234.51	222.49	207.45
0.83	226.58	214.75	198.92
0.92	219.53	209.84	186.54
1.00	212.05	200.40	180.35
1.08	204.93	193.20	170.48
1.17	197.23	189.44	164.70
1.25	190.34	181.19	158.33
1.33	183.04	173.98	149.15
1.42	175.94	165.42	142.76
1.50	168.64	159.97	128.27
1.58	161.54	152.75	119.79
1.67	154.53	146.62	110.64
1.75	147.33	137.69	105.68
1.83	140.17	130.02	97.84
1.92	133.33	119.32	89.97
2.00	119.22	101.09	81.31
2.08	116.33	92.32	72.79
2.17	112.36	84.64	68.48
2.25	105.54	72.59	60.72
2.33	98.17	69.32	56.64
2.42	90.96	60.07	50.53
2.50	84.44	52.73	45.98
2.58	77.69	46.92	37.22
2.67	70.65	39.73	30.04
2.75	63.68	30.22	24.71
2.83	56.95	24.17	18.70

2.92	50.14	18.43	12.16
3.00	43.45	11.23	8.82
3.08	36.88	7.31	1.65
3.17	30.24	2.76	0.00
3.25	23.55	0.16	0.00
3.33	16.57	0.00	0.00
3.42	12.33	0.00	0.00
3.50	9.56	0.00	0.00
3.58	3.19	0.00	0.00
3.67	1.94	0.00	0.00
3.75	0.00	0.00	0.00
3.83	0.00	0.00	0.00
3.92	0.00	0.00	0.00
4.00	0.00	0.00	0.00
4.08	0.00	0.00	0.00
4.17	0.00	0.00	0.00
4.25	0.00	0.00	0.00
4.33	0.00	0.00	0.00
4.42	0.00	0.00	0.00
4.50	0.00	0.00	0.00
4.58	0.00	0.00	0.00
4.67	0.00	0.00	0.00
4.75	0.00	0.00	0.00
4.83	0.00	0.00	0.00
4.92	0.00	0.00	0.00
5.00	0.00	0.00	0.00
5.08	0.00	0.00	0.00
5.17	0.00	0.00	0.00
5.25	0.00	0.00	0.00
5.33	0.00	0.00	0.00
5.42	0.00	0.00	0.00
5.50	0.00	0.00	0.00
5.58	0.00	0.00	0.00
5.67	0.00	0.00	0.00
5.75	0.00	0.00	0.00
5.83	0.00	0.00	0.00
5.92	0.00	0.00	0.00
6.00	0.00	0.00	0.00
6.08	0.00	0.00	0.00
6.17	0.00	0.00	0.00
6.25	0.00	0.00	0.00
6.33	0.00	0.00	0.00

6.42	0.00	0.00	0.00
6.50	0.00	0.00	0.00
6.58	0.00	0.00	0.00
6.67	0.00	0.00	0.00
6.75	0.00	0.00	0.00
6.83	0.00	0.00	0.00
6.92	0.00	0.00	0.00
7.00	0.00	0.00	0.00
7.08	0.00	0.00	0.00
7.17	0.00	0.00	0.00
7.25	0.00	0.00	0.00
7.33	0.00	0.00	0.00
7.42	0.00	0.00	0.00
7.50	0.00	0.00	0.00
7.58	0.00	0.00	0.00
7.67	0.00	0.00	0.00
7.75	0.00	0.00	0.00
7.83	0.00	0.00	0.00
7.92	0.00	0.00	0.00
8.00	0.00	0.00	0.00
8.08	0.00	0.00	0.00
8.17	0.00	0.00	0.00
8.25	0.00	0.00	0.00
8.33	0.00	0.00	0.00
8.42	0.00	0.00	0.00
8.50	0.00	0.00	0.00
8.58	0.00	0.00	0.00
8.67	0.00	0.00	0.00
8.75	0.00	0.00	0.00
8.83	0.00	0.00	0.00
8.92	0.00	0.00	0.00
9.00	0.00	0.00	0.00
9.08	0.00	0.00	0.00
9.17	0.00	0.00	0.00
9.25	0.00	0.00	0.00
9.33	0.00	0.00	0.00
9.42	0.00	0.00	0.00
9.50	0.00	0.00	0.00
9.58	0.00	0.00	0.00
9.67	0.00	0.00	0.00
9.75	0.00	0.00	0.00
9.83	0.00	0.00	0.00

9.92	0.00	0.00	0.00
10.00	0.00	0.00	0.00
10.08	0.00	0.00	0.00
10.17	0.00	0.00	0.00
10.25	0.00	0.00	0.00
10.33	0.00	0.00	0.00
10.42	0.00	0.00	0.00
10.50	0.00	0.00	0.00
10.58	0.00	0.00	0.00
10.67	0.00	0.00	0.00
10.75	0.00	0.00	0.00
10.83	0.00	0.00	0.00
10.92	0.00	0.00	0.00
11.00	0.00	0.00	0.00
11.08	0.00	0.00	0.00
11.17	0.00	0.00	0.00
11.25	0.00	0.00	0.00
11.33	0.00	0.00	0.00
11.42	0.00	0.00	0.00
11.50	0.00	0.00	0.00
11.58	0.00	0.00	0.00
11.67	0.00	0.00	0.00
11.75	0.00	0.00	0.00
11.83	0.00	0.00	0.00
11.92	0.00	0.00	0.00
12.00	0.00	0.00	0.00
12.08	0.00	0.00	0.00
12.17	0.00	0.00	0.00
12.25	0.00	0.00	0.00
12.33	0.00	0.00	0.00
12.42	0.00	0.00	0.00
12.50	0.00	0.00	0.00
12.58	0.00	0.00	0.00
12.67	0.00	0.00	0.00
12.75	0.00	0.00	0.00
12.83	0.00	0.00	0.00
12.92	0.00	0.00	0.00
13.00	0.00	0.00	0.00
13.08	0.00	0.00	0.00
13.17	0.00	0.00	0.00
13.25	0.00	0.00	0.00
13.33	0.00	0.00	0.00

13.42	0.00	0.00	0.00
13.50	0.00	0.00	0.00
13.58	0.00	0.00	0.00
13.67	0.00	0.00	0.00
13.75	0.00	0.00	0.00
13.83	0.00	0.00	0.00
13.92	0.00	0.00	0.00
14.00	0.00	0.00	0.00
14.08	0.00	0.00	0.00
14.17	0.00	0.00	0.00
14.25	0.00	0.00	0.00
14.33	0.00	0.00	0.00
14.42	0.00	0.00	0.00
14.50	0.00	0.00	0.00
14.58	0.00	0.00	0.00
14.67	0.00	0.00	0.00
14.75	0.00	0.00	0.00
14.83	0.00	0.00	0.00
14.92	0.00	0.00	0.00
15.00	0.00	0.00	0.00
15.08	0.00	0.00	0.00
15.17	0.00	0.00	0.00
15.25	0.00	0.00	0.00
15.33	0.00	0.00	0.00
15.42	0.00	0.00	0.00
15.50	0.00	0.00	0.00
15.58	0.00	0.00	0.00
15.67	0.00	0.00	0.00
15.75	0.00	0.00	0.00
15.83	0.00	0.00	0.00
15.92	0.00	0.00	0.00
16.00	0.00	0.00	0.00
16.08	0.00	0.00	0.00
16.17	0.00	0.00	0.00
16.25	0.00	0.00	0.00
16.33	0.00	0.00	0.00
16.42	0.00	0.00	0.00
16.50	0.00	0.00	0.00
16.58	0.00	0.00	0.00
16.67	0.00	0.00	0.00
16.75	0.00	0.00	0.00
16.83	0.00	0.00	0.00

16.92	0.00	0.00	0.00
17.00	0.00	0.00	0.00
17.08	0.00	0.00	0.00
17.17	0.00	0.00	0.00
17.25	0.00	0.00	0.00
17.33	0.00	0.00	0.00
17.42	0.00	0.00	0.00
17.50	0.00	0.00	0.00
17.58	0.00	0.00	0.00
17.67	0.00	0.00	0.00
17.75	0.00	0.00	0.00
17.83	0.00	0.00	0.00
17.92	0.00	0.00	0.00
18.00	0.00	0.00	0.00
18.08	0.00	0.00	0.00
18.17	0.00	0.00	0.00
18.25	0.00	0.00	0.00
18.33	0.00	0.00	0.00
18.42	0.00	0.00	0.00
18.50	0.00	0.00	0.00
18.58	0.00	0.00	0.00
18.67	0.00	0.00	0.00
18.75	0.00	0.00	0.00
18.83	0.00	0.00	0.00
18.92	0.00	0.00	0.00
19.00	0.00	0.00	0.00
19.08	0.00	0.00	0.00
19.17	0.00	0.00	0.00
19.25	0.00	0.00	0.00
19.33	0.00	0.00	0.00
19.42	0.00	0.00	0.00
19.50	0.00	0.00	0.00
19.58	0.00	0.00	0.00
19.67	0.00	0.00	0.00
19.75	0.00	0.00	0.00
19.83	0.00	0.00	0.00
19.92	0.00	0.00	0.00
20.00	0.00	0.00	0.00
20.08	0.00	0.00	0.00
20.17	0.00	0.00	0.00
20.25	0.00	0.00	0.00
20.33	0.00	0.00	0.00

20.42	0.00	0.00	0.00
20.50	0.00	0.00	0.00
20.58	0.00	0.00	0.00
20.67	0.00	0.00	0.00
20.75	0.00	0.00	0.00
20.83	0.00	0.00	0.00
20.92	0.00	0.00	0.00
21.00	0.00	0.00	0.00
21.08	0.00	0.00	0.00
21.17	0.00	0.00	0.00
21.25	0.00	0.00	0.00
21.33	0.00	0.00	0.00
21.42	0.00	0.00	0.00
21.50	0.00	0.00	0.00
21.58	0.00	0.00	0.00
21.67	0.00	0.00	0.00
21.75	0.00	0.00	0.00
21.83	0.00	0.00	0.00
21.92	0.00	0.00	0.00
22.00	0.00	0.00	0.00
22.08	0.00	0.00	0.00
22.17	0.00	0.00	0.00
22.25	0.00	0.00	0.00
22.33	0.00	0.00	0.00
22.42	0.00	0.00	0.00
22.50	0.00	0.00	0.00
22.58	0.00	0.00	0.00
22.67	0.00	0.00	0.00
22.75	0.00	0.00	0.00
22.83	0.00	0.00	0.00
22.92	0.00	0.00	0.00
23.00	0.00	0.00	0.00
23.08	0.00	0.00	0.00
23.17	0.00	0.00	0.00
23.25	0.00	0.00	0.00
23.33	0.00	0.00	0.00
23.42	0.00	0.00	0.00
23.50	0.00	0.00	0.00
23.58	0.00	0.00	0.00
23.67	0.00	0.00	0.00
23.75	0.00	0.00	0.00
23.83	0.00	0.00	0.00

23.92	0.00	0.00	0.00
24.00	0.00	0.00	0.00
24.08	0.00	0.00	0.00
24.17	0.00	0.00	0.00
24.25	0.00	0.00	0.00
24.33	0.00	0.00	0.00
24.42	0.00	0.00	0.00
24.50	0.00	0.00	0.00
24.58	0.00	0.00	0.00
24.67	0.00	0.00	0.00
24.75	0.00	0.00	0.00
24.83	0.00	0.00	0.00
24.92	0.00	0.00	0.00
25.00	0.00	0.00	0.00
25.08	0.00	0.00	0.00
25.17	0.00	0.00	0.00
25.25	0.00	0.00	0.00
25.33	0.00	0.00	0.00
25.42	0.00	0.00	0.00
25.50	0.00	0.00	0.00
25.58	0.00	0.00	0.00
25.67	0.00	0.00	0.00
25.75	0.00	0.00	0.00
25.83	0.00	0.00	0.00
25.92	0.00	0.00	0.00
26.00	0.00	0.00	0.00
26.08	0.00	0.00	0.00
26.17	0.00	0.00	0.00
26.25	0.00	0.00	0.00
26.33	0.00	0.00	0.00
26.42	0.00	0.00	0.00
26.50	0.00	0.00	0.00
26.58	0.00	0.00	0.00
26.67	0.00	0.00	0.00
26.75	0.00	0.00	0.00
26.83	0.00	0.00	0.00
26.92	0.00	0.00	0.00
27.00	0.00	0.00	0.00
27.08	0.00	0.00	0.00
27.17	0.00	0.00	0.00
27.25	0.00	0.00	0.00
27.33	0.00	0.00	0.00

27.42	0.00	0.00	0.00
27.50	0.00	0.00	0.00
27.58	0.00	0.00	0.00
27.67	0.00	0.00	0.00
27.75	0.00	0.00	0.00
27.83	0.00	0.00	0.00
27.92	0.00	0.00	0.00
28.00	0.00	0.00	0.00
28.08	0.00	0.00	0.00
28.17	0.00	0.00	0.00
28.25	0.00	0.00	0.00
28.33	0.00	0.00	0.00
28.42	0.00	0.00	0.00
28.50	0.00	0.00	0.00
28.58	0.00	0.00	0.00
28.67	0.00	0.00	0.00
28.75	0.00	0.00	0.00
28.83	0.00	0.00	0.00
28.92	0.00	0.00	0.00
29.00	0.00	0.00	0.00
29.08	0.00	0.00	0.00
29.17	0.00	0.00	0.00
29.25	0.00	0.00	0.00
29.33	0.00	0.00	0.00
29.42	0.00	0.00	0.00
29.50	0.00	0.00	0.00
29.58	0.00	0.00	0.00
29.67	0.00	0.00	0.00
29.75	0.00	0.00	0.00
29.83	0.00	0.00	0.00
29.92	0.00	0.00	0.00
30.00	0.00	0.00	0.00
30.08	0.00	0.00	0.00
30.17	0.00	0.00	0.00
30.25	0.00	0.00	0.00
30.33	0.00	0.00	0.00
30.42	0.00	0.00	0.00
30.50	0.00	0.00	0.00
30.58	0.00	0.00	0.00
30.67	0.00	0.00	0.00
30.75	0.00	0.00	0.00
30.83	0.00	0.00	0.00

30.92	0.00	0.00	0.00
31.00	0.00	0.00	0.00
31.08	0.00	0.00	0.00
31.17	0.00	0.00	0.00
31.25	0.00	0.00	0.00
31.33	0.00	0.00	0.00
31.42	0.00	0.00	0.00
31.50	0.00	0.00	0.00
31.58	0.00	0.00	0.00
31.67	0.00	0.00	0.00
31.75	0.00	0.00	0.00
31.83	0.00	0.00	0.00
31.92	0.00	0.00	0.00
32.00	0.00	0.00	0.00
32.08	0.00	0.00	0.00
32.17	0.00	0.00	0.00
32.25	0.00	0.00	0.00
32.33	0.00	0.00	0.00
32.42	0.00	0.00	0.00
32.50	0.00	0.00	0.00
32.58	0.00	0.00	0.00
32.67	0.00	0.00	0.00
32.75	0.00	0.00	0.00
32.83	0.00	0.00	0.00
32.92	0.00	0.00	0.00
33.00	0.00	0.00	0.00
33.08	0.00	0.00	0.00
33.17	0.00	0.00	0.00
33.25	0.00	0.00	0.00
33.33	0.00	0.00	0.00
33.42	0.00	0.00	0.00
33.50	0.00	0.00	0.00
33.58	0.00	0.00	0.00
33.67	0.00	0.00	0.00
33.75	0.00	0.00	0.00
33.83	0.00	0.00	0.00
33.92	0.00	0.00	0.00
34.00	0.00	0.00	0.00
34.08	0.00	0.00	0.00
34.17	0.00	0.00	0.00
34.25	0.00	0.00	0.00
34.33	0.00	0.00	0.00

34.42	0.00	0.00	0.00
34.50	0.00	0.00	0.00
34.58	0.00	0.00	0.00
34.67	0.00	0.00	0.00
34.75	0.00	0.00	0.00
34.83	0.00	0.00	0.00
34.92	0.00	0.00	0.00
35.00	0.00	0.00	0.00
35.08	0.00	0.00	0.00
35.17	0.00	0.00	0.00
35.25	0.00	0.00	0.00
35.33	0.00	0.00	0.00
35.42	0.00	0.00	0.00
35.50	0.00	0.00	0.00
35.58	0.00	0.00	0.00
35.67	0.00	0.00	0.00
35.75	0.00	0.00	0.00
35.83	0.00	0.00	0.00
35.92	0.00	0.00	0.00
36.00	0.00	0.00	0.00
36.08	0.00	0.00	0.00
36.17	0.00	0.00	0.00
36.25	0.00	0.00	0.00
36.33	0.00	0.00	0.00
36.42	0.00	0.00	0.00
36.50	0.00	0.00	0.00
36.58	0.00	0.00	0.00
36.67	0.00	0.00	0.00
36.75	0.00	0.00	0.00
36.83	0.00	0.00	0.00
36.92	0.00	0.00	0.00
37.00	0.00	0.00	0.00
37.08	0.00	0.00	0.00
37.17	0.00	0.00	0.00
37.25	0.00	0.00	0.00
37.33	0.00	0.00	0.00
37.42	0.00	0.00	0.00
37.50	0.00	0.00	0.00
37.58	0.00	0.00	0.00
37.67	0.00	0.00	0.00
37.75	0.00	0.00	0.00
37.83	0.00	0.00	0.00

37.92	0.00	0.00	0.00
38.00	0.00	0.00	0.00
38.08	0.00	0.00	0.00
38.17	0.00	0.00	0.00
38.25	0.00	0.00	0.00
38.33	0.00	0.00	0.00
38.42	0.00	0.00	0.00
38.50	0.00	0.00	0.00
38.58	0.00	0.00	0.00
38.67	0.00	0.00	0.00
38.75	0.00	0.00	0.00
38.83	0.00	0.00	0.00
38.92	0.00	0.00	0.00
39.00	0.00	0.00	0.00
39.08	0.00	0.00	0.00
39.17	0.00	0.00	0.00
39.25	0.00	0.00	0.00
39.33	0.00	0.00	0.00
39.42	0.00	0.00	0.00
39.50	0.00	0.00	0.00
39.58	0.00	0.00	0.00
39.67	0.00	0.00	0.00
39.75	0.00	0.00	0.00
39.83	0.00	0.00	0.00
39.92	0.00	0.00	0.00
40.00	0.00	0.00	0.00
40.08	0.00	0.00	0.00
40.17	0.00	0.00	0.00
40.25	0.00	0.00	0.00
40.33	0.00	0.00	0.00
40.42	0.00	0.00	0.00
40.50	0.00	0.00	0.00
40.58	0.00	0.00	0.00
40.67	0.00	0.00	0.00
40.75	0.00	0.00	0.00
40.83	0.00	0.00	0.00
40.92	0.00	0.00	0.00
41.00	0.00	0.00	0.00
41.08	0.00	0.00	0.00
41.17	0.00	0.00	0.00
41.25	0.00	0.00	0.00
41.33	0.00	0.00	0.00

41.42	0.00	0.00	0.00
41.50	0.00	0.00	0.00
41.58	0.00	0.00	0.00
41.67	0.00	0.00	0.00
41.75	0.00	0.00	0.00
41.83	0.00	0.00	0.00
41.92	0.00	0.00	0.00
42.00	0.00	0.00	0.00
42.08	0.00	0.00	0.00
42.17	0.00	0.00	0.00
42.25	0.00	0.00	0.00
42.33	0.00	0.00	0.00
42.42	0.00	0.00	0.00
42.50	0.00	0.00	0.00
42.58	0.00	0.00	0.00
42.67	0.00	0.00	0.00
42.75	0.00	0.00	0.00
42.83	0.00	0.00	0.00
42.92	0.00	0.00	0.00
43.00	0.00	0.00	0.00
43.08	0.00	0.00	0.00
43.17	0.00	0.00	0.00
43.25	0.00	0.00	0.00
43.33	0.00	0.00	0.00
43.42	0.00	0.00	0.00
43.50	0.00	0.00	0.00
43.58	0.00	0.00	0.00
43.67	0.00	0.00	0.00
43.75	0.00	0.00	0.00
43.83	0.00	0.00	0.00
43.92	0.00	0.00	0.00
44.00	0.00	0.00	0.00
44.08	0.00	0.00	0.00
44.17	0.00	0.00	0.00
44.25	0.00	0.00	0.00
44.33	0.00	0.00	0.00
44.42	0.00	0.00	0.00
44.50	0.00	0.00	0.00
44.58	0.00	0.00	0.00
44.67	0.00	0.00	0.00
44.75	0.00	0.00	0.00
44.83	0.00	0.00	0.00

44.92	0.00	0.00	0.00
45.00	0.00	0.00	0.00
45.08	0.00	0.00	0.00
45.17	0.00	0.00	0.00
45.25	0.00	0.00	0.00
45.33	0.00	0.00	0.00
45.42	0.00	0.00	0.00
45.50	0.00	0.00	0.00
45.58	0.00	0.00	0.00
45.67	0.00	0.00	0.00
45.75	0.00	0.00	0.00
45.83	0.00	0.00	0.00
45.92	0.00	0.00	0.00
46.00	0.00	0.00	0.00
46.08	0.00	0.00	0.00
46.17	0.00	0.00	0.00
46.25	0.00	0.00	0.00
46.33	0.00	0.00	0.00
46.42	0.00	0.00	0.00
46.50	0.00	0.00	0.00
46.58	0.00	0.00	0.00
46.67	0.00	0.00	0.00
46.75	0.00	0.00	0.00
46.83	0.00	0.00	0.00
46.92	0.00	0.00	0.00
47.00	0.00	0.00	0.00
47.08	0.00	0.00	0.00
47.17	0.00	0.00	0.00
47.25	0.00	0.00	0.00
47.33	0.00	0.00	0.00
47.42	0.00	0.00	0.00
47.50	0.00	0.00	0.00
47.58	0.00	0.00	0.00
47.67	0.00	0.00	0.00
47.75	0.00	0.00	0.00
47.83	0.00	0.00	0.00
47.92	0.00	0.00	0.00
48.00	0.00	0.00	0.00
48.08	0.00	0.00	0.00
48.17	0.00	0.00	0.00
48.25	0.00	0.00	0.00
48.33	0.00	0.00	0.00

48.42	0.00	0.00	0.00
48.50	0.00	0.00	0.00
48.58	0.00	0.00	0.00
48.67	0.00	0.00	0.00
48.75	0.00	0.00	0.00
48.83	0.00	0.00	0.00
48.92	0.00	0.00	0.00
49.00	0.00	0.00	0.00
49.08	0.00	0.00	0.00
49.17	0.00	0.00	0.00
49.25	0.00	0.00	0.00
49.33	0.00	0.00	0.00
49.42	0.00	0.00	0.00
49.50	0.00	0.00	0.00
49.58	0.00	0.00	0.00
49.67	0.00	0.00	0.00
49.75	0.00	0.00	0.00
49.83	0.00	0.00	0.00
49.92	0.00	0.00	0.00
50.00	0.00	0.00	0.00
50.08	0.00	0.00	0.00
50.17	0.00	0.00	0.00
50.25	0.00	0.00	0.00
50.33	0.00	0.00	0.00
50.42	0.00	0.00	0.00
50.50	0.00	0.00	0.00
50.58	0.00	0.00	0.00
50.67	0.00	0.00	0.00
50.75	0.00	0.00	0.00
50.83	0.00	0.00	0.00
50.92	0.00	0.00	0.00
51.00	0.00	0.00	0.00
51.08	0.00	0.00	0.00
51.17	0.00	0.00	0.00
51.25	0.00	0.00	0.00
51.33	0.00	0.00	0.00
51.42	0.00	0.00	0.00
51.50	0.00	0.00	0.00
51.58	0.00	0.00	0.00
51.67	0.00	0.00	0.00
51.75	0.00	0.00	0.00
51.83	0.00	0.00	0.00

51.92	0.00	0.00	0.00
52.00	0.00	0.00	0.00
52.08	0.00	0.00	0.00
52.17	0.00	0.00	0.00
52.25	0.00	0.00	0.00
52.33	0.00	0.00	0.00
52.42	0.00	0.00	0.00
52.50	0.00	0.00	0.00
52.58	0.00	0.00	0.00
52.67	0.00	0.00	0.00
52.75	0.00	0.00	0.00
52.83	0.00	0.00	0.00
52.92	0.00	0.00	0.00
53.00	0.00	0.00	0.00
53.08	0.00	0.00	0.00
53.17	0.00	0.00	0.00
53.25	0.00	0.00	0.00
53.33	0.00	0.00	0.00
53.42	0.00	0.00	0.00
53.50	0.00	0.00	0.00
53.58	0.00	0.00	0.00
53.67	0.00	0.00	0.00
53.75	0.00	0.00	0.00
53.83	0.00	0.00	0.00
53.92	0.00	0.00	0.00
54.00	0.00	0.00	0.00
54.08	0.00	0.00	0.00
54.17	0.00	0.00	0.00
54.25	0.00	0.00	0.00
54.33	0.00	0.00	0.00
54.42	0.00	0.00	0.00
54.50	0.00	0.00	0.00
54.58	0.00	0.00	0.00
54.67	0.00	0.00	0.00
54.75	0.00	0.00	0.00
54.83	0.00	0.00	0.00
54.92	0.00	0.00	0.00
55.00	0.00	0.00	0.00
55.08	0.00	0.00	0.00
55.17	0.00	0.00	0.00
55.25	0.00	0.00	0.00
55.33	0.00	0.00	0.00

55.42	0.00	0.00	0.00
55.50	0.00	0.00	0.00
55.58	0.00	0.00	0.00
55.67	0.00	0.00	0.00
55.75	0.00	0.00	0.00
55.83	0.00	0.00	0.00
55.92	0.00	0.00	0.00
56.00	0.00	0.00	0.00
56.08	0.00	0.00	0.00
56.17	0.00	0.00	0.00
56.25	0.00	0.00	0.00
56.33	0.00	0.00	0.00
56.42	0.00	0.00	0.00
56.50	0.00	0.00	0.00
56.58	0.00	0.00	0.00
56.67	0.00	0.00	0.00
56.75	0.00	0.00	0.00
56.83	0.00	0.00	0.00
56.92	0.00	0.00	0.00
57.00	0.00	0.00	0.00
57.08	0.00	0.00	0.00
57.17	0.00	0.00	0.00
57.25	0.00	0.00	0.00
57.33	0.00	0.00	0.00
57.42	0.00	0.00	0.00
57.50	0.00	0.00	0.00
57.58	0.00	0.00	0.00
57.67	0.00	0.00	0.00
57.75	0.00	0.00	0.00
57.83	0.00	0.00	0.00
57.92	0.00	0.00	0.00
58.00	0.00	0.00	0.00
58.08	0.00	0.00	0.00
58.17	0.00	0.00	0.00
58.25	0.00	0.00	0.00
58.33	0.00	0.00	0.00
58.42	0.00	0.00	0.00
58.50	0.00	0.00	0.00
58.58	0.00	0.00	0.00
58.67	0.00	0.00	0.00
58.75	0.00	0.00	0.00
58.83	0.00	0.00	0.00

58.92	1.28	0.00	0.00
59.00	1.26	0.00	0.00
59.08	1.31	0.00	0.00
59.17	1.31	0.00	0.84
59.25	1.30	0.00	0.86
59.33	1.32	0.00	0.88
59.42	1.29	0.00	0.91
59.50	1.31	0.00	0.93
59.58	1.31	0.97	0.94
59.67	1.32	0.99	0.96
59.75	1.32	0.99	0.96
59.83	1.30	1.00	0.97
59.92	1.32	1.03	0.99
60.00	1.31	1.08	0.99

Appendix C

Efficiency Curve Data

Table C.1: Calculated data at 200℃ for dark fly ash sample

Time (mins)	Run 1	Run 2	Run 3
0.00	0.00	0.00	0.00
0.08	2.52	4.51	1.12
0.17	5.21	7.50	11.08
0.25	7.71	9.19	17.57
0.33	10.20	14.03	21.59
0.42	12.76	16.27	23.73
0.50	15.29	17.88	27.44
0.58	17.77	20.41	30.50
0.67	20.27	23.44	31.16
0.75	22.61	26.51	31.57
0.83	25.23	29.07	34.38
0.92	27.55	30.69	38.47
1.00	30.02	33.81	40.51
1.08	32.37	36.18	43.76
1.17	34.91	37.43	45.67
1.25	37.19	40.15	47.77
1.33	39.59	42.53	50.80
1.42	41.94	45.36	52.91
1.50	44.35	47.16	57.69
1.58	46.69	49.55	60.48
1.67	49.00	51.57	63.50
1.75	51.38	54.52	65.14
1.83	53.74	57.06	67.73
1.92	56.00	60.59	70.32
2.00	61.61	66.61	73.18
2.08	60.65	69.51	75.99
2.17	62.92	72.04	77.41
2.25	65.17	76.02	79.97
2.33	67.60	77.10	81.32
2.42	69.98	80.16	83.33
2.50	72.13	82.58	84.83
2.58	74.36	84.50	87.72

2.67	76.68	86.88	90.09
2.75	78.99	90.02	91.85
2.83	81.21	92.02	93.83
2.92	83.45	93.91	95.99
3.00	85.66	96.29	97.09
3.08	87.83	97.59	99.46
3.17	90.02	99.09	100.00
3.25	92.23	99.95	100.00
3.33	94.53	100.00	100.00
3.42	95.93	100.00	100.00
3.50	96.85	100.00	100.00
3.58	98.95	100.00	100.00
3.67	99.36	100.00	100.00
3.75	100.00	100.00	100.00
3.83	100.00	100.00	100.00
3.92	100.00	100.00	100.00
4.00	100.00	100.00	100.00
4.08	100.00	100.00	100.00
4.17	100.00	100.00	100.00
4.25	100.00	100.00	100.00
4.33	100.00	100.00	100.00
4.42	100.00	100.00	100.00
4.50	100.00	100.00	100.00
4.58	100.00	100.00	100.00
4.67	100.00	100.00	100.00
4.75	100.00	100.00	100.00
4.83	100.00	100.00	100.00
4.92	100.00	100.00	100.00
5.00	100.00	100.00	100.00
5.08	100.00	100.00	100.00
5.17	100.00	100.00	100.00
5.25	100.00	100.00	100.00
5.33	100.00	100.00	100.00
5.42	100.00	100.00	100.00
5.50	100.00	100.00	100.00
5.58	100.00	100.00	100.00
5.67	100.00	100.00	100.00
5.75	100.00	100.00	100.00
5.83	100.00	100.00	100.00
5.92	100.00	100.00	100.00
6.00	100.00	100.00	100.00
6.08	100.00	100.00	100.00

6.17	100.00	100.00	100.00
6.25	100.00	100.00	100.00
6.33	100.00	100.00	100.00
6.42	100.00	100.00	100.00
6.50	100.00	100.00	100.00
6.58	100.00	100.00	100.00
6.67	100.00	100.00	100.00
6.75	100.00	100.00	100.00
6.83	100.00	100.00	100.00
6.92	100.00	100.00	100.00
7.00	100.00	100.00	100.00
7.08	100.00	100.00	100.00
7.17	100.00	100.00	100.00
7.25	100.00	100.00	100.00
7.33	100.00	100.00	100.00
7.42	100.00	100.00	100.00
7.50	100.00	100.00	100.00
7.58	100.00	100.00	100.00
7.67	100.00	100.00	100.00
7.75	100.00	100.00	100.00
7.83	100.00	100.00	100.00
7.92	100.00	100.00	100.00
8.00	100.00	100.00	100.00
8.08	100.00	100.00	100.00
8.17	100.00	100.00	100.00
8.25	100.00	100.00	100.00
8.33	100.00	100.00	100.00
8.42	100.00	100.00	100.00
8.50	100.00	100.00	100.00
8.58	100.00	100.00	100.00
8.67	100.00	100.00	100.00
8.75	100.00	100.00	100.00
8.83	100.00	100.00	100.00
8.92	100.00	100.00	100.00
9.00	100.00	100.00	100.00
9.08	100.00	100.00	100.00
9.17	100.00	100.00	100.00
9.25	100.00	100.00	100.00
9.33	100.00	100.00	100.00
9.42	100.00	100.00	100.00
9.50	100.00	100.00	100.00
9.58	100.00	100.00	100.00

9.67	100.00	100.00	100.00
9.75	100.00	100.00	100.00
9.83	100.00	100.00	100.00
9.92	100.00	100.00	100.00
10.00	100.00	100.00	100.00
10.08	100.00	100.00	100.00
10.17	100.00	100.00	100.00
10.25	100.00	100.00	100.00
10.33	100.00	100.00	100.00
10.42	100.00	100.00	100.00
10.50	100.00	100.00	100.00
10.58	100.00	100.00	100.00
10.67	100.00	100.00	100.00
10.75	100.00	100.00	100.00
10.83	100.00	100.00	100.00
10.92	100.00	100.00	100.00
11.00	100.00	100.00	100.00
11.08	100.00	100.00	100.00
11.17	100.00	100.00	100.00
11.25	100.00	100.00	100.00
11.33	100.00	100.00	100.00
11.42	100.00	100.00	100.00
11.50	100.00	100.00	100.00
11.58	100.00	100.00	100.00
11.67	100.00	100.00	100.00
11.75	100.00	100.00	100.00
11.83	100.00	100.00	100.00
11.92	100.00	100.00	100.00
12.00	100.00	100.00	100.00
12.08	100.00	100.00	100.00
12.17	100.00	100.00	100.00
12.25	100.00	100.00	100.00
12.33	100.00	100.00	100.00
12.42	100.00	100.00	100.00
12.50	100.00	100.00	100.00
12.58	100.00	100.00	100.00
12.67	100.00	100.00	100.00
12.75	100.00	100.00	100.00
12.83	100.00	100.00	100.00
12.92	100.00	100.00	100.00
13.00	100.00	100.00	100.00
13.08	100.00	100.00	100.00

13.17	100.00	100.00	100.00
13.25	100.00	100.00	100.00
13.33	100.00	100.00	100.00
13.42	100.00	100.00	100.00
13.50	100.00	100.00	100.00
13.58	100.00	100.00	100.00
13.67	100.00	100.00	100.00
13.75	100.00	100.00	100.00
13.83	100.00	100.00	100.00
13.92	100.00	100.00	100.00
14.00	100.00	100.00	100.00
14.08	100.00	100.00	100.00
14.17	100.00	100.00	100.00
14.25	100.00	100.00	100.00
14.33	100.00	100.00	100.00
14.42	100.00	100.00	100.00
14.50	100.00	100.00	100.00
14.58	100.00	100.00	100.00
14.67	100.00	100.00	100.00
14.75	100.00	100.00	100.00
14.83	100.00	100.00	100.00
14.92	100.00	100.00	100.00
15.00	100.00	100.00	100.00
15.08	100.00	100.00	100.00
15.17	100.00	100.00	100.00
15.25	100.00	100.00	100.00
15.33	100.00	100.00	100.00
15.42	100.00	100.00	100.00
15.50	100.00	100.00	100.00
15.58	100.00	100.00	100.00
15.67	100.00	100.00	100.00
15.75	100.00	100.00	100.00
15.83	100.00	100.00	100.00
15.92	100.00	100.00	100.00
16.00	100.00	100.00	100.00
16.08	100.00	100.00	100.00
16.17	100.00	100.00	100.00
16.25	100.00	100.00	100.00
16.33	100.00	100.00	100.00
16.42	100.00	100.00	100.00
16.50	100.00	100.00	100.00
16.58	100.00	100.00	100.00

16.67	100.00	100.00	100.00
16.75	100.00	100.00	100.00
16.83	100.00	100.00	100.00
16.92	100.00	100.00	100.00
17.00	100.00	100.00	100.00
17.08	100.00	100.00	100.00
17.17	100.00	100.00	100.00
17.25	100.00	100.00	100.00
17.33	100.00	100.00	100.00
17.42	100.00	100.00	100.00
17.50	100.00	100.00	100.00
17.58	100.00	100.00	100.00
17.67	100.00	100.00	100.00
17.75	100.00	100.00	100.00
17.83	100.00	100.00	100.00
17.92	100.00	100.00	100.00
18.00	100.00	100.00	100.00
18.08	100.00	100.00	100.00
18.17	100.00	100.00	100.00
18.25	100.00	100.00	100.00
18.33	100.00	100.00	100.00
18.42	100.00	100.00	100.00
18.50	100.00	100.00	100.00
18.58	100.00	100.00	100.00
18.67	100.00	100.00	100.00
18.75	100.00	100.00	100.00
18.83	100.00	100.00	100.00
18.92	100.00	100.00	100.00
19.00	100.00	100.00	100.00
19.08	100.00	100.00	100.00
19.17	100.00	100.00	100.00
19.25	100.00	100.00	100.00
19.33	100.00	100.00	100.00
19.42	100.00	100.00	100.00
19.50	100.00	100.00	100.00
19.58	100.00	100.00	100.00
19.67	100.00	100.00	100.00
19.75	100.00	100.00	100.00
19.83	100.00	100.00	100.00
19.92	100.00	100.00	100.00
20.00	100.00	100.00	100.00
20.08	100.00	100.00	100.00

20.17	100.00	100.00	100.00
20.25	100.00	100.00	100.00
20.33	100.00	100.00	100.00
20.42	100.00	100.00	100.00
20.50	100.00	100.00	100.00
20.58	100.00	100.00	100.00
20.67	100.00	100.00	100.00
20.75	100.00	100.00	100.00
20.83	100.00	100.00	100.00
20.92	100.00	100.00	100.00
21.00	100.00	100.00	100.00
21.08	100.00	100.00	100.00
21.17	100.00	100.00	100.00
21.25	100.00	100.00	100.00
21.33	100.00	100.00	100.00
21.42	100.00	100.00	100.00
21.50	100.00	100.00	100.00
21.58	100.00	100.00	100.00
21.67	100.00	100.00	100.00
21.75	100.00	100.00	100.00
21.83	100.00	100.00	100.00
21.92	100.00	100.00	100.00
22.00	100.00	100.00	100.00
22.08	100.00	100.00	100.00
22.17	100.00	100.00	100.00
22.25	100.00	100.00	100.00
22.33	100.00	100.00	100.00
22.42	100.00	100.00	100.00
22.50	100.00	100.00	100.00
22.58	100.00	100.00	100.00
22.67	100.00	100.00	100.00
22.75	100.00	100.00	100.00
22.83	100.00	100.00	100.00
22.92	100.00	100.00	100.00
23.00	100.00	100.00	100.00
23.08	100.00	100.00	100.00
23.17	100.00	100.00	100.00
23.25	100.00	100.00	100.00
23.33	100.00	100.00	100.00
23.42	100.00	100.00	100.00
23.50	100.00	100.00	100.00
23.58	100.00	100.00	100.00

23.67	100.00	100.00	100.00
23.75	100.00	100.00	100.00
23.83	100.00	100.00	100.00
23.92	100.00	100.00	100.00
24.00	100.00	100.00	100.00
24.08	100.00	100.00	100.00
24.17	100.00	100.00	100.00
24.25	100.00	100.00	100.00
24.33	100.00	100.00	100.00
24.42	100.00	100.00	100.00
24.50	100.00	100.00	100.00
24.58	100.00	100.00	100.00
24.67	100.00	100.00	100.00
24.75	100.00	100.00	100.00
24.83	100.00	100.00	100.00
24.92	100.00	100.00	100.00
25.00	100.00	100.00	100.00
25.08	100.00	100.00	100.00
25.17	100.00	100.00	100.00
25.25	100.00	100.00	100.00
25.33	100.00	100.00	100.00
25.42	100.00	100.00	100.00
25.50	100.00	100.00	100.00
25.58	100.00	100.00	100.00
25.67	100.00	100.00	100.00
25.75	100.00	100.00	100.00
25.83	100.00	100.00	100.00
25.92	100.00	100.00	100.00
26.00	100.00	100.00	100.00
26.08	100.00	100.00	100.00
26.17	100.00	100.00	100.00
26.25	100.00	100.00	100.00
26.33	100.00	100.00	100.00
26.42	100.00	100.00	100.00
26.50	100.00	100.00	100.00
26.58	100.00	100.00	100.00
26.67	100.00	100.00	100.00
26.75	100.00	100.00	100.00
26.83	100.00	100.00	100.00
26.92	100.00	100.00	100.00
27.00	100.00	100.00	100.00
27.08	100.00	100.00	100.00

27.17	100.00	100.00	100.00
27.25	100.00	100.00	100.00
27.33	100.00	100.00	100.00
27.42	100.00	100.00	100.00
27.50	100.00	100.00	100.00
27.58	100.00	100.00	100.00
27.67	100.00	100.00	100.00
27.75	100.00	100.00	100.00
27.83	100.00	100.00	100.00
27.92	100.00	100.00	100.00
28.00	100.00	100.00	100.00
28.08	100.00	100.00	100.00
28.17	100.00	100.00	100.00
28.25	100.00	100.00	100.00
28.33	100.00	100.00	100.00
28.42	100.00	100.00	100.00
28.50	100.00	100.00	100.00
28.58	100.00	100.00	100.00
28.67	100.00	100.00	100.00
28.75	100.00	100.00	100.00
28.83	100.00	100.00	100.00
28.92	100.00	100.00	100.00
29.00	100.00	100.00	100.00
29.08	100.00	100.00	100.00
29.17	100.00	100.00	100.00
29.25	100.00	100.00	100.00
29.33	100.00	100.00	100.00
29.42	100.00	100.00	100.00
29.50	100.00	100.00	100.00
29.58	100.00	100.00	100.00
29.67	100.00	100.00	100.00
29.75	100.00	100.00	100.00
29.83	100.00	100.00	100.00
29.92	100.00	100.00	100.00
30.00	100.00	100.00	100.00
30.08	100.00	100.00	100.00
30.17	100.00	100.00	100.00
30.25	100.00	100.00	100.00
30.33	100.00	100.00	100.00
30.42	100.00	100.00	100.00
30.50	100.00	100.00	100.00
30.58	100.00	100.00	100.00

30.67	100.00	100.00	100.00
30.75	100.00	100.00	100.00
30.83	100.00	100.00	100.00
30.92	100.00	100.00	100.00
31.00	100.00	100.00	100.00
31.08	100.00	100.00	100.00
31.17	100.00	100.00	100.00
31.25	100.00	100.00	100.00
31.33	100.00	100.00	100.00
31.42	100.00	100.00	100.00
31.50	100.00	100.00	100.00
31.58	100.00	100.00	100.00
31.67	100.00	100.00	100.00
31.75	100.00	100.00	100.00
31.83	100.00	100.00	100.00
31.92	100.00	100.00	100.00
32.00	100.00	100.00	100.00
32.08	100.00	100.00	100.00
32.17	100.00	100.00	100.00
32.25	100.00	100.00	100.00
32.33	100.00	100.00	100.00
32.42	100.00	100.00	100.00
32.50	100.00	100.00	100.00
32.58	100.00	100.00	100.00
32.67	100.00	100.00	100.00
32.75	100.00	100.00	100.00
32.83	100.00	100.00	100.00
32.92	100.00	100.00	100.00
33.00	100.00	100.00	100.00
33.08	100.00	100.00	100.00
33.17	100.00	100.00	100.00
33.25	100.00	100.00	100.00
33.33	100.00	100.00	100.00
33.42	100.00	100.00	100.00
33.50	100.00	100.00	100.00
33.58	100.00	100.00	100.00
33.67	100.00	100.00	100.00
33.75	100.00	100.00	100.00
33.83	100.00	100.00	100.00
33.92	100.00	100.00	100.00
34.00	100.00	100.00	100.00
34.08	100.00	100.00	100.00

34.17	100.00	100.00	100.00
34.25	100.00	100.00	100.00
34.33	100.00	100.00	100.00
34.42	100.00	100.00	100.00
34.50	100.00	100.00	100.00
34.58	100.00	100.00	100.00
34.67	100.00	100.00	100.00
34.75	100.00	100.00	100.00
34.83	100.00	100.00	100.00
34.92	100.00	100.00	100.00
35.00	100.00	100.00	100.00
35.08	100.00	100.00	100.00
35.17	100.00	100.00	100.00
35.25	100.00	100.00	100.00
35.33	100.00	100.00	100.00
35.42	100.00	100.00	100.00
35.50	100.00	100.00	100.00
35.58	100.00	100.00	100.00
35.67	100.00	100.00	100.00
35.75	100.00	100.00	100.00
35.83	100.00	100.00	100.00
35.92	100.00	100.00	100.00
36.00	100.00	100.00	100.00
36.08	100.00	100.00	100.00
36.17	100.00	100.00	100.00
36.25	100.00	100.00	100.00
36.33	100.00	100.00	100.00
36.42	100.00	100.00	100.00
36.50	100.00	100.00	100.00
36.58	100.00	100.00	100.00
36.67	100.00	100.00	100.00
36.75	100.00	100.00	100.00
36.83	100.00	100.00	100.00
36.92	100.00	100.00	100.00
37.00	100.00	100.00	100.00
37.08	100.00	100.00	100.00
37.17	100.00	100.00	100.00
37.25	100.00	100.00	100.00
37.33	100.00	100.00	100.00
37.42	100.00	100.00	100.00
37.50	100.00	100.00	100.00
37.58	100.00	100.00	100.00

37.67	100.00	100.00	100.00
37.75	100.00	100.00	100.00
37.83	100.00	100.00	100.00
37.92	100.00	100.00	100.00
38.00	100.00	100.00	100.00
38.08	100.00	100.00	100.00
38.17	100.00	100.00	100.00
38.25	100.00	100.00	100.00
38.33	100.00	100.00	100.00
38.42	100.00	100.00	100.00
38.50	100.00	100.00	100.00
38.58	100.00	100.00	100.00
38.67	100.00	100.00	100.00
38.75	100.00	100.00	100.00
38.83	100.00	100.00	100.00
38.92	100.00	100.00	100.00
39.00	100.00	100.00	100.00
39.08	100.00	100.00	100.00
39.17	100.00	100.00	100.00
39.25	100.00	100.00	100.00
39.33	100.00	100.00	100.00
39.42	100.00	100.00	100.00
39.50	100.00	100.00	100.00
39.58	100.00	100.00	100.00
39.67	100.00	100.00	100.00
39.75	100.00	100.00	100.00
39.83	100.00	100.00	100.00
39.92	100.00	100.00	100.00
40.00	100.00	100.00	100.00
40.08	100.00	100.00	100.00
40.17	100.00	100.00	100.00
40.25	100.00	100.00	100.00
40.33	100.00	100.00	100.00
40.42	100.00	100.00	100.00
40.50	100.00	100.00	100.00
40.58	100.00	100.00	100.00
40.67	100.00	100.00	100.00
40.75	100.00	100.00	100.00
40.83	100.00	100.00	100.00
40.92	100.00	100.00	100.00
41.00	100.00	100.00	100.00
41.08	100.00	100.00	100.00

41.17	100.00	100.00	100.00
41.25	100.00	100.00	100.00
41.33	100.00	100.00	100.00
41.42	100.00	100.00	100.00
41.50	100.00	100.00	100.00
41.58	100.00	100.00	100.00
41.67	100.00	100.00	100.00
41.75	100.00	100.00	100.00
41.83	100.00	100.00	100.00
41.92	100.00	100.00	100.00
42.00	100.00	100.00	100.00
42.08	100.00	100.00	100.00
42.17	100.00	100.00	100.00
42.25	100.00	100.00	100.00
42.33	100.00	100.00	100.00
42.42	100.00	100.00	100.00
42.50	100.00	100.00	100.00
42.58	100.00	100.00	100.00
42.67	100.00	100.00	100.00
42.75	100.00	100.00	100.00
42.83	100.00	100.00	100.00
42.92	100.00	100.00	100.00
43.00	100.00	100.00	100.00
43.08	100.00	100.00	100.00
43.17	100.00	100.00	100.00
43.25	100.00	100.00	100.00
43.33	100.00	100.00	100.00
43.42	100.00	100.00	100.00
43.50	100.00	100.00	100.00
43.58	100.00	100.00	100.00
43.67	100.00	100.00	100.00
43.75	100.00	100.00	100.00
43.83	100.00	100.00	100.00
43.92	100.00	100.00	100.00
44.00	100.00	100.00	100.00
44.08	100.00	100.00	100.00
44.17	100.00	100.00	100.00
44.25	100.00	100.00	100.00
44.33	100.00	100.00	100.00
44.42	100.00	100.00	100.00
44.50	100.00	100.00	100.00
44.58	100.00	100.00	100.00

44.67	100.00	100.00	100.00
44.75	100.00	100.00	100.00
44.83	100.00	100.00	100.00
44.92	100.00	100.00	100.00
45.00	100.00	100.00	100.00
45.08	100.00	100.00	100.00
45.17	100.00	100.00	100.00
45.25	100.00	100.00	100.00
45.33	100.00	100.00	100.00
45.42	100.00	100.00	100.00
45.50	100.00	100.00	100.00
45.58	100.00	100.00	100.00
45.67	100.00	100.00	100.00
45.75	100.00	100.00	100.00
45.83	100.00	100.00	100.00
45.92	100.00	100.00	100.00
46.00	100.00	100.00	100.00
46.08	100.00	100.00	100.00
46.17	100.00	100.00	100.00
46.25	100.00	100.00	100.00
46.33	100.00	100.00	100.00
46.42	100.00	100.00	100.00
46.50	100.00	100.00	100.00
46.58	100.00	100.00	100.00
46.67	100.00	100.00	100.00
46.75	100.00	100.00	100.00
46.83	100.00	100.00	100.00
46.92	100.00	100.00	100.00
47.00	100.00	100.00	100.00
47.08	100.00	100.00	100.00
47.17	100.00	100.00	100.00
47.25	100.00	100.00	100.00
47.33	100.00	100.00	100.00
47.42	100.00	100.00	100.00
47.50	100.00	100.00	100.00
47.58	100.00	100.00	100.00
47.67	100.00	100.00	100.00
47.75	100.00	100.00	100.00
47.83	100.00	100.00	100.00
47.92	100.00	100.00	100.00
48.00	100.00	100.00	100.00
48.08	100.00	100.00	100.00

48.17	100.00	100.00	100.00
48.25	100.00	100.00	100.00
48.33	100.00	100.00	100.00
48.42	100.00	100.00	100.00
48.50	100.00	100.00	100.00
48.58	100.00	100.00	100.00
48.67	100.00	100.00	100.00
48.75	100.00	100.00	100.00
48.83	100.00	100.00	100.00
48.92	100.00	100.00	100.00
49.00	100.00	100.00	100.00
49.08	100.00	100.00	100.00
49.17	100.00	100.00	100.00
49.25	100.00	100.00	100.00
49.33	100.00	100.00	100.00
49.42	100.00	100.00	100.00
49.50	100.00	100.00	100.00
49.58	100.00	100.00	100.00
49.67	100.00	100.00	100.00
49.75	100.00	100.00	100.00
49.83	100.00	100.00	100.00
49.92	100.00	100.00	100.00
50.00	100.00	100.00	100.00
50.08	100.00	100.00	100.00
50.17	100.00	100.00	100.00
50.25	100.00	100.00	100.00
50.33	100.00	100.00	100.00
50.42	100.00	100.00	100.00
50.50	100.00	100.00	100.00
50.58	100.00	100.00	100.00
50.67	100.00	100.00	100.00
50.75	100.00	100.00	100.00
50.83	100.00	100.00	100.00
50.92	100.00	100.00	100.00
51.00	100.00	100.00	100.00
51.08	100.00	100.00	100.00
51.17	100.00	100.00	100.00
51.25	100.00	100.00	100.00
51.33	100.00	100.00	100.00
51.42	100.00	100.00	100.00
51.50	100.00	100.00	100.00
51.58	100.00	100.00	100.00

51.67	100.00	100.00	100.00
51.75	100.00	100.00	100.00
51.83	100.00	100.00	100.00
51.92	100.00	100.00	100.00
52.00	100.00	100.00	100.00
52.08	100.00	100.00	100.00
52.17	100.00	100.00	100.00
52.25	100.00	100.00	100.00
52.33	100.00	100.00	100.00
52.42	100.00	100.00	100.00
52.50	100.00	100.00	100.00
52.58	100.00	100.00	100.00
52.67	100.00	100.00	100.00
52.75	100.00	100.00	100.00
52.83	100.00	100.00	100.00
52.92	100.00	100.00	100.00
53.00	100.00	100.00	100.00
53.08	100.00	100.00	100.00
53.17	100.00	100.00	100.00
53.25	100.00	100.00	100.00
53.33	100.00	100.00	100.00
53.42	100.00	100.00	100.00
53.50	100.00	100.00	100.00
53.58	100.00	100.00	100.00
53.67	100.00	100.00	100.00
53.75	100.00	100.00	100.00
53.83	100.00	100.00	100.00
53.92	100.00	100.00	100.00
54.00	100.00	100.00	100.00
54.08	100.00	100.00	100.00
54.17	100.00	100.00	100.00
54.25	100.00	100.00	100.00
54.33	100.00	100.00	100.00
54.42	100.00	100.00	100.00
54.50	100.00	100.00	100.00
54.58	100.00	100.00	100.00
54.67	100.00	100.00	100.00
54.75	100.00	100.00	100.00
54.83	100.00	100.00	100.00
54.92	100.00	100.00	100.00
55.00	100.00	100.00	100.00
55.08	100.00	100.00	100.00

55.17	100.00	100.00	100.00
55.25	100.00	100.00	100.00
55.33	100.00	100.00	100.00
55.42	100.00	100.00	100.00
55.50	100.00	100.00	100.00
55.58	100.00	100.00	100.00
55.67	100.00	100.00	100.00
55.75	100.00	100.00	100.00
55.83	100.00	100.00	100.00
55.92	100.00	100.00	100.00
56.00	100.00	100.00	100.00
56.08	100.00	100.00	100.00
56.17	100.00	100.00	100.00
56.25	100.00	100.00	100.00
56.33	100.00	100.00	100.00
56.42	100.00	100.00	100.00
56.50	100.00	100.00	100.00
56.58	100.00	100.00	100.00
56.67	100.00	100.00	100.00
56.75	100.00	100.00	100.00
56.83	100.00	100.00	100.00
56.92	100.00	100.00	100.00
57.00	100.00	100.00	100.00
57.08	100.00	100.00	100.00
57.17	100.00	100.00	100.00
57.25	100.00	100.00	100.00
57.33	100.00	100.00	100.00
57.42	100.00	100.00	100.00
57.50	100.00	100.00	100.00
57.58	100.00	100.00	100.00
57.67	100.00	100.00	100.00
57.75	100.00	100.00	100.00
57.83	100.00	100.00	100.00
57.92	100.00	100.00	100.00
58.00	100.00	100.00	100.00
58.08	100.00	100.00	100.00
58.17	100.00	100.00	100.00
58.25	100.00	100.00	100.00
58.33	100.00	100.00	100.00
58.42	100.00	100.00	100.00
58.50	100.00	100.00	100.00
58.58	100.00	100.00	100.00

58.67	100.00	100.00	100.00
58.75	100.00	100.00	100.00
58.83	100.00	100.00	100.00
58.92	99.58	100.00	100.00
59.00	99.58	100.00	100.00
59.08	99.57	100.00	100.00
59.17	99.57	100.00	99.72
59.25	99.57	100.00	99.72
59.33	99.57	100.00	99.71
59.42	99.57	100.00	99.70
59.50	99.57	100.00	99.69
59.58	99.57	99.68	99.69
59.67	99.56	99.67	99.68
59.75	99.57	99.67	99.68
59.83	99.57	99.67	99.68
59.92	99.56	99.66	99.67
60.00	99.57	99.64	99.67